

Universidade do Minho
Escola de Ciências

Flávia Couto Brandão Pereira

**Understanding the role of KRAS hotspot
mutations in KRAS/Galectin-3/p16^{INK4a} axis
regulation in colorectal cancer**



Universidade do Minho
Escola de Ciências

Flávia Couto Brandão Pereira

Understanding the role of KRAS hotspot mutations in KRAS/Galectin-3/p16^{INK4a} axis regulation in colorectal cancer

Dissertação de Mestrado

Mestrado em Genética Molecular

Trabalho efetuado sob a orientação de

Prof.^a Doutora Ana Arminda Lopes Preto de Almeida

Prof.^a Doutora Maria José Cardoso Oliveira

Fevereiro de 2018

DECLARAÇÃO

Nome: Flávia Couto Brandão Pereira

Endereço eletrónico: flaviabrandao.fcbp@gmail.com Telemóvel: +351 914 495 296

Cartão do Cidadão: 14593818 2 ZY2

Título da dissertação: Understanding the role of KRAS hotspot mutations in KRAS/Galectin-3/p16^{INK4a} axis regulation in colorectal cancer

Orientadoras

Professora Doutora Ana Arminda Lopes Preto de Almeida

Professora Doutora Maria José Cardoso Oliveira

Ano de conclusão: 2018

Mestrado em Genética Molecular

DE ACORDO COM A LEGISLAÇÃO EM VIGOR, NÃO É PERMITIDA A REPRODUÇÃO DE QUALQUER PARTE DESTA TESE/TRABALHO.

Universidade do Minho, ____/____/____

Assinatura:

AGRADECIMENTOS/ACKNOWLEDGMENTS



Um agradecimento à Fundação para a Ciência e Tecnologia (FCT), através do projeto PEst-OE/BIA/UI4050/2014, ao projeto *European Marie Curie Initial Training Networks (ITN): FP7-PEOPLE-2012-ITN: “GLYCOPHARM: The sugar code: from (bio)chemical concept to clinics”* e ao Norte 2020 pelo financiamento. Outro enorme agradecimento ao Centro de Biologia Molecular e Ambiental (CBMA), ao Instituto de Investigação e Inovação em Saúde (i3s), em especial ao Instituto Nacional de Engenharia Biomédica (INEB) pelo acolhimento, hospitalidade e, sobretudo, pela oportunidade concedida de desenvolver esta dissertação em instituições tão promissoras para o desenvolvimento de trabalhos graças à qualidade das instalações, promoção de trabalhos colaborativos, e o bom ambiente que neles se vivenciam.

Em seguida, mas definitivamente não menos importante, queria agradecer às minhas duas queridas orientadoras, à Ana Preto e à Maria José Oliveira. Primeiro de tudo queria agradecer pela oportunidade de desenvolver este projeto desafiador. Obrigada por terem apostado e acreditado em mim. Obrigada também por todo o vosso apoio incondicional durante todos estes longos meses, em especial, o vosso acompanhamento em TODAS as várias apresentações públicas que, sem dúvida, me fizeram sentir apoiada a 200%. Não posso deixar de elogiar o vosso perfil entusiasta e todo o empenho dedicado a este projeto e a mim. O meu muito obrigada às duas professoras, orientadoras e amigas com quem tive o privilégio de conhecer e trabalhar. Um enorme obrigada à Doutora Maria Lázaro pertencente ao Centro de Bioimagem de Biomateriais e Terapias Regenerativas (b.IMAGE) do i3s/INEB. Agradeço toda a disponibilidade para me ensinar e ajudar, a sua ajuda foi enorme. Esta foi uma colaboração muito gratificante, a qual nos permitiu tirar uma das conclusões fundamentais desta tese. Queria agradecer também à Doutora Ana João Rodrigues e à sua aluna de doutoramento Carina Cunha, do Instituto de Investigação em Ciências da Vida e Saúde (ICVS).

Também não me poderia esquecer de agradecer àqueles que me acompanharam neste árduo percurso, o grupo da Ana Preto. Ao Tiago Moreira e à Giulia Cazzanelli gostaria de agradecer todos os ensinamentos, que foram fundamentais para chegar até aqui e toda a boa disposição que sempre os acompanharam. Um muito obrigado às minhas meninas Ana Almeida, Rita Brás e à Sara Gomes que foram as minhas companheiras de laboratório (e de todas as ocasiões) e que me mostraram o verdadeiro e puro espírito de equipa. Foi espetacular e muitíssimo importante este crescimento conjunto e este apoio que nos demos umas às outras. Um obrigada

aos novos membros também, a Adriana Mendes e o Jorge Macedo, que trouxeram novas ideias para o grupo e que também me acompanharam e apoiaram. Queria também agradecer aos elementos do divertido grupo da Maria José Oliveira, que me receberam tão bem e que foram fundamentais. Um especial agradecimento à Ângela Costa, à Marta Laranjeiro Pinto e à Patrícia Cardoso, por todos os ensinamentos e discussões de resultados que foram essenciais. Obrigada às Flávias, Flávia Castro e Flávia Martins, pelo acompanhamento, pela ajuda, pelo apoio e por toda a diversão, e por vezes desafio, que foi sermos 3 Flávias no mesmo grupo. Um obrigada também à Rosa Oliveira, a minha colega de infância que agora se tornou minha colega de trabalho, a tua boa disposição é contagiante. Agradeço também ao Diogo Adão e à Catarina Cunha pela companhia. Um obrigado vai também para o grupo Cancer Drug Resistance (CDR), que foram excelentes companhias para todas as ocasiões. Obrigada Hugo Caires, Cristina Xavier, Alexandra Teixeira, Joana Pereira, Inês Castro, Tamara Marcelo, Pedro Nunes, André Pina e Sara Alves. Um enorme obrigada também aos meus colegas de mestrado, especialmente à Leslie Amaral, à Rita Costa e à Beatriz Rodrigues.

Por último, mas não menos importante quero agradecer à minha família, por estarem sempre lá “para tudo o que der e vier”. Em destaque fundamental, um obrigado aos meus pais, pois sem eles, rigorosamente, nada disto era possível. Obrigada por me acompanharem em todas as ambições, derrotas e vitórias, por acreditarem em mim mais do que eu própria e, fundamentalmente, por me darem a oportunidade de, a pouco e pouco, realizar os meus sonhos. Esta tese é fruto, não só do meu trabalho, mas também de tudo o que vós meus pais me educaram a ser. Sei que dificilmente irei alguma vez conseguir exprimir o quão agradecida vos estou, mas um muito obrigado cheio de amor por todos os sacrifícios que fizeram para que eu chegasse até aqui. Obrigada ao meu irmão também por todo o apoio. Um muito obrigado também ao meu namorado, foi um pilar e um companheiro fundamental e insubstituível em toda esta longa caminhada. Obrigada por me fazeres sentir uma guerreira e me ajudares quando tudo corria menos bem. Um especial obrigado à minha estrelinha, o meu avô, que sei que estaria super orgulhoso de me ver a terminar mais uma etapa e que se pudesse estaria no dia da minha defesa na fila da frente a apoiar me.

Obrigada a todas as outras pessoas que tive a oportunidade de conhecer e trabalhar.

ABSTRACT

Colorectal Cancer (CRC) is a heterogeneous complex disease, which is the third most commonly diagnosed cancer worldwide. Despite the intensive follow-up and the novel therapeutic options for CRC patients, it remains as one of the most leading causes of cancer-related deaths. CRC carcinogenesis results mainly from the serrated or from the adenoma-carcinoma pathways, being associated with several mutations in key molecules.

KRAS mutations are a very frequent event present in CRC being the hotspot mutations the following: KRAS^{G13D}, KRAS^{G12D} and KRAS^{G12V}. These mutations can lead to constitutively activation of KRAS proteins, which contribute to colorectal tumorigenesis, and no specific inhibitors are available what constitutes a clinical problem to overcome. Galectin-3 (Gal-3) belongs to galectins family and its function depends on its subcellular localization. Its abnormal localization is common in many types of human cancers, including CRC, and is correlated with cancer cell invasion and tumor angiogenesis. Recent studies shown that Gal-3 overexpression is associated with increased KRAS signal output, leading to increased cell proliferation, survival and migration. However, the interactions between Gal-3 and active KRAS are not fully understood. On its turn, p16^{INK4a} is a tumor suppressor protein, G1 cyclin-dependent kinase (CDK) inhibitor which loss occurs during malignant transformation. Since overexpression of KRAS can be induced by loss of p16^{INK4a} the latter has been appointed with a crucial role in CRC carcinogenesis.

In the present project, we aimed to study the role of KRAS in the regulation of KRAS/Galectin-3/p16^{INK4a} triple axis in CRC and the impact of the complex in CRC invasion and invasion-associated activities.

Our results demonstrated for the first time using normal colon and CRC cells, that KRAS/Galectin-3/p16^{INK4a} interact, forming a multiprotein complex which showed a feedback loop regulation. Moreover, we provided evidences that this complex might be a new mechanism of inactivation of the tumor suppressor gene p16^{INK4a} by forcing its re-localization from the nucleus to the cytoplasm. Our data also identified KRAS and Gal-3 as important players in CRC migration and invasion.

This work opens a new field of research, as understanding the role of KRAS/Galectin-3/p16^{INK4a} complex regulation on colorectal carcinogenesis might have relevant therapeutic implications.

RESUMO

O cancro colorretal é uma doença heterogénea complexa, que corresponde ao terceiro cancro mais frequentemente diagnosticado no mundo. Apesar do acompanhamento intensivo dos pacientes e dos últimos avanços terapêuticos, é ainda uma das principais causas de morte associadas a cancro. O seu processo de carcinogénese resulta principalmente das vias serrada e adenoma-carcinoma, estando associado a mutações em moléculas chave.

As mutações do gene KRAS são eventos muito frequentes no cancro colorretal sendo as mutações mais comuns as seguintes: KRAS^{G13D}, KRAS^{G12D} e KRAS^{G12V}. Estas mutações podem levar à ativação constitutiva das proteínas KRAS, contribuindo para a tumorigénese, não havendo inibidores específicos do KRAS o que é um problema clínico que precisa de resolução. A Galectina-3 pertence à família das galectinas e a sua função depende da sua localização subcelular. A sua localização anormal é frequente em vários tipos de cancros, incluindo no cancro colorretal, e está relacionada com a invasão e angiogénese do tumor. Estudos recentes demonstraram que a sobreexpressão da proteína Gal-3 está associada ao aumento da sinalização mediada pelo KRAS, resultando no acréscimo da proliferação, sobrevivência e migração celulares. No entanto, as interações entre a Galectina-3 e a proteína KRAS ativada não estão ainda completamente compreendidas. Por sua vez, a p16^{INK4a} é uma proteína supressora de tumores, inibidora G1 da cinase dependente de ciclina cuja perda ocorre frequentemente durante a transformação maligna dos tumores. Uma vez que a sobreexpressão da proteína KRAS pode ser induzida pela perda da expressão da p16^{INK4a}, pensa-se que a última tenha também um papel muito importante na carcinogénese colorretal.

No presente projeto, pretendemos estudar o papel da proteína KRAS na regulação do eixo KRAS/Galectin-3/p16^{INK4a} no cancro colorretal e o impacto deste complexo na invasão e nas atividades associadas à invasão tumoral. Os nossos estudos, utilizando linhas celulares colorretais normais e cancerígenas, demonstraram, pela primeira vez, que as proteínas KRAS/Galectin-3/p16^{INK4a} interagem entre si formando um complexo de regulação recíproca. Apresentamos ainda, evidências de que este complexo pode ser um novo mecanismo de inativação da proteína supressora tumoral p16^{INK4a}, por forçar a sua realocação do núcleo para o citoplasma. Os nossos dados também identificaram o KRAS e a Galectina-3 como intervenientes importantes na migração e invasão das células colorretais.

Este trabalho abre novas perspetivas de investigação sobre o papel da regulação do complexo KRAS/Galectin-3/p16^{INK4a} na carcinogénese colorretal que poderá ter implicações terapêuticas relevantes.

LIST OF CONTENTS

AGRADECIMIENTOS/ACKNOWLEDGMENTS	III
ABSTRACT	V
RESUMO	VII
LIST OF FIGURES	XI
LIST OF TABLES	XII
LIST OF ABBREVIATIONS AND ACRONYMS	XIII
THESIS OUTLINE	1
CHAPTER I. STATE OF THE ART	3
1.1 COLORECTAL CANCER	4
1.1.1 <i>Incidence and mortality of colorectal cancer</i>	4
1.1.2 <i>Colorectal cancer stages</i>	5
1.1.3 <i>Colorectal cancer subtypes according to genetic markers</i>	7
1.1.4 <i>Colorectal carcinogenesis</i>	8
1.1.5 <i>The influence of diet in colorectal cancer</i>	12
1.2 RAS SUPERFAMILY	13
1.2.1 <i>Ras proto-oncogenes</i>	14
1.2.2 <i>RAS signaling</i>	16
1.2.3 <i>The role of KRAS oncogene in cancer</i>	19
1.2.4 <i>The role of KRAS oncogene in colorectal cancer</i>	20
1.2.5 <i>KRAS dimers and multimers</i>	21
1.2.5.1 <i>KRAS dimers and RAS-RAF-MAPK signaling axis</i>	22
1.3 GALECTINS	23
1.3.1 <i>Galectin-3</i>	25
1.3.2 <i>The role of galectin-3 in cancer</i>	26
1.3.3 <i>The role of galectin-3 in colorectal cancer</i>	28
1.4 p16 ^{INK4A}	30
1.4.1 <i>The role of p16^{INK4a} in cancer</i>	32
1.4.2 <i>The role of p16^{INK4a} in colorectal cancer</i>	36
1.5 THE INTERPLAY BETWEEN KRAS, GALECTIN-3 AND p16 ^{INK4A}	37
1.6 RATIONALE AND AIMS.....	39
CHAPTER II. MATERIALS AND METHODS	41
2.1 CELL LINES AND CULTURE CONDITIONS	42
2.2 KRAS/GALECTIN-3/PP6 ^{INK4A} NANOCUSTER ANALYSIS	43
2.2.1 <i>Immunoprecipitation assay</i>	43
2.2.2 <i>Co-localization studies through immunofluorescence assay</i>	45

2.2.2.1	Immunofluorescence assay	45
2.2.2.2	Co-localization analysis by ImageJ software.....	47
2.3	SILENCING OF KRAS AND/OR GALECTIN-3 BY RNA INTERFERENCE	48
2.3.1	<i>KRAS and galectin-3 localization through immunofluorescence assay</i>	49
2.3.3	<i>Time-Lapse migration assays</i>	50
2.3.3.1	Time-Lapse wound-healing migration assay	50
2.3.3.2	Time-lapse single-cell migration assay	50
2.3.4	<i>Matrigel invasion assay</i>	51
2.3.5	<i>Gelatin zymography assay</i>	51
2.3.6	<i>Senescence-associated β-galactosidase assay</i>	52
2.3.7	<i>Western blot analysis</i>	52
2.4	STATISTICAL ANALYSIS	53
CHAPTER III. RESULTS		55
3.1	CO-IMMUNOPRECIPITATION AND CO-LOCALIZATION STUDIES EVIDENCE THAT KRAS/GALECTIN-3/P16 ^{INK4A} INTERACT AS A MULTIPROTEIN COMPLEX	56
3.1.1	<i>Co-immunoprecipitation studies on colon cell lines</i>	56
3.1.2	<i>Co-localization studies on NCM460 cell lines transfected with Flag-KRAS hotspot mutations</i>	59
3.2	<i>KRAS/GALECTIN-3/P16^{INK4A} EXHIBIT A FEEDBACK LOOP REGULATION</i>	68
3.3	<i>GALECTIN-3 SILENCING LEADS TO AN INCREASED P16^{INK4A} LOCALIZATION AT THE NUCLEUS</i>	69
3.4	<i>KRAS AND GALECTIN-3 ENHANCE CANCER CELL INVASION WITHOUT ACTIVATION OF MATRIX METALLOPROTEINASE MMP-2 AND MMP-9</i>	71
3.5	<i>KRAS AND/OR GALECTIN-3 ENHANCE CANCER CELL MIGRATION</i>	72
3.6	<i>KRAS AFFECTS INVASION-ASSOCIATED SIGNALING PATHWAY ERK</i>	74
3.7	<i>KRAS AND GALECTIN-3 SEEM TO AFFECT PROLIFERATION AND SURVIVAL SIGNALING PATHWAY PI3K-AKT</i>	75
CHAPTER IV. DISCUSSION AND CONCLUDING REMARKS		77
CHAPTER V. FUTURE PERSPECTIVES		87
I.	REFERENCES	93

LIST OF FIGURES

FIGURE 1 – ESTIMATED NUMBER OF INCIDENT CASES OF CANCER WORLDWIDE IN 2012.....	4
FIGURE 2 – WORLDWIDE INCIDENCE AND MORTALITY OF DIFFERENT CANCERS IN BOTH SEXES IN 2012.	5
FIGURE 3 – COLORECTAL CANCER STAGES.	6
FIGURE 4 – SCHEMATIC REPRESENTATION OF CLASSICAL AND SERRATED PATHWAYS OF COLORECTAL CARCINOGENESIS AND THEIR RELATIONSHIP WITH HISTOLOGICAL STATES AND GENETIC FEATURES.	9
FIGURE 5 - COLORECTAL CANCER CARCINOGENESIS BY CHROMOSOMAL INSTABILITY AND MICROSATELLITE INSTABILITY PATHWAYS. ..	11
FIGURE 6 - RAS SUPERFAMILY AND THEIR FIVE BRANCHES RAS, RHO, ARF/SAR, RAN AND RAB.....	13
FIGURE 7 – CYCLE OF ACTIVE RAS-GTP AND INACTIVE RAS-GDP.	14
FIGURE 8 – HRAS, NRAS AND KRAS PROTEINS.....	15
FIGURE 9 - RAS SIGNALING PATHWAY.....	18
FIGURE 10 – THE FAMILY OF 15 MAMMALIAN GALACTOSIDE-BINDING PROTEINS DIVIDED IN PROTOTYPE, CHIMERA-TYPE AND TANDEM- REPEAT TYPE SUBGROUPS ACCORDING TO STRUCTURAL DIFFERENCES.....	23
FIGURE 11 – LOCALIZATION AND FUNCTIONS OF MULTIFUNCTIONAL GALECTINS ON CANCER.	24
FIGURE 12 – GALECTIN-3 MONOMER AND PENTAMER REPRESENTATION FOCUSING THEIR STRUCTURAL DOMAINS.	25
FIGURE 13 - EFFECTS OF GALECTIN-3 ON TUMOR CELL APOPTOSIS.	27
FIGURE 14 – INK4B/ARF/INK4A LOCUS ON CHROMOSOME 9P21.....	30
FIGURE 15 – <i>CDKN2A</i> GENE ORGANIZATION AND CELL-CYCLE FUNCTIONS OF ENCODING PROTEINS P6 ^{INK4A} AND P14 ^{ARF}	31
FIGURE 16 – P16 ^{INK4A} LEVELS DURING TUMORIGENESIS.	34
FIGURE 17 – CELLULAR COMPARTMENTALIZATION AND FUNCTIONS OF P16 ^{INK4A}	35
FIGURE 18 – <i>RATIONALE</i> OF THIS WORK.	40
FIGURE 19 - ANALYSIS OF KRAS, GAL-3, AND P16INK4A CO-IMMUNOPRECIPITATIONS IN SW480 THROUGH PROTEIN G SEPHAROSE BEADS FOLLOWED BY WESTERN BLOT.	58
FIGURE 20 - CONFOCAL IMMUNOFLUORESCENCE MICROSCOPE ANALYSIS OF SINGLE STAINING AND CONTROL CONDITIONS FOR GAL-3 LOCALIZATION IN NCM460 FLAG-KRAS ^{WT}	60
FIGURE 21 - CONFOCAL IMMUNOFLUORESCENCE MICROSCOPE ANALYSIS OF SINGLE STAINING AND CONTROL CONDITIONS FOR P16 ^{INK4A} LOCALIZATION IN NCM460 FLAG-KRAS ^{WT}	60
FIGURE 22- CONFOCAL IMMUNOFLUORESCENCE MICROSCOPE ANALYSIS OF SINGLE STAINING AND CONTROL CONDITIONS FOR FLAG LOCALIZATION IN NCM460 <i>FLAG-KRAS</i> ^{WT}	61
FIGURE 23 - CONFOCAL FLUORESCENCE MICROSCOPE ANALYSIS OF DOUBLE STAINING FOR GAL-3 + P16 ^{INK4A} , GAL-3 + FLAG-KRAS, FLAG-KRAS + P16 ^{INK4A} CO-LOCALIZATION IN NCM460 <i>FLAG-KRAS</i> ^{WT} CELL LINES.	62
FIGURE 24 - CONFOCAL FLUORESCENCE MICROSCOPE ANALYSIS OF DOUBLE STAINING FOR GAL-3 + FLAG-KRAS LOCALIZATION IN NCM460 <i>FLAG-KRAS</i> TRANSFECTED CELL LINES.....	63
FIGURE 25 - CONFOCAL FLUORESCENCE MICROSCOPE ANALYSIS OF DOUBLE STAINING FOR GAL-3 + P16 ^{INK4A} LOCALIZATION IN NCM460 <i>FLAG-KRAS</i> TRANSFECTED CELL LINES.....	64
FIGURE 26 - CONFOCAL FLUORESCENCE MICROSCOPE ANALYSIS OF DOUBLE STAINING FOR FLAG-KRAS + P16 ^{INK4A} LOCALIZATION IN NCM460 <i>FLAG-KRAS</i> TRANSFECTED CELL LINES.....	65

FIGURE 27 - ANALYSES OF KRAS, GALECTIN-3 AND P16 ^{INK4A} EXPRESSION LEVELS AFTER <i>KRAS</i> AND/OR <i>LGALS3</i> SILENCING UPON RNAI IN HCT116 CELL LINE. (A) WESTERN BLOT ANALYSIS. (B) PROTEIN LEVEL AFTER RNAI EXPERIMENTS.	69
FIGURE 28 - IMPACT OF KRAS AND GAL-3 ON GAL-3 AND P16 ^{INK4A} LOCALIZATION ASSESSED BY CONFOCAL FLUORESCENCE MICROSCOPE ANALYSIS.	70
FIGURE 29 - EFFECT OF KRAS AND GALECTIN-3 ON CELL INVASION.	71
FIGURE 30 - MATRIX METALLOPROTEINASES ACTIVITY ANALYSIS THROUGH GELATIN ZYMOGRAPHY OF HCT116 SILENCING FOR KRAS AND/OR GAL-3 UPON RNAI.	72
FIGURE 31 - EFFECT OF KRAS AND GALECTIN-3 ON CELL MIGRATION BY WOUND-HEALING ASSAY. (A) WOUND-HEALING ASSAY. (B) THE PERCENTAGE OF WOUND CLOSURE.	73
FIGURE 32 - EFFECT OF KRAS AND GALECTIN-3 ON CELL MIGRATION BY SINGLE-CELL MIGRATION ASSAY. (A) MIGRATION DISTANCE AND (B) MIGRATION VELOCITY WERE ANALYZED FOR SINGLE-CELL MIGRATION ASSAY.	74
FIGURE 33 - ANALYSIS OF KRAS AND GALECTIN-3 IMPACT ON INVASION-ASSOCIATED ERK SIGNALING PATHWAY. (A) WESTERN BLOT ANALYSIS. (B) PROTEIN LEVEL AFTER RNAI EXPERIMENTS.	75
FIGURE 34 - ANALYSIS OF KRAS AND GALECTIN-3 IMPACT ON CELL PROLIFERATION AND SURVIVAL PI ₃ K-AKT SIGNALING PATHWAY. (A) WESTERN BLOT ANALYSIS. (B) PROTEIN LEVEL AFTER RNAI EXPERIMENTS.	76
FIGURE 35 - KRAS/GALECTIN-3/P16 ^{INK4A} AXIS REGULATION ON COLORECTAL CANCER.	86
FIGURE 36 - PRINCIPLE OF PLA TECHNIQUE SINCE PROTEIN RECOGNITION UNTIL PROTEIN-PROTEIN INTERACTION DETECTION.	88
FIGURE 37 - PRINCIPLE OF FAR-WESTERN BLOT TECHNIQUE.	89

LIST OF TABLES

TABLE 1 – PRIMARY AND SECONDARY ANTIBODIES USED FOR IMMUNOFLUORESCENCE ASSAY.	46
TABLE 2 - PRIMARY AND SECONDARY ANTIBODIES USED IN GAL-3 AND P16 ^{INK4A} CO-LOCALIZATION ANALYSIS BY IMMUNOFLUORESCENCE ASSAY.	49
TABLE 3 - VALUES OF GAL-3/FLAG-KRAS, P16 ^{INK4A} /FLAG-KRAS AND GAL-3/ P16 ^{INK4A} COLOCALIZATION ANALYSIS IN NCM460 FLAG-KRAS CELLS.	67

LIST OF ABBREVIATIONS AND ACRONYMS

AE1 - <u>A</u> nion <u>E</u> xchanger <u>1</u>	FLIM-FRET - <u>F</u> luorescence <u>L</u> ifetime
APC - <u>A</u> denomatous <u>P</u> olyposis <u>C</u> oli	<u>I</u> maging & <u>F</u> luorescence <u>R</u> esonance <u>E</u> nergy
APN - <u>A</u> minopeptidase <u>N</u> /CD13	<u>T</u> ransfer
ARF - <u>A</u> lternative <u>R</u> eadin <u>F</u> rame	G proteins - <u>G</u> uanine Nucleotide-Binding
b.IMAGE - Centro de Bioimagem de	<u>P</u> roteins
Biomateriais e Terapias Regenerativas	Gal-3 - <u>G</u> alectin- <u>3</u>
BAT26 - <u>B</u> ig <u>A</u> denine <u>T</u> ract <u>26</u>	Galβ1,3GalNAcα-, TF - <u>T</u> homsen-
bFGF - <u>B</u> asic <u>F</u> ibroblast <u>G</u> rowth <u>F</u> actor	<u>F</u> riedenreich Carbohydrate
CBMA - <u>C</u> entro de <u>B</u> iologia <u>M</u> olecular e	GAPs - <u>G</u> TPase- <u>A</u> ctivating <u>P</u> roteins
<u>A</u> mbiental	G-CSF - <u>G</u> ranulocyte <u>C</u> olony- <u>S</u> timulating
CBP-30 - <u>C</u> arbohydrate-Binding <u>P</u> rotein <u>30</u>	<u>F</u> actor
CBP-35 - <u>C</u> arbohydrate-Binding <u>P</u> rotein <u>35</u>	GDP - <u>G</u> uanine <u>D</u> iphosphate
CDK - <u>C</u> yclin- <u>D</u> ependent <u>K</u> inase	GEFs - <u>G</u> uanine-Nucleotide <u>E</u> xchange <u>F</u> actors
CDK4I - <u>C</u> yclin- <u>D</u> ependent <u>K</u> inase <u>4</u> <u>I</u> nhibitor	GM-CSF - <u>G</u> ranulocyte- <u>M</u> acrophage <u>C</u> olony-
<u>A</u>	<u>S</u> timulating <u>F</u> actor
CDKN2A - <u>C</u> yclin- <u>D</u> ependent <u>K</u> inase <u>I</u> nhibitor	GSK-3β - <u>G</u> lycogen <u>S</u> ynthase <u>K</u> inase- <u>3β</u>
<u>2A</u>	GTP - <u>G</u> uanine <u>T</u> riphosphate
CIMP - <u>C</u> pg <u>I</u> sland <u>M</u> ethylator <u>P</u> henotype	HBSS - <u>H</u> ank's <u>B</u> alanced <u>S</u> alt <u>S</u> olution
CIN - <u>C</u> hromosomal <u>I</u> nstability	HNPCC - <u>H</u> ereditary <u>N</u> on- <u>P</u> olyposis
CK1 - <u>C</u> asein <u>K</u> inase <u>1</u>	<u>C</u> olorectal <u>C</u> ancer
Co-IP - <u>C</u> o- <u>I</u> mmunoprecipitation	HPP - <u>H</u> yperplastic <u>P</u> olyps
Control - Control cells	HRAS - <u>H</u> arvey <u>R</u> AS
CRC - <u>C</u> olorectal <u>C</u> ancer	HVR - <u>H</u> ypervariable <u>R</u> egion
CRDs - <u>C</u> arbohydrate <u>R</u> ecognition <u>D</u> omains	I3S - <u>I</u> nstituto de <u>I</u> nvestigação e <u>I</u> novação em
CREB - <u>c</u> AMP <u>R</u> esponsive <u>E</u> lement <u>B</u> inding	<u>S</u> áude
CTNBI - <u>C</u> atenin cadherin-associated	ICAM-1 - <u>I</u> nter <u>c</u> ellular <u>A</u> dhesion <u>M</u> olecule <u>1</u>
protein <u>B</u> eta <u>1</u>	ICVS - Instituto de Investigação em Ciências
DAG - <u>D</u> iacylglycerol	da Vida e Saúde
DLS - <u>D</u> ynamic <u>L</u> ight <u>S</u> cattering	IgEBP - <u>I</u> gE-binding protein
dsRNA - <u>D</u> ouble <u>S</u> tranded <u>R</u> NA	IL-6 - <u>I</u> nterleukin <u>6</u>
FAP - <u>F</u> amilial <u>A</u> denomatous <u>P</u> olyposis	INEB - Instituto Nacional de Engenharia
FBS - <u>F</u> etal <u>B</u> ovine <u>S</u> erum	<u>B</u> iomédica
FCT - Fundação para a <u>C</u> iência e <u>T</u> ecnologia	IP - <u>I</u> mmunoprecipitation
	IP Gal-3 - <u>I</u> mmunoprecipitation of Gal-3
	IP KRAS - <u>I</u> mmunoprecipitation of KRAS

IP p16 - Immunoprecipitation of p16^{INK4a}
ITN - European Marie Curie Initial Training Networks
JACoP - Just Another Colocalization Plugin
KRAS – Kirsten RAS
KRAS siRNA - siRNA abrogating the expression of KRAS
LGALS3 siRNA - siRNA abrogating the expression of Gal-3
LGALS3 siRNA+KRAS siRNA - siRNA abrogating expression of both proteins Gal-3+KRAS
MAP - MUTYH-Associated Polyposis
MDR - Multidrug Resistance
MEFs - Mouse Embryonic-Fibroblasts
MLH1 - MutL homolog 1
MMPs - Matrix Metalloproteinases
MMR-D - Deficient Mismatch Repair
MMR-P - Proficiant Mismatch Repair
MOC - Mander's Overlap Coefficient
MSH2 - MutS homolog 2
MSI - Microsatellite Instability
MSS - Microsatellite Stability
MTS-1 - Multiple Tumor Suppressor 1
MUC1 - Mucin Protein
NRAS – Neuroblastoma RAS
NSAIDs - Non-Steroidal Anti-Inflammatory Drugs
OC - Overlap Coefficient
ORF - Open ReadinFrame
pAKT - Phosphorylated AKT
PBS-T - PBS-Tween20
PCC - Pearson's Correlation Coefficient
Pen-Strep - Penicillin-Streptomycin
pERK - Phosphorylated ERK
PFA - Paraformaldehyde

PI3K - phosphatidyInositol 4,5 bisphosphate 3-kinase
PIK3CA^{H1047R} - catalytic subunit α of phosphatidyInositol-4,5-bisphosphate 3-kinase
PLA - Proximity Ligation Assay
pRb - Phosphorylate Retinoblastoma Protein
PTM - Post-Translational Modifications
RCA - Rolling Circle Amplification
RNAi - RNA interference
ROS - Reactive Oxygen Species
SA-β-Gal - Senescence-associated expression of β-Galactosidase
SCFA - Short-Chain Fatty Acids
SDS - Sodium Dodecyl Sulphate
sICAM-1 - Soluble Intercellular Adhesion Molecule-1
siRNA - small interfering RNA
SSA/P - Sessile Serrated Adenoma/Polyp
TP53 - Tumor Suppressor protein p53
TRAIL - Tumor Necrosis Factor-Related Appoptosis-Inducing Ligand
TSA - Traditional Serrated Adenomas
TTF-1 - Th thyroid Transcription Factor-1
VCAM-1 - Vascular Cell Adhesion Molecule 1
VEGF - Vascular Endothelial Growth Factor

THESIS OUTLINE

For sake of simplicity we decided to divide the present dissertation in the following chapters:

Chapter I comprises the state of the art, which is a general introduction on the subject of study and the *rationale* and aims of this work.

In the stated of the art we first focus on CRC, mainly on the characterization and development of the disease. Then we highlight RAS superfamily and RAS family members converging in KRAS proteins, their mutations and impact on cancer specially on CRC. Further, we explore the Galectins focusing on Gal-3, its role and impact on cancer and CRC. Next, we describe p16^{INK4a}, its role and impact on cancer and CRC. Finally, we describe what is already known about the interplay between KRAS, Gal-3 and p16^{INK4a}.

Chapter II describes the materials and methods used to perform all the experimental work being subdivided by techniques.

Chapter III comprises the results obtained, which are subdivided in subchapters.

Chapter IV comprises an extensive discussion on the results obtained and the overall conclusions of this work with a schematic representation.

Chapter V presents the suggestions for future perspectives on the project.

CHAPTER I. STATE OF THE ART

Some sections of this chapter are part of the following publication (Annex I):

Cazzanelli G, **Pereira F**, Alves S, Francisco R, Azevedo L, Carvalho PD, Almeida A, Côrte-Real M, Oliveira MJ, Lucas C, Sousa MJ, and Preto A. (2018) *The Yeast Saccharomyces cerevisiae as a Model for Understanding RAS Proteins and Their Role in Human Tumorigenesis. Cells* (Vol. 7). <https://doi.org/10.3390/cells7020014>

1.1 Colorectal Cancer

1.1.1 Incidence and mortality of colorectal cancer

CRC is the third most commonly diagnosed cancer accounting for more than 1.3 million new cases worldwide in 2012 (Norton *et al.*, 2015; Qi *et al.*, 2015; Rosa *et al.*, 2015; Szyllberg *et al.*, 2015; Wong *et al.*, 2015) (**Figure 1**).

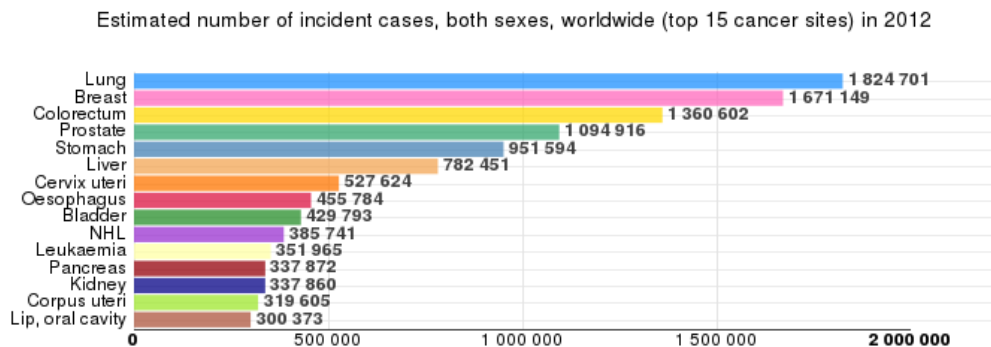


Figure 1 – Estimated number of incident cases of cancer worldwide in 2012.

Colorectal cancer is the third most diagnosed cancer worldwide with 1,360,602 of new cases. This incidence is only exceeded by lung cancer with 1,824,701 cases and breast cancer accounting with 1,671,149 incident cases. The graph was obtained from Global Cancer Observatory based on GLOBOCAN 2012 information. Reproduced from: Ferlay *et al.*, 2014.

Importantly, about 70% of these CRC cases are sporadic (Korkmaz *et al.*, 2016) and approximately 20-25% of the newly diagnosed CRCs correspond to stage IV with synchronous CRC liver metastases present in 15–25% of these cases (Adam *et al.*, 2015; Ghidini *et al.*, 2016; Sakellariou *et al.*, 2016). The liver is often the first site of metastatic disease, but CRC also metastasizes to the lung, peritoneum, bone, spleen, brain and distant lymph nodes (Hugen *et al.*, 2014; Qi *et al.*, 2015).

Despite the intensive follow-up for CRC patients, it is the fourth leading cause of cancer-related death in men and the third in women with 693,600 deaths, corresponding to 8% of all cancer deaths worldwide occurred in 2012 (Alberti *et al.*, 2015; Alves *et al.*, 2015; Qi *et al.*, 2015; Rosa *et al.*, 2015; Sylvester and Vakiani, 2015; Szyllberg *et al.*, 2015; Wong *et al.*, 2015; Yanai, Nakamura and Matsumoto, 2015) (**Figure 2**).

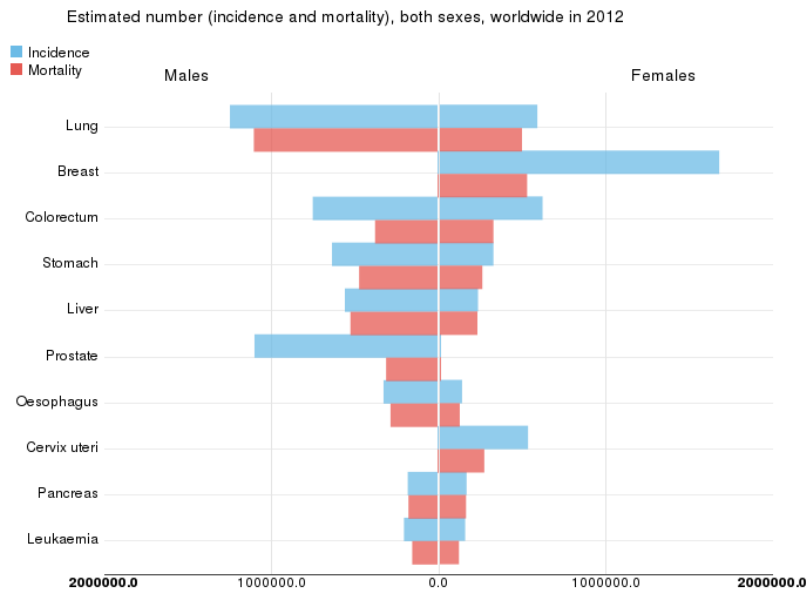


Figure 2 – Worldwide incidence and mortality of different cancers in both sexes in 2012.

Colorectal cancer is the fourth leading cause of cancer-related death in men and the third in women. In men, the first leading cause of cancer-related death is lung cancer, followed by liver and stomach cancers. In women, mortality estimated number for colorectal is exceeded by breast and lung cancers. The graph was obtained from Global Cancer Observatory based on GLOBOCAN 2012 information. Reproduced from: Ferlay et al., 2014.

Moreover, approximately one-third of CRC patients die 5 years after diagnosis (Roper and Hung, 2013; El-Sham *et al.*, 2015). Over the years, this situation is being reverted with the increased rates of CRC screening, advances in early detection and treatment (El-Sham *et al.*, 2015). With survivors increase, efforts have been provided to prevention of CRC recurrence and of new primary CRC as well as to minimize both short and long term adverse effects and improve the modalities used to treat it (El-Sham *et al.*, 2015).

1.1.2 Colorectal cancer stages

CRC is a heterogeneous complex disease that can be divided into five stages: 0, I, II, III and IV (Patai *et al.*, 2013; American Cancer Society, 2015; Cancer treatment centers of America, 2015) (Erro! A origem da referência não foi encontrada.). At Stage 0 cancer does not grow beyond the inner layer of the colon or rectum. It is known as carcinoma *in situ* or intramucosal carcinoma (American Cancer Society, 2015; Cancer treatment centers of America, 2015). At stage I cancer grows into the layers of colon wall, but it does not spread outside the colon wall itself. This cancer grows through the mucosa and into the submucosa or it may also grows into the muscularis propria (American Cancer Society, 2015; Cancer treatment centers of America, 2015). At stage II CRC is divided into three subcategories based on spread of cancer: IIA, IIB and IIC. IIA is characterized by a cancer that grows into the outermost layers of colon or rectum,

but it does not grow through them. IIB is relative to cancer that grows through all the layers of colon or rectum, but it does not grow into other organs or tissues. IIC CRC grows through all the layers of colon or rectum and into nearby organs or tissues. In conclusion, these cancers grow through the wall of colon or rectum and possibly into nearby tissue, but they are not yet spread to the lymph nodes (American Cancer Society, 2015; Cancer treatment centers of America, 2015). CRC at stage III is divided into three categories based on spread and how many lymph nodes are affected: IIIA, IIIB and IIIC. IIIA is characterized by a cancer that grows into the submucosa and possibly into the *muscularis propria* and spreads to 1-3 lymph nodes near the site of the primary tumor. IIIB CRC grows into the outermost layer of the colon or rectum, it can reach nearby organs and spreads to 1-3 lymph nodes near the primary site. IIIC CRC may or may not grow through the wall of colon or rectum, but it spreads to four or more lymph nodes near the primary site. In conclusion, cancers at stage III only spread to nearby lymph nodes, but they are not yet spread to other parts of the body (American Cancer Society, 2015; Cancer treatment centers of America, 2015). At stage IV, CRCs reach other organs in the body, forming metastases at distant sites, such as liver or lungs. These types of cancers can also be divided into IVA and IVB. If spreads to one unique organ it is considered IVA, but if the disease affects more than one organ with multiple organ metastases it is considered as IVB cancer (American Cancer Society, 2015; Cancer treatment centers of America, 2015).

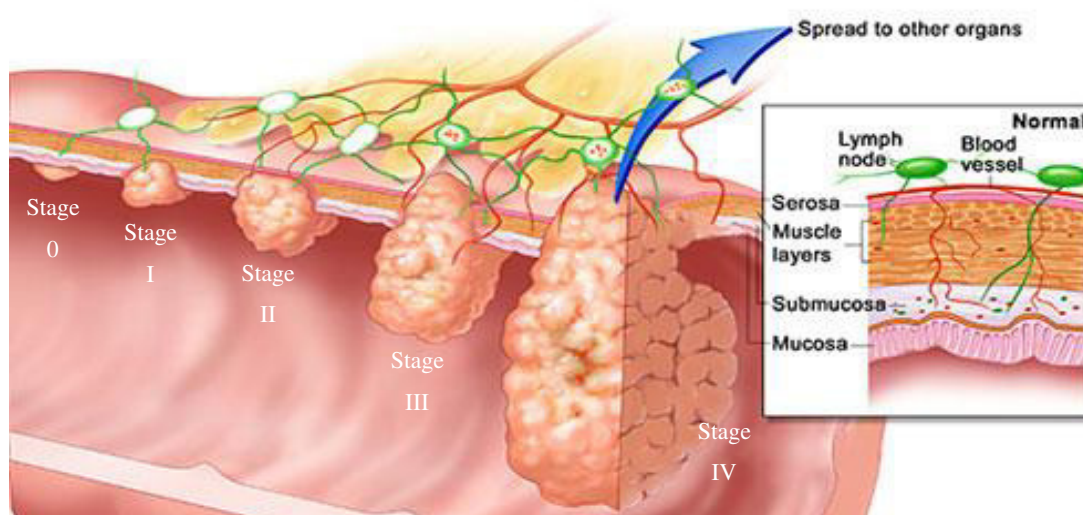


Figure 3 – Colorectal cancer stages.

CRC can be divided into five stages. At stage 0, cancer does not grow beyond the inner layer of the colon or rectum. At stage I, cancer grows into the layers of the colon wall without spread outside wall itself. The stage II is subdivided into IIA, IIB and IIC based on spread of cancer. These cancers grow through the wall of colon or rectum and possibly into nearby tissue, but they are not yet spread to the lymph nodes. CRC at stage III is divided into three categories based on spread and how many lymph nodes are affected: IIIA, IIIB and IIIC. These cancers at stage III only spread to nearby lymph nodes, but they are not yet spread to other parts of the body. At stage IV, CRCs reach other organs in the body, forming metastasizes at to distant sites, such as liver or lungs. These types of cancers can also be divided into IVA and IVB. Adapted from: Terese Winslow, 2005.

CRC results from different combinations of genetic and epigenetic alterations such as DNA methylation and histone modifications (Kim *et al.*, 2012; Blanco-Calvo *et al.*, 2015; Setaffy and Langner, 2015; Xue, Lai and Wang, 2015; Gibson and Odze, 2016). This disease manifests through variable clinical scenarios and it has important divergences in response to treatment (Blanco-Calvo *et al.*, 2015; Gibson and Odze, 2016). This variability is shown through histopathological analysis and through genetic and biological heterogeneity between and inside tumors (Simmonds *et al.*, 2006; Blanco-Calvo *et al.*, 2015). However, histopathological analysis are being displaced in favor of more precise and multi-parametric molecular classifications (Blanco-Calvo *et al.*, 2015). Therefore, a molecular classification has been done to identify similar characteristics among individual tumors and to predict the pathogenesis and biological behavior of a particular tumor (Setaffy and Langner, 2015). So, currently CRC subtypes can be divided based upon combinations of genetic markers and histological subtypes (Hugen *et al.*, 2014; Setaffy and Langner, 2015; Tamas *et al.*, 2015).

1.1.3 Colorectal cancer subtypes according to genetic markers

I. Chromosomal instability

Chromosomal Instability (CIN) occurs in approximately two thirds of sporadic CRCs (Setaffy and Langner, 2015), but it is also present in the inherited condition familial adenomatous polyposis (FAP) (Setaffy and Langner, 2015; Tamas *et al.*, 2015). CIN is characterized by an accelerated rate of gains and losses of whole or large portions of chromosomes, resulting in chromosomal number imbalance and a higher frequency of loss of heterozygosity (Setaffy and Langner, 2015; Tamas *et al.*, 2015). Activating KRAS mutations are an important feature of sporadic CIN tumors (Tamas *et al.*, 2015).

II. Microsatellite instability

Microsatellites are short repetitive DNA nucleotide sequences, which have 1 to 6 base pair units scattered throughout the genome. These repetitive sequences are susceptible to frame shift mutations and base-repair substitutions during DNA replication due to their propensity to DNA strand slippage (Worthley and Leggett, 2010; Setaffy and Langner, 2015). Thus, microsatellite instability (MSI) is defined as a hypermutable phenotype caused by DNA deficient mismatch repair (MMR-D), deletions and insertions resulting in length change of repeating units (Davies, Miller and Coleman, 2005; Watson, 2007; Walther *et al.*, 2009; Worthley and Leggett, 2010; Setaffy and Langner, 2015; Tamas *et al.*, 2015). Big Adenine Tract 26 (BAT26) is the

microsatellite region altered in almost MMR-D CRCs (Davies, Miller and Coleman, 2005). MSI may be caused by inactivating germline mutations, such as Lynch syndrome, or by MutL homolog 1 (MLH1) promoter hypermethylation present in sporadic carcinomas (Walther *et al.*, 2009; Setaffy and Langner, 2015; Tamas *et al.*, 2015).

III. CpG island methylator phenotype (CIMP)

CpG islands are clusters of cytosine-guanosine residues, which are present in promoters of human genome. Hypermethylation in these CpG-rich promoters have been recognized as a common feature of human neoplasia, leading to transcriptional inactivation of tumor suppressor genes or of other tumor-related genes. Although hypermethylation can have different degrees, CIMP corresponds to the highest, which is characterized by “epigenetic instability” (Setaffy and Langner, 2015). The “classical” CRC CIMP markers are p16, *MINT1*, *MINT2*, *MINT31* and *hMLH1* (Kim *et al.*, 2012).

1.1.4 Colorectal carcinogenesis

In the 1980s researchers proposed a four-step progression of gene alterations in colonic epithelium that includes transformation of normal epithelium to an adenoma, then to carcinoma *in situ*, and ultimately to invasive and metastatic tumors (Pino and Chung, 2010; Liu, Jakubowski and Hunt, 2011; Armaghany *et al.*, 2012; Blanco-Calvo *et al.*, 2015) (**Figure 4**). This progression is the result of activating mutations of oncogenes coupled with inactivating mutations of tumor suppressor genes (Sancho, Batlle and Clevers, 2004; Armaghany *et al.*, 2012). These mutations can occur through both genetic and environmental factors, such as invasion by pathogens, toxins, stress conditions, polyamines and generation of reactive oxygen species (ROS) (Sancho, Batlle and Clevers, 2004; Armaghany *et al.*, 2012; Roper and Hung, 2013). These alterations can also be classified into deterministic and stochastic events. The deterministic events generate cell subtypes with phenotype and physiology similar to those found in normal tissue through variations in the transcriptional activity of genes. The stochastic events cause cell-to-cell heterogeneity by transcriptional noise or variations in the amount of signaling components (Blanco-Calvo *et al.*, 2015). Based on these events, Blanco-Calvo and co-workers investigated the alterations in different tumors and found that the majority are concentrated in a few signaling pathways (Blanco-Calvo *et al.*, 2015). While the Wnt pathway is the most affected one, the RAS-RAF-MEK-ERK-MAPK, TGF- β and PI3K pathways are others commonly altered pathways (Lee *et al.*, 2013; Blanco-Calvo *et al.*, 2015). In the altered Wnt pathway, the most commonly initiating event is the mutated adenomatous polyposis coli

(*APC*) gene (Sylvester and Vakiani, 2015). Activating mutations on RAS-RAF-MEK-ERK-MAPK pathway promote tumor growth and adenoma formation. Mutations in *TP53*, *SMAD4* genes or other components of TGF- β pathway lead to clonal expansion and transition from adenoma to invasive carcinoma (Sylvester and Vakiani, 2015). In the non-hypermethylated tumors, Blanco-Calvo and co-workers found primary mutations affecting the p53 pathway (Blanco-Calvo *et al.*, 2015). Furthermore, nearly all tumors showed alterations in the expression of MYC transcriptional targets (Blanco-Calvo *et al.*, 2015).

In fact, CRC carcinogenesis develops by two main pathways, the classical and the serrated pathways (**Figure 4**). The classical pathway, also known as the adenoma-carcinoma sequence, CIN or suppressor pathway, originates 80-90% of all CRCs (Yamane *et al.*, 2014; Setaffy and Langner, 2015; Gibson and Odze, 2016). This pathway is developed through a series of progressive mutations in several genes, such as *APC*, *KRAS*, *SMAD4* and *TP53*. Approximately 10-20 % of all CRCs are believed to arise from sessile serrated adenoma/polyp (SSA/P) precursor lesions via the serrated pathway. This pathway results from CIMP and it is characterized by *BRAF* mutations, MSI and MMR-D. Serrated pathway is mainly sporadic, however approximately 5% may arise from well-defined inherited syndromes, including Lynch syndrome, FAP, *MUTYH*-associated polyposis (MAP) and certain hamartomatous polyposis conditions (Bettington *et al.*, 2013; Norton *et al.*, 2015; Setaffy and Langner, 2015; Szyllberg *et al.*, 2015).

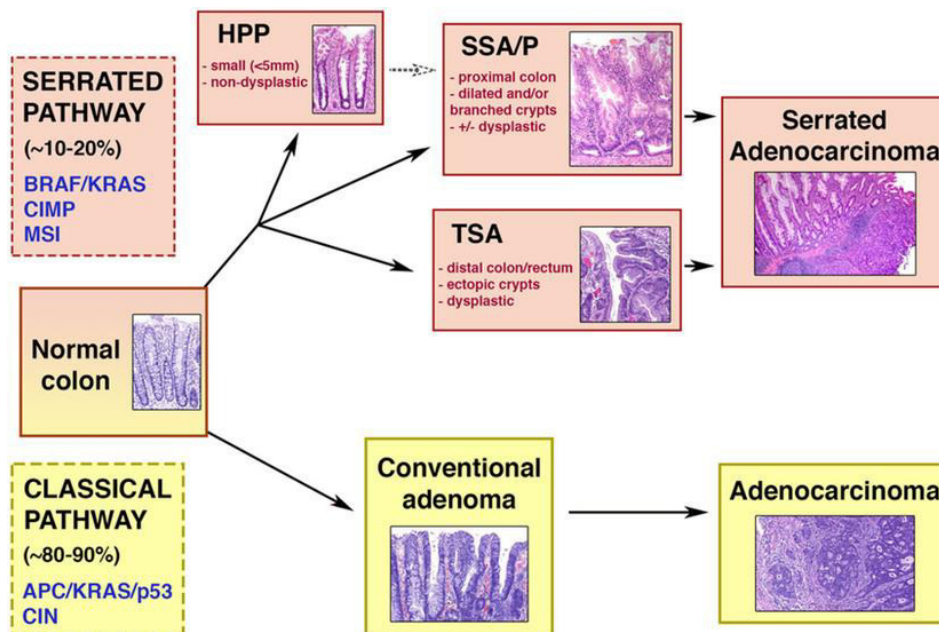


Figure 4 – Schematic representation of classical and serrated pathways of colorectal carcinogenesis and their relationship with histological states and genetic features.

Classical pathway also known as adenoma-carcinoma pathway is responsible for 80-90 % of CRCs. Serrated pathway account for 10-20 % of CRC. Serrated adenocarcinoma arises from hyperplastic polyps (HPP) and/or SSA/P or traditional serrated adenomas (TSA). Reproduced from: Baker *et al.*, 2015.

I. Classical pathway

The classical pathway is the most well characterized cancer progression pathway also known as CIN, traditional pathway or adenoma-carcinoma sequence (Yamane *et al.*, 2014; Setaffy and Langner, 2015). This pathway is frequently characterized by gains in chromosomes 8q, 13q and 20q and losses in the 1p, 8p, 17p and 18q chromosomal regions (Sylvester and Vakiani, 2015). Moreover, the resulting adenocarcinomas are microsatellite stable (MSS) and proficient mismatch repair (MMR-P) (Gibson and Odze, 2016). Conventional adenomas, which are associated with loss of APC and/or loss of chromosome 5q that includes the *APC* gene, are the main precursors of this pathway (Walther *et al.*, 2009; Pino and Chung, 2010; Smith *et al.*, 2010; Worthley and Leggett, 2010; Roper and Hung, 2013; Setaffy and Langner, 2015). Thus, APC is known as the “gatekeeper” of colonic carcinogenesis (Bennecke *et al.*, 2010). Normally, the binding of APC to β -catenin helps to suppress the Wnt signaling pathway, which regulates growth, apoptosis and differentiation (Worthley and Leggett, 2010). The loss of APC function leads to β -catenin cytoplasmic accumulation, which can translocate to the nucleus leading to Wnt signaling activation, driving cell proliferation (Pino and Chung, 2010; Gibson and Odze, 2016) and epithelial-to-mesenchymal transitions. This mutation also leads to additional mutations in tumor suppressors genes and oncogenes along the adenoma-carcinoma sequence, such as small GTPase KRAS, followed by loss of chromosome 18q with SMAD4 and mutations in the tumor suppressor protein p53 (TP53), and ultimately resulting in invasive cancers (Walther *et al.*, 2009; Bennecke *et al.*, 2010; Roper and Hung, 2013; Yamane *et al.*, 2014) (**Figure 5**). SMAD4 is involved in the TGF- β signaling pathway, which is important in regulating tumor growth and apoptosis (Worthley and Leggett, 2010). TP53 acts to increase the expression of cell-cycle genes to slow the cell cycle and to provide sufficient time for DNA repair (Worthley and Leggett, 2010). Although genetic alterations occurs according with this preferred sequence, the total accumulation of changes rather than their order is responsible for tumors biologic properties (Sancho, Batlle and Clevers, 2004).

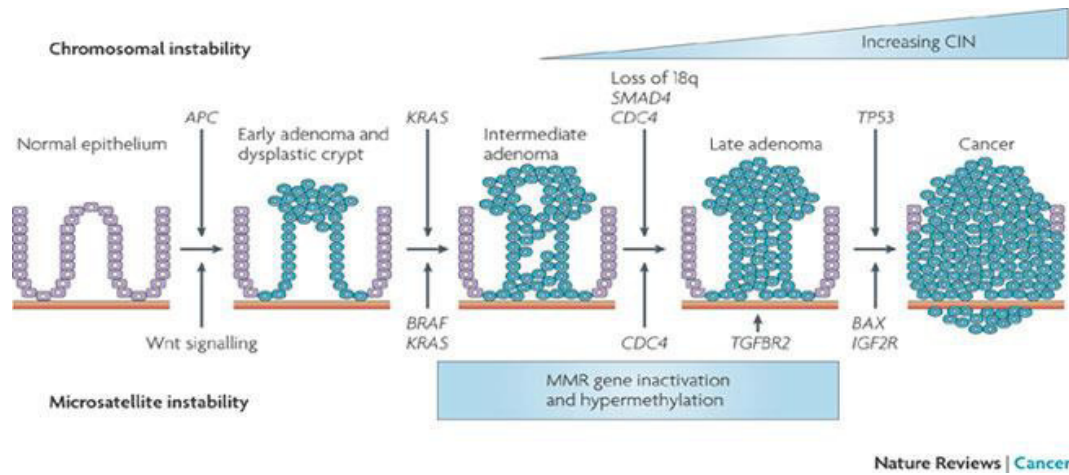


Figure 5 - Colorectal cancer carcinogenesis by chromosomal instability and microsatellite instability pathways.

CIN pathway is characterized by gains in chromosomes 8q, 13q and 20q and losses in the 1p, 8p, 17p and 18q chromosomal regions resulting APC loss and KRAS, SMAD4 and TP53 mutations. MSI pathway is characterized by BRAF or KRAS mutations, MSI and MMR-D. Reproduced from: Walther *et al.*, 2009.

II. Serrated pathway

Most serrated pathway related tumors develop sporadically and comprises a heterogeneous group ranging from hyperplastic polyps (HP), SSA/P, traditional serrated adenomas (TSA) and mixed polyps to serrated carcinoma (Watson, 2007; Bennecke *et al.*, 2010; Leggett and Whitehall, 2010; Worthley and Leggett, 2010; Bettington *et al.*, 2013; Szyllberg *et al.*, 2015). SSA/P develops by the accumulation of insertion or deletion mutations throughout the genome, leading to genomic instability and resulting in MSI and CIMP rather than CIN (Goldstein, 2006; Patai *et al.*, 2013; Sylvester and Vakiani, 2015). In this pathway, carcinoma progresses through malignant transformation of SSA/P precursor lesions. This pathway results from CIMP and it is characterized by *BRAF* or *KRAS* mutations, MSI and MMR-D (Goldstein, 2006; Watson, 2007; Bennecke *et al.*, 2010; Leggett and Whitehall, 2010; Bettington *et al.*, 2013; Kedrin and Gala, 2015; Gibson and Odze, 2016) (**Figure 5**). The activation of RAS-RAF-MEK-ERK-MAPK axis has been suggested as the initiating event of serrated carcinogenesis (Goldstein, 2006; Bennecke *et al.*, 2010).

The minor part of serrated pathway related tumors are not sporadic arising from well-defined inherited syndromes (Bettington *et al.*, 2013; Norton *et al.*, 2015; Setaffy and Langner, 2015; Szyllberg *et al.*, 2015). Two main syndromes caused by germline mutations play a role in the occurrence of CRCs. One of them is FAP, which is associated with mutated *APC* tumor suppressor gene. These patients develop tumors in distal colon in 60% of the cases and in the rectum in 25% of the cases. The other syndrome is Lynch syndrome also known as hereditary non-polyposis colorectal cancer (HNPCC), which results from inactivating mutations in DNA MMR genes, such as *MLH1* and *MutS homolog 2* (*MSH2*). These patients develop tumors in

the proximal colon in 55% of the cases and in the rectum in 15% of the cases (Tamas *et al.*, 2015).

1.1.5 The influence of diet in colorectal cancer

CRC can be both positively and negatively influenced by lifestyle and diet. Among the dietary factors, several plants have been reported as CRC protectors, while the higher intake of red meat is associated with enhanced CRC risk (Qi *et al.*, 2015). Diets with high content in fiber such as bread may reduce the risk of incident CRC, while very low intake of fibers may increase the risk (Qi *et al.*, 2015). Another protector factor documented is the regular long-term use of aspirin or non-steroidal anti-inflammatory drugs (NSAIDs), especially after 10 years of use (Wong *et al.*, 2015). Recently, proprionibacteria found in fiber-rich food and dairy products were also identified as a cancer prevention strategy. This bacteria produces short-chain fatty acids (SCFA), mainly propionate and acetate, which induce apoptosis of CRC cells (Marques *et al.*, 2013). Several studies about the relationship between meat consumption and incidence of CRC were published but the results are not in agreement (Chan *et al.*, 2011). Both significant and non-statistically significant increase in CRC risk were reported with increasing consumption of red meat and processed meat (Chan *et al.*, 2011; Richi *et al.*, 2015). Others recognized risk factors include age, obesity, diabetes, male gender, current smoking, history of colonic polyps or CRC, HNPCC, history of inflammatory bowel diseases, long-term insulin use in patients with type 2 diabetes, FAP, certain Asian ethnicities like Japanese, Koreans and Chinese, as well as unhealthy lifestyle habits such as excessive alcohol drinking and low fruit and vegetable intake (Itzkowitz and Yio, 2004; Wong *et al.*, 2015; Sakellariou *et al.*, 2016).

1.2 RAS superfamily

The RAS superfamily comprises five major families, classified according to their primary aminoacid sequence and functional similarities, and divided as RAS, RHO, ARF/SAR, RAN and RAB proteins (Wennerberg et al., 2005, Arozarena et al., 2011, Jančík et al., 2009, Ihle, 2012, Colicelli, 2010, Rojas et al., 2012) (**Figure 6**). The RAS family is involved in cell proliferation, gene expression, differentiation, migration and apoptosis (Ihle, 2012, Wittinghofer, 2014, Arrington et al., 2012b, Liu et al., 2016, Smith et al., 2010). The RHO is associated with cytoskeleton dynamics, gene expression, cell cycle progression, cell polarity and haematopoiesis (Rojas *et al.*, 2012; Vetter, 2014). RAB and ARF/SAR families regulate vesicular transport (Rojas *et al.*, 2012; Vetter, 2014). Finally, the RAN family determines the direction of nucleocytoplasmic transport and it is involved in mitotic spindle organization (Rojas et al., 2012, Wittinghofer, 2014). KRAS belongs to the oncoprotein RAS family that also includes NRAS and HRAS (Colicelli, 2004; Sancho, Batlle and Clevers, 2004; Jančík *et al.*, 2010; Krasinskas, 2011; Arrington *et al.*, 2012; Ihle, 2012; Phipps *et al.*, 2013).

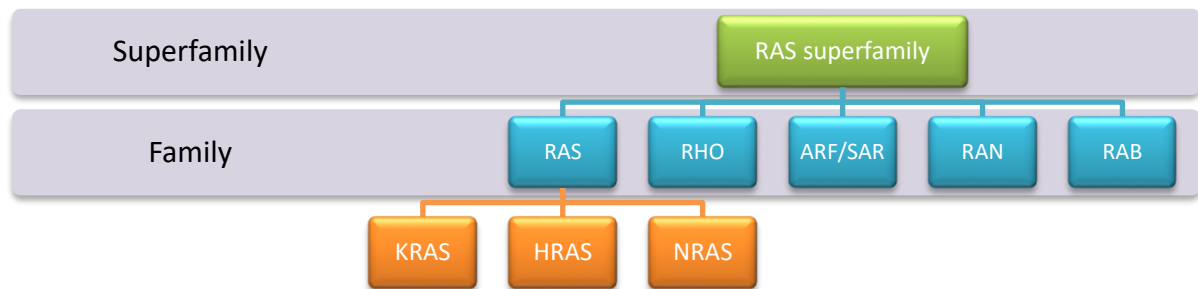


Figure 6 - RAS superfamily and their five branches RAS, RHO, ARF/SAR, RAN and RAB.

The Ras superfamily comprises five major families according to primary aminoacid sequence and functional similarities, and divided as RAS, RHO, ARF/SAR, RAN and RAB.

The RAS family is the most studied small GTPases, which share similarities to the heterotrimeric G proteins, but lack the presence of the G β and G γ subunits as additional regulators (Ihle, 2012, Jančík et al., 2009). Small GTPases belong to Guanine nucleotide-binding proteins (G proteins) that are transducers of extracellular stimuli and activate intracellular signaling cascades (Kratz *et al.*, 2006; Schubert, Shannon and Bollag, 2007).

RAS proteins exist in two forms, either bound to GDP (RAS-GDP) making them inactive or bound to GTP (RAS-GTP) switching to the active state and making them capable of engaging multiple effector proteins (Ihle, 2012; Tan and Du, 2012; Vetter, 2014) (**Figure 7**). RAS-GTP directly binds effectors, changes their conformation and creates an active state (Ihle, 2012; Vetter, 2014). This activation is caused by interaction of γ -phosphate of GTP with two switch

regions of RAS protein (threonine 35 and glycine 60), pulling them together into a “loaded spring” conformation. This conformation consists in a position that the switch regions are contorted in such a fashion that effector binding becomes favorable. Thus, RAS proteins can act on their own nucleotide, stimulating self-hydrolyze of their own GTP molecule to GDP, resulting in de-activation. However, this process needs to be amplified with additional regulatory proteins for appropriate physiological activity. These regulatory proteins are of two major types: the guanine-nucleotide exchange factors (GEFs) that activate GTPases by stimulating the release of guanine diphosphate (GDP) to allow binding to guanine triphosphate (GTP); and the GTPase-activating proteins (GAPs) that lead to GTPases de-activation by stimulation of GTP hydrolysis (Bos, Rehmann and Wittinghofer, 2007).

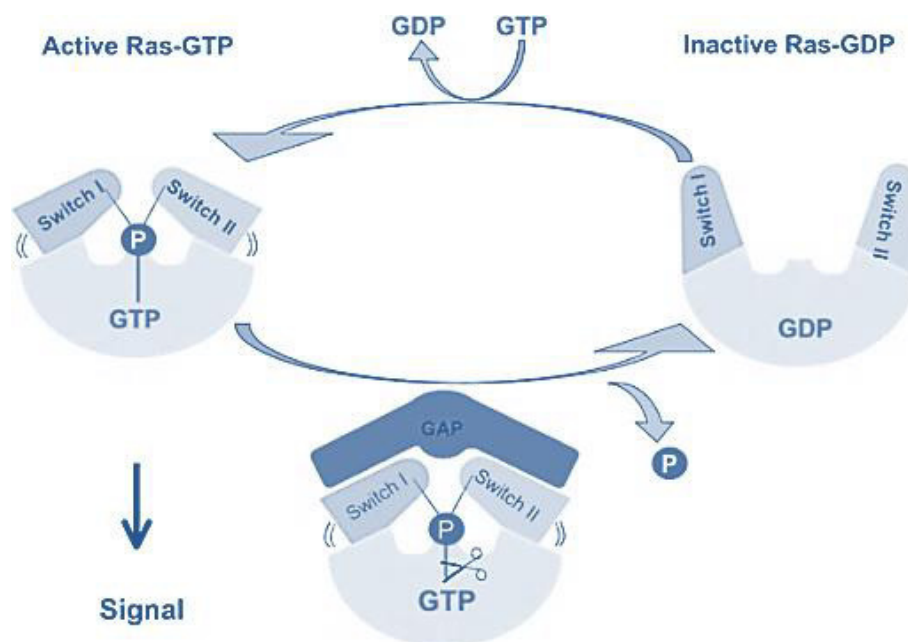


Figure 7 – Cycle of active Ras-GTP and inactive RAS-GDP.

RAS exists in two forms, either bound to GDP making them inactive or bound to GTP switching to the active state and making them capable of engaging multiple effector proteins. Adapted from: Kratz et al. 2006.

1.2.1 Ras proto-oncogenes

The “classical” RAS proto-oncogenes (Harvey (H-)RAS, Kirsten (K-) RAS and Neuroblastoma (N-) RAS are the most extensively studied from all RAS family members. RAS interest began with the discovery of Harvey and Kirsten rat sarcoma retroviruses in the 1960’s identified as viral genes transduced from the rodent genome and responsible for causing tumors in mice. Nevertheless, v-HRAS and v-KRAS intensive studied began after mutated activated forms of these genes had been identified in human cancer cell lines. However, it was only in 1983 that a third isoform NRAS was identified (Malumbres and Barbacid, 2003).

In humans, the three *RAS* genes encode four homologous proteins: HRAS, NRAS and KRAS4A and KRAS4B (Schubbert et al., 2007) (**Figure 8**). These RAS isoforms share 85-90% sequence homology in the G-domain and diverge mainly at the C-terminal, known as the hypervariable region (HVR). The G-domain contains G motifs which bind directly to GDP or GTP, such as switch I and II and the P-loop. The C-terminal differences are caused by post-translational modifications (PTMs) that specifically occur in a string of residues termed the HVR responsible for appropriate localization membrane interaction and cellular trafficking of the proteins (Rosseland, Wierod and Flinder, 2007; Ihle, 2012; Chen *et al.*, 2016). In fact, KRAS has a polybasic region required for plasma membrane localization, HRAS and NRAS are palmitoylated and, therefore, more likely to partition into lipid rafts (Simons and Toomre, 2000; Ahearn *et al.*, 2008). Recent studies suggest that activated KRAS is not a raft resident protein (Niv *et al.*, 2002).

KRAS4A and KRAS4B are protein products generated through alternative gene splicing of the fourth exon of the *KRAS* gene, which that determines the presence or absence of exon 4A. The common activating mutations occur in exons 1 or 2, so both splice variants are oncogenic. The alternative fourth exon encodes the HVRs responsible for membrane targeting. Thus, KRAS4A is palmitoylated, whereas KRAS4B is not, because it lacks a site of palmitoylation (Tsai *et al.*, 2015). For this reason, KRAS4A HVR shows higher sequence homology with NRAS (Tsai *et al.*, 2015). KRAS4A is expressed at low levels, but KRAS4B (hereafter referred to as KRAS) is ubiquitously expressed and accounts for 90-99% of all KRAS mRNA (Ihle, 2012, Wang et al., 2001).

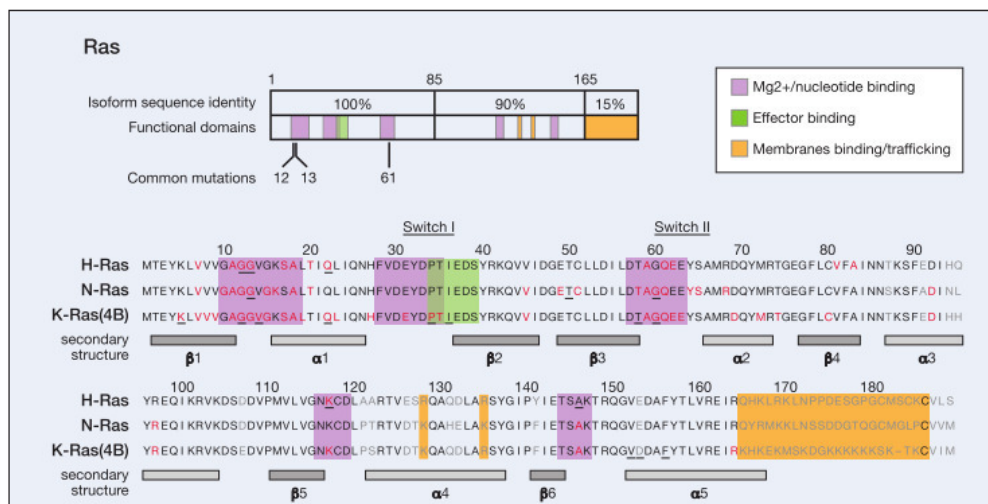


Figure 8 – HRAS, NRAS and KRAS proteins.

The three RAS proteins share approximately 85-90% sequence homology differing mainly at a C-terminus in a string of residues termed the HVR responsible for their appropriate localization (here represented as Membranes binding/trafficking). Reproduced from: Prior, Lewis, and Mattos 2012.

Despite their high homology, Ras proteins functions also differ significantly and do not display redundant functionality. This is particularly surprising since the regions of the proteins that interact with downstream effectors are identical between the three RAS isoforms (Prior and Hancock, 2012). Therefore, their specific roles may be explained by various others factors, such as cellular context, differential interaction with effectors, compartmentalized signaling and PTMs (Arozarena et al., 2011). HRAS, KRAS4A and NRAS are described as dispensable for normal development in mice. In contrast, KRAS4B knockout is embryonically lethal and thought to be caused by hematopoietic defects in result of a dysfunctional microenvironment in the fetal liver. Although these defects, many tissues undergo normal growth and differentiation, despite no compensatory increases in HRAS or NRAS protein expression being observed (Ihle, 2012). Thus, these homologous proteins, encoded by the three canonical members of the RAS gene family, act as central control elements in signal transduction pathways including proliferation, differentiation, apoptosis, survival, motility and adhesion, among many others (Fernandez-Medarde and Santos, 2011), being the impact of these genes on cellular homeostasis evident.

1.2.2 RAS signaling

RAS is involved in a complex signaling pathway, which is activated in response to growth factors (Figure 9). Growth factors bind to the extracellular domain of the receptor, leading to conformational changes and phosphorylation of tyrosine residues on its intracellular region. Such phosphorylation stimulates the binding of proteins containing SH2 domains, also known as adaptor proteins, to the phosphorylated tyrosine residues and activates GEFs. Grb2 is an adaptor molecule that binds directly or through binding to other adaptor proteins present on growth factor receptors such as IRS. Grb2 associates to Sos1, which is a GEF, activating the RAS-RAF-MEK-ERK-MAPK pathway (Fröjdö, Vidal and Pirola, 2009; Ihle, 2012). GEFs interact and activate RAS promoting dissociation of GDP and binding of GTP (Sancho, Battle and Clevers, 2004; Levy *et al.*, 2011; Knickelbein and Zhang, 2015). The RAS-GEF Cdc25 makes the connection between the adenylate cyclase and RAS pathway. Wild-type RAS molecules alternate between an inactive state, the Ras molecule bound to GDP, and an active state, the Ras molecule bound to GTP (Niv *et al.*, 1999). RAS in active state transduces intracellular signals through other GTPases and kinases, thus linking the presence of extracellular growth factors to intracellular signaling cascades. There are several downstream signaling proteins activated by KRAS. The first is RAF1, which is an activator of MEK-ERK

signal transduction, important for growth and development. The catalytic subunits of phosphatidylinositol 4,5 bisphosphate 3-kinase (PI3K) is another downstream signaling protein which is responsible for converting the membrane lipid PIP2 to PIP3 and subsequent plasma membrane recruitment of PIP3-binding pleckstrin homology domain proteins such as protein kinases AKT1 and PDK1. AKT plays an important role in growth and metabolism. RAS also binds to PLC ϵ 44, a phospholipase C isoform responsible for RAS mediated production of the membrane lipid diacylglycerol (DAG) which results in calcium release and activation of the PKC signaling cascade. Finally, RAS binds also to Tiam1 enzyme, involved in integrin signaling and plays an extensive role in T cell trafficking through its control of the chemokine and S1P response making it necessary for the mounting of an appropriate immune response. RASSF is another effector associated with apoptosis (44,45).

RAS also has an intrinsic GTPase activity removing the γ -phosphate of GTP to yields GDP, however this reaction is accelerated by p120 RAS-GAP enzyme that binds RAS enzymes and accelerates the rate of hydrolysis of GTP by 300 fold (Ihle, 2012; Knickelbein and Zhang, 2015). NF2 also act as a RAS-GAP, increasing the hydrolysis of GTP bound RAS (Ihle, 2012).

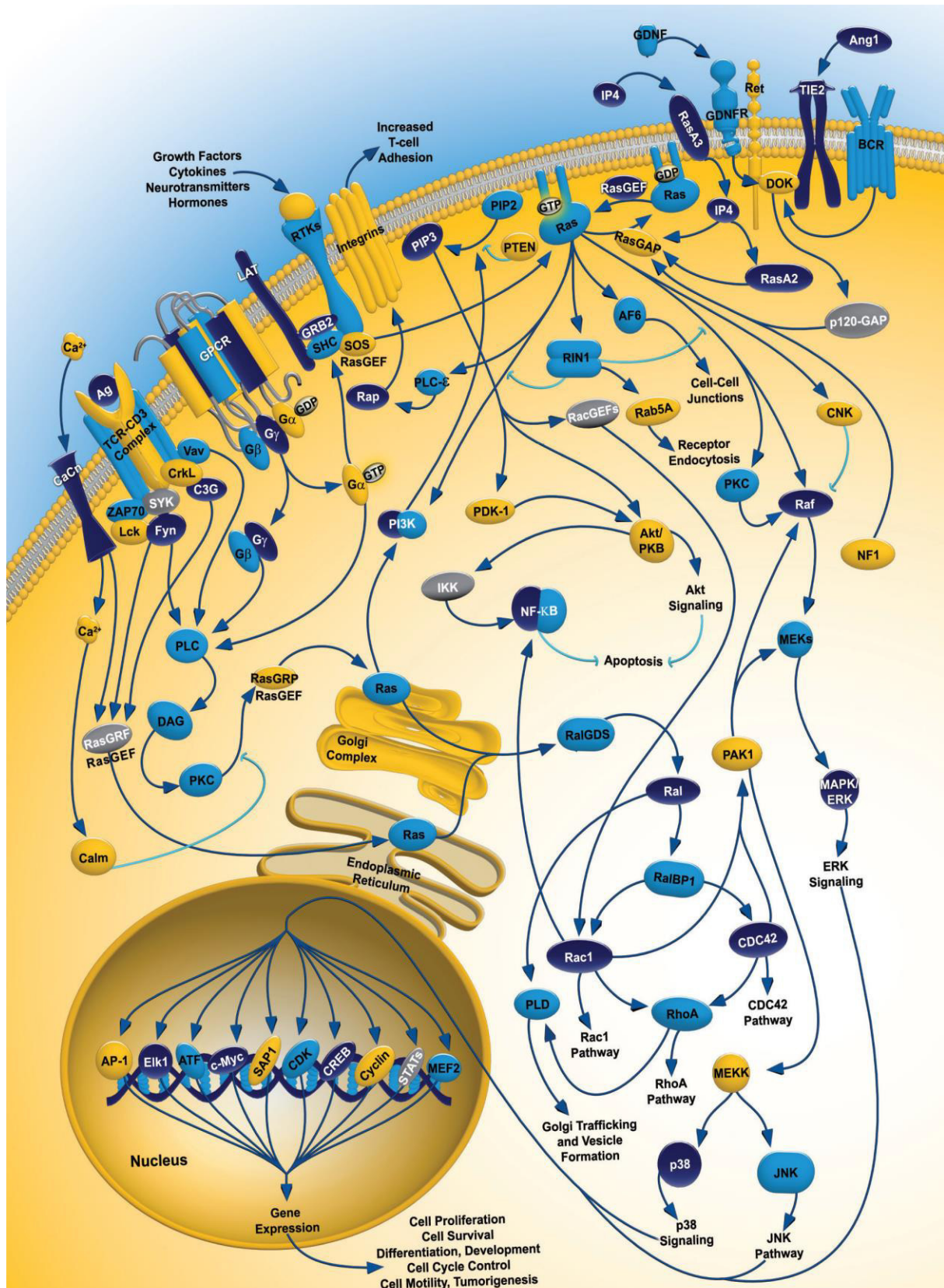


Figure 9 - Ras signaling pathway.

Ras signaling pathway is activated in response to growth factors, resulting in a cascade of events on cells. Reproduced from: Jančík et al., 2010.

1.2.3 The role of KRAS oncogene in cancer

The role of RAS proteins in carcinogenesis is well established and their RAS activating point mutations were reported in approximately 30% of all human cancers, with pancreas (60-90%), colon (30-50%) and lung (20-30%) cancers displaying the highest frequency (Downward, 2003, Forbes et al., 2011, Schubbert et al., 2007). *KRAS* mutations are common in pancreatic, colorectal, endometrial, biliary tract, lung and cervical cancers. *NRAS* mutations are more prevalent in myeloid leukemia and *HRAS* mutations predominate in bladder cancer (Forbes et al., 2011, Karnoub and Weinberg, 2008, Schubbert et al., 2007).

Activating mutations of *KRAS* occur mainly by substitutions in codons 12, 13 and 61, but substitutions at codon 12 are the most frequent. Thus, the most common mutations are *KRAS*^{G13D}, *KRAS*^{G12D} and *KRAS*^{G12V} (Niv et al., 2002; Nagasaka et al., 2004; Jančík et al., 2010; Pino and Chung, 2010; Smith et al., 2010; Krasinskas, 2011; Liu, Jakubowski and Hunt, 2011; Arrington et al., 2012; Ihle, 2012; Tan and Du, 2012; Roper and Hung, 2013). Glycine, which has not side chain, is the amino acid found at 12 and 13 positions in the wild type *KRAS* protein. The introduction of any side chain containing amino acid at these positions, with the exception of proline, leads to hyperactive *KRAS* enzyme, because glycine inhibit the formation of Van der Waals bonds between RAS-GAP and RAS, by disrupting the proper orientation of the catalytic glutamine for the γ -phosphate of GTP found at codon 61 (Ihle, 2012). These mutations result in insensitivity to RAS-GAP increasing time in the GTP bound state (Sancho, Batlle and Clevers, 2004; Pino and Chung, 2010; Worthley and Leggett, 2010; Krasinskas, 2011; Ihle, 2012; Bruera et al., 2013; Roper and Hung, 2013; Hammond et al., 2015). In another words, *KRAS* mutations lead to loss of intrinsic GTPase activity, prevent GAPs from promoting GTP hydrolysis resulting the constitutively activation of the RAS-RAF-MEK-ERK-MAPK pathway (Worthley and Leggett, 2010; Bettington et al., 2013; Hammond et al., 2015; Knickelbein and Zhang, 2015). Different amino acid substitutions activate different *KRAS* downstream signaling pathways as well as different clonogenic growth potential and responses to targeted therapies. It happens because different mutations influence the *KRAS*-effectors behavior (Ihle, 2012; Hammond et al., 2015). Codon 12 mutations increase aggressiveness by the differential regulation of *KRAS* downstream pathways that lead to inhibition of apoptosis, enhanced loss of contact inhibition and increased predisposition to anchorage-independent growth. Codon 13 mutations lead to reduced transforming capacity compared to codon 12 mutations (Bruera et al., 2013). Alternatively, codon 61 substitutions occur less frequently, activate *KRAS* through a similar mechanism indicating the essential nature of codon 61 in *KRAS* deactivation (Ihle,

2012). These constitutively active RAS proteins contribute to cell proliferation, suppression of apoptosis, altered cell metabolism and changes in the tumor microenvironment, which lead to tumorigenesis, tumor maintenance, invasion and metastasis (Levy *et al.*, 2010; Smith *et al.*, 2010; Bettington *et al.*, 2013; Knickelbein and Zhang, 2015). The GTP-bound KRAS increases cell proliferation by upregulation of growth and transcriptional factors, such as c-JUN and c-FOS. The activated KRAS suppresses apoptosis through its effector PI3K, which in turn activates AKT, a potent pro-survival kinase. AKT inhibits apoptosis by the inhibitory phosphorylation of the pro-apoptotic Bcl-2 family protein BAD, and the inhibitory phosphorylation of the initiator caspase-9 (Knickelbein and Zhang, 2015).

1.2.4 The role of KRAS oncogene in colorectal cancer

The *KRAS* mutation is a hallmark of cancer being a very frequent event in many cancers, including CRC (30-50 %). Oncogene *KRAS* activating mutations: *KRAS*^{G13D}, *KRAS*^{G12D} and *KRAS*^{G12V} are the most frequent *KRAS* mutations, being codon 12 the most frequently mutated (70%) followed by codon 13 (30%). These mutations are an early important event in colon carcinogenesis and they are well conserved between primary tumor and corresponding metastases (Akande *et al.*, 1998; Krasinskas, 2011; Reinacher-Schick *et al.*, 2012; Bettington *et al.*, 2013; Alves *et al.*, 2015). *KRAS* mutations have also been associated with poor overall survival and increased tumor aggressiveness (Arrington *et al.*, 2012b).

Cell lines harbouring RAS mutations, such as CRC cells, have high levels of autophagy, which is an evolutionary conserved catabolic process that targets cellular components for lysosomal degradation to maintain cellular homeostasis (Alves *et al.*, 2015). Alves and co-workers (Alves *et al.*, 2015) found that expression of activating *KRAS* mutations increases Atg8p levels, which is an autophagic marker (Alves *et al.*, 2015). *KRAS*-induced autophagy is mediated through upregulation of the RAS-RAF-MEK-ERK-MAPK pathway and downregulation of the PI3K/AKT pathway, known to activate the autophagy inhibitor mTOR (Alves *et al.*, 2015). Both pathways are commonly deregulated in CRC (Alves *et al.*, 2015). They also demonstrated that *KRAS*-induced autophagy supports the survival of CRC-derived cells exposed to stressful conditions like nutrients limitation (Alves *et al.*, 2015). Moreover, autophagy is an issue to be concerned because this process is implicated as a potential mechanism of resistance to anticancer agents, as it aids in the response of tumor cells to cellular stress and/or increased metabolic demands (Alves *et al.*, 2015). Therefore, inhibition of *KRAS* or autophagy could be a promising therapeutic strategy for CRC cells harbouring *KRAS* mutations (Alves *et al.*, 2015).

Not only KRAS, but also KRAS downstream effectors can be deregulated in CRC (Malumbres and Barbacid, 2003). *BRAF* mutations is seen in 10% of CRC (Barras, 2015) and mutated *BRAF*^{V600E} is characterized by a highly transforming and oncogenic activity comparing with *BRAF*^{WT} (Oliveira *et al.*, 2007). Mutations of *PI3K*, an KRAS effector, are also frequently found in approximately 40% of CRCs (Parsons *et al.*, 2005). These mutations are responsible for a high ability of cell proliferation and survival under environmental stress and confer apoptosis resistance and metastatic potential (Parsons *et al.*, 2005). Furthermore, *PI3K* mutations co-occur frequently with other mutations, such *KRAS* or *BRAF*, suggesting a synergic effect for an efficient malignant transformation (Velho *et al.*, 2005). *AKT* mutations or up-regulations as also *PTEN* tumor suppressor gene loss or down-regulation are seen in disease playing an essential role in CRC progression (Danielsen *et al.*, 2015).

Overall, *KRAS* and its downstream effectors have been associated with CRC progression, being therefore attractive targets for CRC therapy.

1.2.5 KRAS dimers and multimers

RAS dimers and higher order protein clusters have been studied through the years. It is believed that RAS nanoclusters may act as signaling platforms increasing signal output and enhancing cooperativity with effectors, such as RAF and MAPK (Muratcioglu *et al.*, 2015; Chen *et al.*, 2016). Moreover, nanoclusters could also restrict binding events, avert redundant signaling and prevent external stimuli from causing repetitive cellular firing (Muratcioglu *et al.*, 2015).

Muratcioglu and co-workers (Muratcioglu *et al.*, 2015) evaluate the oligomerization state of KRAS G-domain by dynamic light scattering (DLS). KRAS4B₁₋₁₆₆-GDP analysis showed predominant species of 18 kDa molecular mass, which corresponds to a G-domain monomer. However, KRAS4B₁₋₁₆₆-GTP- γ -S corresponds to a globular protein with a molecular mass of 41 kDa (Muratcioglu *et al.*, 2015). High-resolution mass spectrometry was also performed to confirm the absence of a covalent dimer that could be formed through oxidation of cysteine residues. The resulting data suggest that KRAS4B₁₋₁₆₆-GTP- γ -S forms stable non-covalent dimers, while KRAS4B₁₋₁₆₆-GDP may have a reduced tendency to self-associate. Thus, Muratcioglu and co-workers (Muratcioglu *et al.*, 2015) demonstrate that GTP-bound, but not GDP-bound KRAS4B catalytic domain can form stable homodimers.

Furthermore, modelling results of Muratcioglu and co-workers (Muratcioglu *et al.*, 2015) also suggest that both KRAS4B₁₋₁₈₀ GTP- and GDP-bound states can form homodimers through the same interface, although KRAS4B-GTP form more stable homodimers.

Moreover, it is thought that galectin interferes in tetramerization driven by farnesylated KRAS4B on the inner plasma membrane which confers higher specificity and cellular control.

1.2.5.1 KRAS dimers and RAS-RAF-MAPK signaling axis

It was demonstrated that monomeric RAS can bind to RAF protein, however, the normal RAF activation requires its dimerization, which can be promoted by RAS proteins (Muratcioglu *et al.*, 2015). Recently, it was observed that c-RAF forms dimers, trimers, and tetramers in the presence of RAS-GTP, suggesting that RAS plays a significant role in RAF dimerization. All three RAS isoforms, HRAS, NRAS, and KRAS activate RAF at variable degrees, being however KRAS the most potent activator.

The MAPK is also activate by RAS-GTP dimers (Nana *et al.*, 2015). Nana and co-workers (Nana *et al.*, 2015) demonstrate that at endogenous expression levels KRAS^{G12D} forms dimers, and that at higher expression levels, KRAS^{G12D} forms RAS protein clusters. Both activates MAPK. However, at lower expression levels, KRAS^{G12D} turns monomeric and the activation of MAPK only occur when KRAS is artificially dimerized (Nana *et al.*, 2015).

1.3 Galectins

Galectins are a family of 15 mammalian galactoside-binding proteins, which share a consensus amino acid sequence in their carbohydrate recognition domains (CRDs). They are divided into three types according to structural differences: the prototype, chimera-type and tandem-repeat type (**Figure 10**). The prototype or mono-CRD galectins, which contain a single CRD in their polypeptide sequence, include the galectins 1, 2, 5, 7, 10, 11, 13, 14, and 15. These galectins can be active as monomers or homodimers, as result from non-covalent ligation between monomers. The chimera-type galectins are composed by galectin-3, which has a non-lectin domain linked to a C-terminal CRD. This type of galectins can form oligomers, more specifically pentamers. The tandem-repeat type or bi-CRD galectins are characterized by galectins with two distinct CRDs and include galectins 4, 6, 8, 9, and 12 (Barrow, Rhodes and Yu, 2011; Johannes, Wunder and Shafaq-Zadah, 2016).

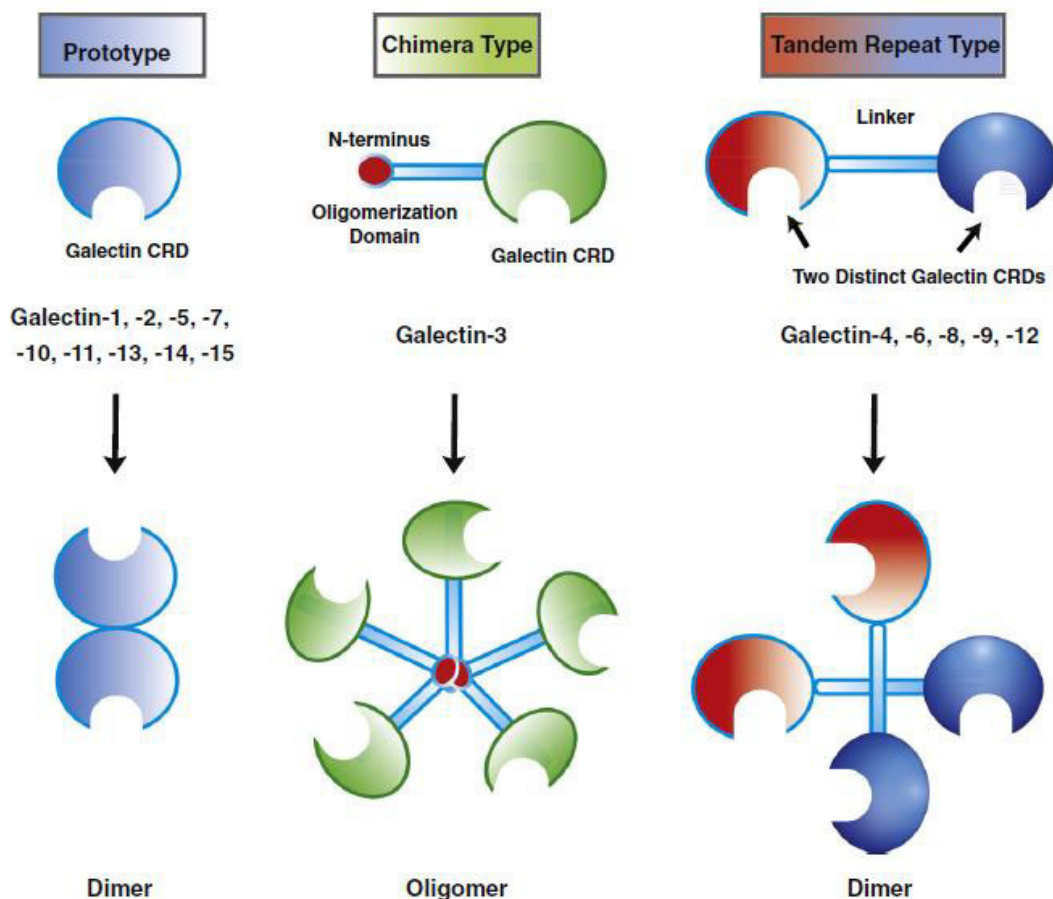


Figure 10 – The family of 15 mammalian galactoside-binding proteins divided in prototype, chimera-type and tandem-repeat type subgroups according to structural differences.

The prototype galectins are constituted by one CRD domain and include galectins 1, 2, 5, 7, 10, 11, 13, 14, and 15. This type of galectins can be active as monomers or homodimers. The chimera-type galectins are composed by a CRD domain and a collagen-like domain. This chimera-type is composed by Galectin-3, which can form pentamers. The tandem-repeat type has two distinct CRD domains linked to each other. This type of galectins is composed by galectins 4, 6, 8, 9, and 12. Reproduced from: Johannes, Wunder and Shafaq-Zadah, 2016.

Galectins are widely expressed in human tissues being found in various intracellular compartments (Barrow, Rhodes and Yu, 2011). Moreover, all galectins are multifunctional proteins involved in cell adhesion, migration, differentiation, angiogenesis, proliferation, mRNA splicing and apoptosis (Hill *et al.*, 2010; Barrow *et al.*, 2011). The study of their functions in cancer is a challenge, because galectins can either have pro- or anti-tumoral properties depending on cancer type (**Figure 11**). It can be explained by their large diversity of binding partners (Vladoiu, Labrie and St-Pierre, 2014). However, these dual functionalities have also been reported due to distinct compartmentalization of galectins within cells. It means that galectins can have different functions depending on their localization within the cell, which differs between cell type and tumor stage (Vladoiu, Labrie and St-Pierre, 2014). Galectins 1, 3, 4 and 8 are expressed in human colon and rectum and exhibit significant alterations in their expression levels during the tumorigenesis process (Barrow, Rhodes and Yu, 2011). These significant alterations are correlated with pro- and anti-tumor functions in cancer cell apoptosis, adhesion, migration, cell transformation, tumor growth, angiogenesis, immune escape, invasion and metastasis (Barrow, Rhodes and Yu, 2011; Vladoiu, Labrie and St-Pierre, 2014) (**Figure 11**).

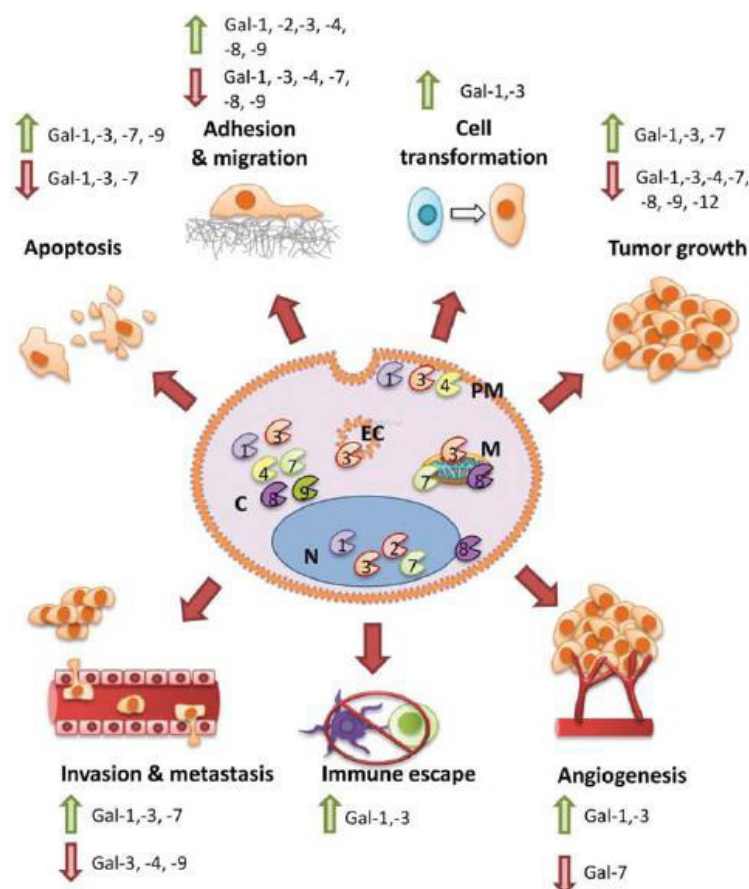


Figure 11 – Localization and functions of multifunctional galectins on cancer.

Galectins are multifunctional proteins with pro- and anti-tumor functions in many features of tumor progression such as apoptosis, adhesion, migration, cell transformation, tumor growth, angiogenesis, immune escape, invasion and metastasis. Galectins can be found at the nucleus (N), cytoplasm (C), inner plasma membrane (PM), endosomal compartments (EC) and mitochondria (M). Reproduced from: Vladoiu, Labrie and St-Pierre, 2014.

1.3.1 Galectin-3

Gal-3 is one of the most extensively studied galectins and is widely expressed in the human gastrointestinal tract including colon and rectum (Hill *et al.*, 2010; Yu, 2010; Barrow, Rhodes and Yu, 2011; Wu *et al.*, 2012; Korkmaz *et al.*, 2016; Suthahar *et al.*, 2018). Gal-3 was firstly described as Mac-2 antigen on the surface of murine macrophages, but it is also known as Carbohydrate-bunding protein 30 (CBP-30), Carbohydrate-bunding protein 35 (CBP-35) and IgE-bunding protein (IgEBP) (Newlaczyl and Yu, 2011).

Gal-3 is a small protein with molecular weight of 29-35 kDa encoded by *LGALS3* gene, also known as *MAC2* (Hill *et al.*, 2010; Yu, 2010; Wu *et al.*, 2012; Korkmaz *et al.*, 2016). It is composed by three distinct structural domains: (1) a N-terminal domain composed by 12 amino acids that controls its cellular targeting and it is essential for Gal-3 homo-dimerization, (2) a C-terminal domain formed by β -sheet layers and composed by a single CRD and (3) a repetitive collagen-like sequence rich in glycine, tyrosine, and proline, which links the other two domains and acts as a substrate for matrix metalloproteinases (MMPs) (Mazurek *et al.*, 2012) (**Figure 12**). Interestingly, Gal-3 contains the NWGR amino acid motif, which is a highly conserved sequence within the BH1 domain of Bcl-2 family proteins (Shalom-FFF, 2005).

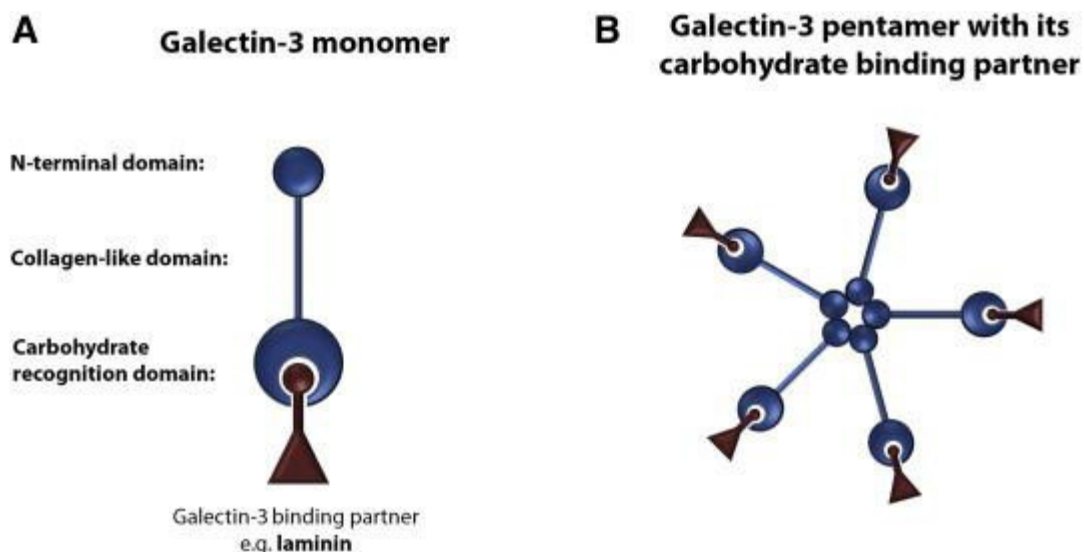


Figure 12 – Galectin-3 monomer and pentamer representation focusing their structural domains.

(A) Gal-3 monomer and its distinct structural domains: (1) N-terminal domain, (2) C-terminal carbohydrate recognition domain (CRD) and (3) repetitive collagen-like domain. (B) Gal-3 pentamer representation illustrating the main functions of each domain. N-terminal domain is essential for homo-dimerization, C-terminal is the CRD and the collagen-like domain links the N- to the C-terminus. Reproduced from: Filipe *et al.*, 2015.

Gal-3 is a multifunctional protein that interacts with distinct molecules, playing a variety of different roles (Hittelet *et al.*, 2003; Shi *et al.*, 2007; Hill *et al.*, 2010; Korkmaz *et al.*, 2016). Interestingly, Gal-3 functions depend on its subcellular localization (Hill *et al.*, 2010). Gal-3

can be expressed in the nucleus, cytoplasm as well as on cell surface and be release into the surrounding extracellular matrix (Hill *et al.*, 2010; Barrow *et al.*, 2011; Chen *et al.*, 2013). In the nucleus, Gal-3 localizes in the dense fibrillar network of the nucleolus, as well as the periphery of the fibrillar centers (Barrow, Rhodes and Yu, 2011). Gal-3 has also been found in the interchromatic spaces and along the borders of condensed chromatin of the nucleoplasm, where pre-mRNA synthesis and splicing occurs (Barrow, Rhodes and Yu, 2011). Moreover, in the nucleus, Gal-3 promotes pre-mRNA splicing promoter, has a pro-apoptotic activity, and probably regulates, at the transcriptional levels, the gene expression of cyclin D1, cAMP responsive element binding (CREB), the nuclear factor SP1 and Thyroid transcription factor-1 (TTF-1) (Hill *et al.*, 2010; Yu, 2010; Barrow *et al.*, 2011; Barrow, Rhodes and Yu, 2011). Extracellular Gal-3 mediates cell migration, adhesion and cell to cell interactions (Hill *et al.*, 2010). Cytoplasmic Gal-3 interacts with anti-apoptotic BCL-2, synexin (annexin VII), β -catenin and oncogenic KRAS,, regulating apoptosis by suppressing mitochondrial depolarization and preventing the release of cytochrome c (Hill *et al.*, 2010; Yu, 2010; Barrow *et al.*, 2011; Dawson, André and Karamitopoulou, 2013). The cell surface-associated galectins promote cell to cell and cell to matrix interactions and facilitate cancer progression and metastasis (Barrow *et al.*, 2011; Chen *et al.*, 2013).

1.3.2 The role of galectin-3 in cancer

Gal-3 has been shown to promote tumor angiogenesis by interaction with aminopeptidase N/CD13 (APN), an endothelial cell surface enzyme and by influencing the function of vascular endothelial growth factor (VEGF) and of basic fibroblast growth factor (bFGF) (Barrow, Rhodes and Yu, 2011). More specifically, Gal-3 binds to $\alpha\beta 3$ integrin on the endothelial cell surface, inducing integrin clustering followed by activation of focal adhesion kinase and VEGF and bFGF-mediated endothelial migration and vessel branching. Thus, Gal-3 can influence tumor angiogenesis by interactions with several endothelial cell surface receptors (Barrow, Rhodes and Yu, 2011).

Gal-3 has a dual conversely effect on apoptosis (**Figure 13**)Figure 13. Gal-3 prevents apoptosis due to a functional anti-death NWGR motif in its amino acid sequence, which is conserved in the BH1 domain of the Bcl2 gene family (Barrow, Rhodes and Yu, 2011). Before apoptosis stimulation, the intracellular Gal-3 interacts with Bcl-2 and synexin and translocates to the mitochondrial membrane at the peri-nuclear region where it prevents mitochondrial depolarization and cytochrome c release. This galectin can also complex with CD95/Fas

Receptor, inhibiting CD95/Fas-mediated caspase-8 activation and apoptosis (Barrow, Rhodes and Yu, 2011). Its anti-apoptotic role is regulated by the phosphorylation/dephosphorylation status of its Ser-6 residue, which acts as an “on/off” switch in regulating the binding of Gal-3 to its ligands (Barrow, Rhodes and Yu, 2011). Thus, mutations at Ser-6 residue, such as the substitution of this residue by Ala decrease the anti-apoptotic activity of Gal-3 (Barrow, Rhodes and Yu, 2011). Interestingly, exogenous Gal-3 promotes apoptosis by ligation to the cell surface CD29 (integrin β 1)/CD7 complex and triggers mitochondrial release of cytochrome c and caspase-3 activation (Barrow, Rhodes and Yu, 2011). Interestingly, is a cluster of differentiation marker that identifies multiple CD8 T cell effector subsets. Other studies demonstrate that Gal-3 inhibits apoptosis through binding to tumor necrosis factor-related apoptosis-inducing ligand (TRAIL) (Korkmaz *et al.*, 2016).

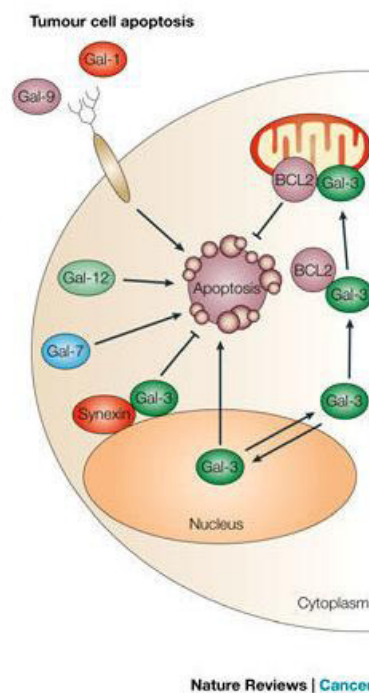


Figure 13 - Effects of galectin-3 on tumor cell apoptosis.

Gal-3 has a dual conversely effect on apoptosis process. Gal-3 prevents apoptosis due to a NWGR motif, which is conserved in the BH1 domain of the Bcl2 gene family. Before apoptosis stimulation, the intracellular Gal-3 interacts with Bcl-2 and synexin and translocates to the mitochondrial membrane at the peri-nuclear region where prevents mitochondrial depolarization and cytochrome c release. Its anti-apoptotic role is regulated by the phosphorylation/dephosphorylation status of its Ser-6 residue, which acts as an “on/off” switch in regulating the binding of Gal-3 to its ligands. Adapted from: Liu and Rabinovich, 2005.

Gal-3 also induces secretion of several metastasis-promoting cytokines such as Interleukin 6 (IL-6), Granulocyte colony-stimulating factor (G-CSF), soluble intercellular adhesion molecule-1 (sICAM-1) and Granulocyte-macrophage colony-stimulating factor (GM-CSF)

from blood vascular endothelial cells in vitro and in mice enhancing metastasis. These cytokines autocrinely or paracrinely interact with the vascular endothelium increasing the expression of the endothelial cell surface adhesion molecules integrin α v β 1, E-selectin, Intercellular Adhesion Molecule 1 (ICAM-1) and Vascular cell adhesion molecule 1 (VCAM-1), resulting in increased cancer cell-endothelial cell adhesion, endothelial cell migration and tubule formation. Recently, Chen and co-workers (Chen *et al.*, 2013) demonstrated that the increased circulation of Gal-3 in cancer promotes cancer metastasis in an animal model. This effect is partly attributed to its interaction with oncofetal Thomsen-Friedenreich carbohydrate (Gal β 1,3GalNAc α -, TF) antigen on the transmembrane mucin protein (MUC1) expressed by cancer cells. The Gal-3-TF/MUC1 interaction induces MUC1 cell surface polarization, exposure of adhesion molecules, increased tumor cell heterotypic adhesion to blood vascular endothelium and increased tumor cell homotypic aggregation in the circulation (Chen *et al.*, 2013). Thus, Gal-3 is now being explored as a promising target for therapeutic strategies to prevent metastasis.

1.3.3 The role of galectin-3 in colorectal cancer

Loss of nuclear Gal-3 and its cytoplasm accumulation are commonly seen in many types of human cancers, including CRC. Gal-3 is also significantly increased in the sera of patients with CRC. These accumulations are correlated with cancer cell survival caused by apoptosis inhibition, cancer cell invasion, and tumor angiogenesis (Hittelet *et al.*, 2003; Yu, 2010, 2014; Barrow, Rhodes and Yu, 2011; Chen *et al.*, 2013; Korkmaz *et al.*, 2016). Recently, Gal-3 has also been associated with carcinogenesis, cancer progression and metastasis by interaction with various galactoside-terminated cell surface glycans (Hill *et al.*, 2010; Yu, 2014).

Gal-3 regulates metastasis by binding to cell adhesion-related molecules and by inhibiting cell-cell and cell-matrix interactions, promoting cancer cell detachment and mobility (Barrow, Rhodes and Yu, 2011; Wu *et al.*, 2012). Wu and co-workers tested Gal-3 expression effects on colon cancer cells migration, in particular in: Caco-2 and DLD-1 cells (Wu *et al.*, 2012). They concluded that Caco-2 cells express more Gal-3 than DLD-1, which apparently reflects in a faster migration pattern of Caco-2 against DLD-1 cells, as demonstrated by wound-healing assay. They also evidenced that knockdown of Gal-3 expression significantly decreased the cell migration rate, while the overexpression of Gal-3 increases significantly the rate of cell migration. Wu and co-workers also demonstrated the relation between Gal-3 and enhanced cancer cell invasion, usually correlated with lamellipodia formation, evident membrane

protrusions at the leading edge of actively migrating cells (Wu *et al.*, 2012). Altogether, this suggests that cells overexpressing Gal-3 exhibit higher adhesion, migration, invasion and metastatic potential. They also evaluated the p-RAF, pERK1/2, p38 expression levels, and JNK MAPK action, to determine the mechanisms underlying Gal-3-induced DLD-1 cell migration. They concluded that cell lines overexpressing Gal-3 had higher levels of pRAF and pERK1/2 and non-affected levels of p38 and JNK MAPK activation. Interestingly, the silencing of KRAS by RNAi also decreases the migration rate, particularly in cell lines overexpressing Gal-3. Therefore, a possible and undiscovered relation between Gal-3 and KRAS can be considered. Moreover, extracellular Gal-3 is known to modulate each phase of metastasis in human colon cancer. Additionally, higher Gal-3 expression levels in colon cancer patients are associated with an increased risk of metastasis and it has been suggested to be a useful prognostic marker (Barrow, Rhodes and Yu, 2011). However it remains unclear how Gal-3 affects colon cancer cells intracellular signaling, migration and metastasis potential (Wu *et al.*, 2012).

Gal-3 has also been reported as involved in the Wnt pathway. In CRC, Gal-3 is described to upregulate β -catenin expression, to bind to β -catenin and to promote its translocation into the nucleus. At the same time, Gal-3 augments Wnt pathway in CRC by regulating glycogen synthase kinase-3 β (GSK-3 β) phosphorylation and activity, via the PI3K/AKT pathway (Shi *et al.*, 2007; Lee *et al.*, 2013; Korkmaz *et al.*, 2016). Gal-3 also regulates various pathways to activate Multidrug resistance (MDR) mechanism (Lee *et al.*, 2013). Thus, Gal-3 inhibition via RNA interference (RNAi) is being explored as a potential to overcome resistance to some anticancer drugs (Lee *et al.*, 2013). The Gal-3 RNAi treatment induces apoptosis, as demonstrated by chromatin condensation, a higher sub-G1 phase proportion and increased caspase-3 and caspase-9 activity, indicating a mitochondrial apoptosis pathway.

1.4 p16^{INK4a}

p16^{INK4a} also known as cyclin-dependent kinase inhibitor 2A (*CDKN2A*), cyclin-dependent kinase 4 inhibitor A (CDK4I) and multiple tumor suppressor 1 (*MTS-1*) is one of the most commonly studied proteins in the pathogenesis of human neoplasia. It is one of the most direct links between cell-cycle control and cancer (Serrano, 1997; Ortega, Malumbres and Barbacid, 2002). This protein belongs to the INK4A/ARF family of suppressors of CDKs and is the founder member of a family of proteins that inhibit CDK4 and CDK4-related kinase CDK6 (Serrano, 1997). The other members of this family are p15^{INK4b}, p18^{INK4c} and p19^{INK4d}, which are also tumor suppressor proteins (Serrano, 1997; Zhang, Rosen and Yao, 2006). These proteins have similar biochemical properties linking to CDK4 and CDK6 and inhibiting the activity of the CDK4-6 with D-type cyclins complex (Serrano, 1997; Zhang, Rosen and Yao, 2006).

p16^{INK4a} is encoded by *CDKN2*, *CDKN2A*, *INK4b/ARF/INK4a locus* or *MTS-1*, which is the gene localized on chromosome 9p21 (Gorgoulis, Koutroumbi and Kotsinas, 1998; Yoruker, Mert and Bugra, 2012; Bagci *et al.*, 2016). Interestingly, this gene encodes three important tumor suppressor proteins p14^{ARF}, p15^{INK4b}, and p16^{INK4a} (**Figure 14, Figure 15A**). Comparing to p16^{INK4a}, P14^{ARF} is translated in alternative reading frame (ARF) sharing the exon 2 and 3 and differing in exon 1. INK4a and ARF are transcribed independently, because each one has its own independent promoters. On its turn, p15^{INK4b} have its own independent structure (Popov and Gil, 2010).

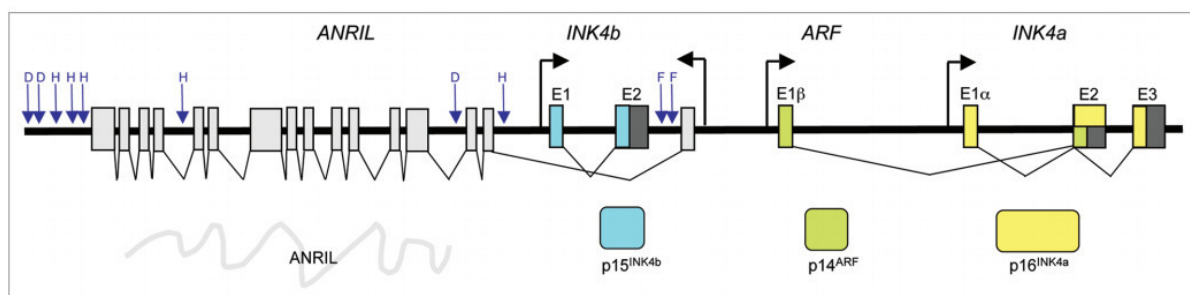


Figure 14 – INK4b/ARF/INK4a locus on chromosome 9p21.

INK4b/ARF/INK4a locus encodes p14^{ARF}, p15^{INK4b}, and p16^{INK4a}. p16^{INK4a} and p14^{ARF} are translated in alternative reading frame sharing the exon 2 and 3 (not represented) and differing in exon 1. P15^{INK4b} have its own independent structure. Reproduced from: Popov and Gil, 2010.

p16^{INK4a} is a G1 CDK inhibitor that regulates the cell cycle negatively competing with cyclin-D for binding to CDK4, which in turn inhibits the formation of enzymatically active complexes CDK4-6/cycD within the cell cytoplasm (**Figure 15b**). Thus, p16^{INK4a} obstructs the ability of CDK4-6 to phosphorylate retinoblastoma protein (pRb). Preserving the hypophosphorylated

state of retinoblastoma protein, the cell cycle progression is blocked by inhibition of dissociation of pRb-E2F complex resulting in G1 arrest before the entry into the S-phase. At the same time, hypophosphorylated active pRb can repress p16 expression, whereas inactivation of pRb by phosphorylation leads to p16^{INK4a} expression. Therefore, p16^{INK4a} expression triggers cellular senescence through activation of retinoblastoma tumor suppressor (Romagosa *et al.*, 2011; Kim *et al.*, 2012; Yoruker, Mert and Bugra, 2012; McLaughlin-Drubin, Park and Munger, 2013; X. Zhang *et al.*, 2013; Shi, Wang and Xia, 2016). P15^{INK4b} also as p16^{INK4a} is an inhibitor of CDKs, promoting G1 arrest by preventing phosphorylation of pRb. p14^{ARF} is an indirect regulator of p53. Accordingly, p14^{ARF} inhibits MDM2 by its sequestration to the nucleus, which in turn activates p53 promoting cell-cycle arrest or apoptosis (**Figure 15c**).

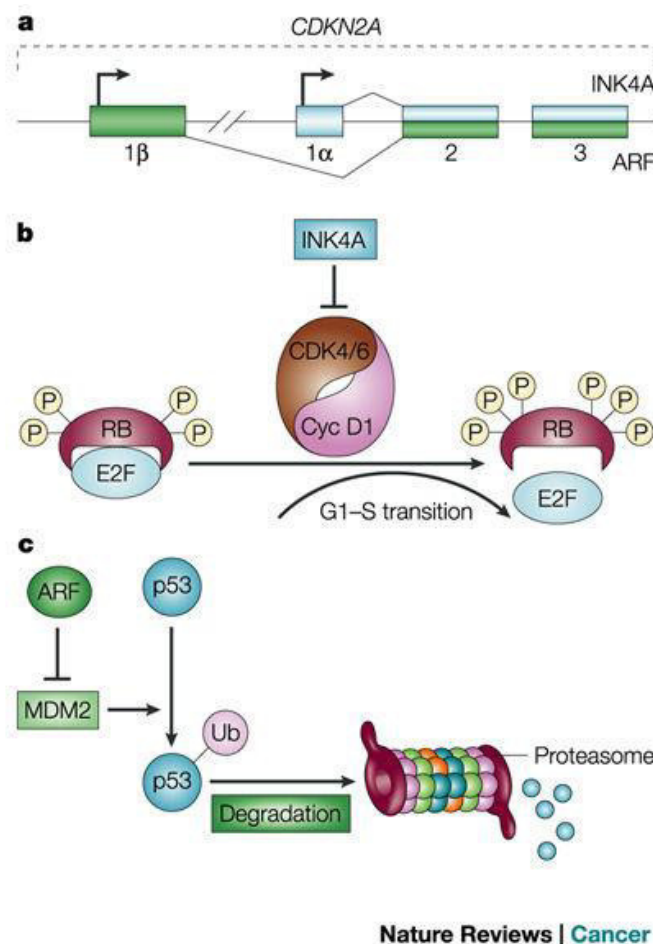


Figure 15 – *CDKN2A* gene organization and cell-cycle functions of encoding proteins p16^{INK4a} and p14^{ARF}.

(A) Organization of *CDKN2A* gene, which encodes p16^{INK4a} and p14^{ARF} tumor suppressor proteins. p16^{INK4a} and p14^{ARF} share the exon 2 and 3 and differ in exon 1. (B) G1-S transition CDK inhibition function of P16^{INK4a}. INK4a competes with cyclin-D for CDK4-6 binding, inhibiting the formation of CDK4-6/cycD active complexes and in turn the phosphorylation of pRb. Thus, cell cycle progression is blocked because E2F remains in association with pRb. (C) p14^{ARF} function. ARF inhibits MDM2 by the sequestration of MDM2 in the nucleus that in turn activates p53 promoting cell-cycle arrest or apoptosis. Reproduced from: Chin, 2003.

p16^{INK4a} can also be linked to oncogene-induced senescence, which is a process characterized by an irreversible growth arrest as a consequence of oncogene activation due to KRAS or BRAF mutation (Kriegl *et al.*, 2011). The senescent process was originally defined in fibroblasts, which were characterized metabolically active but in a growth-arrested state at the G1 phase. This extremely stable process protects cells from hyperproliferative signals and various types of stress and it is activated during ageing – **replicative senescence** - or in response to several stress stimuli, such as DNA damage, oxidative stress or exposure to drugs – **premature senescence** (Zhang, Rosen and Yao, 2006; Romagosa *et al.*, 2011). It is the rupture of this process of senescence that initiates an important mechanism for malignant transformation, leading to the immortalization of senescence cells (Zhang, Rosen and Yao, 2006; Kriegl *et al.*, 2011). p16^{INK4}, as also p14^{ARF} and p15^{INK4b} has been recently identified as a senescence marker (Zhang, Rosen and Yao, 2006).

1.4.1 The role of p16^{INK4a} in cancer

p16^{INK4a} expression ranges from its loss or downregulation to its clear overexpression in several cancer types (Romagosa *et al.*, 2011) (**Figure 16**). Under physiological conditions, the p16^{INK4a} is expressed at low levels in normal proliferating cells prior to extensive rounds of cell division, suggesting a late-stage, anti-proliferative role as in replicate cell senescence (Cammatt, Luo and Peng, 2003; Shi, Wang and Xia, 2016). However, it is specifically induced by replicative cellular senescence and oncogenic stress due to KRAS or BRAF mutations (Kriegl *et al.*, 2011; Kim *et al.*, 2012; Shi, Wang and Xia, 2016). During premature senescence, particularly during oncogene-induced senescence, and in benign and premalignant lesions with senescent cells, p16^{INK4a} is overexpressed (Ortega, Malumbres and Barbacid, 2002; Zhang, Rosen and Yao, 2006; Kriegl *et al.*, 2011; Shi, Wang and Xia, 2016). p16^{INK4a} overexpression results in an increase of CDK4-6/p16^{INK4a} complex formation and a decrease of CDK4-6/cyclin D complex, blocking tumor cells in S-phase (X. Zhang *et al.*, 2013; Bagci *et al.*, 2016) (**Figure 15**). During the tumorigenic process, the p16^{INK4a} function is lost, which allows irreversible progression into S-phase and, ultimately, to a growth advantage essential in tumorigenesis. This loss is observed in most tumor types such as head and neck, esophagus, biliary tract, lung, bladder, colon, breast, leukemias, lymphomas, and glioblastomas with frequencies ranging between 25 to 70% (Serrano, 1997; William Y. Kim and Sharpless, 2016). A minor group of cancer can also have p16^{INK4a} overexpressed, such as cervical cancer, head and neck (Romagosa *et al.*, 2011). This exceptional p16^{INK4a} overexpression has been associated with high-risk genotype HPV

infections (Romagosa *et al.*, 2011). HPV E6 and E7 oncoproteins are responsible for tumor suppressor p53 degradation and pRb inactivation, respectively. After pRb inactivation increasing levels of p16^{INK4a} are seen due to p16^{INK4a} release from the negative feedback with pRb. Thus, p16^{INK4a} overexpression can be seen as an unsuccessful attempt to stop cell proliferation (Romagosa *et al.*, 2011).

The genetic events that impair p16^{INK4a} function include homozygous deletions, epigenetic silencing and mutations at INK4a/ARF locus (Serrano, 1997; Gorgoulis, Koutroumbi and Kotsinas, 1998; Cammett, Luo and Peng, 2003; Semczuk *et al.*, 2004; Jung *et al.*, 2011; Kriegl *et al.*, 2011; Romagosa *et al.*, 2011). Epigenetic silencing can be caused by *CDKN2A* promoter hypermethylation associated with CIMP (Vinci, Perdelli and Banelli, 2005; Kriegl *et al.*, 2011; Kim *et al.*, 2012; Sameer *et al.*, 2012; Yoruker, Mert and Bugra, 2012; McLaughlin-Drubin, Park and Munger, 2013). This phenomena is considered to be the second most common defect in human cancers (Yoruker, Mert and Bugra, 2012). However, Bagci and co-workers (Bagci *et al.*, 2016) verified that any fully hypermethylation was not detected for *CDKN2A* gene but only one partially hypermethylation. The mutations of p16^{INK4a} are distributed through Ankyrin repeats protein, which are involved in protein-protein interactions, leading to the disruption of the native secondary and/or tertiary structures resulting in protein unfolding, aggregation, and loss of function (Serrano, 1997; Cammett, Luo and Peng, 2003). Moreover, the mutations at INK4a/ARF locus are particularly oncogenic because INK4a open reading frame (ORF) overlaps with the tumor suppressor ARF, thus INK4a/ARF encodes two tumor suppressor proteins, p16^{INK4a} and p14^{ARF} (Cammett, Luo and Peng, 2003). In conclusion, p16^{INK4a} induction is seen in premalignant lesions, while p16^{INK4a} loss occurs during malignant transformation supporting p16^{INK4a} as an important factor of carcinogenesis (Vinci, Perdelli and Banelli, 2005; Bennecke *et al.*, 2010; Kriegl *et al.*, 2011). Thus, p16^{INK4a} has been proposed as a marker for malignant transformation (Jung *et al.*, 2011). Moreover, these findings suggest that the capability to bypass senescence is the key molecular mechanism involved in the transformation of premalignant to malignant cells (Shi, Wang and Xia, 2016).

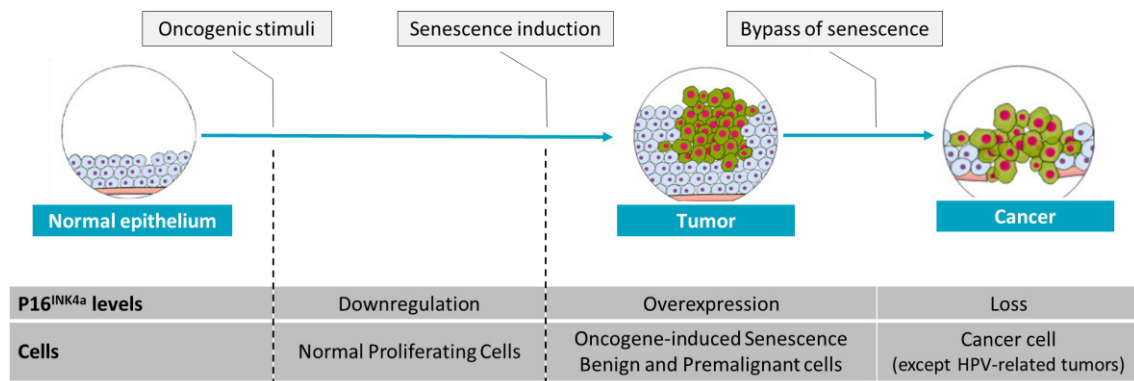


Figure 16 – p16^{INK4a} levels during tumorigenesis.

p16^{INK4a} expression ranges from its loss or downregulation to its clear overexpression in several cancer types. Downregulation is seen in normal proliferating cells. p16^{INK4a} overexpression occurs in premature senescence, particularly during oncogene-induced senescence, and in benign and premalignant lesions. p16^{INK4a} loss is observed in most tumor types such as head and neck esophagus, biliary tract, lung, bladder, colon, breast, leukemias, lymphomas, and glioblastomas.

p16^{INK4a} distinct cellular localizations have also been described (Shi, Wang and Xia, 2016). In CRC, breast cancer, and non-epithelial tumors, p16^{INK4a} shows strong nuclear/cytoplasmic-positive expression in adenomas and adenocarcinomas, whereas negative or low nuclear expression is observed in normal mucosa and in benign conditions (Romagosa *et al.*, 2011; Shi, Wang and Xia, 2016). These results suggest that p16^{INK4a} functions may vary according to different subcellular localizations (Romagosa *et al.*, 2011; Shi, Wang and Xia, 2016). It has also been hypothesized that p16^{INK4a} cellular compartmentalization may result from different mRNA splicing or posttranslational protein modifications, but not an alteration of *CDKN2A* gene itself (Romagosa *et al.*, 2011; Shi, Wang and Xia, 2016). Moreover, it has been suggested that cytoplasmic localization of p16^{INK4a} may be due to CDK4 sequestration in neoplastic cells as an indirect phenomenon of an alteration in Rb pathway (Romagosa *et al.*, 2011) (**Figure 17**). Anion Exchanger 1 (AE1) is another protein related to aberrant p16^{INK4a} accumulation in the cytoplasm (Romagosa *et al.*, 2011) (**Figure 17**). AE1 is a transmembrane protein that interacts with p16^{INK4a}, sequestering the p16^{INK4a} in the cytoplasm resulting in the co-accumulation of both proteins. Interestingly, small interfering RNA-mediated silencing of AE1 induces the release of p16^{INK4a} from the cytoplasm to the nucleus, leading to cell death and inhibition of tumor cell growth (Romagosa *et al.*, 2011).

p16^{INK4a} also modulates the N/O-glycosylation and galectin expression to induce anoikis in human pancreatic carcinoma cells (Amano *et al.*, 2012). p16^{INK4} is known to upregulate Galectin-1 (Gal-1) and makes cell surfaces susceptible for Gal-1 binding to fibronectin receptor to induce anoikis via downregulation of alpha 2,6-sialylation (Amano *et al.*, 2012). p16^{INK4a} is also described to control oncogenic KRAS function in human pancreatic cancer cells (Rabien *et al.*, 2012). It was demonstrated that reintroduction of p16^{INK4a} reversed anoikis resistance and

clonogenicity of human pancreatic cancer cells, properties commonly attributed to the transforming potential of oncogenic KRAS. Therefore, it seems like p16^{INK4a} can negatively influences KRAS (Rabien *et al.*, 2012). p16^{INK4a} might also induce tumor cell migration and invasion in cooperation with laminin-5 γ 2, as it has been demonstrated in a keratinocyte model of squamous cell carcinomas (Wassermann *et al.*, 2009; Romagosa *et al.*, 2011) (**Figure 17**). Interestingly, laminin-5 γ 2 is another β -catenin/TCF4 target gene, thus β -catenin might be an integrator of malignant transformation. In endometrial carcinomas, it was proven that p16^{INK4a} and p21^{Cip1/Waf1} are regulated via the action of β -catenin in the absence of TCF4, however, the mechanism of regulation of p16^{INK4a} might differ in CRC, as this is already proved for p21 (Wassermann *et al.*, 2009). Initially, Wassermann and co-workers (Wassermann *et al.*, 2009) proposed that p16^{INK4a} might be a target gene of β -catenin because nuclear expression of β -catenin correlates with the expression of p16^{INK4a} in human CRCs in a highly significant manner. Thus, they analyzed the interaction between both molecules and conclude that both molecules indeed interact (Wassermann *et al.*, 2009). Moreover, other studies have demonstrated that p16^{INK4a} overexpression may induce apoptosis in a p53-dependent or independent manner in various cancer cell lines (Romagosa *et al.*, 2011). Considering all the herein summarized data, a role of p16^{INK4a} as a universal cancer suppressor acting to block several pro-neoplastic cell capabilities, such as proliferation, cell invasion and angiogenesis, can be hypothesized (Romagosa *et al.*, 2011) (**Figure 17**).

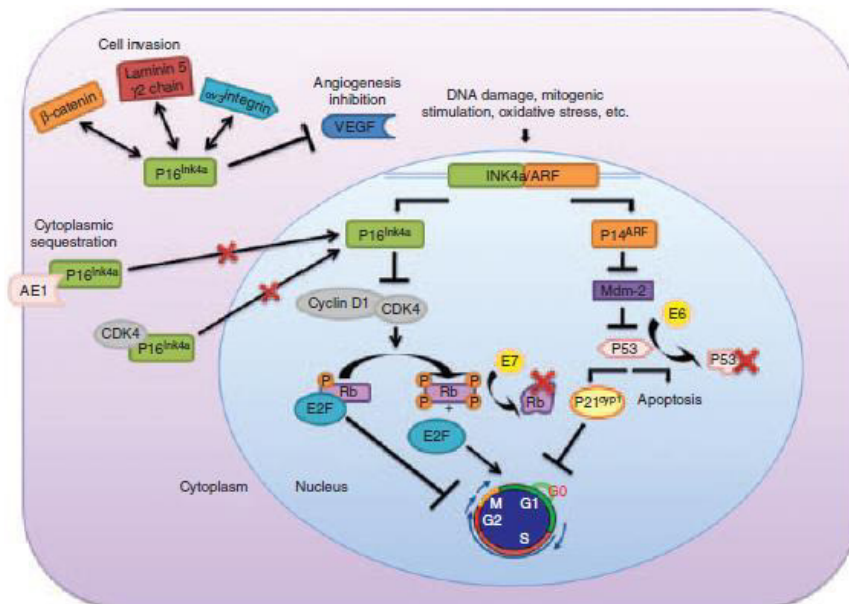


Figure 17 – Cellular compartmentalization and functions of p16^{INK4a}.

p16^{INK4a} functions vary according to its different subcellular localizations that may result from different mRNA splicing or posttranslational protein modifications, but not alterations of p16 gene itself. Aberrant cytoplasmic p16^{INK4a} accumulation may be due to CDK4 sequestration in neoplastic cells, as an indirect phenomenon of an alteration in Rb pathway. It can also be caused by AE1 that interact with p16^{INK4a}, sequestering the p16^{INK4a} in the cytoplasm. p16^{INK4a} has also been implicated in migration and invasion of tumor cells in cooperation with laminin-5 γ 2 and β -catenin. p16^{INK4a} has also been related to angiogenesis. Reproduced from: Romagosa *et al.*, 2011.

1.4.2 The role of p16^{INK4a} in colorectal cancer

Krieger and co-workers (Kriegl *et al.*, 2011) observed that all serrated lesions with low-grade intraepithelial neoplasia are characterized by low or high expression levels of p16^{INK4a}, while serrated lesions with high-grade intraepithelial neoplasia express high levels of p16^{INK4a} or loss of p16^{INK4a}. However, all ex-adenoma serrated adenocarcinomas show a loss of p16^{INK4a}. These results evidenced the loss of p16^{INK4a} during the process of malignant transformation and an up and down regulation of p16^{INK4a} in the serrated route to colon cancer (Kriegl *et al.*, 2011).

Krieger and co-workers (Kriegl *et al.*, 2011) suggested a process in human serrated polyps where oncogene-induced senescence driven by BRAF mutations cause a growth arrest and stop the malignant transformation. However, the characteristic loss of p16^{INK4a} due to hypermethylation of CDKN2A lead to overcome the senescence barrier and enable the progression of the tumor into invasive colon cancer (Kriegl *et al.*, 2011). They also studied the impact of KRAS mutations in a mouse model (Kriegl *et al.*, 2011). Interestingly, their study shows that KRAS^{G12D} also induce murine serrated polyps, which were characterized by p16^{INK4a} overexpression and induction of senescence. After INK4a/ARF locus deletion in these mice, tumors turned morphological and molecular comparable to human KRAS-mutated serrated carcinomas (Kriegl *et al.*, 2011).

Hypermethylation of the CpG islands of p16^{INK4a} is a frequent event in CRC (Kim *et al.*, 2012). This event is associated with CIMP of CRC, which implies widespread promoter methylation including CDKN2A (Kriegl *et al.*, 2011). Kim and co-workers (Kim *et al.*, 2012) had shown that p16^{INK4a} hypermethylation is significantly associated with KRAS mutations and CIMP positivity. Patients with p16^{INK4a} unmethylated tumors had significant longer time to progression and overall survival comparing with p16^{INK4a} methylated tumors. Patients with both p16^{INK4a} and KRAS aberrancy had markedly shortened time to progression than those with either KRAS or p16^{INK4a} aberrancy or those with neither (Kim *et al.*, 2012). In CRC, p16^{INK4a} shows strong nuclear/cytoplasmic-positive expression in adenomas and adenocarcinomas, whereas negative or low nuclear expression is observed in normal mucosa and in benign conditions (Romagosa *et al.*, 2011; Shi, Wang and Xia, 2016). These results suggest that p16^{INK4a} nuclear localization might be associated with the acquisition of a malignant state.

1.5 The interplay between KRAS, Galectin-3 and p16^{INK4a}

The first insights about KRAS/Gal-3 emerge by the observation of their similar activities, both are capable to prevent apoptosis and promote cell proliferation (Shalom-Feuerstein *et al.*, 2005). Interestingly, Gal-3 overexpression is associated with increased KRAS signal output leading to increased cell proliferation, survival, and migration (Levy *et al.*, 2010, 2011; Li *et al.*, 2015). These Gal-3-mediated effects result from a selective binding to KRAS-GTP, leading to increased nanoclustering in the cell membrane, stabilization of KRAS in its active state (KRAS-GTP), and robust RAS signaling (Shalom-Feuerstein *et al.*, 2008; Levy *et al.*, 2011). Moreover, Shalom-Feuerstein and co-workers demonstrated that the cytosolic level of Gal-3 determines the magnitude of KRAS-GTP nanoclustering and signal output (Shalom-Feuerstein *et al.*, 2008). However, for this interaction KRAS/Gal-3 to occur, Gal-3 must be translocated from the nucleus to the cytoplasm, which is regulated by its serine 6 phosphorylation catalyzed by casein kinase 1 (CK1). Thus, this phosphorylation promotes the translocation of Gal-3 from nucleus to cytoplasm and hence the stability of KRAS-GTP at the plasma membrane. Levy and co-workers (Levy *et al.*, 2011) also demonstrated that Gal-3 also interferes with KRAS localization by fluorescent confocal microscopy. They confirmed KRAS plasma membrane localization in wt and Gal-1^{-/-} mouse embryonic-fibroblasts (MEFs). Interestingly, KRAS plasma membrane localization was no longer detected in Gal-3^{-/-} MEFs, corresponding to MEFs with Gal-3-knockout, and in cell lines pre-treated with CK1 inhibitor D4476, which prevents the Gal-3 cytosol translocation. Levy and co-workers (Levy *et al.*, 2011) also proved that Gal-3 attenuates KRAS protein degradation. Moreover, when this group examined the RAS downstream effectors ERK and AKT, they also verified that pERK and pAKT levels were significantly lower in Gal-3^{-/-} MEFs comparing with wt MEFs. These results suggest that Gal-3 can activate downstream signals to ERK and AKT. Shalom-Feuerstein and co-workers also proved that Gal-3^{WT} coimmunoprecipitates and co-localizes with oncogenic KRAS leading to RAS signaling pathway radical activation (Shalom-Feuerstein *et al.*, 2005). Moreover, KRAS/Gal-3 complex formation might turn KRAS insensitive to RAS GTPase-activating proteins, perhaps because the linking domain of KRAS is blocked by Gal-3 (Shalom-Feuerstein *et al.*, 2005). Thus, important questions arise concerning the control of KRAS by Gal-3.

Induction of senescence or tumorigenesis depends on cell cycle regulatory proteins, such as p16^{INK4a} which was already associated with KRAS mutations (Rustgi, 2013). It was demonstrated that SSA progression to cancer is not achieved due to p16^{INK4a}-mediated senescence and intact p53 (Rustgi, 2013). In fact, they observed KRAS-mutated mice develop

epithelial hyperplasia and crypt architecture changes in the colon, instead of carcinomas (Rustgi, 2013). This phenomena is accompanied by p16^{INK4a} overexpression which is the result of senescence inducted through oncogenic KRAS (Rustgi, 2013). It was further investigated and the mutant-KRAS mice was deleted for *CDKN2A*, gene that encode p16^{INK4a}, resulting in senescence prevention and development of carcinomas in mutant-KRAS mice. Therefore, KRAS mutations induce p16^{INK4a}-mediated senescence and p16^{INK4a} inactivation might to be induced to KRAS-driven carcinoma (Rustgi, 2013). Other authors reported that oncogenic KRAS itself can inactivate p16^{INK4a} bypassing senescence (Lee and Bar-Sagi, 2010).

p16^{INK4a} also modulates the N/O-glycosylation and galectin expression to induce anoikis in human pancreatic carcinoma cells (Amano *et al.*, 2012). p16^{INK4} upregulates Galectin-1 (Gal-1) and makes cell surfaces susceptible for Gal-1 binding to fibronectin receptor to induce anoikis via downregulation of alpha 2,6-sialylation (Amano *et al.*, 2012). Gal-3 inversely protects cells from anoikis by interacting with Gal-1. Additionally, Sanchez-Ruderisch and co-workers shown that p16^{INK4a} not only affects Gal-1, but also Gal-3 (Sanchez-Ruderisch *et al.*, 2010).

Overall, these evidences encouraged our investigation on the existence of a possible KRAS, Gal-3, p16^{INK4a} axis in CRC.

1.6 Rationale and aims

CRC is the third most commonly diagnosed cancer worldwide and one of the leading causes of cancer related death (Ferlay *et al.*, 2014). Over the years, this situation is being reverted with the increased rates of CRC screening, advances in early detection and treatment (El-Sham *et al.*, 2015). Therefore, it is important to elucidate some physiopathology issues of CRC in order to be able to reverse this situation with more effective treatments.

KRAS, Gal-3 and/or p16^{INK4a} alterations have been associated in some types of cancer, including CRC. Oncogene *KRAS* mutations are among the most frequent events found in CRC and play a role in the genesis and progression of this cancer (Roper and Hung, 2013; Alves *et al.*, 2015). So far no KRAS inhibitors are available at the clinics despite all the efforts of the pharmaceutical companies. Moreover, CRC harbouring KRAS mutations and EGFR overexpression are resistant to EGFR inhibitors what constitute a relevant clinical problem that urges a resolution. Gal-3 is a multifunctional protein, which is reported to interact with KRAS affecting cell proliferation, survival and migration in several cancers including CRC (Shalom-Feuerstein *et al.*, 2008; Levy *et al.*, 2011). p16^{INK4a} was reported to downregulate Gal-3 and KRAS exerting its tumor suppressor function (Rabien *et al.*, 2012). p16^{INK4a} loss of function is a very frequent event during malignant transformation, which has been associated with KRAS mutation being an important factor for carcinogenesis (Li, Poi and Ming-Daw, 2012).

There are evidences for a possible relation between KRAS, Gal-3, p16^{INK4a} and, but little is known about the role of KRAS in the regulation of KRAS/Galectin-3/p16^{INK4a} triple axis in CRC.

In this project we aimed to understand how KRAS hot spot mutations, KRAS^{G13D}, KRAS^{G12D} and KRAS^{G12V}, regulate the KRAS interaction with Gal-3 and p16^{INK4a} to form a complex. We also aimed to uncover the impact of the KRAS/Galectin-3/p16^{INK4a} triple axis complex regulation in the induction of phenotypic alterations namely invasion and invasion-associated activities in CRC cells.

For that matter we will use as model NCM460 normal colon cells that were previously stably transfected with Flag-KRAS^{WT} and with the KRAS hotspot mutations: Flag-KRAS^{G12V}, Flag-KRAS^{G12D} and Flag-KRAS^{G13D}. We will also use CRC derived cell lines harbouring KRAS mutations (SW480 with a KRAS^{G12V} and HCT116 with a KRAS^{G13D}), in which we will silence KRAS and/or Gal-3 by RNAi.

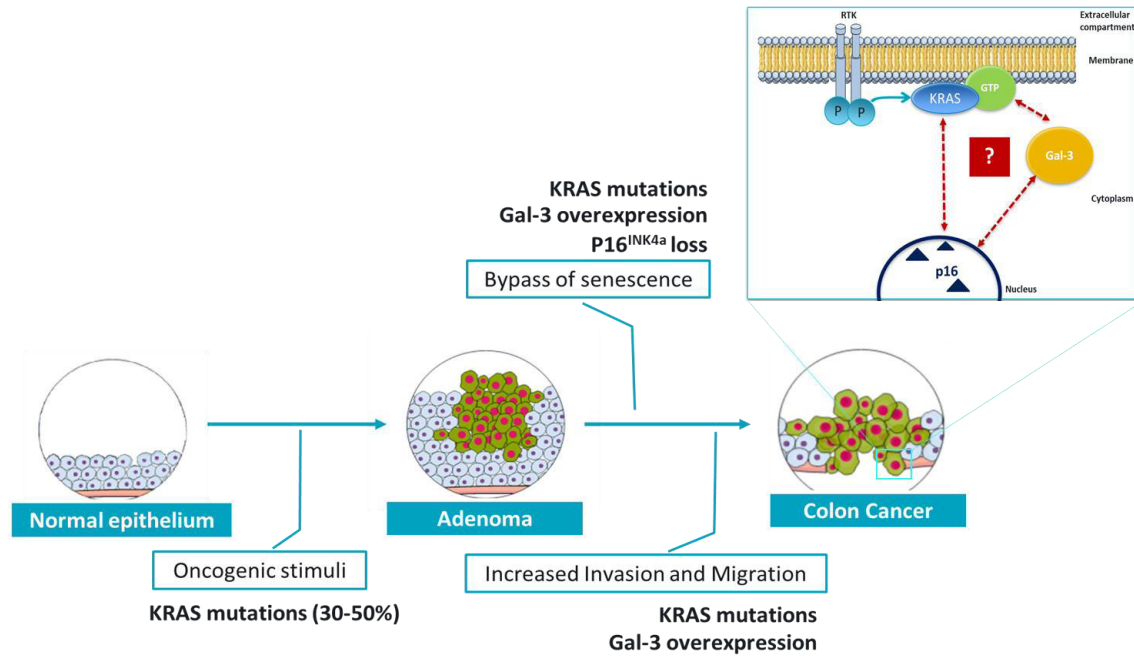


Figure 18 – Rationale of this work.

KRAS, Gal-3 and/or p16^{INK4a} have been associated in some types of cancer, including CRC. Oncogene KRAS mutations is a very frequent initial event in CRC. p16^{INK4a} is a tumor suppressor protein frequently loss during malignant transformation, which has been associated with KRAS mutations. Gal-3 is a multifunctional protein, which is reported to interact with KRAS, affecting cell proliferation, survival and migration in several cancers including CRC. Thus, we aimed to study the regulation of the KRAS/Galectin-3/p16^{INK4a} triple axis in CRC. Moreover, we intended to study if there is a direct KRAS/Galectin-3/p16^{INK4a} interaction and what are the phenotypic alterations induced by the silencing of KRAS and/or Gal-3 in the CRC model.

CHAPTER II. MATERIALS AND METHODS

2.1 Cell lines and culture conditions

In the present work we used human colorectal derived cell lines with different genetic backgrounds and normal non-cancer cell lines. The human cancer cell lines used were SW480 (ATCC® CCL-228™) and HCT116 (ATCC® CCL-247™). SW480 is an aneuploid cell line derived from a primary tumor that harbors *KRAS*^{G12V} mutation (Tomita *et al.*, 1992), overexpression and mutation of p53 (*TP53*^{R273H:P309S}) and *MYC* amplification (Knutsen *et al.*, 2010; Ahmed *et al.*, 2013). HCT116 is a diploid cell line that harbors multiple mutations, such as, *KRAS*^{G13D} (Ahmed *et al.*, 2013), *PIK3CA*^{H1047R} (catalytic subunit alpha of phosphatidylinositol-4,5-bisphosphate 3-kinase), an insertion mutation on *CDKN2A* and a deletion mutation on oncogene *CTNNB1* (Catenin cadherin-associated protein Beta 1) (ATCC, 2016). This cell line was provided by Muriel Priault (IBGC, CNRS). NCM460 cell lines are non-cancer colon cells derived from normal human colon mucosa epithelium, obtained from INCELL (San Antonio, TX) (Moyer *et al.*, 1996). NCM460 cells were previously transfected with p3XFLAG-CMV vectors containing *KRAS*^{WT}, *KRAS*^{G12V}, *KRAS*^{G13D} and *KRAS*^{G12D} mutations (Alves *et al.*, 2015). Four NCM460 cell lines were obtained expressing: wild-type *KRAS* (*Flag-KRAS*^{wt}), *KRAS* mutated in codon 12 (*Flag-KRAS*^{G12V} and *Flag-KRAS*^{G12D}), and *KRAS* mutated in codon 13 (*Flag-KRAS*^{G13D}) (Alves *et al.*, 2015).

SW480 and NCM460 Flag-*KRAS* cells were grown in RPMI-1640 medium (Gibco), while HCT116 cells were maintained in McCoy's 5A medium (Biowest). Both media were supplemented with 1% penicillin–streptomycin (Pen-Strep; Gibco, Invitrogen) and 10% heat inactivated fetal bovine serum (FBS; Gibco, Invitrogen). All cell lines were maintained in a humidified atmosphere of 5% CO₂ at 37°C. The medium was renewed once a week and the cells were subcultured every week, when the confluence reached values close to 80% by detachment with 0.05% trypsin (Sigma-Aldrich). Cells were used for the assays when they reached > 80% confluence.

2.2 KRAS/Galectin-3/Pp6^{INK4a} nanocluster analysis

2.2.1 Immunoprecipitation assay

Co-Immunoprecipitation (Co-IP) was used to identify physical protein-protein interactions. Through the use of specific antibodies, Co-IP not only enables the capture and purification of a primary protein target, but also the capture and identification of its interactome, namely, the proteins that interact physically with this primary target.

For the evaluation of KRAS/Galectin-3/p16^{INK4a} as a nanocluster, co-IP assay was performed followed by western blot analysis. SW480 and HCT116 cell lines were grown in 75 cm² culture flasks until they reached >90% of confluence. The medium was collected and frozen at -80°C for further analysis and the cells were washed with PBS 1× and lysed for 15 minutes on ice in RIPA buffer (1% NP-40, 150 mM NaCl, 50 mM Tris-HCl (pH 7.5), 2 mM EDTA) supplemented with a mix of protease and phosphatase inhibitors (10 µg/mL NaF, 20 µg/mL Na₃VO₄, 10 µg/mL PMSF, 10 µg/mL Aprotinin, 10 µg/mL Leupeptin and 50 µg/mL Na₄P₂O₇). Cell monolayer was scraped, resuspended and collected. The resulting cell suspension was centrifuged (10 minutes, 14000 rpm, 4°C), the supernatant was transferred to an eppendorf tube on ice and the pellet was discarded. The supernatant was then subjected to protein quantification using DC protein assay Kit (Bio-Rad Laboratories). Standard BSA concentrations 0.25, 0.5, 0.75, 1, 1.5, 3 mg/mL were used, and the absorbance was determined at 655 nm in the SynergyTM Mx (BioTek). Finally, a calibration curve was designed, using BSA standards absorbance, and the concentration of the samples was then extrapolated.

For the isolation of a target, from a mixture of many other proteins, we took advantage of antibody specificity. Thus, Protein G sepharose beads (GE Healthcare) were centrifuged (12 seconds; 14000 rpm; 4°C), to remove the ethanol fraction, and washed with buffer C (Catenin lysis buffer: [1% Triton X-100 + 1% NP-40], 5 mg/mL Na₄P₂O₇ and 1% NaF) with short spins between the washes, to remove supernatant. Dynabeads® Protein G (LifeTechnologies) were prepared in PBS-Tween20 (PBS-T) and washes were performed through the application of a magnetic field. Finally, beads were resuspended in PBS. Then, both types of beads were blocked overnight at 4°C with 1% BSA in PBS-T and under agitation, to avoid proteins unspecific binding. Afterwards, samples were pre-cleared by adding 15 µL of beads suspension to each 1000 µg protein, under agitation for 30 minutes at 4°C. Then, supernatants were collected to new eppendorfs and the respective primary antibodies, as anti-KRAS (Sigma), anti-

Gal-3 (Santa Cruz Biotechnology) or anti-p16 (Santa Cruz Biotechnology), were added (5 $\mu\text{g}/1000 \mu\text{g}$ protein) to the respective tubes and incubated overnight at 4°C under agitation. To the pellets, which correspond to pre-cleared samples, we added 25 μL loading buffer 1.5 \times . These samples were then denatured (5 minutes; 95°C) and frozen.

On the following day, a new bead suspension was added to each sample previously incubated with the primary antibody. After incubation (1 h; 4°C; under agitation) to complex the **target-protein-antibody-bead**, a short spin was made, in the case of sepharose beads, or a magnetic field was applied, in the case of Dynabeads, and supernatants were discarded. Pellets, which contain beads-antibody-antigen complex, were washed 3 times and, in the last wash, supernatants were completely removed. Finally, 50 μL loading buffer 1.5 \times were added and the samples were subjected to denaturing conditions (5 minutes; 95°C) to dissociate the complex. Lastly, all samples were centrifuged (14000 rpm; 5 minutes; 4°C) and 20 μL of each sample was loaded to the respective lane of a SDS-polyacrylamide gel. Proteins were then separated in 15% polyacrylamide gels and transferred to a nitrocellulose membrane (GE Healthcare) for 2h at 100V. Next, membranes were blocked during 45 minutes with 5% milk in PBS-T in order to block nonspecific binding sites. After blocking, membranes were briefly washed in PBST and then incubated overnight at 4°C under agitation with anti-KRAS (1:1000, Sigma), anti-Gal-3 (1:500, Santa Cruz Biotechnology) and anti-p16 antibodies (1:500, ProteinTech Group), in order to assess the presence of these proteins in the immunoprecipitated samples. Membranes were washed 4 times in PBST for 5 minutes. Secondary antibodies used were anti-mouse (1:2000, Santa Cruz Biotechnology), anti-goat (1:2000, Santa Cruz Biotechnology), and anti-rabbit (1:2000, GE Healthcare). Membranes were washed 6 times in PBST for 5 minutes. Protein bands were then revealed with ECL Western Blotting Detection Kit (Life Science). When Bio-Rad revealing solution was used, all secondary antibodies were diluted at 1:10000 dilution.

2.2.2 Co-localization studies through immunofluorescence assay

To confirm the formation of a KRAS/Galectin-3/p16^{INK4a} nanocluster and complement the immunoprecipitation (IP) results, protein localization was assessed by immunofluorescence assay, followed by high resolution confocal microscopy analysis. Co-localization were quantified by ImageJ Software, namely, Just Another Colocalization Plugin (JACoP).

2.2.2.1 Immunofluorescence assay

To study the co-localization of KRAS/Galectin-3/p16^{INK4a}, single and double immunostainings and the respective controls were prepared. Single immunostainings and other controls were made on NCM460 *Flag-KRAS^{WT}* to define the best acquisition settings for each fluorochrome and to exclude cross-reactions. Double staining was prepared to obtain the images for future co-localization studies. For that, **NCM460 *Flag-KRAS^{wt}*, *Flag-KRAS^{G12V}*, *Flag-KRAS^{G12D}*, and *Flag-KRAS^{G13D}*** cells were seeded on glass coverslips at 2×10^5 cells/well in 24-well plates for 48 hours. Then, cells were fixed with 4% paraformaldehyde (PFA), permeabilized with 0.1% Triton X-100, blocked with 10% FBS, and incubated overnight at 4°C with primary antibodies: anti-FLAG (1:25, Sigma), anti-Gal-3 (1:25, Santa Cruz Biotechnology) and anti-p16 (1:25, ProteinTech Group). The secondary antibodies Donkey anti-goat Alexa 488 (1:200), Chicken anti-rabbit Alexa 647 (1:200), Donkey anti-mouse Alexa 488 (1:200), and Chicken anti-mouse Alexa 594 (1:200) were incubated for 1 hour at room temperature (RT). All conditions with needed for co-localization studies are listed below (**Table 1**). Finally, coverslips were mounted with Vectashield Mounting Medium with DAPI (Vectashield, Vector Laboratories) over a microscope slide and sealed with nail polish.

Images were acquired with a laser confocal microscopy Leica TCS SP5II using a HCX PL APO CS 63x 1.40 OIL UV objective. All images were acquired with identical laser power, gain and offset, which were defined previously for each fluorochrome with single immunostainings and respective controls. Moreover, the obtained images were acquired with zoom 1.0, format 1024x1024 at 200 Hz and the orthogonal projections were derived from stack images acquired with zoom 3.2, format 1024x1024 at 200 Hz.

Table 1 – Primary and secondary antibodies used for immunofluorescence assay.

Cell line	Condition	Primary antibodies (1°)	Dilution	Secondary Antibodies (2°)	Dilution
NCM460 KRAS ^{wt}	<i>P16 (1°+2°)</i>	P16	1:25	Chicken anti-rabbit Alexa 647	1:200
	<i>P16 (2°)</i>	-	-	Chicken anti-rabbit Alexa 647	1:200
	<i>P16 (1°) + Flag-KRAS (2°)</i>	P16	1:25	Goat anti-mouse Alexa 488	1:200
	<i>P16 (1°) + Gal-3 (2°)</i>	P16	1:25	Donkey anti-goat Alexa 488	1:200
	<i>Flag-KRAS (1°+2°)</i>	Flag-KRAS	1:25	Goat anti-mouse Alexa 488	1:200
	<i>Flag-KRAS (2°)</i>	-	-	Goat anti-mouse Alexa 488	1:200
	<i>Flag-KRAS (1°) + p16 (2°)</i>	Flag-KRAS	1:25	Chicken anti-rabbit Alexa 647	1:200
	<i>Flag-KRAS (1°+2°)</i>	Flag-KRAS	1:25	Chicken anti-mouse Alexa 594	1:200
	<i>Flag-KRAS (2°)</i>	-	-	Chicken anti-mouse Alexa 594	1:200
	<i>Flag-KRAS (1°) + Gal-3 (2°)</i>	Flag-KRAS	1:25	Donkey anti-goat Alexa 488	1:200
	<i>Gal-3 (1°+2°)</i>	Gal-3	1:25	Donkey anti-goat Alexa 488	1:200
	<i>Gal-3 (2°)</i>	-	-	Donkey anti-goat Alexa 488	1:200
	<i>Gal-3 (1°) + Flag-KRAS (2°)</i>	Gal-3	1: 25	Chicken anti-mouse Alexa 594	1:200
	<i>Gal-3 (1°) + P16 (2°)</i>	Gal-3	1: 25	Chicken anti-rabbit Alexa 647	1:200
	<i>Gal-3 (1°+2°) + Flag-KRAS (1°+2°)</i>	Gal-3	1: 25	Donkey anti-goat Alexa 488	1:200
		Flag-KRAS	1: 25	Chicken anti-mouse Alexa 594	1:200
	<i>Gal-3 (2°) + Flag-KRAS (2°)</i>	-	-	Donkey anti-goat Alexa 488	1:200
		-	-	Chicken anti-mouse Alexa 594	1:200
	<i>Gal-3 (1°+2°) + P16 (1°+2°)</i>	Gal-3	1: 25	Donkey anti-goat Alexa 488	1:200
		P16	1: 25	Chicken anti-rabbit Alexa 647	1:200
	<i>Gal-3 (2°) + P16 (2°)</i>	-	-	Donkey anti-goat Alexa 488	1:200
		-	-	Chicken anti-rabbit Alexa 647	1:200
	<i>P16 (1°+2°) + Flag-KRAS (1°+2°)</i>	P16	1: 25	Chicken anti-rabbit Alexa 647	1:200
FLAG-KRAS		1: 25	Goat anti-mouse Alexa 488	1:200	
<i>P16 (2°) + Flag-KRAS (2°)</i>	-	-	Chicken anti-rabbit Alexa 647	1:200	
	-	-	Goat anti-mouse Alexa 488	1:200	
NCM460 KRAS ^{G12V}	<i>Gal-3 (1°+2°) + Flag-KRAS (1°+2°)</i>	Gal-3	1: 25	Donkey anti-goat Alexa 488	1:200
		Flag-KRAS	1: 25	Chicken anti-mouse Alexa 594	1:200
	<i>Gal-3 (1°+2°) + P16 (1°+2°)</i>	Gal-3	1: 25	Donkey anti-goat Alexa 488	1:200
		P16	1: 25	Chicken anti-rabbit Alexa 647	1:200
	<i>P16 (1°+2°) + Flag-KRAS (1°+2°)</i>	P16	1: 25	Chicken anti-rabbit Alexa 647	1:200
		FLAG-KRAS	1: 25	Goat anti-mouse Alexa 488	1:200

NCM460 KRAS ^{G12D}	<i>Gal-3 (1°+2°) + Flag-KRAS (1°+2°)</i>	Gal-3	1: 25	Donkey anti-goat Alexa 488	1:200
		Flag-KRAS	1: 25	Chicken anti-mouse Alexa 594	1:200
	<i>Gal-3 (1°+2°) + P16 (1°+2°)</i>	Gal-3	1: 25	Donkey anti-goat Alexa 488	1:200
		P16	1: 25	Chicken anti-rabbit Alexa 647	1:200
	<i>P16 (1°+2°) + Flag-KRAS (1°+2°)</i>	P16	1: 25	Chicken anti-rabbit Alexa 647	1:200
		FLAG-KRAS	1: 25	Goat anti-mouse Alexa 488	1:200
NCM460 KRAS ^{G13D}	<i>Gal-3 (1°+2°) + Flag-KRAS (1°+2°)</i>	Gal-3	1: 25	Donkey anti-goat Alexa 488	1:200
		Flag-KRAS	1: 25	Chicken anti-mouse Alexa 594	1:200
	<i>Gal-3 (1°+2°) + P16 (1°+2°)</i>	Gal-3	1: 25	Donkey anti-goat Alexa 488	1:200
		P16	1: 25	Chicken anti-rabbit Alexa 647	1:200
	<i>P16 (1°+2°) + Flag-KRAS (1°+2°)</i>	P16	1: 25	Chicken anti-rabbit Alexa 647	1:200
		FLAG-KRAS	1: 25	Goat anti-mouse Alexa 488	1:200

2.2.2.2 Co-localization analysis by ImageJ software

After immunofluorescence images were obtained, the co-localization analysis of the KRAS/Galectin-3/p16^{INK4a} protein complex was processed with JACoP of ImageJ software, a toolbox for subcellular co-localization. Of note, images with at least 50 cells/condition were necessary. For these analyses, a common threshold for each fluorochrome was defined and applied to all conditions. Then, the images were treated with JACoP plugin and the Pearson's coefficient, M1 & M2 coefficients, and overlap coefficients, k1 & k2 were obtained for each image. All data were collected, analyzed and the mean for each condition was obtained and compared for main conclusions.

2.3 Silencing of KRAS and/or galectin-3 by RNA interference

To achieve the key roles of KRAS and Gal-3 in cells, their silencing was performed by RNAi. RNAi technique is based on the physiological regulatory mechanism that control gene activity through small double stranded RNA (dsRNA) molecules, also known as small interfering RNA (siRNA). These siRNA molecules are recognized by the RNAi enzymatic machinery, namely the RISC complex, and function as a homology-dependent guide to degrade specific mRNA transcripts resulting in targeted and transient post-transcriptional gene silencing (Aagaard and Rossi, 2007). Thus, Hs_KRAS2_8 siRNA (5'AAGGAGAATTTAATAAAGATA3') and Hs_LGALS3_3 siRNA (5'CACGGTGAAGCCCAATGCAAA3') were the selected siRNAs to silence KRAS and Gal-3 proteins, respectively. AllStars negative control siRNA (5'AATTCTCCGAACGTGTCACGT3') was used as the non-silencing control.

Briefly, HCT116 cells were plated at 2×10^5 cells/well in 6-well plates with McCoy's 5A medium supplemented with 1% Pen-Strep and 10% FBS. After 24 hours, the McCoy's 5A supplemented medium was replaced by McCoy's 5A non-supplemented and the transfection was performed in OPI-MEM medium (to 1/5 of the total medium). Control cells (**Control -**) were left untreated, **non-silencing siRNA** condition was transfected using 6 μ L lipofectamine 2000 (Invitrogen) as transfection reagent and 150 nM of non-silencing siRNA, **KRAS siRNA** condition was transfected using 6 μ L lipofectamine 2000 + 150 nM of KRAS siRNA, **LGALS3 siRNA** condition was transfected with 6 μ L lipofectamine 2000 + 50 nM of LGALS3 siRNA and finally, **KRAS + LGALS3 siRNA** was transfected using 6 μ L lipofectamine 2000 + 150 nM of KRAS siRNA + 50 nM of LGALS3 siRNA. After 14 hours (time 0) of transfection, the medium was replaced by McCoy's supplemented with 10% FBS and 1% Pen-Strep and cells were prepared for additional experiments and maintained for 48 hours. All procedures were performed under RNase free conditions.

2.3.1 KRAS and galectin-3 localization through immunofluorescence assay

During HCT116 RNAi for *KRAS* and/or *LGALS3*, the p16^{INK4a} and Gal-3 localization were evaluated to understand if KRAS and/or Gal-3 silencing have any impact on their localization. For that, at time 0 of HCT116 silencing, these cells were plated on glass coverslips at 2×10^5 cells/well in 24-well plate for 48 hours. Then, cells were fixed with 4% PFA, permeabilized with 0.1% TritonX-100, blocked with 10% FBS, and incubated with primary antibodies: anti-Gal-3 (1:25, Santa Cruz Biotechnology), and anti-p16 (1:25, ProteinTech Group) overnight at 4°C. Then, the secondary antibodies incubation was performed for 1 hour at RT with Donkey anti-goat Alexa 488 (1:200) and Chicken anti-rabbit Alexa 647 (1:200). All conditions needed for Gal-3 and p16^{INK4a} co-localization studies are listed below (**Table 2**).

Lastly, coverslips were mounted with Vectashield Mounting Medium with DAPI (Vectashield, Vector Laboratories) over a microscope slide and sealed with nail polish. Images were acquired with a laser confocal microscopy Leica TCS SP5II using a HCX PL APO CS 63x 1.40 OIL UV objective. All images were acquired with identical laser power, gain and offset, with zoom 1.0 and at format 1024x1024 at 200 Hz.

Table 2 - Primary and secondary antibodies used in Gal-3 and p16^{INK4a} co-localization analysis by immunofluorescence assay.

Cell line	Condition	Primary antibodies (1°)	Dilution	Secondary Antibodies	Dilution
HCT116	<i>Control</i> - <i>P16</i> (1°+2°) + <i>Gal-3</i> (1°+2°)	P16	1:25	Chicken anti-rabbit Alexa 647	1:200
		Gal-3	1:25	Donkey anti-goat Alexa 488	1:200
	<i>Control</i> - <i>P16</i> (2°) + <i>Gal-3</i> (2°)	-	-	Chicken anti-rabbit Alexa 647	1:200
		-	-	Donkey anti-goat Alexa 488	1:200
	<i>Non-silencing control</i> - <i>P16</i> (1°+2°) + <i>Gal-3</i> (1°+2°)	P16	1:25	Chicken anti-rabbit Alexa 647	1:200
		Gal-3	1:25	Donkey anti-goat Alexa 488	1:200
	<i>LGALS3 siRNA</i> - <i>P16</i> (1°+2°)	P16	1:25	Chicken anti-rabbit Alexa 647	1:200
	<i>KRAS siRNA</i> - <i>P16</i> (1°+2°) + <i>Gal-3</i> (1°+2°)	P16	1:25	Chicken anti-rabbit Alexa 647	1:200
		Gal-3	1:25	Donkey anti-goat Alexa 488	1:200
	<i>LGALS3</i> + <i>KRAS siRNAs</i> - <i>P16</i> (1°+2°)	P16	1:25	Chicken anti-rabbit Alexa 647	1:200

2.3.3 Time-Lapse migration assays

Migration is an essential activity for invasion and metastasis to occur, thus, HCT116 transfected cells migration rates were evaluated through wound-healing and single-cell migration assays as described below.

2.3.3.1 Time-Lapse wound-healing migration assay

Wound-healing assay enables the *in vitro* study of cell migration and motility that occurs in various biological processes, such as cancer metastasis. This assay is based on the closure analysis of a given “wound” created by scratching a confluent monolayer culture. The “wound” is monitored and measured periodically, and the rate of wound closure is calculated over time (Zaritsky *et al.*, 2015).

The migration assay was performed in HCT116 cell lines upon RNAi for *KRAS* and/or *LGALS3*. At time 0 of silencing, the cells were plated to a 24-well plate to reach 95% of confluence at 48 hours. At that time, a mimic wound was made using a plastic pipette tip in the well. Culture medium was carefully removed to eliminate free-floating cells and debris, and the wound-closure was followed. To analyze cell motility a bright field image was taken every 5 minutes for 20 hours, using the 10x objective of a high-resolution inverted Leica DMI 6000B time-lapse microscope and the LAS AF (Leica) software. The images obtained were analyzed using the ImageJ software. For that, the wound size was measured over time and the ratios of wound closure were quantified.

2.3.3.2 Time-lapse single-cell migration assay

Single-cell migration assay was also performed to study cell migration of individual cells. Single-cell analysis is important due to heterogeneity within the tumor.

Thus, migration was also evaluated by a single-cell assay in which cells are followed individually. After 32 hours of silencing for *KRAS* and/or *LGALS3*, HCT116 were plated at 1.5×10^4 cells/well to a 24-well plate. Then, cells were allowed to adhere through an overnight incubation at 37°C and a 5% CO₂ humidified atmosphere. At 48 hours of silencing, cell migration was analyzed taking a bright field image every 5 minutes, for 20 hours, using the 10x objective of a high-resolution inverted Leica DMI 6000B time-lapse microscope and the LAS AF (Leica) software. Ultimately, the images obtained were analyzed using the ImageJ software.

2.3.4 Matrigel invasion assay

To understand Gal-3 and/or KRAS impact on invasion, Matrigel invasion assay were performed to mimic the process of cell invasion and extravasation through the extracellular matrix (Justus *et al.*, 2014). For that, Matrigel-coated invasion inserts of 8 µm pore-size filters were used to mimic the basement membrane and McCoy's medium supplemented with 20% FBS function as a chemo-attractant. At 24 hours of RNAi experiment, the inserts (**Corning® BioCoat™ Insert**) were transferred, thaw and rehydrated in a 24-well plate with McCoy's medium and maintained at the incubator at 37°C and 5% CO₂ humidified atmosphere for 2 hours. After rehydration, the medium of the well was renewed for a complete McCoy's medium with 20% FBS as a stimulus for invasion. The medium of the insert chamber was also discarded and HCT116 was plated on that at 1.5×10^5 cells/ condition. Then, the 24-well plate containing the insert chambers were incubated for additional at 37°C and 5% CO₂ humidified atmosphere. After that, supernatants were collected for MMP's activity analysis, and the inserts were rinsed with PBS, fixed with 4% PFA, and the non-invading cells, at the top of the insert, were scrubbed. Then, the insert was again rinsed, and the membranes were collected and mounted, with invading cells to the top, onto a microscope slide with Vectashield Mounting Medium with DAPI (Vectashield, Vector Laboratories). At that time, a coverslip was placed on the top of the membrane, and it was sealed with nail polish. Then, filters were visualized through a Leica DM2000 fluorescence microscope (Leica Microsystems) to count nuclei of invading cells.

2.3.5 Gelatin zymography assay

Gelatin zymography was used to evaluate the matrix metalloproteinase (MMP) activity, namely, MMP-2 and MMP-9 that have the highest gelatinase activity. MMP are known as degrading agents of extracellular matrix proteins, which facilitate cell invasion and metastasis. Thus, to better understand the impact of silencing *KRAS* and/or *LGALS3* on cancer cell invasion gelatin zymography was performed. This technique is based on the principle that active MMP with gelatinase activity digest gelatin-polyacrylamide gel creating detectable clear bands contrasting with a blue stained background after Coomassie staining.

For that, after 24 hours of invasion assay, the medium was collected, centrifuged (6000 rpm; 3 minutes; 4°C) to eliminate dead cells and the supernatant transferred to a new eppendorf. Then, the samples were quantified using the DC protein assay Kit (Bio-Rad Laboratories). Finally, samples were prepared mixing 10 µg of protein samples with a non-reducing sample buffer (10% sodium dodecyl sulphate (SDS), 4% sucrose and 0.03% bromophenol blue in 0.5 M Tris

HCl, pH 6.8) and PBS 1x without denaturation of the sample. After that, separating and stacking polyacrylamide zymogram gels were prepared and the samples loaded to the respective lane of the polyacrylamide gel. Samples were then separated in 10% polyacrylamide zymogram gels with 0.1% gelatin (Sigma-Aldrich) at 80V for 4 hours. After electrophoresis, the gel was washed with 2% TritonX-100 for protein renaturation and incubated with MMP substrate buffer (50 mM Tris-HCl, pH 7.5, 10 mM CaCl₂, and 0.5% NaN₃) containing essential cofactors to allow the degradation of the gelatin through gelatinases, at 37°C for 16 hours. Then, the gel was incubated with Coomassie blue solution (Sigma-Aldrich) for 30 minutes, followed by a gentle destain to intensify the white proteolytic bands that correspond to degraded gelatin zones as a result of MMP activity. Finally, the gel was scanned, and the gelatinolytic bands analyzed.

2.3.6 Senescence-associated β -galactosidase assay

Senescent cells have an increased senescence-associated expression of β -galactosidase (SA- β -Gal) activity which can be detected through senescence-associated β -galactosidase assay in cultured cells. To understand KRAS and Gal-3 impact on senescence either directly or indirectly through p16^{INK4a} induction alterations, HCT116 cells were evaluated during the silencing for *KRAS* and/or *LGALS3* upon RNAi.

At time 0 of HCT116 silencing, the cells were plated on glass coverslips at 2×10^5 cells/well in 24-well plate for 48h. At 48h, cells were fixed with 4% PFA, incubated with β -galactosidase staining solution (staining solution 1x in water; 20 mg X-Gal in dimethylformamide (DMF); 10 uL Staining Supplement A; 10 uL Staining Supplement B; pH 5.9-6.1) ON at 37°C. Then, coverslips were mounted with Vectashield solution onto a microscope slide and sealed with nail polish. Finally, blue senescence cells were counted.

2.3.7 Western blot analysis

To understand how KRAS, Gal-3 and p16^{INK4a} regulate each other, their expression levels were analyzed after *KRAS* and/or *LGALS3* silencing by RNA interference. The KRAS and Gal-3 protein expression levels were investigated not only to verify if they regulate each other but also to confirm the silencing. Moreover, the expression levels of total and phosphorylated ERK (pERK) and AKT proteins were also analyzed to investigate KRAS and/or Gal-3 impact on cancer cell invasion and survival. For that, KRAS and Gal-3 proteins were silenced through *LGALS3* siRNA and *KRAS* siRNA both alone and in combination as described previously.

At 48 hours of silencing, cells were trypsinized, counted with Trypan Blue and processed for western blot analysis to confirm silencing efficiency. The procedure was initiated by the collection of the trypsinized cells, their centrifugation (2000 rpm; 10 minutes; 4°C), washing with PBS 1× followed by centrifugations (6000 rpm; 5 minutes; 4°C). Then, cells were lysed for 30 minutes on ice in RIPA buffer (1% NP-40, 150 mM NaCl, 50 mM Tris-HCl (pH 7.5), 2 mM EDTA) supplemented with a mix of phosphatase and protease inhibitors (10 µg/mL NaF, 20 µg/mL Na₃VO₄, 10 µg/mL PMSF, 10 µg/mL Aprotinin, 10 µg/mL Leupeptin and 50 µg/mL Na₄P₂O₇). After that, cells were centrifuged (10 minutes, 14000 rpm, 4°C), the supernatants were transferred to new eppendorfs on ice and pellets were discarded. The supernatants were store on ice until protein quantification using the DC protein assay Kit (Bio-Rad Laboratories). Finally, 50 µg of protein were dissolved in Laemmli buffer 4x (0.5 M Tris-HCl pH 6.8, 9.2 g SDS, 40 mL Glycerol, 5% β-mercaptoethanol, 5% bromophenol blue). Then, samples were subjected to denaturing conditions (5 minutes; 95°C). Finally, samples were loaded to the respective lane of a polyacrylamide gel. Proteins were separated in 15% polyacrylamide gel and transferred to a nitrocellulose membrane (GE Healthcare) for 2h at 100V. Next, membranes were blocked for 45 minutes with 5% milk in PBS-T in order to block nonspecific binding sites. After blocking, membranes were briefly washed in PBST and then incubated with anti-KRAS (1:1000, Sigma), anti-Gal-3 antibodies (1:500, Santa Cruz Biotechnology), anti-p16 (1:500, ProteinTech Group), anti-actin (1:1000, Cell Signaling), anti-pERK (1:1000, Cell Signaling), anti-ERK 1/2 (1:1000, Cell Signaling), anti-pAKT (1:1000, Cell Signaling) or anti-AKT (1:1000, Cell Signaling) antibodies to confirm the protein expression levels of proteins of interest. Membranes were washed 4 times in PBST for 5 minutes. Secondary antibodies used were anti-mouse (1:2000, Santa Cruz Biotechnology), anti-goat (1:2000, Santa Cruz Biotechnology), and anti-rabbit (1:2000, GE Healthcare). Membranes were washed 6 times in PBST for 5 minutes. Protein bands were then revealed with ECL Western Blotting Detection Kit (Life Science).

2.4 Statistical Analysis

All statistical analyses were performed using the Graph Pad Prism 6.0 software.

All experiments were treated as means ± SD and Two and One-way ANOVA tests followed by Dunnett's multiple comparison test were performed. Statistically significant values were presented as * for $p \leq 0.05$; ** for $p \leq 0.01$; *** for $p \leq 0.001$.

CHAPTER III. RESULTS

3.1 Co-immunoprecipitation and co-localization studies evidence that KRAS/Galectin-3/p16^{INK4a} interact as a multiprotein complex

We started by testing our hypothesis that KRAS/Galectin-3/p16^{INK4a} may form a multiprotein complex. Preliminary results from our group (data not published) provided evidences, by western blot analysis and immunofluorescence experiments, that KRAS, Gal-3 and p16^{INK4a} might exhibit a reciprocal regulation and could establish proximity. Here, we decided to confirm the results obtained by performing both co-localization and co-IP assays to better understand if they are close enough to interact and/or if they physically interact.

3.1.1 Co-immunoprecipitation studies on colon cell lines

Co-immunoprecipitation studies were performed in order to confirm KRAS/Galectin-3/p16^{INK4a} physical interaction (**Figure 19**). KRAS, Gal-3 and p16^{INK4a} were immunoprecipitated from total cell lysates of CRC cells, namely SW480, HCT116 and normal colon cells stably transfected with KRAS (NCM460 *Flag-KRAS^{WT}* and NCM460 *Flag-KRAS^{G12V}*). The IP was assessed through Protein G Sepharose beads, followed by western blot analysis. For preclear (PREC) preparation, total cell lysates were incubated, during 1 hour, with beads pre-treated with 1%, 2% or 5% BSA (PREC or PREC 1%, 2% or 5% BSA, respectively), to minimize beads unspecific protein binding. Lysate preclears correspond then to the resulting pellet, serving as IP control to exclude unspecific binding of the protein of interest to the beads, while the respective supernatants were used for immunoprecipitation with the respective antibodies.

For immunoprecipitation of p16^{INK4a} (IP p16), of Gal-3 (IP Gal-3), or of KRAS (IP KRAS), supernatants of the precleared lysates were incubated with the anti-p16^{INK4a}, the anti-Gal-3 or the anti-KRAS primary antibodies, respectively. The protein of interest-primary antibody complexes were then incubated, for 1 hour, with the 1% BSA pre-treated beads, leading to their capture for further elution in denaturing sample buffer. Of note, each IP not only captures the specific protein recognized by the antibody, but also the protein-interacting partners that physically interact with the primary protein target. Thus, by western blot, using antibodies to detect these putative interacting proteins, we can verify if they are indeed captured by the beads as part of the multiprotein complex.

In SW480 cells, western blot against KRAS on IP KRAS revealed the existence of two proteins, one of approximately 50 kDa and another of approximately 22 kDa, of the same molecular weight as the bands found on total lysates (TL) (**Figure 19**). These suggest that both bands are

recognized by the anti-KRAS antibody. While the lower molecular weight protein is appointed as KRAS, no information could be found regarding the identity of the protein of higher molecular weight. In principle, the denaturing conditions of our experiments would prevent the formation of KRAS duplets that could be possibly appointed. Further experiments should be performed, excising and digesting the 50 kDa band, for further identification through proteomics. Importantly, one should mention that the same bands were recognized on preclear lysates PREC, what could indicate unspecific binding of these KRAS antibody-recognized proteins to the beads. The pre-treatment of our beads with 1% BSA (Preclear 1% BSA) was very effective in reducing such unspecific binding, and therefore, always used in further experiments. Interestingly, IP Gal-3 captured both 50 kDa and the 22 kDa KRAS antibody-recognized proteins, while the IP p16 only captured the protein of higher molecular weight. Altogether, these results indicate that Gal-3, but not p16, co-immunoprecipitate with the 22 kDa KRAS protein. In addition, Gal-3 and p16 co-immunoprecipitate with another higher molecular weight protein, recognized by the anti-KRAS antibody, but which remains to be identified.

On its turn, the western blot using the anti-Gal-3 antibody evidenced unspecific binding of Gal-3 to the beads, which impaired further analysis of the KRAS and of the p16^{INK4a} immunoprecipitates (**Figure 19**). However, the western blot using the anti-p16^{INK4a} antibody revealed the existence of a thin band of approximately 16 kDa in the IP p16. The same thin band, apparently different from the one present in the preclears, was also observed in the Gal-3 and KRAS immunoprecipitates. These results may suggest that both proteins co-immunoprecipitate with p16^{INK4a}. To confirm these, we would like to repeat these immunoprecipitation studies with other beads, having minor background, and to identify the co-immunoprecipitated proteins by proteomics.

Further immunoprecipitation studies with other cells as HCT116, and NCM460 *Flag-KRAS*^{WT} and NCM460 *Flag-KRAS*^{G12V} revealed unspecific binding of the proteins of interest to the beads, which might be certainly cell line dependent, but that impaired all co-immunoprecipitation analysis. This means that we cannot control the protein binding to the beads, not being sure if the proteins are linked directly to the protein complex recognized by the antibody or directly to the beads. We tried to overcome these problems of unspecific beads binding by testing different concentrations and sources of BSA, without success.

In summary, in SW480 cells, we confirmed that Gal-3 co-immunoprecipitates with KRAS and we believe to have evidences that p16^{INK4a} also co-immunoprecipitates with Gal-3 and with KRAS, forming a multiprotein complex. Further experiments are however being performed to support these findings.

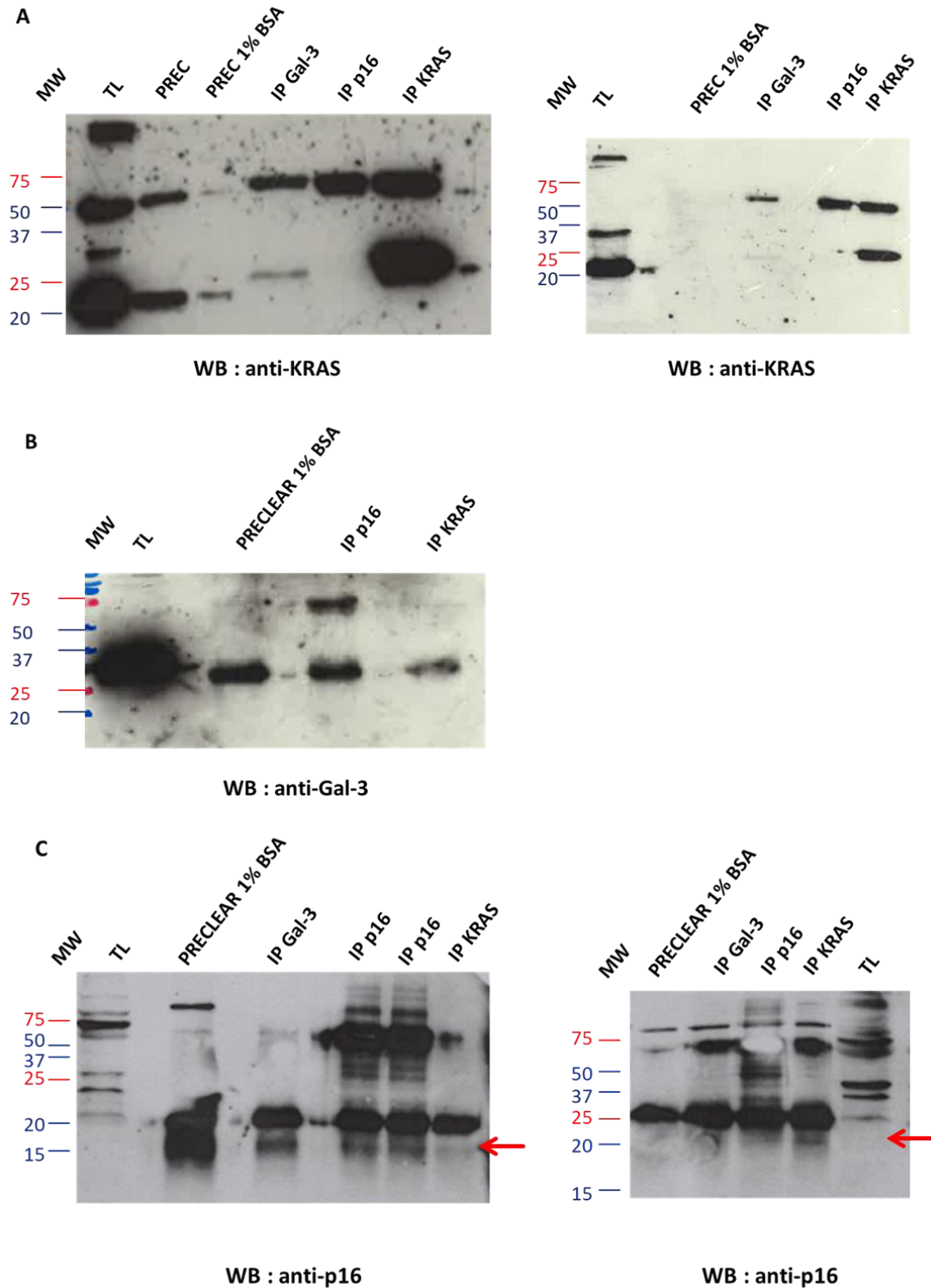


Figure 19 - Analysis of KRAS, Gal-3, and p16^{INK4a} co-immunoprecipitations in SW480 through Protein G Sepharose beads followed by Western Blot.

KRAS, Gal-3, and p16^{INK4a} were immunoprecipitated from SW480 total cell lysates using Protein G Sepharose beads and the samples were analysed by western blot using the polyacrylamide gel at 15% of concentration. (A) Western Blot anti-KRAS: Membranes were incubated with anti-KRAS primary antibody at optimal dilution 1:1000 followed by anti-mouse secondary antibody at dilution 1:10000 (reproduced twice). Western Blot anti-Gal-3: Membrane was incubated with anti-Gal-3 primary antibody at optimal dilution 1:500 and anti-goat secondary antibody at dilution 1:5000 (reproduced once). Western Blot anti-p16: Membranes were incubated with anti-p16 antibody at optimal dilution 1:250 and anti-goat secondary antibody at dilution 1:5000 (reproduced twice). All blots were revealed with Clarity Western ECL Substrate.

3.1.2 Co-localization studies on NCM460 cell lines transfected with Flag-KRAS hotspot mutations

To confirm and complement previous IP results suggesting that KRAS/Galectin-3/p16^{INK4a} form a multiprotein complex, we decided to evaluate the co-localization of these proteins through high-resolution confocal microscopy. However, since the commercially available KRAS antibodies are not suitable for immunofluorescence, co-localization studies could not be performed on SW480 or on HCT116 cells expressing endogenous KRAS mutations. Therefore, cells stably transfected with KRAS wild-type: NCM460 *Flag-KRAS*^{WT}, or with KRAS hotspot mutations: NCM460 *Flag-KRAS*^{G12V}, NCM460 *Flag-KRAS*^{G13D}, and NCM460 *Flag-KRAS*^{G12D} were used to perform co-localization studies. These cell lines, previously established in our laboratory, have the advantage of possessing a Flag linked to KRAS proteins, thus allowing KRAS recognition through the anti-Flag antibody. Double immunostainings were then performed using antibodies targeting anti-Flag to recognize KRAS-Flag in combination with anti-Gal-3 or anti-p16; and targeting anti-Gal-3 in combination with anti-p16. Single immunostainings and other controls, lacking one or both primary antibodies, were made on NCM460 *Flag-KRAS*^{WT} to define the best acquisition settings for each fluorochrome and to exclude cross-reactions (Figure 20, **Figure 21**, **Figure 22**). Of note, the same acquisition settings were applied to all cell lines to have comparable results between the different cell lines. Analyzing the control microphotographs obtained for NCM460 *Flag-KRAS*^{WT}, it was possible to observe that the antibodies used for Flag-KRAS, Gal-3 and p16^{INK4a} stainings exhibited specific cell signals with weak unspecificity (Figure 20, **Figure 21**, **Figure 22**). The respective negative controls, lacking primary antibodies and presenting only secondary antibodies (Gal-3 negative control, p16^{INK4a} negative control and Flag-KRAS negative control) had, in general, a reduced background (Figure 20, **Figure 21**, **Figure 22**). Similarly, controls with the secondary antibody for Gal-3 and the primary antibodies for Flag-KRAS (Flag-KRAS+Donkey anti-goat Alexa 488) and p16^{INK4a} (p16+Donkey anti-goat Alexa 488) displayed a weak background noise (Figure 20). The same happened for controls with the secondary antibody for p16^{INK4a} and the primary antibodies for Flag-KRAS (Flag-KRAS+Chicken anti-rabbit Alexa 647) and Gal-3 (Gal-3+Chicken anti-rabbit Alexa 647) (**Figure 21**); and for the controls with the secondary antibody for Flag-KRAS and the primary antibody for p16^{INK4a} (p16+ Goat anti-mouse Alexa 488) (**Figure 22**). However, the controls for the Flag-KRAS secondary antibody Chicken anti-mouse Alexa 594, exhibited a higher background noise comparing with the Flag-KRAS secondary antibody Goat anti-mouse Alexa 488, as demonstrated by the stainings

without Flag-KRAS primary antibody (Flag negative control) and the primary antibody for Gal-3 (Gal-3+Chicken anti-mouse Alexa 594) (**Figure 22**).

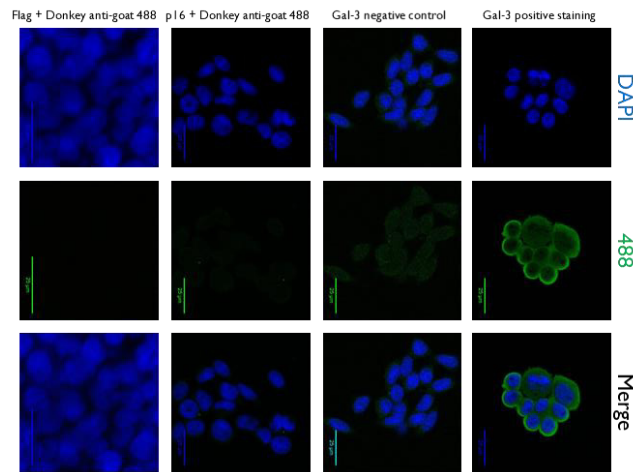


Figure 20 - Confocal immunofluorescence microscope analysis of single staining and control conditions for Gal-3 localization in NCM460 Flag-KRAS^{WT}.

Single staining plus further controls for Gal-3 staining. NCM460 Flag-KRAS^{WT} cells were cultured on coverslips with no treatment and fixed with 4% PFA. Gal-3 was stained with secondary antibody Donkey anti-goat Alexa 488 (green) and cell nuclei were counterstained with DAPI (blue). Gal-3 positive staining with primary and secondary antibodies for Gal-3 (higher panels), Gal-3 negative control with only secondary antibody and controls with the secondary antibody for Gal-3 and the primary antibodies for Flag-KRAS (Flag-KRAS+Donkey anti-goat Alexa 488) and p16^{INK4a} (p16+Donkey anti-goat Alexa 488) displayed a weak signal of unspecificity demonstrating that Donkey anti-goat Alexa 488 secondary antibody is a good antibody with weak signals of unspecificity and without cross-reaction with the primary antibodies that we intended to use for co-localization studies.

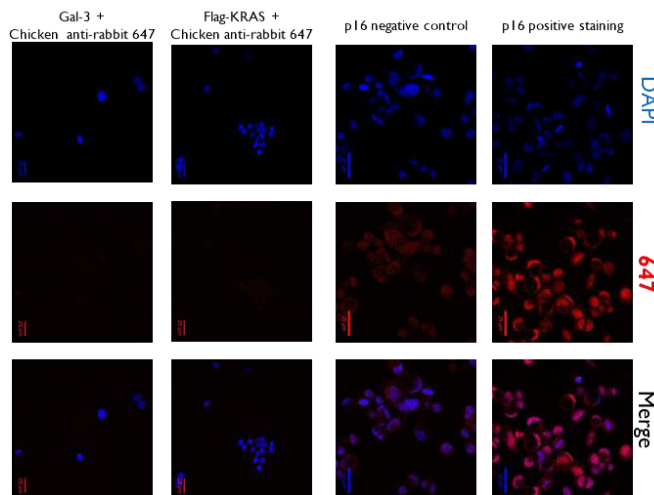


Figure 21 - Confocal immunofluorescence microscope analysis of single staining and control conditions for P16^{INK4a} localization in NCM460 Flag-KRAS^{WT}.

Single staining and further controls for p16^{INK4a}. NCM460 Flag-KRAS^{WT} cells were cultured on coverslips with no treatment and fixed with 4% PFA. p16^{INK4a} was stained with the secondary antibody Chicken anti-rabbit Alexa 647 (red) and cell nuclei were counterstained with DAPI (blue). p16^{INK4a} positive staining with primary and secondary antibodies for p16 (higher panels), p16^{INK4a} negative control with only secondary antibody and controls with the secondary antibody for p16^{INK4a} and the primary antibodies for Flag-KRAS (Flag-KRAS+Chicken anti-rabbit Alexa 647) and Gal-3 (Gal-3+Chicken anti-rabbit Alexa 647) showed some unspecificity without cross-reaction with the primary antibodies that we intended to use for co-localization studies.

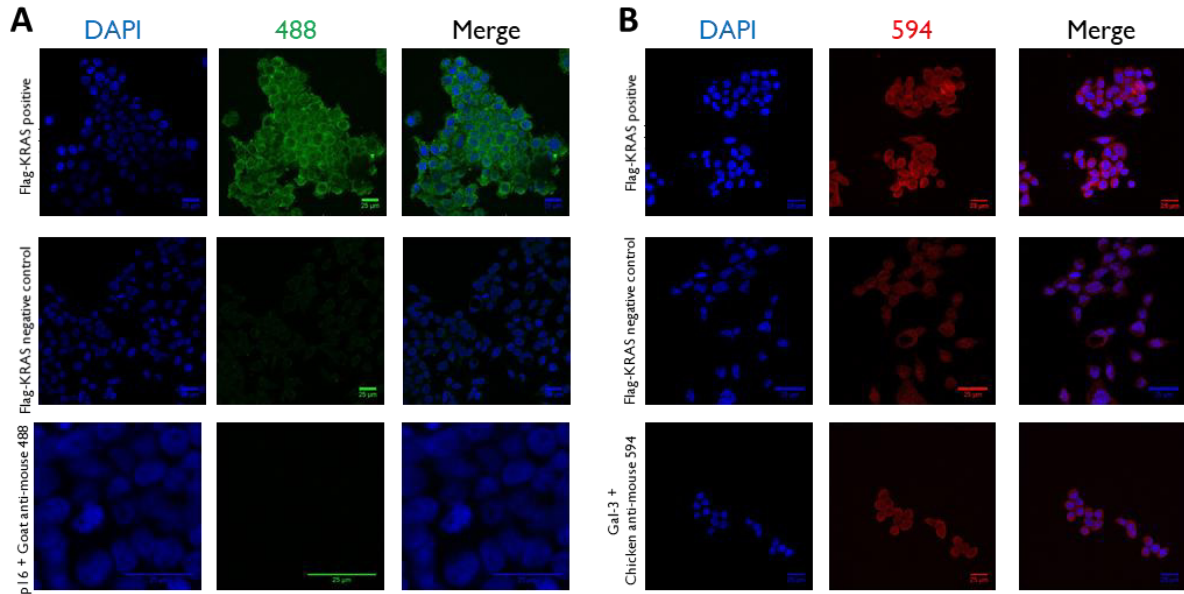


Figure 22- Confocal immunofluorescence microscope analysis of single staining and control conditions for FLAG localization in NCM460 *Flag-KRAS*^{WT}.

Single staining and further controls for Flag-KRAS. NCM460 *Flag-KRAS*^{WT} cells were cultured on coverslips with no treatment and fixed with 4% PFA. Flag was stained with **secondary antibody Goat anti-mouse Alexa 488 (green)** (A); or **secondary antibody Chicken anti-mouse Alexa 594 (red)** (B) and cell nuclei were counterstained with DAPI (blue). **A** - Flag positive staining with primary and secondary antibodies for Flag (higher panels), Flag negative control with only secondary antibody and controls with the secondary antibody for Flag-KRAS and the primary antibody for p16^{INK4a} (p16+ Goat anti-mouse Alexa 488) showed a weak signal of unspecificity demonstrating that Donkey anti-goat Alexa 488 secondary antibody is a good antibody with weak signals of unspecificity and without cross-reaction with the primary antibodies that we intended to use for co-localization studies. However, this antibody can not be used for double staining with Gal-3, because Gal-3 is an antibody produced in goat, so to overcome cross-reaction between them, another secondary antibody was considered: **B** - Flag positive staining with primary and secondary antibodies for Flag (higher panels), Flag negative control with only secondary antibody and/or with the primary antibody for Gal-3 (Gal-3+Chicken anti-mouse Alexa 594) showed some unspecificity without cross-reaction with the primary antibodies that we intended to use for co-localization studies.

Although some problems of background noise, we discarded the hypothesis of secondary antibodies cross-reactions and the double immunostainings were performed firstly on NCM460 *Flag-KRAS*^{WT} (**Figure 23**). A careful analysis demonstrated that *Flag-KRAS*, Gal-3 and p16^{INK4a} localization patterns were very similar to the ones observed through single immunostainings, confirming that double immunostainings did not affect protein localization. Images evidenced that Gal-3 is mainly cytoplasmic and perinuclear, but it exhibits also membrane and residual nuclear stainings. p16^{INK4a} is mainly cytoplasmic, preferentially located at the perinuclear zone, with residual nuclear localization. On its turn, *Flag-KRAS* is preferentially located at the membrane and at the cytoplasm with, however, residual nuclear localization (**Figure 23**). Interestingly, the co-immunofluorescence analysis revealed that *Flag-KRAS* and Gal-3 but also the *Flag-KRAS* and p16^{INK4a} and the p16^{INK4a} and Gal-3 seem to colocalize in specific dots spread throughout the cytoplasm. Overall, in NCM460 *Flag-KRAS*^{WT} the double immunostainings suggest that KRAS might co-localize with Gal-3 and p16^{INK4A} and that Gal-3 might co-localize with p16^{INK4A} what is suggestive of the existence of a multiprotein complex.

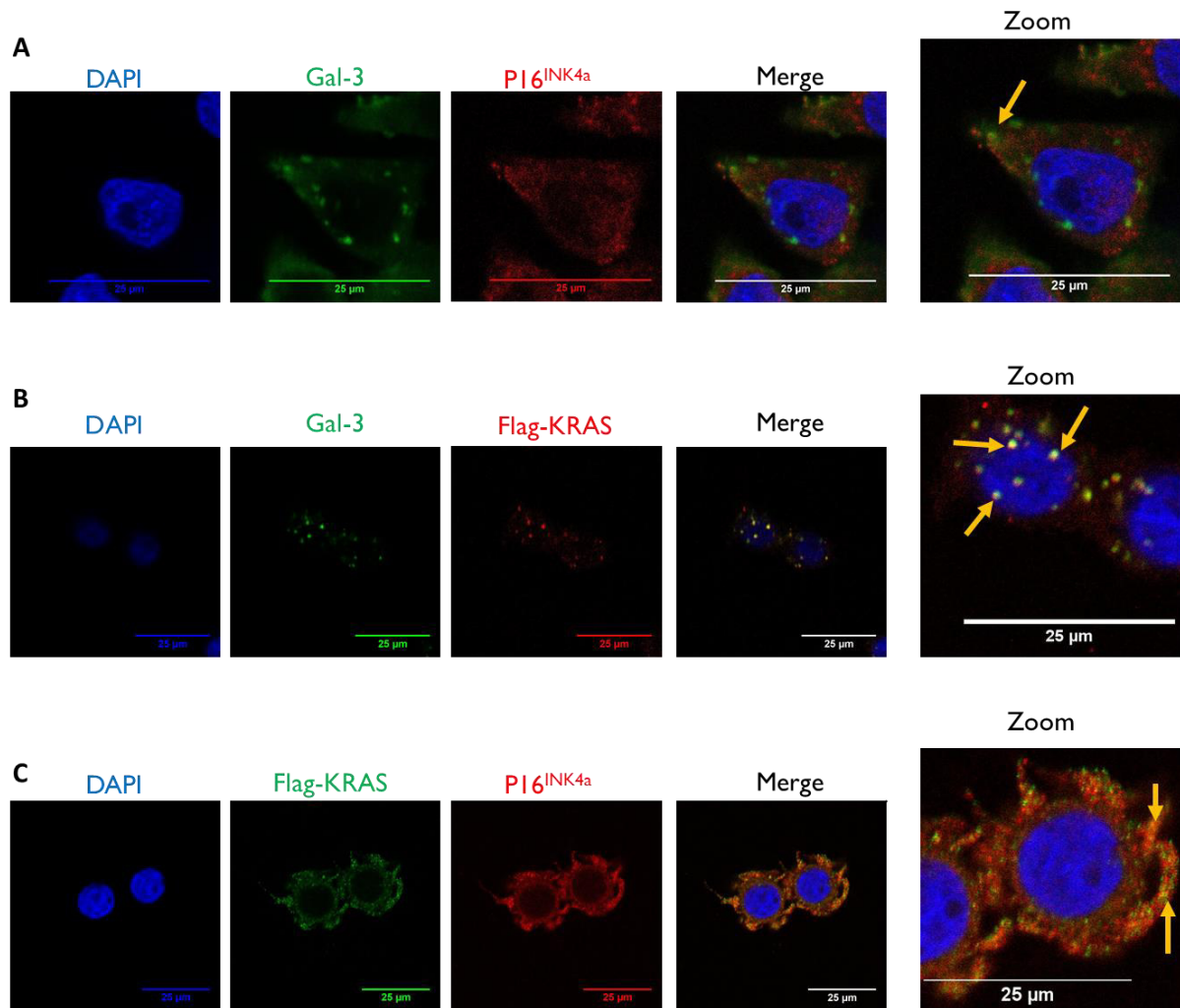


Figure 23 - Confocal fluorescence microscope analysis of double staining for Gal-3 + p16^{INK4a}, Gal-3 + Flag-KRAS, Flag-KRAS + p16^{INK4a} co-localization in NCM460 *Flag-KRAS*^{WT} cell lines.

NCM460 *Flag-KRAS*^{WT} cells were fixed in PFA and cell nuclei stained through DAPI. A – Cells were stained simultaneously with primary antibodies Gal-3 and p16 and their respective secondary antibodies, Donkey anti-goat Alexa 488 (green) and Chicken anti-rabbit Alexa 647 (red). B – Cells were stained simultaneously with primary antibodies Gal-3 and Flag and their respective secondary antibodies, Donkey anti-goat Alexa 488 (green) and Chicken anti-mouse Alexa594 (red). C – Cells were stained with primary antibodies Flag-KRAS and p16^{INK4a} and their respective secondary antibodies, Goat anti-mouse Alexa 488 (green) and Chicken anti-rabbit Alexa647 (red). All images were obtained through the laser confocal microscopy Leica TCS SP5II using a HCX PL APO CS 63x 1.40 OIL UV objective.

Double immunostainings were repeated on NCM460 *Flag-KRAS* harbouring mutated KRAS isoforms in order to evaluate the influence of KRAS mutations on the KRAS/Galectin-3/p16^{INK4a} axis. New microphotographs were acquired corresponding to double immunostainings in NCM460 *Flag-KRAS*^{WT} in comparison with NCM460 *Flag-KRAS*^{G12V}, NCM460 *Flag-KRAS*^{G13D}, and NCM460 *Flag-KRAS*^{G12D} with the same acquisition settings in order to have comparable results (**Figure 24**, **Figure 25**, **Figure 26**). Interestingly, *Flag-KRAS*/Gal-3 double stainings demonstrated that both proteins exhibit a very similar pattern, being mainly cytoplasmic with residual nuclear localization (**Figure 24**). Although very similar

amongst all NCM460 *Flag-KRAS* cell lines, the presence of double staining dots, suggesting both proteins co-localization seems to be higher in mutant versus wildtype cells.

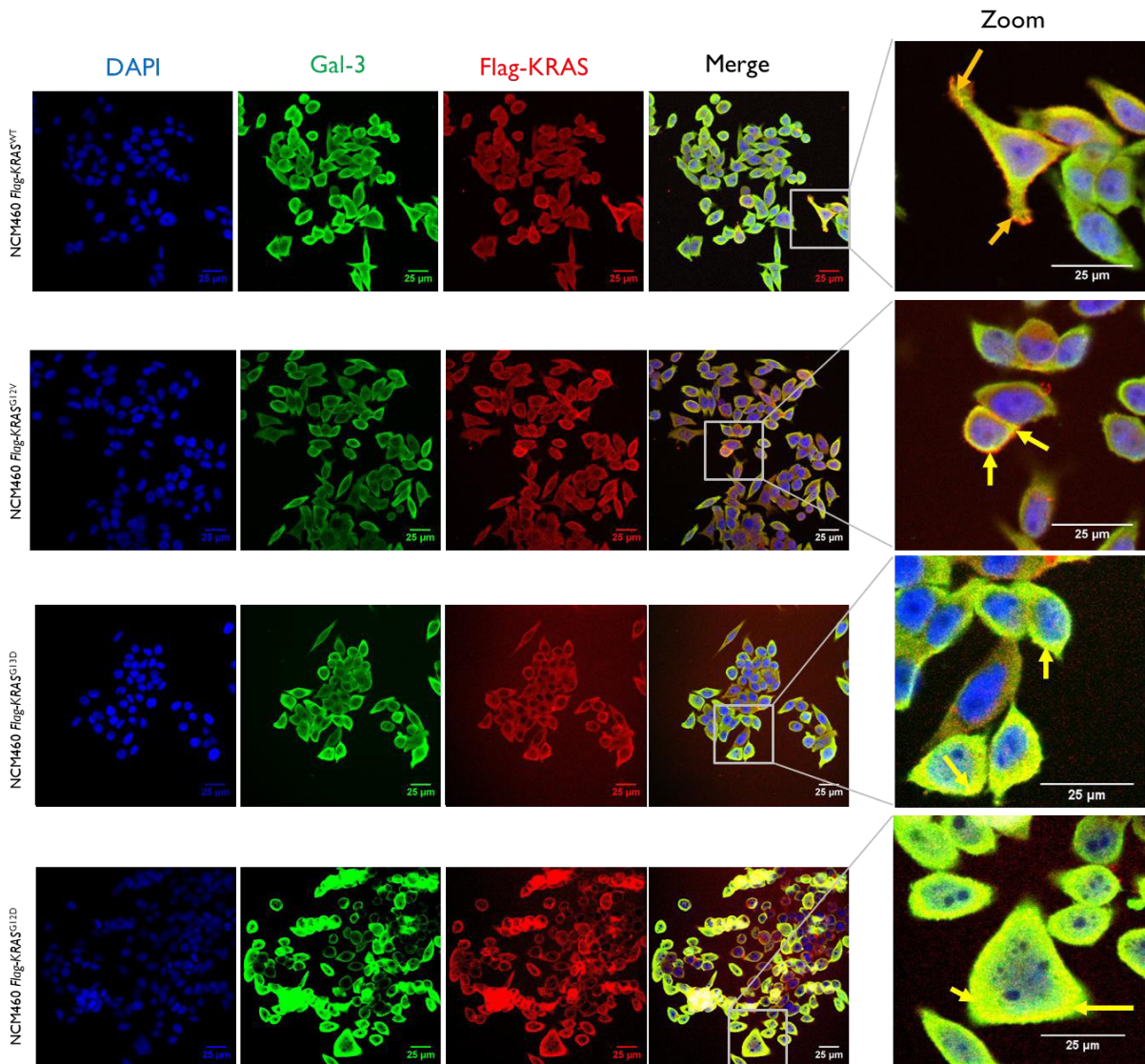


Figure 24 - Confocal fluorescence microscope analysis of double staining for Gal-3 + Flag-KRAS localization in NCM460 *Flag-KRAS* transfected cell lines.

NCM460 *Flag-KRAS*^{WT}, NCM460 *Flag-KRAS*^{G12V}, NCM460 *Flag-KRAS*^{G13D}, and NCM460 *Flag-KRAS*^{G12D} cells were fixed in PFA and stained simultaneously with primary antibodies Gal-3 and Flag and their respective secondary antibodies, Donkey anti-goat Alexa 488 (green) and Chicken anti-mouse Alexa 594 (red). Cell nuclei were also stained through DAPI. The confocal immunofluorescence photomicrographs were obtained through the laser confocal microscopy Leica TCS SP5II using a HCX PL APO CS 63x 1.40 OIL UV objective.

Gal-3/p16^{INK4a} co-immunostainings revealed also differences regarding protein localization amongst the cell lines with different KRAS status. Gal-3 showed mainly cytoplasmic with residual nuclear localization, which was particularly evident in the NCM460 *Flag-KRAS*^{G13D} and the NCM460 *Flag-KRAS*^{G12D} cells. However, while in NCM460 *Flag-KRAS*^{wt}, p16^{INK4a} is mainly cytoplasmic, being preferentially located at the perinuclear zone with residual nuclear exclusion, in all cell lines harbouring KRAS mutations (NCM460 *Flag-KRAS*^{G12V}, NCM460

Flag-KRAS^{G13D} and NCM460 *Flag-KRAS^{G12D}*) p16^{INK4a} exhibits increased and evident nuclear staining. The co-localization yellow dots are not so evident in NCM460 *Flag-KRAS^{wt}* and NCM460 *Flag-KRAS^{G12V}* and this might be because Gal-3 is an overexpressed protein and p16^{INK4a} is a protein expressed at very low levels, thus the p16^{INK4a} signal might be masked by the Gal-3 staining. In contrast, in NCM460 *Flag-KRAS^{G13D}* and NCM460 *Flag-KRAS^{G12D}* the co-localization dots are more evident and are both localized nuclear and perinuclear areas (Figure 25).

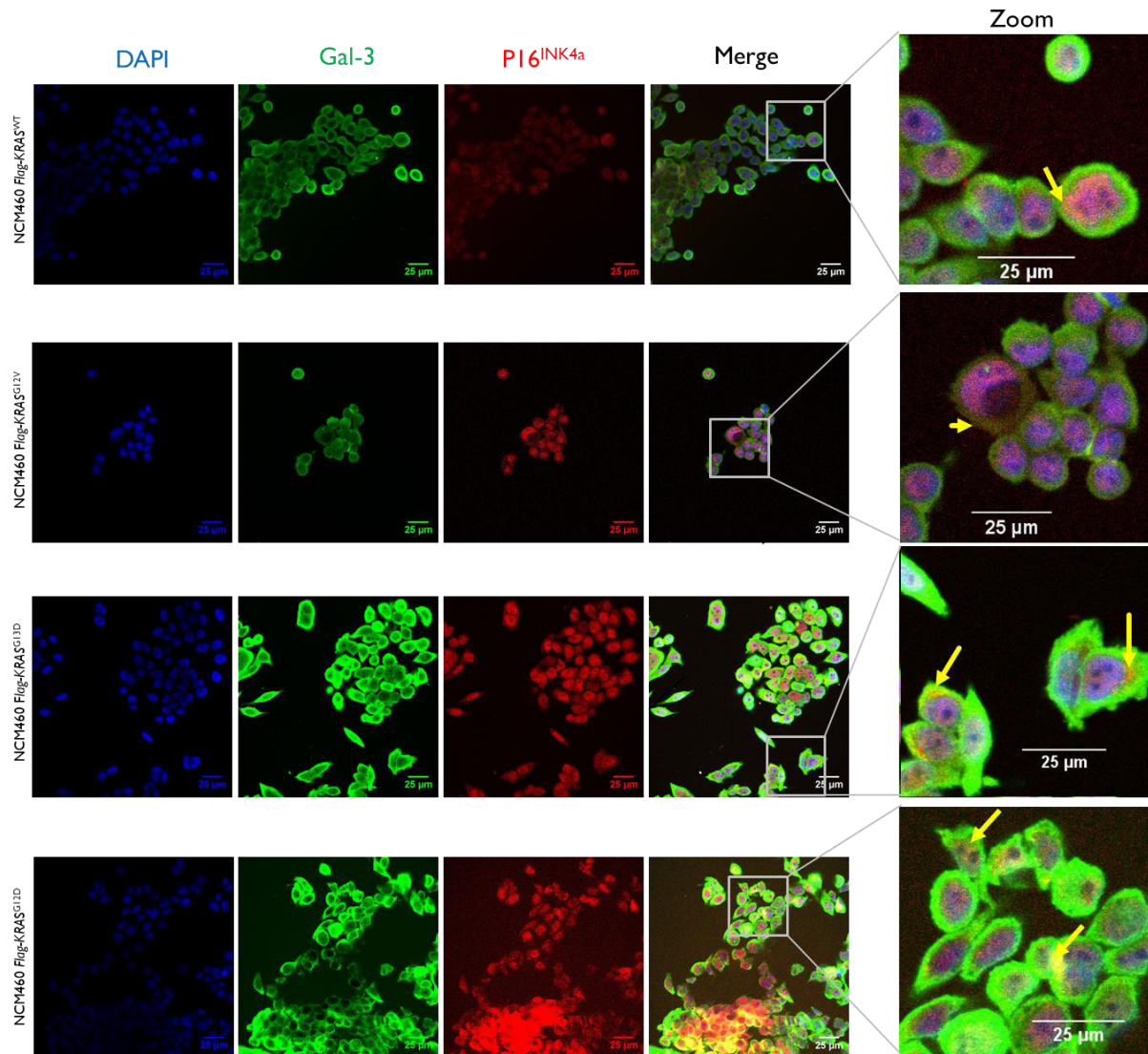


Figure 25 - Confocal fluorescence microscope analysis of double staining for Gal-3 + p16^{INK4a} localization in NCM460 *Flag-KRAS* transfected cell lines.

NCM460 *Flag-KRAS^{WT}*, NCM460 *Flag-KRAS^{G12V}*, NCM460 *Flag-KRAS^{G13D}*, and NCM460 *Flag-KRAS^{G12D}* cells were fixed in PFA and stained simultaneously with primary antibodies Gal-3 and p16^{INK4a} and their respective secondary antibodies, Donkey anti-goat Alexa 488 (green) and Chicken anti-rabbit Alexa 647 (red). Cell nuclei were also stained through DAPI. The confocal immunofluorescence photomicrographs were obtained through the laser confocal microscopy Leica TCS SP5II using a HCX PL APO CS 63x 1.40 OIL UV objective.

KRAS/p16^{INK4a} double immunostainings analysis evidenced also differences between cell lines, revealing an impact of KRAS mutations (**Figure 26**). In NCM460 *Flag-KRAS*^{WT} we observe low levels of both KRAS and p16^{INK4a} proteins with double staining dots preferentially localized at the cell periphery. In NCM460 *Flag-KRAS*^{G12V} and preferentially in NCM460 *Flag-KRAS*^{G13D}, a higher content of both Flag-KRAS and p16^{INK4a} levels were observed. Considering the co-staining dots, they were more evident and preferentially cytoplasmic in the NCM460 *Flag-KRAS*^{G13D} cells, while in the NCM460 *Flag-KRAS*^{G12D} cells they were less abundant and preferentially located at the nucleus.

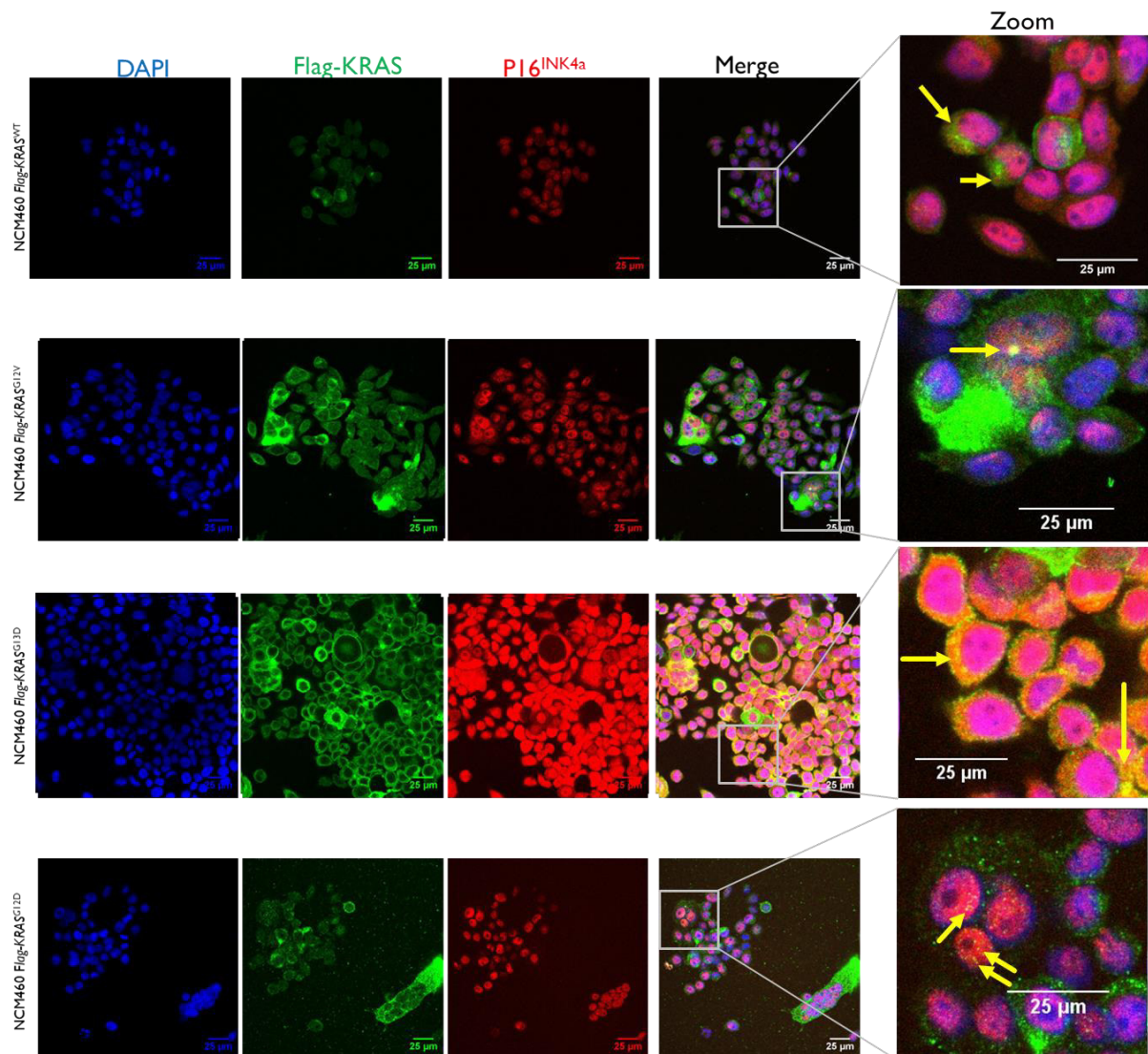


Figure 26 - Confocal fluorescence microscope analysis of double staining for Flag-KRAS + p16^{INK4a} localization in NCM460 *Flag-KRAS* transfected cell lines.

NCM460 *Flag-KRAS*^{WT}, NCM460 *Flag-KRAS*^{G12V}, NCM460 *Flag-KRAS*^{G13D}, and NCM460 *Flag-KRAS*^{G12D} cells were fixed in PFA and stained simultaneously with primary antibodies Flag-KRAS and p16^{INK4a} and their respective secondary antibodies, Goat anti-mouse Alexa 488 (green) and Chicken anti-rabbit Alexa 647 (red). Cell nuclei were also stained through DAPI. The confocal immunofluorescence photomicrographs were obtained through the laser confocal microscopy Leica TCS SP5II using a HCX PL APO CS 63x 1.40 OIL UV objective.

Overall, our results suggest that KRAS mutations might have an impact on KRAS/Gal-3, on KRAS/p16^{INK4a} and on Gal-3/p16^{INK4a} double immunostainings. In fact, the detailed analyses suggested co-localization between Flag-KRAS/Gal-3, Gal-3/p16^{INK4a}, and Flag-KRAS/p16^{INK4a} (**Figure 24, Figure 25, Figure 26**) which can be observed by the presence of yellow dots, more evidently present at the cytoplasm of NCM460 *Flag-KRAS^{G13D}* cells. The yellow stainings may however result from the overlap or close proximity between green and red signals. To exclude close proximity from overlap staining, which indicates co-localization, we performed pixel analysis by JACoP under ImageJ software to obtain Pearson's Correlation Coefficient (PCC), Overlap Coefficient (OC) and their k1 and k2, and Mander's Overlap Coefficient (MOC), M1 and M2. The values obtained are represented on **Table 3** **Erro! A origem da referência não foi encontrada.**, and they are a mean result of the analysis of at least 50 cells per condition, in at least 2 independent experiments.

PCC, ranging from -1 to 1, can estimate the association strength between two proteins, but it is not a real value of colocalization quantification. Thus, looking at PCC, the values between 1 and 0.5 indicates a positive correlation, namely for KRAS/Gal-3 and Gal-3/p16^{INK4a} in all NCM460 *Flag-KRAS* cells and for KRAS/p16^{INK4a} in NCM460 *Flag-KRAS^{WT}* (**Table 3**). However, values between -0.5 and 0.5 do not allow conclusions, namely, KRAS/p16^{INK4a} in NCM460 *Flag-KRAS^{G12V}*, NCM460 *Flag-KRAS^{G13D}* and NCM460 *Flag-KRAS^{G12D}*. Although PCC is a good parameter because it is independent of background noise, it also is insensitive to differences in signal intensities. Thus, because we are working with very low p16^{INK4a} expression levels, and with two other proteins of high expressions, KRAS and Gal-3, the colocalization values could be masked. Thus, the need to analyze the colocalization through other parameters became very important.

Therefore, the OC, k1 and k2, a variation of PCC, were also collected and analyzed. OC is an upgrade of PCC that considers the differences in intensities between two channels and the background noise. Thus, this value must be adjusted to a common threshold for all conditions, and specifically for each fluorochrome. OC values varying between 0 and 1 mean no or full colocalization, respectively. K₁ and K₂ are the estimation of the amount of colocalization from one channel over another. Here K₁ is the estimation of amount of colocalization of channel (1) over the channel (2) and K₂ corresponds to channel (2) over the channel (1), as identified in each condition on table. Considering these analyses, our results suggested colocalization for KRAS/Gal-3, KRAS/p16^{INK4a}, and Gal-3/p16^{INK4a} in all transfected cell lines, and Gal-3 is the main contributor for these colocalization in both KRAS/Gal-3 and Gal-3/p16^{INK4a}, whereas KRAS is the key contributor on KRAS/p16^{INK4a} colocalization (**Table 3**).

PCC and OC are suitable for comparative analysis and not for the estimation of the quantity of colocalization, by this way MOC was also calculated in order to have an estimation of the colocalization quantity. Moreover, M1 and M2, which varies from 0 to 1, are the estimation of the amount of colocalization from one channel over the other, so it indicates the percentage of overlapping pixels, normalized against the total pixel intensity. Therefore, Mander's can be considered as a real quantification of colocalization. Our results suggested that KRAS/Gal-3, KRAS/p16^{INK4a} and Gal-3/p16^{INK4a} colocalize in all cell lines, since high levels for M1 and M2, and different from zero, were obtained (Table 3).

Table 3 - Values of Gal-3/Flag-KRAS, p16^{INK4a}/Flag-KRAS and Gal-3/ p16^{INK4a} colocalization analysis in NCM460 Flag-KRAS cells. Pearson's Coefficient, Overlap Coefficient and their respective K1&K2 values, and Mander's coefficients M1&M2 were obtained performing the colocalization analysis by JACoP. Overlap Coefficient, K1&K2, and Mander's coefficients M1&M2 were adjusted to the threshold pre-defined for each fluorochrome and applied for all conditions in order to have comparable results. The values showed are a mean of at least 50 cells/ condition in NCM460 Flag-KRAS^{WT}, NCM460 Flag-KRAS^{G12V}, NCM460 Flag-KRAS^{G13D} and NCM460 Flag-KRAS^{G12D}.

Double immunostaining Gal-3 (1) + Flag-KRAS (2)						
	PCC	OC	K1	K2	M1	M2
NCM460 Flag-KRAS ^{WT}	0,536	0,794	1,08	0,54	0,654	0,275
NCM460 Flag-KRAS ^{G12V}	0,842	0,55	0,637	0,485	0,87	0,433
NCM460 Flag-KRAS ^{G13D}	0,648	0,764	1,24	0,367	0,697	0,435
NCM460 Flag-KRAS ^{G12D}	0,528	0,204	0,353	0,119	0,842	0,264
Double immunostaining p16 (1) + Flag-Kras (2)						
	PCC	OC	K1	K2	M1	M2
NCM460 Flag-KRAS ^{WT}	0,5245	0,801	0,463	1,254	0,165	0,524
NCM460 Flag-KRAS ^{G12V}	0,5	0,805	0,487	1,386	0,215	0,406
NCM460 Flag-KRAS ^{G13D}	0,48	0,659	0,34	1,266	0,932	0,975
NCM460 Flag-KRAS ^{G12D}	0,208	0,756	0,439	1,319	0,247	0,539
Double immunostaining Gal-3 (1) + p16 (2)						
	PCC	OC	K1	K2	M1	M2
NCM460 Flag-KRAS ^{WT}	0,526	0,934	2,642	0,348	0,337	0,488
NCM460 Flag-KRAS ^{G12V}	0,749	0,927	1,499	0,586	0,759	0,458
NCM460 Flag-KRAS ^{G13D}	0,753	0,405	0,616	0,267	0,924	0,93
NCM460 Flag-KRAS ^{G12D}	0,518	0,726	1,319	0,247	0,456	0,724

In detail, KRAS/Gal-3 seems to have a higher colocalization on NCM460 Flag-KRAS^{G12V} and NCM460 Flag-KRAS^{G12D} cells, suggesting a high impact of KRAS^{G12V} and KRAS^{G12D} mutations on KRAS/Gal-3 axis, while the Mander's values were similar for NCM460 Flag-KRAS^{WT} and NCM460 Flag-KRAS^{G13D}. In KRAS/p16^{INK4a} double immunostainings, a higher impact of KRAS^{G13D} mutation on KRAS/p16^{INK4a} axis was clearly observed. For Gal-3/p16^{INK4a} double

immunostainings, either KRAS^{G12V} and KRAS^{G13D} have a positive impact on the co-localization of both proteins.

In conclusion, co-IP and co-localization studies may lead us to suggest, for the first time, that KRAS/Galectin-3/p16^{INK4A} form a multiprotein complex, and that KRAS mutations might be important for its regulation. However, more precise techniques should be applied in the future to confirm the existence of such KRAS/Galectin-3/p16^{INK4a} complex and to understand its implication for disease progression.

3.2 *KRAS/Galectin-3/p16^{INK4a} exhibit a feedback loop regulation*

To understand how KRAS, Gal-3 and p16^{INK4a} regulate each other expression, their protein levels were analyzed after *KRAS* and/or *LGALS3* silencing by RNAi technology. Therefore, HCT116 CRC cells were transiently transfected, for 48 hours, with siRNA abrogating the expression of Gal-3 (*LGALS3* siRNA), the expression of KRAS (*KRAS* siRNA), or the expression of both proteins (*LGALS3* siRNA+*KRAS* siRNA). Non-transfected cells (control-) or cells transfected with non-silencing siRNA, were used as negative controls (**Figure 27**). The levels of silencing, reached in average along three independent experiments, were 42% of KRAS expression levels in *KRAS* siRNA condition, 24% of Gal-3 expression levels in *LGALS3* siRNA condition, and 0% of KRAS expression levels and 22% of Gal-3 expression levels in *LGALS3*+*KRAS* silencing, respectively. When the double silencing was performed, the silence efficiency of *KRAS* siRNA increased, being statistically significant. Our results showed that both KRAS and/or Gal-3 affect the expression of each other, but also of its interacting partner p16^{INK4a}. Indeed, the silencing of *KRAS* seems to result in a slight increase of Gal-3 expression and the silencing of *LGALS3* in a slight increase of KRAS levels, with no relevant statistically significant differences. Moreover, p16^{INK4a} expression levels were also enhanced upon *KRAS* and/or *LGALS3* silencing. It is possible to observe an increase of p16^{INK4a} expression levels in single *KRAS* and single *LGALS3* silencing conditions, being more evident in single *KRAS* silencing, although not statistically significant. These results suggest the existence of a feedback loop regulation between KRAS/Galectin-3/p16^{INK4a} proteins.

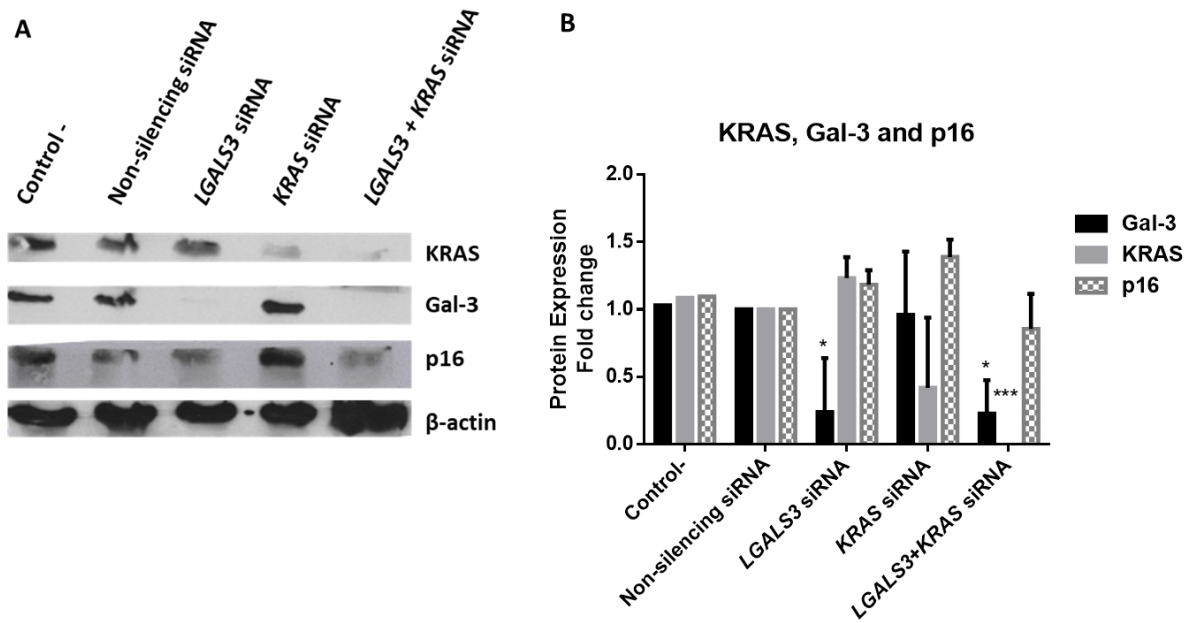


Figure 27 - Analyses of KRAS, Galectin-3 and p16^{INK4a} expression levels after KRAS and/or LGALS3 silencing upon RNAi in HCT116 cell line. (A) Western Blot analysis. (B) Protein level after RNAi experiments.

KRAS and Gal-3 proteins were silenced by RNAi both alone and in conjunction in HCT116. The level of KRAS, Gal-3, and p16^{INK4a} were measured by Western Blot analysis after three independent silencing experiments at 48h using ImageJ software. The levels of proteins were compared to the control β -actin level and normalized for non-silencing siRNA condition, which represents the protein expression fold change 1. Values are the average of at least 3 independent experiments \pm SD. Two-way ANOVA statistical analysis was performed, and the results are shown: *p-value \leq 0.05 and ***p-value \leq 0.001.

3.3 Galectin-3 silencing leads to an increased p16^{INK4a} localization at the nucleus

To understand the impact of silencing one of the proteins of the complex, on the localization of the other partners, immunofluorescences were performed on HCT116 cells silenced for KRAS and/or LGALS3 by siRNA. Of note, we only investigated Gal-3 and p16^{INK4a} cellular localizations, given the absence of specific commercial antibodies directed to KRAS. Remarkably, our results evidenced a weak p16^{INK4a} nuclear localization in most cells under control and non-silencing siRNA transfection. Nevertheless, when LGALS3 and LGALS3+KRAS were silenced, the p16^{INK4a} staining became stronger, as also suggested by western blot analysis, which may indicate increase of its expression, decrease of its degradation and/or alteration of its localization (**Figure 28**). Further immunostaining analyses revealed that p16^{INK4a} indeed increased its nuclear localization when LGALS3 and LGALS3+KRAS were silenced (**Figure 28**). The fact that KRAS silencing does not affect p16^{INK4a} nuclear localization suggests that Gal-3 is the crucial partner which sustains the maintenance of p16 at the cytoplasm (**Figure 28**).

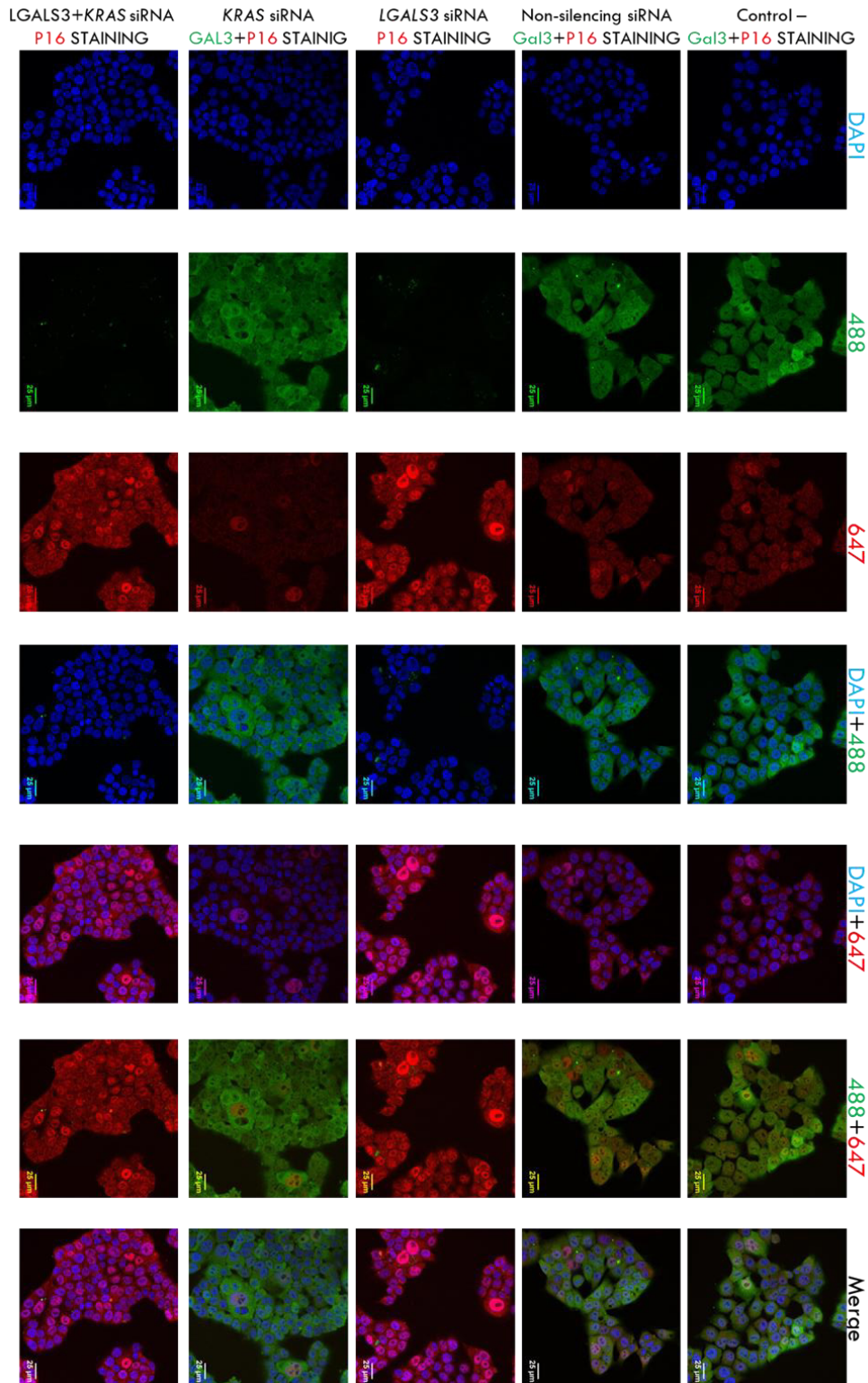


Figure 28 - Impact of KRAS and Gal-3 on Gal-3 and p16^{INK4a} localization assessed by confocal fluorescence microscope analysis.

HCT116 silenced for KRAS and/or Gal-3 upon RNAi were cultured on coverslips with no treatment and fixed with 4% PFA. Gal-3 was stained with Donkey anti-goat Alexa 488, p16^{INK4a} was stained with the Chicken anti-rabbit Alexa 647 secondary antibody (red), and cell nuclei were counterstained with DAPI (blue). All images were obtained through the laser confocal microscopy Leica TCS SP5II using a HCX PL APO CS 63x 1.40 OIL UV objective.

3.4 *KRAS and Galectin-3 enhance cancer cell invasion without activation of matrix metalloproteinase MMP-2 and MMP-9*

To understand KRAS and/or Gal-3 impact on cancer cell invasion and proteolysis, Matrigel invasion assays, and gelatin zymograms to evaluate MMP activity, were performed. For Matrigel invasion assays, the invasion ability of HCT116 cells, silenced or not for *KRAS* and/or *LGALS3*, was evaluated using 20% FBS in McCoy's medium as an invasive stimulus. Our results showed a significant decrease in the invasion of silenced *KRAS* and/or *LGALS3*, in comparison with the non-silencing siRNA condition, being more evident for siRNA *LGALS3+KRAS* (**Figure 29**). The results obtained suggest that KRAS and Gal-3 might have a synergic effect on cancer cell invasion.

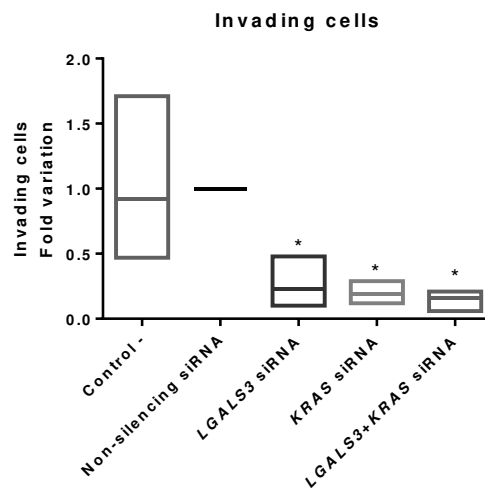


Figure 29 - Effect of KRAS and Galectin-3 on cell invasion.

Matrigel invasion assay was performed during 24 to 48h of silencing experiment on HCT116 silenced for KRAS and/or Gal-3 upon RNAi. At time 48h, the number of invading cells were counted and normalized for non-silencing siRNA control, which was estimated as a fold variation of 1. Results are an average of 3 independent experiments \pm SD. Dunnett's multiple comparisons test was performed and statistically significant differences are shown: * p-value \leq 0.05.

Because invasive cancer cells may exhibit enhanced proteolytic activity, as a mechanism to degrade the extracellular matrix, facilitating tumor growth, invasion and metastasis, this activity was further investigated through gelatin zymography. Our results showed that silencing of *KRAS* and/or *LGALS3* do not activate endogenous cancer cell MMP-2 and MMP-9 activities (**Figure 30**). Therefore, our results strongly suggest that KRAS and Gal-3 are crucial inducers of cancer cell invasion through MMP-2 and MMP-9 independent mechanisms.

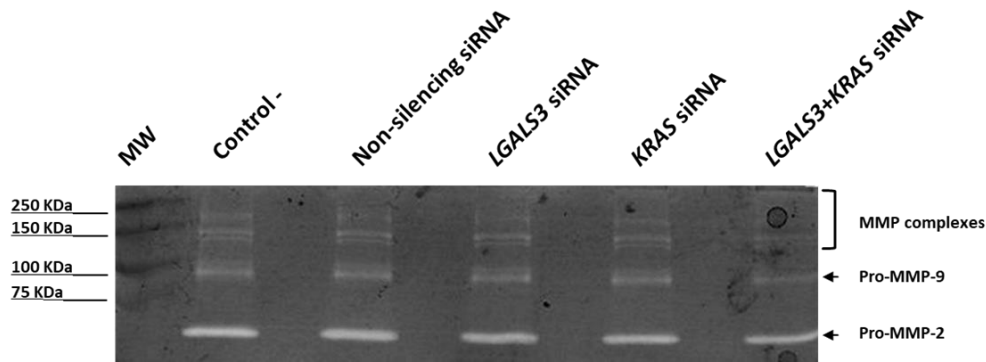


Figure 30 - Matrix Metalloproteinases activity analysis through gelatin zymography of HCT116 silencing for KRAS and/or Gal-3 upon RNAi.

After invasion assay, the medium was collected and analyzed for MMP's activity through gelatin zymography. The activity of MMP-9 and MMP-2 was analyzed. Here is shown the one representative zymogram from five independent experiments.

3.5 *KRAS and/or Galectin-3 enhance cancer cell migration*

Migration is an essential feature for cancer cell invasion and metastasis. Thus, HCT116 cells silenced for KRAS and/or LGALS3 were evaluated through wound-healing and single-cell migration assays to assess the silencing impact on cell migration.

In wound-healing migration assay, wound closure was analyzed for 20 hours and it was quantified through ImageJ software. Our results showed a delay on wound closure in *KRAS* and/or *LGALS3* siRNA conditions, being the impact more evident on siRNA *KRAS* (**Figure 31**). Interestingly, after 2h of silencing, we already have differences, however, they only became statistically significant at 6h after wound for *KRAS* siRNA, and at 8h after wound for *LGALS3* siRNA and for *LGALS3+KRAS* siRNA.

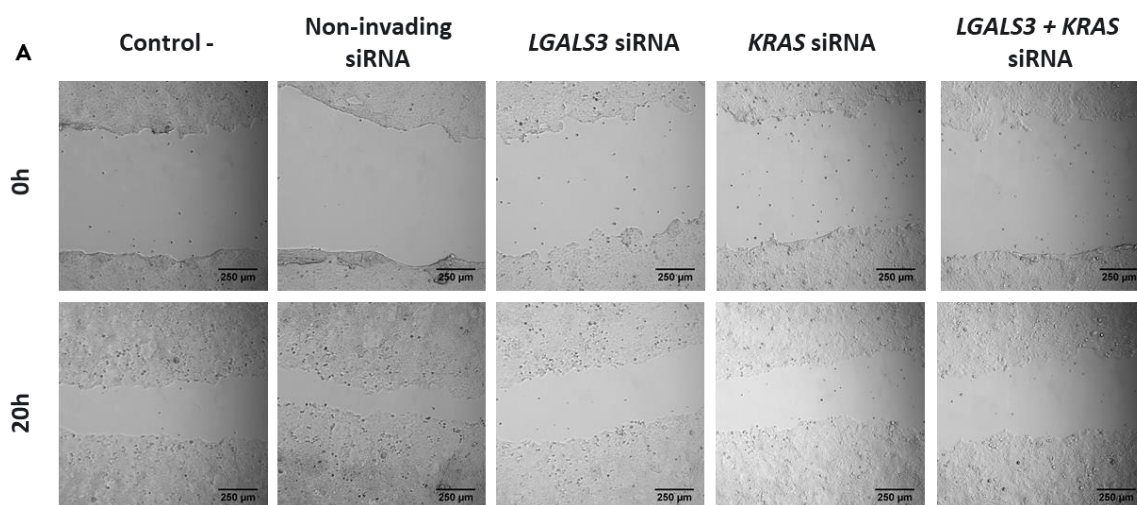


Figure 31 - Effect of KRAS and Galectin-3 on cell migration by wound-healing assay. (A) Wound-healing assay. (B) The percentage of wound closure (Continued)

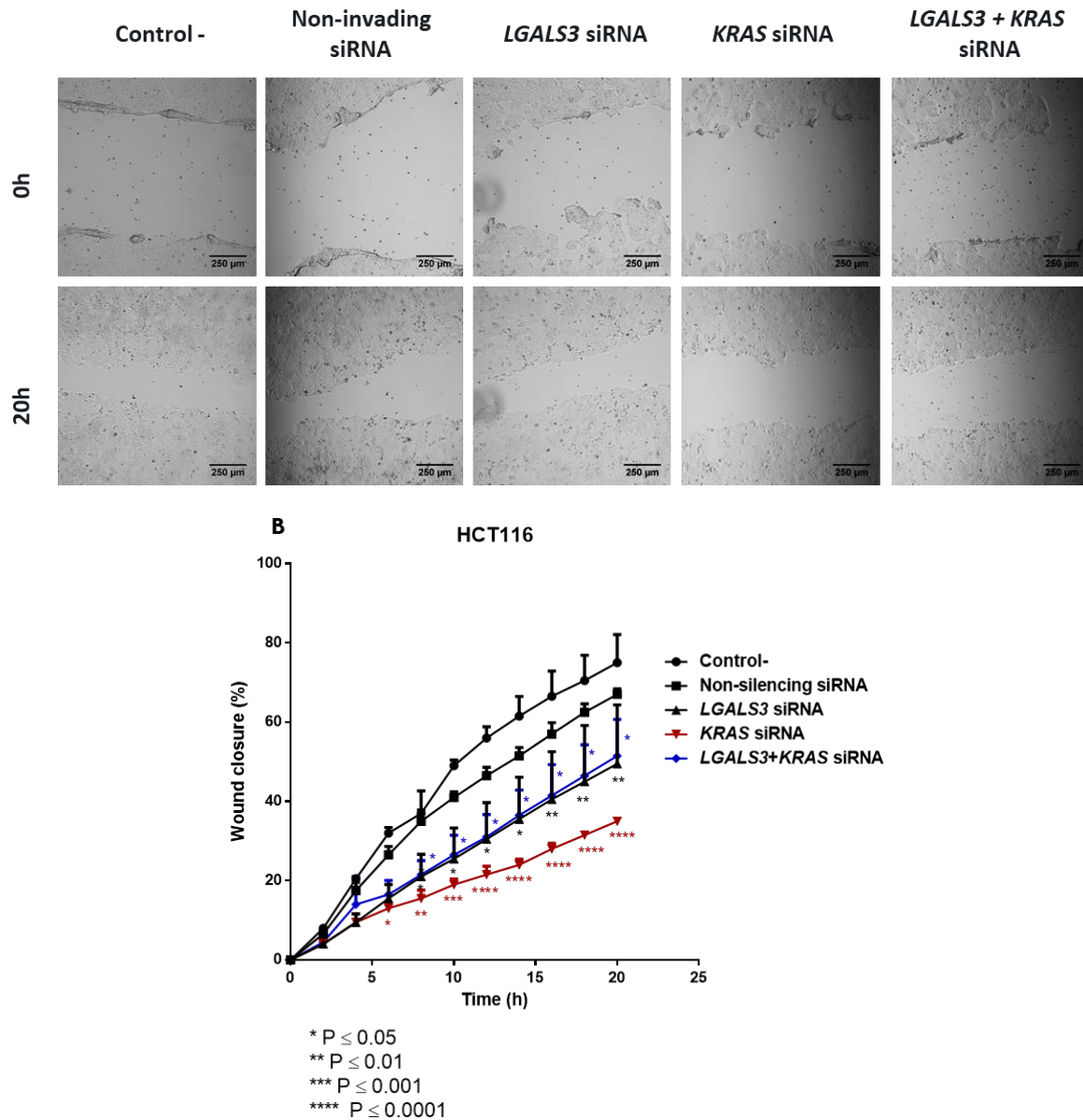


Figure 31 - Effect of KRAS and Galectin-3 on cell migration by wound-healing assay. (A) Wound-healing assay. (B) The percentage of wound closure.

Wound-healing assay was performed to analyze the cell migration on HCT116 silenced for KRAS and/or Gal-3 upon RNAi. Images were captured at each 5 minutes during 20h and the wound closure was quantified through ImageJ. Values are an average of 2 independent experiments \pm SD (shown in A). Dunnett's multiple comparisons test was performed and statistically significant differences are shown: * p-value \leq 0.05; ** p-value \leq 0.01; *** p-value \leq 0.001 and **** p-value \leq 0.0001.

Single-cell migration analyses were also performed to study, through high-resolution time-lapse confocal microscopy, individual cell migration. For that, individual cells were followed for 20 hours and the distance and velocity of migration for each cell were obtained (**Figure 32**). Interestingly, the distance and velocity of migration decreased on *KRAS* and/or *LGALS3* silencing conditions, being this decrease more evident in *LGALS3+KRAS* siRNA cells.

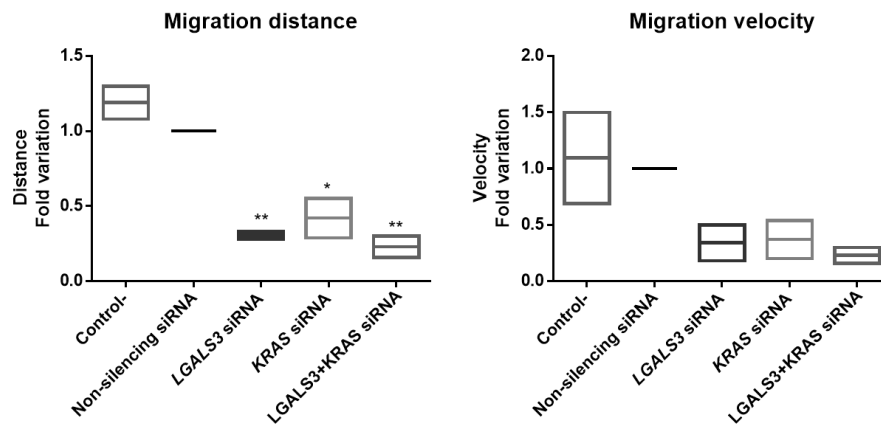


Figure 32 - Effect of KRAS and Galectin-3 on cell migration by Single-cell migration assay. (A) Migration distance and (B) Migration velocity were analyzed for single-cell migration assay.

Single-cell migration assay was performed to study cell migration of individual HCT116 silenced for KRAS and/or Gal-3 upon RNAi. Images were captured at each 5 minutes during 20h and analyzed through ImageJ. The distance and velocity of migration for each individual cell were obtained and the mean was calculated and presented here. Values are an average of 2 independent experiments \pm SD. Dunnett's multiple comparisons test was performed using the non-silencing siRNA condition as a control which represents fold change of 1. Statistically significant differences are shown: * p-value \leq 0.05 and ** p-value \leq 0.01.

Therefore, both migration assays allow us to conclude that silencing of *KRAS* and/or *LGALS3* seems to decrease cell migration rates, suggesting that these proteins are crucial for cancer cell migration. Moreover, *LGALS3+KRAS* silencing show a higher decrease suggesting that Gal-3/*KRAS* axis regulation is relevant for the regulation of cancer cell migration.

3.6 *KRAS* affects invasion-associated signaling pathway ERK

Because ERK signaling pathway is associated with cancer cell invasion, the expression of total and pERK proteins was explored on HCT116 silenced cells for *KRAS* and/or *LGALS3*. The levels of pERK and total ERK were measured by Western Blot analysis and normalized for the control protein β -actin (**Figure 33**). For a more precise analysis, the ratio between phosphorylated ERK/totalERK/ β -actin was determined. The obtained levels lead us to conclude that the silencing for *KRAS* induced a decrease on ERK phosphorylation. Moreover, when we silenced *KRAS* and *LGALS3* simultaneously, the proteins levels of pERK decrease even more (**Figure 33**). However, the silencing for *LGALS3* seems not to affect the phosphorylation of ERK comparing with non-silencing control. Nevertheless, preliminary results showed that *KRAS* may regulate the ERK signaling pathway but additional independent experiments, will be carefully repeated (**Figure 33**).

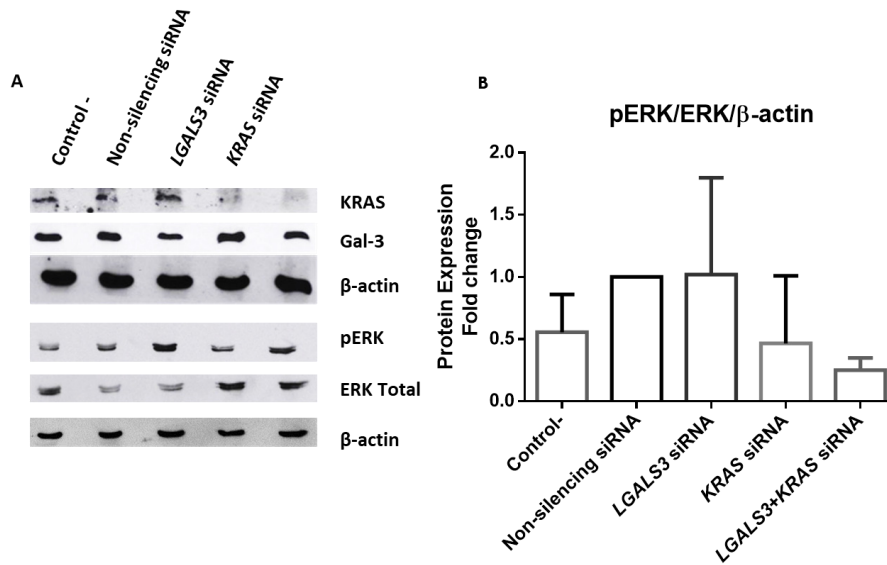


Figure 33 - Analysis of KRAS and Galectin-3 impact on invasion-associated ERK signaling pathway. (A) Western Blot analysis. (B) Protein level after RNAi experiments.

KRAS and Gal-3 proteins were silenced by RNAi both alone and in conjunction in HCT116. The levels of pERK were measured by Western Blot analysis after two independent silencing experiments at 48h and normalized for the control protein β-actin. The ratio pERK/ERK/β-actin were estimated and the protein expression levels was normalized using the values of the protein level in control cells subjected to non-silencing siRNA, which represents fold change of 1. Dunnett's multiple comparisons test was performed and the differences were not statistically significant.

3.7 *KRAS and Galectin-3 seem to affect proliferation and survival signaling pathway PI₃K-AKT*

PI₃K-AKT signaling pathway, which is frequently involved in human cancers, controls cell proliferation and survival, through the phosphorylation of AKT and of a variety of interacting substrates. In this study, the expression of total and phosphorylated AKT (pAKT) proteins was analyzed on HCT116 silenced cells for *KRAS* and/or *LGALS3*. The levels of pAKT and total AKT were measured by Western Blot analysis, normalized for the control protein β-actin, and the ratio for phosphorylated AKT/total AKT/β-actin was determined (**Figure 34**).

Our results showed an increase on pAKT levels after *KRAS* and/or *LGALS3* silencing comparing with non-silencing control. However, all these differences were not statistically significant. Therefore, these results allow us to infer that *KRAS* and/or *Gal-3* seems to downregulate the PI₃K-AKT signaling pathway, but further studies will be performed for confirmation.

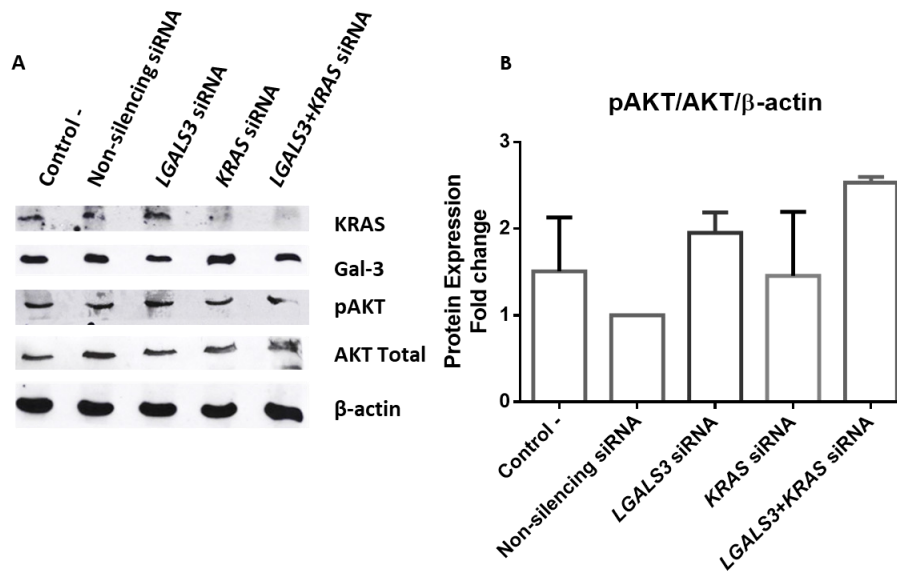


Figure 34 - Analysis of KRAS and Galectin-3 impact on cell proliferation and survival PI₃K-AKT signaling pathway. (A) Western Blot analysis. (B) Protein level after RNAi experiments.

KRAS and Gal-3 proteins were silenced by RNAi both alone and in conjunction in HCT116. The levels of pAKT were measured by Western Blot analysis after two independent silencing experiments at 48h and normalized to the control protein β-actin. The bands intensity was measured using ImageJ software, the ratio pAKT/AKT/β-actin was determined and normalized for non-silencing siRNA control, which was considered the fold change 1. Dunnett's multiple comparisons test was performed and the differences were not statistically significant.

CHAPTER IV. DISCUSSION AND CONCLUDING REMARKS

CRC is the third most commonly diagnosed cancer worldwide and one of the leading causes of cancer related deaths (Ferlay *et al.*, 2014). Over the years, this situation is being improved by the increased rates of CRC screenings, advances in early detection and development of novel therapeutic strategies (El-Sham *et al.*, 2015). Therefore, it is important to elucidate some physiopathology issues of CRC in order to be able to reverse this situation with more effective treatments.

Oncogene *KRAS* mutations are among the most frequent events found in CRC and play a role in the genesis and progression of this type of tumors (Roper and Hung, 2013; Alves *et al.*, 2015). On its turn, p16^{INK4a} was reported to downregulate Gal-3 and *KRAS*, exerting tumor suppressor functions (Rabien *et al.*, 2012), but also as an important factor of colon carcinogenesis (Li, Poi and Ming-Daw, 2012). Gal-3 is a multifunctional protein, which is reported to interact with *KRAS*, promoting cell proliferation, survival and migration in several cancers, including CRC (Shalom-Feuerstein *et al.*, 2008; Levy *et al.*, 2011).

There are evidences for a possible association between p16^{INK4a}, Gal-3 and *KRAS* (Smetana *et al.*, 2013), but little is known about the role of *KRAS* in the regulation of *KRAS*/Galectin-3/p16^{INK4a} triple axis in CRC, which we aimed to study in this work. Moreover, we intended to study if there is a direct *KRAS*/Galectin-3/p16^{INK4a} interaction and what are the phenotypic alterations induced by the silencing of *KRAS* and/or Gal-3 in such protein complex and in the CRC model.

Despite the technical problems associated to the co-IP, our results provided good evidences that *KRAS* and Gal-3 physically interact in SW480 cells. Previous unpublished data from our group also demonstrated in SW480 cells that both *KRAS* and Gal-3 also interact with each other *in vitro* on SW480 cells and that both proteins also interact with p16^{INK4a} (Cazzanelli, Preto and Lucas, 2017). It was already proved that *KRAS*/Gal-3 co-IP in human breast cancer cells BT-549 (Shalom-Feuerstein *et al.*, 2008). These authors showed that not only Gal-3^{WT} but also Gal-3^{V125A} co-immunoprecipitates with GFP-*KRAS*^{G12V}. Nevertheless, *KRAS*/p16^{INK4a}, Gal-3/p16^{INK4a} and more importantly *KRAS*/Galectin-3/p16^{INK4A} multiprotein complex was not so far proved, to the best of our knowledge. However, Rabien and co-workers also tried unsuccessfully to evaluate the *KRAS*/p16^{INK4a} axis by co-IP, to understand if there is a direct interaction between both proteins, as p16^{INK4a} selectively inhibits *KRAS* activity by decreasing *KRAS* protein stability in the human pancreatic cancer cells Capan-1. Authors described, using low-stringent buffers to overcome technical problems, that low amounts of *KRAS* may indeed co-immunoprecipitate with p16^{INK4a} (Rabien *et al.*, 2012). *KRAS* is mostly associated to the membrane and being more difficult to release higher-stringent buffers were needed, whereas

p16^{INK4a} with nuclear localization requires a low-stringent buffer. However, high-stringent buffers are not indicated for co-IP since they may affect the native protein conformations, absolutely necessary to protein-protein interaction to occur. Moreover, KRAS and p16^{INK4a} different localization difficulties protein extraction as also co-IP studies (Rabien *et al.*, 2012). In conclusion, our result on KRAS/Gal-3 direct interaction is in accordance with the already described by us and others (Shalom-Feuerstein *et al.*, 2008).

Curiously, in all tested cell lines (SW480, HCT116, NCM460 *Flag-KRAS*^{WT} and NCM460 *Flag-KRAS*^{G12V}), western blot against KRAS revealed a constant 40-50 kDa band in TL conditions that are extended to IP KRAS, IP Gal-3 and IP p16, being apparently what might be a KRAS dimer. If we could prove that this band may correspond to KRAS dimers, we may conclude that single KRAS only interact with Gal-3, while KRAS dimers may interact with Gal-3 and p16^{INK4a}. These interesting and unexpected results highlighted an important issue: the KRAS dimerization. In this respect, Muratcioglu and co-workers demonstrated, through DLS, that KRAS4B₁₋₁₆₆-GDP have a molecular weight of 18 kDa and the KRAS4B₁₋₁₆₆-GTP- γ -S of 41 kDa (Muratcioglu *et al.*, 2015). Interestingly, this KRAS4B₁₋₁₆₆-GTP- γ -S have a similar molecular weight, as the unknown band of 40-50 kDa, detected by us on IP studies and after western blot analysis, using a specific KRAS antibody. If this is confirmed, our results might suggest that only the active KRAS (KRAS-GTP) co-immunoprecipitate with both Gal-3 and p16^{INK4a} and that probably, the inactive KRAS (KRAS-GDP) only interacts with Gal-3.

Co-localization to determine the multiprotein complex KRAS/Galectin-3/p16^{INK4a} interaction was assessed by immunofluorescence in NCM460 *Flag-KRAS*^{WT, G12V, G13D, G12D}. Our results suggested co-localization for KRAS/Gal-3, KRAS/p16^{INK4a} and Gal-3/p16^{INK4a} in all NCM460 transfected cell lines, according to OC values ranging between 1 and 0.5 and M1 and M2 values being moderate to high levels. According to several authors, OC can only estimate the association strength between two proteins, while Mander's can be considered the real quantification of colocalization (Comeau, Costantino and Wiseman, 2006; Zinchuk, Zinchuk and Okada, 2007; Cordelières and Bolte, 2008; Adler and Parmryd, 2010). Our results suggest that KRAS mutations might be important in the different levels of interaction in the complex. Indeed, we could conclude that KRAS/Gal-3 show a higher colocalization on NCM460 *Flag-KRAS*^{G12V} and NCM460 *Flag-KRAS*^{G12D}, suggesting a higher impact of KRAS^{G12V} and KRAS^{G12D} mutations on KRAS/Gal-3 axis, comparing with NCM460 *Flag-KRAS*^{WT} and NCM460 *Flag-KRAS*^{G13D} where the Mander's values are similar. Moreover, KRAS^{G13D} mutation seems to have a higher impact on KRAS/p16^{INK4a} axis. Importantly, concerning the Gal-3/p16^{INK4a} analysis, KRAS^{G12V} and KRAS^{G13D} seem to have a positive impact on these

proteins interaction. Thus, KRAS^{G12V} mutations seems to colocalize more with their direct partner Gal-3 in NCM460 *Flag-KRAS^{G12V}* and when we analyzed Gal-3/p16^{INK4a} values in these cells, we also see a colocalization increase, in comparison with KRAS^{WT}. The same could be observed in NCM460 *Flag-KRAS^{G13D}*, because KRAS^{G13D} mutation seems to increase the KRAS/p16^{INK4a} colocalization and Gal-3/p16^{INK4a} interaction values, in the same cell. Interestingly, the KRAS^{G12D} mutation also evidences high co-localization with Gal-3 and analyzing the Gal-3/p16^{INK4a} axis, we also see a colocalization increase. Little is known about this triple axis, although it has been proved that KRAS/Gal-3 co-localize at plasma membrane (Shalom-Feuerstein *et al.*, 2008). The authors observed that the mutated Gal-3^{V125A} co-localize with KRAS not only at the plasma membrane, but also in cytosol and other intracellular compartments, suggesting that mutated Gal-3 may interfere with KRAS plasma membrane association. Moreover, this group also demonstrated by Fluorescence Lifetime Imaging & Fluorescence Resonance Energy Transfer (FLIM-FRET) that KRAS/Gal-3 colocalize more in the case of KRAS^{G12V} comparing with KRAS^{WT}. This result is in agreement with our results, showing that KRAS^{G12V} affects positively the KRAS/Gal-3 axis (Shalom-Feuerstein *et al.*, 2008). They also verified that KRAS form two distinct molecular complexes, the KRAS-GTP and the KRAS-GDP and that Gal-3 only affects the KRAS-GTP form as a scaffold protein of formation (Shalom-Feuerstein *et al.*, 2008). In fact, KRAS^{G12V} is constitutively activated in their KRAS-GTP state due to mutation loss of intrinsic GTPase activity (Bettington *et al.*, 2013; Hammond *et al.*, 2015) and it may justify the increased interaction of KRAS/Gal-3, observed by us and other authors (Shalom-Feuerstein *et al.*, 2008). Overall, although the triple colocalization is not possible, the indirect evidences obtained suggest the existence of a triple KRAS/Galectin-3/p16^{INK4a} multiprotein complex in the cell.

Concerning Gal-3/p16^{INK4a} and KRAS/p16^{INK4a}, their interaction was not proved by other researchers, however, some evidences of their relationship were already documented. We further explore the existence of a feedback loop regulation between KRAS/Galectin-3/p16^{INK4a} complex. Although some problems in silencing experiments, such as low efficiency of *KRAS* siRNA and the p16^{INK4a} unspecificity of primary antibody, our experiments lead us to conclude that there is a feedback loop regulation between these proteins.

Upon Gal-3 silencing, we observed an increase of KRAS and p16^{INK4a} levels, being suggestive of a feedback loop regulation between KRAS/Galectin-3/p16^{INK4a}. Previous work from our group, using other cell line, namely the SW480 cells, also showed KRAS increase when Gal-3 is silenced. However, the expression of p16^{INK4a} did not significantly change (Cazzanelli, Preto and Lucas, 2017). Moreover, Gal-3/p16^{INK4a} feedback regulation are in agreement with the

literature, where it was already described a negative correlation between these two proteins in pancreatic cancer cells Capan-1 (Shalom-Feuerstein *et al.*, 2008; Sanchez-Ruderisch *et al.*, 2010). Indeed, it has been demonstrated that overexpressing p16^{INK4a} leads to a Gal-3 downregulation (Shalom-Feuerstein *et al.*, 2008). Sanchez-Ruderisch and co-workers also proved this negative relation *in vivo*, through immunohistochemistry on normal and cancer pancreas tissue, confirming an inverse expression pattern between Gal-3 and p16^{INK4a} (Sanchez-Ruderisch *et al.*, 2010). These results are also in accordance with our immunofluorescence studies, which evidenced that, after Gal-3 silencing, p16^{INK4a} signal increased mainly at the nucleus and at the cytoplasm. Concerning the KRAS/Gal-3 axis, it was expected that the *LGALS3* silencing leads to a downregulation of KRAS, because Gal-3 is described as a protein that attenuates KRAS protein degradation, due partially to the stabilization of active KRAS, inducing KRAS-GTP nanoclustering (Levy *et al.*, 2011). Moreover, Gal-3 also has an impact on KRAS expression levels, by negatively regulating miRNA *let-7*, which itself downregulates also KRAS expression (Levy *et al.*, 2011). However, when we silenced Gal-3, we observed KRAS overexpression, this result make us hypothesize whether HCT116 cells might harbor a Gal-3^{V125A}, as it was already reported to reduce the KRAS expression levels, thus it has to be determined in future work (Shalom-Feuerstein *et al.*, 2008; Levy *et al.*, 2011). Moreover, we may explain this KRAS overexpression as a compensatory mechanism on KRAS/Galectin-3/p16^{INK4a} axis regulation due to the absence of Gal-3. In fact, data from our group with another cell line SW480 also demonstrated KRAS increase when Gal-3 is silenced (Cazzanelli, Preto and Lucas, 2017). Overall the results from the group may indicate that Gal-3 deficiency may induce lower levels of stable KRAS nanocluster what could explain overexpression of KRAS as a compensatory mechanism.

Upon KRAS silencing, we observed an overexpression of Gal-3 and p16^{INK4a}, while previous work from our group using SW480 cell line showed a decrease On Gal-3 and p16^{INK4a}, what could be related with different genetic background of the cell lines. To the best of our knowledge, this is the first report showing the effect of KRAS in the levels of Gal-3, as the only data available only described the effect of Gal-3 over KRAS (Shalom-Feuerstein *et al.*, 2008; Levy *et al.*, 2011). Regarding KRAS/p16^{INK4a}, Rabien and co-workers have found that p16^{INK4a} control the oncogenic KRAS (Rabien *et al.*, 2012). In their experiments, they demonstrated that the reintroduction of p16^{INK4a} in pancreatic cancer cells Capan-1 and DangG and CRC cells SW480 led to a suppression of KRAS^{G12V} activity due to reduction of KRAS protein stability (Rabien *et al.*, 2012). P16^{INK4a} re-introduction also causes Gal-3 downregulation, which could be the direct responsible for KRAS stability decrease, since Gal-3 was already described as a

scaffolding and stabilizer of KRAS (Shalom-Feuerstein *et al.*, 2008; Rabien *et al.*, 2012). Moreover, Lee and co-workers reported that oncogenic KRAS confer senescence bypass, by suppressing the induction of p16^{INK4a} in primary pancreatic duct epithelial cells (PDEC) (Lee and Bar-Sagi, 2010). A different study demonstrated that KRAS mutations can induce tumorigenesis only when p16^{INK4a} inactivation occurs (Rustgi, 2013). Indeed the reported experiment evidenced that KRAS-mutated mice developed epithelial hyperplasia and crypt architecture changes in colon, but no carcinomas (Rustgi, 2013). This was explained by p16^{INK4a} overexpression and senescence induction through activation of oncogenic KRAS^{G12D}. When *CDKN2A* gene, which encodes p16^{INK4a}, was deleted in mutant-KRAS mice induce senescence bypass and carcinomas (Rustgi, 2013). Thus, exogenous expression may induce p16^{INK4a}-mediated senescence and p16^{INK4a} inactivation might to be induced to KRAS-driven carcinoma to occur (Rustgi, 2013). In conclusion, KRAS/p16^{INK4a} feedback loop regulation in HCT116 is in agreement with already reported negative correlation between KRAS/p16^{INK4a} in which decreasing levels of p16^{INK4a} are accompanied by the increasing levels of KRAS (Rabien *et al.*, 2012).

Both KRAS and their downstream effector BRAF mutations appear in CRC development due to ERK signaling abnormalities (Oikonomou *et al.*, 2009). However, these mutations rarely co-exists and further analysis demonstrated both mutations constitutively activates ERK signaling altering remarkably the cell cycle progression (Oikonomou *et al.*, 2009). Moreover, induction of senescence or tumorigenesis depends on cell cycle regulatory proteins, such as p16^{INK4a} that was already associated with KRAS and BRAF mutations (Rustgi, 2013). It was demonstrated that sessile serrated adenoma (SSA) progression to cancer is not achieved due to p16^{INK4a}-mediated senescence and intact p53 (Rustgi, 2013). Moreover, BRAF^{V637E}-mutated mice as well as p16^{INK4a}-deficient mice developed an increase in carcinomas establishing oncogenic BRAF mutations as an inductor of carcinoma, in which carcinoma progression can be accelerated by p53 mutations or p16^{INK4a} inactivation (Rustgi, 2013). The same was not observed in KRAS-mutated mice that develop epithelial hyperplasia and crypt architecture changes in the colon, but not on carcinomas. It is explained by p16^{INK4a} overexpression and senescence induced through oncogenic KRAS^{G12D}. It was further investigated and the *CDKN2A* deletion that encode p16^{INK4a} protein demonstrated senescence prevention and development of carcinomas in mutant-KRAS mice. In fact, both mutated KRAS (Rustgi, 2013) and mutated BRAF (Oikonomou *et al.*, 2009) induction of senescence was already verified. In conclusion, both KRAS and BRAF mutations may induce p16^{INK4a}-mediated senescence, and p16^{INK4a} inactivation might to be induced to KRAS- or BRAF-driven carcinoma (Rustgi, 2013).

Thus, KRAS transfection on NCM460 cells could lead to senescence induction. Instead if senescence is not observed, one may hypothesize that KRAS/p16^{INK4a} interaction occurs as a mechanism to inactivate p16^{INK4a} by sequestering it in the cytoplasm.

When KRAS and Gal-3 were both silenced, we did not observe p16^{INK4a} expression levels what is in accordance to previous results of our group, however, it is an unexpected result due to both KRAS/p16^{INK4a} (Rabien *et al.*, 2012) and Gal-3/p16^{INK4a} (Shalom-Feuerstein *et al.*, 2008; Sanchez-Ruderisch *et al.*, 2010) negative relation already described. At the same time, we see an increase of KRAS silencing, not observed in previous works of our team with another cell line. However, this increase could be explained by the lack of Gal-3 as a stabilizer of KRAS proteins as here described (Shalom-Feuerstein *et al.*, 2008; Rabien *et al.*, 2012).

Overall, the results obtained by us and other authors suggest the existence of a feedback loop regulation between KRAS/Galectin-3/p16^{INK4a} proteins.

To understand if the increased localization of p16^{INK4a} at the nucleus, upon KRAS and/or Gal-3 silencing, we hypothesized that the disruption of the complex might be associated to an increase in the tumor suppression function of p16^{INK4a}, inhibiting cell cycle arrest and thus inducing cellular senescence (Penfield *et al.*, 2013). Thus, in order to test our hypothesis, we evaluated in Gal-3 and/or KRAS silencing cells, the senescence marker β -galactosidase through the β -galactosidase-associated senescence assay, but unfortunately a technical problem with the assay compromised the results (data not showed).

Importantly, we also explored the functional impact of the KRAS/Galectin-3/p16^{INK4a} multicomplex axis on cancer cell migration and invasion. The effect of KRAS and/or Gal-3 on invasion, observed through the inhibition of *KRAS* and *LGALS3* is associated with decreased invasion, being evident a synergic effect of Gal-3 and KRAS. Our results are in accordance with published data showing in CRC SW480 cells that KRAS was responsible for the increase on invasion rates (You *et al.*, 2016). Gal-3 was also described to potentiate invasion on tongue cancer cells SCC-4 and CAL27 and pancreatic cancer cells PanC-1, AsPC-1, and BxPC-3 and specifically extracellular Gal-3 was identified as the regulator of tumor invasiveness (Kobayashi *et al.*, 2011; Song *et al.*, 2012; D. Zhang *et al.*, 2013; Fortuna-Costa *et al.*, 2014). Because invasive cancer cells may exhibit enhanced proteolytic activity, as a mechanism to degrade the extracellular matrix, to facilitate tumor growth, invasion and metastasis, this activity was further investigated, through gelatin zymography, regarding MMP activity (Cheng, Fang and Xu, 2008). Our results revealed that neither silencing for *KRAS* nor for *LGALS3* seem to activate MMP-2 and MMP-9. Therefore, KRAS and Gal-3 seems to stimulate cancer cell invasion, independently of MMP-2 and MMP-9 activities. Only few reports are available

concerning the effect of Gal-3 and/or KRAS in MMP-2 and MMP-9 activation. Gal-3 was reported to interfere with the expression of MMP-9, an important downstream target of the β -catenin signaling pathway in nasopharyngeal carcinoma, without affecting the active state. In pancreatic cancer, silencing of Gal-3 also leads to a reduction of MMP-2 expression via the Wnt signaling pathway (Kobayashi *et al.*, 2011; D. Zhang *et al.*, 2013). As we evaluated MMP-2 and/or MMP-9 activation and not expression levels of Pro-MMP2 and/or Pro-MMP-9 we cannot take conclusions on the changes of expression of these MMP on our study. In conclusion, KRAS and/or Gal-3 stimulate cancer cell invasion, but it is not mediated through the activation of MMP-2 or MMP-9.

Migration is an essential feature for invasion and metastasis in the carcinogenesis process. Thus, the effect of KRAS and/or Gal-3 on migration was also evaluated after its inhibition and revealed a decrease on the rates of wound closure being more evident upon *KRAS* silencing. Because differences on rates of wound closure could be caused either by proliferation and/or migration issues, the single-cell migration assay performed, which allowed studying cell migration of individual cells, to exclude an effect of proliferation. Our results also showed a decrease on distance and velocity of migration after *KRAS* and/or *LGALS3* silencing, being more evident in *LGALS3+KRAS* condition suggesting a synergic effect of KRAS and Gal-3. Altogether our results allow us to conclude that the silencing of KRAS and/or Gal-3 decreased cell migration rates, suggesting KRAS and Gal-3 as important players in CRC cell migration. It has already been demonstrated that Gal-3 also affects the migratory activity of hepatocellular carcinoma cells Hepa1-6 (Serizawa *et al.*, 2015). Interestingly, the KRAS/Gal-3 synergistic effect was also mentioned by the observation of KRAS increased migration rates, particularly in cell lines overexpressing Gal-3 (Wu *et al.*, 2012). Wu and co-workers demonstrated that Gal-3 is expressed at higher levels in Caco2 than in DLD-1 CRC cells and the lower levels of Gal-3 in DLD-1 cells are accompanied with decreased cell migration comparing with Caco2 cells (Wu *et al.*, 2012). They also observed Gal-3 overexpression increased migration rate, while its knockdown decrease cell migration in DLD-1 cells (Wu *et al.*, 2012). Our results show that KRAS and Gal-3 enhance migration, which is in total accordance with reported insights.

It has been showed that ERK signaling pathway is associated with cancer cell invasion reported in invasive human melanoma cell line LOX by observing ARF6-enhanced cell invasion, mediated through the activation of ERK signaling pathway (Tague, Muralidharan and D'Souza-Schorey, 2004). In a previous work from our group, we demonstrated that KRAS regulates the levels of pERKs. In fact, KRAS overexpression is accompanied by increased ERK phosphorylation during starvation observed in NCM460 *Flag-KRAS*^{WT, G13D, G12V} (Alves *et al.*,

2015). Moreover, KRAS downregulation upon *KRAS* silencing also shown a decrease in ERK phosphorylation in HCT116 (Alves *et al.*, 2015). Here we studied the expression of total and pERK proteins after silencing of *KRAS* and/or *LGALS3*. Although preliminary, our data confirmed our previous results showing that pERKs decrease upon *KRAS* silencing, further showing that *LGALS3*+*KRAS* inhibition may also led to the decrease of ERK phosphorylation. However, the silencing of *LGALS3* seems not to affect the phosphorylation of ERK, comparing with the levels of the non-silencing control. The results relative to *KRAS* are in accordance with the already described by us and others (Alves *et al.*, 2015), however, it was already reported that the silencing for Gal-3 lead to a decrease on pERK levels, what is not in accordance to our data (Yeh *et al.*, 2010; Ebrahim *et al.*, 2014). This could be due to the fact that the Gal-3 silencing efficiency was low.

Notably, p13K-AKT signaling pathway, which is frequently involved in human cancer, controls cell proliferation and survival through the phosphorylation of AKT and a variety of substrates (Vara *et al.*, 2004). Our results, although preliminary and not reaching statistical significance, seem to indicate an increase on pAKT levels upon silencing of *KRAS* and/or *LGALS3*. It has been reported that *KRAS* and/or Gal-3 silencing may lead to pAKT downregulation (Kobayashi *et al.*, 2011; Piyush *et al.*, 2017) but it has also been reported by us that at least *KRAS* inhibition induces pAKT increased expression (Alves *et al.*, 2015; Cazzanelli *et al.*, 2018). The low efficiency of *KRAS* and/or Gal-3 silencing may justify the results obtained, and, therefore, we should repeat our RNAi experiments, to achieve higher efficiency on *KRAS* and/or Gal-3 silencing and increase the number of independent experiments.

In conclusion, our results are in favor of the discovery, for the first time, of a novel KRAS/Galectin-3/p16^{INK4a} multiprotein complex axis in CRC cells that seem to interact and exhibit a feedback loop regulation. This complex seems to be important in migration and invasion of CRC cells and thus might be relevant during colorectal carcinogenesis.

Concluding Remarks

Through this study, we aimed at better understanding if KRAS, Gal-3 and p16^{INK4a} form a multiprotein complex and how it was regulated on CRC and which were the consequences of its deregulation for cancer progression. Our results suggested, for the first time, by using normal colon and CRC cells that KRAS/Galectin-3/p16^{INK4a} form a multiprotein complex. We also demonstrated that this complex showed a feedback loop regulation between them. Moreover, we have some evidences that this complex might be a new mechanism of inactivation of the tumor suppressor protein p16^{INK4a} by re-localization from the nucleus to the cytoplasm. Our data also identified KRAS and Gal-3 as important players in the regulation of cell migration and invasion of CRC cells.

Summing-up, in this work we have reasons to suggest a reciprocal protein regulation, in order to maintain equilibrium between oncogenes and tumor suppressor genes, that might contribute to the tumorigenic pathway in CRC.

These findings open a new field of research and further studies are needed in order to better understand the role of KRAS/Galectin-3/p16^{INK4a} complex on colorectal carcinogenesis that might have relevant therapeutic implications.

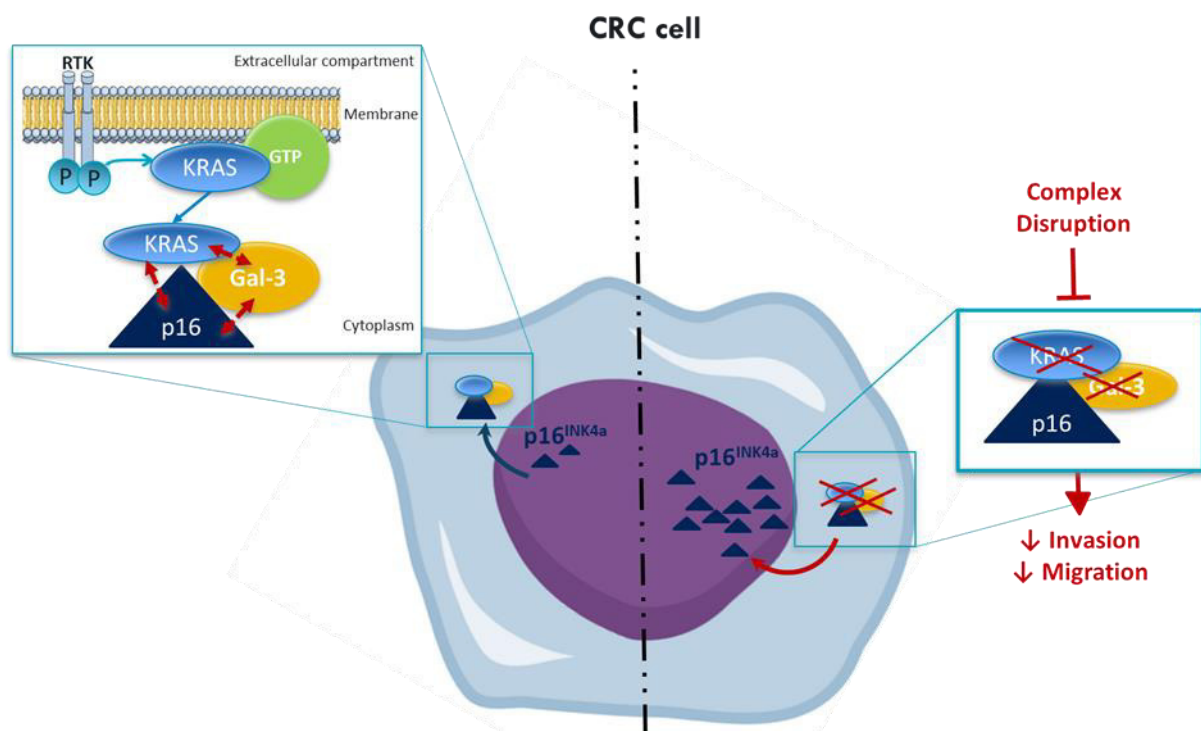


Figure 35 - KRAS/Galectin-3/p16^{INK4a} axis regulation on colorectal cancer.

The proposed model established KRAS, Gal-3 and p16^{INK4a} as a multiprotein complex, which exhibited a feedback loop regulation between them, localized at the cytoplasm. The complex disruption by KRAS and/or Gal-3 silencing leads to a decrease on cancer cell invasion and migration as well as to p16^{INK4a} re-localization at the nucleus.

CHAPTER V. FUTURE PERSPECTIVES

Due to immunoprecipitation technical problems difficult to overcome we will start our future work by focus in a novel complementary technique, Proximity Ligation Assay (PLA), in order to provide more consistent results about the multiprotein complex formed by KRAS/Galectin-3/p16^{INK4a}. Because the study of physic protein-protein interactions through IP revealed some limitations, we tried co-localization studies through immunofluorescence to evaluate the KRAS/Galectin-3/p16^{INK4a} as a complex. However, the pixel resolution of confocal microscopies is limited by the Abbe principle to ~200 nm, which is above to what is needed for resolving protein-protein interactions. Considering this distance, it means that both proteins in analysis can be in the same spot but if they are at 200 nm of distance and might not interact, it may lead to false-positive co-localizations (Xing *et al.*, 2016). Thus, a more suitable complementary technique is needed. PLA conjugated with confocal immunofluorescence microscopy detection is suitable to visualize protein-protein interactions by the detection of protein proximity, theoretically optimal within 40 nm. For that purpose, structures of one pair of primary antibodies covalently linked up to oligonucleotides will be used to behave as templates for the circularization of two additional oligonucleotides. After the dual specific epitope recognition, the circularization of structures is promoted and the rolling circle amplification (RCA) initiates. RCA leads to amplifiable DNA strands, which behave as markers for the detected proteins, through the hybridization of fluorescent-labelled oligonucleotides (**Figure 36**). Finally, the fluorescent signal can be visualized under the confocal immunofluorescence microscopy (Nagy and Szöllosi, 2009; Pacchiana *et al.*, 2014; Greenwood *et al.*, 2015; Zhang *et al.*, 2016; Debaize *et al.*, 2017). Thus, proximity probes are designed to bind to their respective proteins, which must be close to each other to produce signal and suggest protein-protein interactions.

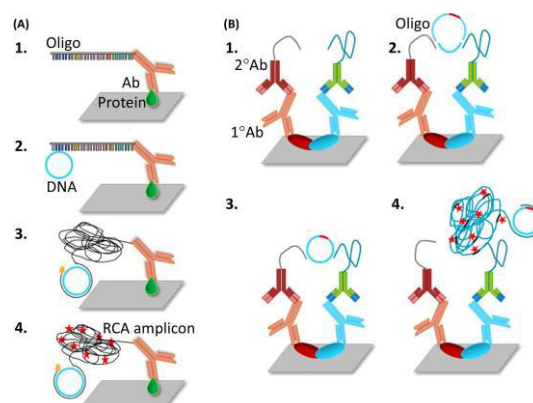


Figure 36 - Principle of PLA technique since protein recognition until protein-protein interaction detection.

PLA is suitable to visualize protein-protein interactions by the detection of protein proximity, theoretically optimal within 40 nm. For that purpose, structures of one pair of primary antibodies covalently linked up to oligonucleotides behave as templates for the circularization of two additional oligonucleotides. After the dual specific epitope recognition, the circularization of structures is promoted and the RCA initiates. RCA leads to amplifiable DNA strands, which behave as markers for the detected proteins, through the hybridization of fluorescent-labelled oligonucleotides. Finally, the fluorescent signal can be visualized under the confocal immunofluorescence microscopy. Reproduced from: Sarkar, Sabhachandani, & Konry, 2017.

In summary, PLA not only exhibits a higher resolution but also higher sensitivity/specificity, and very low nonspecific background than co-localizations already performed. However, because PLA can not substitute IP studies, alternatives for identification of protein-protein interactions are also needed due to all technical problems identified on co-IP studies. Far-Western Blotting could be performed to identify protein-protein interactions. In Far-Western Blotting, as in classical western blotting, lysates containing the unknown “prey” proteins are separated through Sodium Dodecyl Sulphate-Polyacrylamide Gel Electrophoresis (SDS-PAGE) or native PAGE and transferred to a membrane (**Figure 37**). Then, membrane is blocked and probed with a known “bait” protein that should be in the pure form. This step will allow the protein interaction “bait”/“prey” to occur and then, the detection of “bait” protein will allow to identify the corresponding band of the “prey” protein (Thermo Fisher Scientific, 2010). Thus, Far-Western Blotting seems to be a simple technique to identify protein-protein interactions and can substitute IP studies.

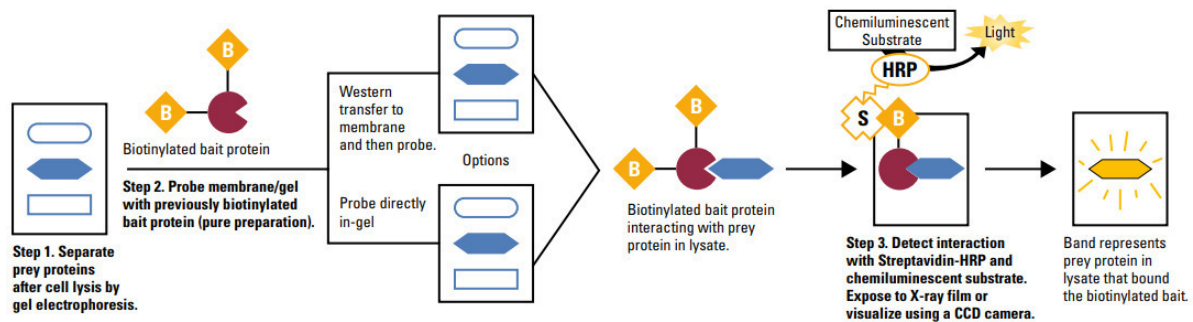


Figure 37 - Principle of Far-Western Blot technique.

In Far-Western Blotting lysates containing the unknown “prey” proteins are separated through SDS-PAGE or native PAGE and transferred to a membrane. Then, membrane is blocked and probed with a known bait protein that should be in the pure form. This step will allow the protein interaction “bait”/“prey” to occur and then, the detection of “bait” protein will allow to identify the corresponding band of the “prey” protein. Reproduced from: Thermo Fisher Scientific, 2010

Other future works will be described based on previous works obtained by our group or reported in the literature. The preliminary study that led us to observe the p16^{INK4a} enrichment at the nucleus after the complex disruption by RNAi emerged some questions. Could the KRAS and/or Gal-3 silencing also changes the KRAS and/or Gal-3 localization? And if we re-introduce the p16^{INK4a}, could p16^{INK4a} also alter the localization of KRAS and/or Gal-3? Thus, it would be interesting to evaluate KRAS localization after Gal-3 silencing, Gal-3 and/or p16^{INK4a} localization after KRAS silencing, and KRAS and/or Gal-3 and/or p16^{INK4a} localization after the re-introduction of p16^{INK4a} through transfection on CRC cells. Moreover, another important question arises through the observation of p16^{INK4a} re-localization at the nucleus: does this re-localization means that the disruption of the complex releases the

inactivated and/or sequestered p16^{INK4a} from the cytoplasm to the nucleus? Thus, to understand if p16^{INK4a} re-localization affects its cell cycle inhibition function, the HCT116 silenced cell line could be evaluated in more detail through (1) Mib-1/ki-67 analysis by flow cytometry, and/or (2) senescence-associated expression of β -galactosidase. In Mib-1/ki-67 analysis by flow cytometry, HCT116 cells silenced for KRAS and/or Gal-3 upon RNAi and Mib-1/Ki-67 will be used, as a proliferative marker. This assay will allow us to observe a high number of cells and to discriminate/estimate the percentage of proliferative and non-proliferative cells in each silencing condition, to understand if Gal-3 and/or KRAS silencing may have any influence in proliferation. Because Mib-1/ki-67 positive cells are an indirect indicator of an inactivated p16^{INK4a} state, this assay will help us to understand if re-localization of p16^{INK4a} to the nucleus activates the p16^{INK4a} function that could be inactivated and/or sequestered in the KRAS/Galectin-3/p16^{INK4a} cytoplasmic nanocluster. p16^{INK4a} functions inducing cell cycle arrest and cellular senescence (Bennecke *et al.*, 2010) could also be evaluated through the senescence-associated β -galactosidase assay. This assay detects the expression of the SA- β -Gal, which has been found increased on senescent cells. Thus, to understand if KRAS and/or Gal-3 may have an impact on the senescent processes, either directly or indirectly through p16^{INK4a} induction alterations, HCT116 could be evaluated after KRAS and/or LGALS3 silencing upon RNA interference. Moreover, because p16^{INK4a} re-introduction on cells lead to a downregulation of KRAS and Gal-3, it is of such relevance to understand if this re-introduction has similar or higher effects than KRAS and/or Gal-3 in some of the studied functions. We can also explore if co-targeting of KRAS and Gal-3 and the re-establishment of p16^{INK4a} could be more attractive strategy to abrogate KRAS and/or Gal-3 identified functions. It can bring some insights that in the future would be applicable to treat CRC.

Our RNAi experiments evidenced low efficacy of KRAS silencing and some results are not statistically significant, thus silencing experiments should be repeated with new siRNAs and the number of independent experiments should be increased to better evaluate the ERK and AKT levels, cell viability, confirm more consistently the feedback loop and to evaluate other functions that the complex could be interfering.

The KRAS dimerization is also an essential theme to be considered for future works. It was demonstrated that Gal-3 only stabilize the KRAS-GTP to form dimers and high order of nanoclusters. It is also important to understand if p16^{INK4a} may also impact in a specific form of KRAS and if it is interfering with KRAS dimerization. Moreover, the bands of 50 kDa detected

by western blot analysis anti-KRAS need to be further evaluated to understand what they represent thus, these bands will be sequenced.

Analyze HCT116 concerning the presence of Gal-3^{WT} and/or Gal-3^{V125A} will also be important to differentiate the impact of each one in the KRAS/Galectin-3/p16^{INK4a} axis. Thus, identification of the presence of either Gal-3^{WT} and/or Gal-3^{V125A} with more specific antibodies will be performed (Shalom-Feuerstein *et al.*, 2008). Since Gal-3 has been reported also as an extracellular protein, with the ability to regulate cell migration and tumor invasion, it would be important to study the Gal-3 presence in conditioned media. The reported alterations of Gal-3 on Pro-MMP-2 and Pro-MMP-9 expression levels should also be evaluated through RT-PCR. However, as already described, further analysis to extensively characterize the complex are needed. In addition to that, understand how microenvironment could modulate this complex is also an interesting study. Therefore, understand what happen to KRAS/Galectin-3/p16^{INK4a} complex in hypoxic and starvation conditions, with and without macrophages will be also very interesting. For that purpose, hypoxic conditions could be simulated using an incubator at 1% O₂, starvation could be stimulated by media replacement by Hank's Balanced Salt Solution (HBSS) and the cultures with macrophages could be established through macrophage-cancer cell indirect co-cultures, using permeable transwell inserts that allows culture media cross-talk but not macrophages-cancer cells direct contact.

Summing up, this work opens a new and underexplored field of research with many and interesting questions to be solved in future.

I. REFERENCES

1. Aagaard, L. and Rossi, J. J. (2007) 'RNAi therapeutics: Principles, prospects and challenges', *Advanced Drug Delivery Reviews*, 59(2–3), pp. 75–86. doi: 10.1016/j.addr.2007.03.005.
2. Adam, R. *et al.* (2015) 'Managing synchronous liver metastases from colorectal cancer: A multidisciplinary international consensus', *Cancer Treatment Reviews*, 41(9), pp. 729–741. doi: 10.1016/j.ctrv.2015.06.006.
3. Adler, J. and Parmryd, I. (2010) 'Quantifying colocalization by correlation: The Pearson correlation coefficient is superior to the Mander's overlap coefficient', *Cytometry Part A*, 77(8), pp. 733–742. doi: 10.1002/cyto.a.20896.
4. Ahearn, I. M. *et al.* (2008) 'Regulating the Regulator: Post-Translational Modification of Ras', *Nature Reviews Molecular Cell Biology*, 13(1), p. 30. doi: 10.3174/ajnr.A1256.Functional.
5. Ahmed, D. *et al.* (2013) 'Epigenetic and genetic features of 24 colon cancer cell lines', *Oncogenesis*, 2. doi: doi:10.1038/oncis.2013.35.
6. Akande, O. F. *et al.* (1998) 'The effects of lag-time and dwell-time on the compaction properties of 1:1 paracetamol/microcrystalline cellulose tablets prepared by pre-compression and main compression', *J Pharm Pharmacol*. 1998/03/21, 50(1), pp. 19–28. Available at: <http://www.ncbi.nlm.nih.gov/pubmed/9504431>.
7. Alberti, L. R. *et al.* (2015) 'How to improve colon cancer screening rates', *World Journal of Gastroenterology*, 7(12), pp. 484–491. doi: 10.4251/wjgo.v7.i12.484.
8. Alves, S. *et al.* (2015) 'Colorectal cancer-related mutant KRAS alleles function as positive regulators of autophagy', *Oncotarget*, 6(31), pp. 30787–30802. doi: 10.18632/oncotarget.5021.
9. Amano, M. *et al.* (2012) 'Tumour suppressor p16(INK4a) - anoikis-favouring decrease in N/O-glycan/cell surface sialylation by down-regulation of enzymes in sialic acid biosynthesis in tandem in a pancreatic carcinoma model.', *The FEBS journal*, 279(21), pp. 4062–80. doi: 10.1111/febs.12001.
10. American Cancer Society (2015) *Treatment of colon cancer, by stage*. Available at: <http://www.cancer.org/cancer/colonandrectumcancer/detailedguide/colorectal-cancer-treating-by-stage-colon> (Accessed: 4 May 2016).
11. Armaghany, T. *et al.* (2012) 'Genetic alterations in colorectal cancer.', *Gastrointestinal cancer research : GCR*, 5(1), pp. 19–27. Available at: <http://www.ncbi.nlm.nih.gov/pubmed/24603996>.
12. Arrington, A. K. *et al.* (2012) 'Prognostic and predictive roles of KRAS mutation in colorectal cancer', *International Journal of Molecular Sciences*, 13(10), pp. 12153–12168. doi: 10.3390/ijms131012153.
13. ATCC (2016) 'Cell Culture Guides', *ATCC online*.
14. Bagci, B. *et al.* (2016) 'KRAS , BRAF oncogene mutations and tissue specific promoter hypermethylation of tumor and p16 genes in colorectal cancer patients', 17, pp. 133–143. doi: 10.3233/CBM-160624.
15. Baker, A.-M. *et al.* (2015) 'Characterization of LGR5 stem cells in colorectal adenomas and carcinomas.', *Nature Scientific reports*, 5(8654), p. 9. doi: 10.1038/srep08654.
16. Barras, D. (2015) 'BRAF Mutation in Colorectal Cancer : An Update', 7, pp. 9–12. doi: 10.4137/BIC.S25248.TYPE.
17. Barrow, H. *et al.* (2011) 'Serum galectin-2, -4, and -8 are greatly increased in colon and breast cancer patients and promote cancer cell adhesion to blood vascular endothelium', *Clinical Cancer Research*, 17(22), pp. 7035–7046. doi: 10.1158/1078-0432.CCR-11-1462.
18. Barrow, H., Rhodes, J. M. and Yu, L.-G. (2011) 'The role of galectins in colorectal cancer progression', *Global Cancer Control*, 129, pp. 1–8. doi: 10.1002/gjc.25945.
19. Bennecke, M. *et al.* (2010) 'Ink4a/Arf and oncogene-induced senescence prevent tumor progression during alternative colorectal tumorigenesis', *Cancer Cell*. Elsevier Ltd, 18(2), pp. 135–146. doi: 10.1016/j.ccr.2010.06.013.
20. Bettington, M. *et al.* (2013) 'The serrated pathway to colorectal carcinoma: Current concepts and challenges', *Histopathology*, 62(3), pp. 367–386. doi: 10.1111/his.12055.
21. Blanco-Calvo, M. *et al.* (2015) 'Colorectal cancer classification and cell heterogeneity: A systems oncology approach', *International Journal of Molecular Sciences*, 16(6), pp. 13610–13632. doi: 10.3390/ijms160613610.
22. Bos, J., Rehmann, H. and Wittinghofer, A. (2007) 'GEFs and GAPs : Critical Elements in the Control of Small G Proteins', *Cell*, 129, pp. 865–877. doi: 10.1016/j.cell.200.
23. Bruera, G. *et al.* (2013) 'Worse prognosis of KRAS c.35 G > A mutant metastatic colorectal cancer (MCR) patients treated with intensive triplet chemotherapy plus bevacizumab (FIR-B/FOX).', *BMC medicine*, 11(1), p. 59. doi: 10.1186/1741-7015-11-59.
24. Cammett, T. J., Luo, L. and Peng, Z. (2003) 'Design and Characterization of a Hyperstable p16 INK4a that Restores Cdk4 Binding Activity when Combined with Oncogenic Mutations', 2836(3), pp. 285–297. doi: 10.1016/S0022-2836(03)00043-3.
25. Cancer treatment centers of America (2015) *Colorectal cancer stages*. Available at: <http://www.cancercenter.com/colorectal-cancer/stages/tab/stage-4/> (Accessed: 4 May 2016).
26. Cazzanelli, G. *et al.* (2018) *The Yeast Saccharomyces cerevisiae as a Model for Understanding RAS Proteins and their Role in Human Tumorigenesis*, *Cells*. doi: 10.3390/cells7020014.
27. Cazzanelli, G., Preto, A. and Lucas, C. (2017) *Study the roles of human galectin-3 using the yeast Saccharomyces cerevisiae and colorectal cancer cells as eukaryotic models*. University of Minho. Available at: <http://hdl.handle.net/1822/48637>.
28. Chan, D. S. M. *et al.* (2011) 'Red and processed meat and colorectal cancer incidence: Meta-analysis of prospective studies', *PLoS ONE*, 6(6). doi: 10.1371/journal.pone.0020456.
29. Chen, C. *et al.* (2013) 'Increased circulation of galectin-3 in cancer induces secretion of metastasis-promoting cytokines from blood vascular endothelium', *Clinical Cancer Research*, 19(7), pp. 1693–1704. doi: 10.1158/1078-0432.CCR-12-2940.
30. Chen, M. *et al.* (2016) 'Ras Dimer Formation as a New Signaling Mechanism and Potential Cancer Therapeutic Target', *Mini-Reviews in Medicinal Chemistry*, 16, pp. 391–403.
31. Cheng, X. C., Fang, H. and Xu, W. F. (2008) 'Advances in assays of matrix metalloproteinases (MMPs) and their inhibitors', *Journal of Enzyme Inhibition and Medicinal Chemistry*, 23(2), pp. 154–167. doi: 10.1080/14756360701511292.
32. Chin, L. (2003) 'The genetics of malignant melanoma: lessons from mouse and man', *Nature Reviews Cancer*, 3(8), pp. 559–570. doi: 10.1038/nrc1145.
33. Colicelli, J. (2004) 'Human RAS Superfamily Proteins and Related GTPases', *Molecular Biology*, 250, pp. 1–53. doi: 10.1126/stke.2502004re13.Human.
34. Comeau, J. W. D., Costantino, S. and Wiseman, P. W. (2006) 'A guide to accurate fluorescence microscopy colocalization measurements', *Biophysical Journal*. Elsevier, 91(12), pp. 4611–4622. doi: 10.1529/biophysj.106.089441.
35. Cordelières, F. P. and Bolte, S. (2008) 'JACoP v2.0 : improving the user experience with co-localization studies', *ImageJ User & Developer Conference*, pp. 174–181.
36. Danielsen, S. A. *et al.* (2015) 'Portrait of the PI3K/AKT pathway in colorectal cancer', *Biochimica et Biophysica Acta (BBA) - Reviews on Cancer*, 1855(1), pp. 104–121. doi: 10.1016/j.bbcan.2014.09.008.
37. Davies, R. J., Miller, R. and Coleman, N. (2005) 'Colorectal cancer screening: prospects for molecular stool analysis.', *Nature reviews*.

- Cancer*, 5(3), pp. 199–209. doi: 10.1038/nrc1545.
38. Dawson, H., André, S. and Karamitopoulou, E. V. A. (2013) 'The Growing Galectin Network in Colon Cancer and Clinical Relevance of Cyttoplasmic Galectin-3 Reactivity', 3060, pp. 3053–3059.
 39. Debaize, L. *et al.* (2017) 'Optimization of proximity ligation assay (PLA) for detection of protein interactions and fusion proteins in non-adherent cells: Application to pre-B lymphocytes', *Molecular Cytogenetics*. *Molecular Cytogenetics*, 10(1), pp. 1–13. doi: 10.1186/s13039-017-0328-2.
 40. Ebrahim, A. H. *et al.* (2014) 'Galectins in cancer: carcinogenesis, diagnosis and therapy.', *Annals of translational medicine*, 2(9), p. 88. doi: 10.3978/j.issn.2305-5839.2014.09.12.
 41. El-Sham, K. *et al.* (2015) 'American Cancer Society Colorectal Cancer Survivorship Care Guidelines', *A cancer Journal for Clinicians*, 65(6), pp. 427–455. doi: 10.3322/caac.21286.
 42. Ferlay, J. *et al.* (2014) 'Cancer incidence and mortality worldwide: sources, methods and major patterns in GLOBOCAN 2012', *International Journal of Cancer*. doi: 10.1002/ijc.29210.
 43. Filipe, M. D. *et al.* (2015) 'Galectin-3 and heart failure: Prognosis, prediction & clinical utility', *Clinica Chimica Acta*, 443, pp. 48–56. doi: 10.1016/j.cca.2014.10.009.
 44. Fortuna-Costa, A. *et al.* (2014) 'Extracellular Galectin-3 in Tumor Progression and Metastasis', *Frontiers in Oncology*, 4(June), pp. 1–9. doi: 10.3389/fonc.2014.00138.
 45. Fröjdö, S., Vidal, H. and Pirola, L. (2009) 'Alterations of insulin signaling in type 2 diabetes: A review of the current evidence from humans', *Biochimica et Biophysica Acta (BBA) - Molecular Basis of Disease*, 1792(2), pp. 83–92. doi: 10.1016/j.bbdis.2008.10.019.
 46. Ghidini, M. *et al.* (2016) 'KRAS mutation in lung metastases from colorectal cancer: prognostic implications', *Cancer medicine*, 5(2), pp. 256–264. doi: 10.1002/cam4.592.
 47. Gibson, J. A. and Odze, R. D. (2016) 'Pathology of premalignant colorectal neoplasia', *Digestive Endoscopy*, 28(3), pp. 312–323. doi: 10.1111/den.12633.
 48. Goldstein, N. S. (2006) 'Serrated Pathway and APC (Conventional)-Type Colorectal Polyps', *American Journal of Clinical Pathology*, 125, pp. 146–153. doi: 10.1309/87BD0C6UCGUG236J.
 49. Gorgoulis, V. G., Koutroumbi, E. N. and Kotsinas, A. (1998) 'Alterations of p16-pRb Pathway and Chromosome Locus 9p21-22 in Sporadic Invasive Breast Carcinomas', *Molecular Medicine*, 4, pp. 807–822.
 50. Greenwood, C. *et al.* (2015) 'Proximity assays for sensitive quantification of proteins', *Biomolecular Detection and Quantification*. Elsevier GmbH, 4, pp. 10–16. doi: 10.1016/j.bdq.2015.04.002.
 51. Hammond, D. E. *et al.* (2015) 'Differential Reprogramming of Isogenic Colorectal Cancer Cells by Distinct Activating KRAS Mutations', *Journal of Proteome Research*, 14(3), pp. 1535–1546. doi: 10.1021/pr501191a.
 52. Hill, M. *et al.* (2010) 'A Novel Clinically Relevant Animal Model for Studying Galectin-3 and Its Ligands During Colon Carcinogenesis', *Journal of Histochemistry and Cytochemistry*, 58(6), pp. 553–565. doi: 10.1369/jhc.2010.955237.
 53. Hittelet, A. *et al.* (2003) 'Upregulation of galectins-1 and -3 in human colon cancer and their role in regulating cell migration', *International Journal of Cancer*, 103(3), pp. 370–379. doi: 10.1002/ijc.10843.
 54. Hugen, N. *et al.* (2014) 'Metastatic pattern in colorectal cancer is strongly influenced by histological subtype', *Annals of Oncology*, 25(3), pp. 651–657. doi: 10.1093/annonc/mdt591.
 55. Ihle, N. (2012) *Differential Activity of the KRAS Oncogene by Method of Activation: Implications for Signaling and Therapeutic Intervention*. The University of Texas.
 56. Itzkowitz, S. H. and Yio, X. (2004) 'Inflammation and cancer IV. Colorectal cancer in inflammatory bowel disease: the role of inflammation.', *American journal of physiology. Gastrointestinal and liver physiology*, 287, pp. G7–G17. doi: 10.1152/ajpgi.00079.2004.
 57. Jančík, S. *et al.* (2010) 'Clinical Relevance of KRAS in Human Cancers', *Journal of Biomedicine and Biotechnology*, 2010, pp. 1–13. doi: 10.1155/2010/150960.
 58. Johannes, L., Wunder, C. and Shafaq-Zadah, M. (2016) 'Glycolipids and Lectins in Endocytic Uptake Processes', *Journal of Molecular Biology*. Elsevier Ltd, 428(24), pp. 4792–4818. doi: 10.1016/j.jmb.2016.10.027.
 59. Jung, S. H. *et al.* (2011) 'Expression of DOG1, PDGFRA, and p16 in Gastrointestinal Stromal Tumors', *Gut and Liver*, 5(2), pp. 171–180. doi: 10.5009/gnl.2011.5.2.171.
 60. Justus, C. R. *et al.* (2014) 'In vitro Cell Migration and Invasion Assays', *Journal of Visualized Experiments*, (88), pp. 1–8. doi: 10.3791/51046.
 61. Kedrin, D. and Gala, M. K. (2015) 'Genetics of the Serrated Pathway to Colorectal Cancer', *Clinical and Translational Gastroenterology*. Nature Publishing Group, 6(4), pp. e84–3. doi: 10.1038/ctg.2015.12.
 62. Kim, S. H. *et al.* (2012) 'P16 (Ink4a) Gene Hypermethylation and Kras Mutation Are Independent Predictors of Folfoxir and Cetuximab Chemotherapy in Patients With Metastatic Colorectal Cancer (Merc)', 48(October), p. 2012.
 63. Knickelbein, K. and Zhang, L. (2015) 'Mutant KRAS as a critical determinant of the therapeutic response of colorectal cancer.', *Genes & Diseases*. Elsevier Ltd, 2(1), pp. 4–12. doi: 10.1016/j.gendis.2014.10.002.
 64. Knutsen, T. *et al.* (2010) 'Definitive Molecular Cytogenetic Characterization of 15 Colorectal Cancer Cell Lines', *Genes Chromosomes Cancer*, 49(3), pp. 204–223. doi: 10.1002/gcc.20730.
 65. Kobayashi, T. *et al.* (2011) 'Transient gene silencing of galectin-3 suppresses pancreatic cancer cell migration and invasion through degradation of β -catenin', *International Journal of Cancer*, 129(12), pp. 2775–2786. doi: 10.1002/ijc.25946.
 66. Korkmaz, G. *et al.* (2016) 'LGALS3 and AXIN1 gene variants playing role in the Wnt/ β -catenin signaling pathway are associated with mucinous component and tumor size in colorectal cancer.', *Bosnian journal of basic medical sciences*, pp. 108–113. doi: 10.17305/bjbm.2016.721.
 67. Krasinskas, A. M. (2011) 'EGFR Signaling in Colorectal Carcinoma.', *Pathology research international*, 2011, p. 932932. doi: 10.4061/2011/932932.
 68. Kratz, C. P. *et al.* (2006) 'Germline mutations in components of the Ras signaling pathway in Noonan syndrome and related disorders', *Cell Cycle*, 5(15), pp. 1607–1611. doi: 10.4161/cc.5.15.3128.
 69. Kriegl, L. *et al.* (2011) 'Up and downregulation of p16(Ink4a) expression in BRAF-mutated polyps/adenomas indicates a senescence barrier in the serrated route to colon cancer.', *Modern pathology: an official journal of the United States and Canadian Academy of Pathology, Inc.* Nature Publishing Group, 24(7), pp. 1015–1022. doi: 10.1038/modpathol.2011.43.
 70. Lee, K. E. and Bar-Sagi, D. (2010) 'Oncogenic KRas suppresses inflammation-associated senescence of pancreatic ductal cells', *Cancer Cell*, 18(5), pp. 448–458. doi: 10.1016/j.ccr.2010.10.020.
 71. Lee, Y. K. *et al.* (2013) 'Galectin-3 silencing inhibits epirubicin-induced ATP binding cassette transporters and activates the mitochondrial apoptosis pathway via β -catenin/GSK-3 β modulation in colorectal carcinoma', *PLoS ONE*, 8(11), pp. 1–14. doi: 10.1371/journal.pone.0082478.
 72. Leggett, B. and Whitehall, V. (2010) 'Role of the Serrated Pathway in Colorectal Cancer Pathogenesis', *Gastroenterology*. Elsevier Inc., 138(6), pp. 2088–2100. doi: 10.1053/j.gastro.2009.12.066.

73. Levy, R. *et al.* (2010) 'Galectin-3 promotes chronic activation of K-Ras and differentiation block in malignant thyroid carcinomas.', *Molecular cancer therapeutics*, 9(8), pp. 2208–2219. doi: 10.1158/1535-7163.MCT-10-0262.
74. Levy, R. *et al.* (2011) 'Galectin-3 mediates cross-talk between K-ras and let-7c tumor suppressor microRNA', *PLoS ONE*, 6(11), pp. 1–10. doi: 10.1371/journal.pone.0027490.
75. Li, J., Poi, M. J. and Ming-Daw, T. (2012) 'The Regulatory Mechanisms of Tumor Suppressor p16^{INK4} and Relevance to cancer', *Biochemistry*, 50(25), pp. 5566–5582. doi: 10.1021/bi200642e.The.
76. Li, Y. *et al.* (2015) 'Senescent mesenchymal stem cells promote colorectal cancer cells growth via galectin-3 expression.', *Cell & Bioscience*. Cell & Bioscience, 5, p. 21. doi: 10.1186/s13578-015-0012-3.
77. Liu, F.-T. and Rabinovich, G. A. (2005) 'Galectins as modulators of tumour progression', *Nature Reviews Cancer*, 5(1), pp. 29–41. doi: 10.1038/nrc1527.
78. Liu, X., Jakubowski, M. and Hunt, J. L. (2011) 'KRAS gene mutation in colorectal cancer is correlated with increased proliferation and spontaneous apoptosis', *American Journal of Clinical Pathology*, 135(2), pp. 245–252. doi: 10.1309/AJCP7FO2VAXIVSTP.
79. Malumbres, M. and Barbacid, M. (2003) 'Timeline: RAS oncogenes: the first 30 years', *Nature Reviews Cancer*, 3(6), pp. 459–465. doi: 10.1038/nrc1097.
80. Marques, C. *et al.* (2013) 'Acetate-induced apoptosis in colorectal carcinoma cells involves lysosomal membrane permeabilization and cathepsin D release.', *Cell death & disease*, 4, p. e507. doi: 10.1038/cddis.2013.29.
81. Mazurek, N. *et al.* (2012) 'Cell-surface galectin-3 confers resistance to TRAIL by impeding trafficking of death receptors in metastatic colon adenocarcinoma cells.', *Cell death and differentiation*, 19(3), pp. 523–33. doi: 10.1038/cdd.2011.123.
82. McLaughlin-Drubin, M. E., Park, D. and Munger, K. (2013) 'Tumor suppressor p16^{INK4A} is necessary for survival of cervical carcinoma cell lines.', *Proceedings of the National Academy of Sciences of the United States of America*, 110(40), pp. 16175–80. doi: 10.1073/pnas.1310432110.
83. Moyer, M. P. *et al.* (1996) 'A normal human colon mucosal epithelial cell line', *In Vitro Cellular & Developmental Biology*, 13, pp. 315–317.
84. Muratcioglu, S. *et al.* (2015) 'GTP-Dependent K-Ras Dimerization', *Structure*, 23(7), pp. 1325–1335. doi: 10.1016/j.str.2015.04.019.
85. Nagasaka, T. *et al.* (2004) 'Colorectal cancer with mutation in BRAF, KRAS, and wild-type with respect to both oncogenes showing different patterns of DNA methylation', *Journal of Clinical Oncology*, 22(22), pp. 4584–4594. doi: 10.1200/JCO.2004.02.154.
86. Nagy, P. and Szöllösi, J. (2009) 'Proximity or no proximity: That is the question - But the answer is more complex', *Cytometry Part A*, 75(10), pp. 813–815. doi: 10.1002/cyto.a.20782.
87. Nana, X. *et al.* (2015) 'Ras-GTP dimers activate the Mitogen-Activated Protein Kinase (MAPK) pathway', *PNAS*, 112(26), pp. 7996–8001. doi: 10.1073/pnas.1509123112.
88. Newlaczyl, A. U. and Yu, L. G. (2011) 'Galectin-3 - A jack-of-all-trades in cancer', *Cancer Letters*. Elsevier Ireland Ltd, 313(2), pp. 123–128. doi: 10.1016/j.canlet.2011.09.003.
89. Niv, H. *et al.* (1999) 'Membrane interactions of a Constitutively Active GFP-Ki-Ras 4B and their role in signaling', *The Journal of Biological Chemistry*, 274(January 2015), pp. 1606–1613.
90. Niv, H. *et al.* (2002) 'Activated K-Ras and H-Ras display different interactions with saturable nonraft sites at the surface of live cells', *The Journal of Cell Biology*, 157(5), pp. 865–872. doi: 10.1083/jcb.200202009.
91. Norton, S. E. *et al.* (2015) 'Immune cell interplay in colorectal cancer prognosis.', *World journal of gastrointestinal oncology*, 7(10), pp. 221–32. doi: 10.4251/wjgo.v7.i10.221.
92. Oikonomou, E. *et al.* (2009) 'BRAF V600E Efficient Transformation and Induction of Microsatellite Instability Versus KRAS G12V Induction of Senescence Markers in Human Colon', *Neoplasia*. Neoplasia Press, Inc., 11(11), pp. 1116–1131. doi: 10.1593/neo.09514.
93. Oliveira, C. *et al.* (2007) 'KRAS and BRAF oncogenic mutations in MSS colorectal carcinoma progression', *Oncogene*, 26(1), pp. 158–163. doi: 10.1038/sj.onc.1209758.
94. Ortega, S., Malumbres, M. and Barbacid, M. (2002) 'Cyclin D-dependent kinases, INK4a inhibitors and cancer', *Biochimica et Biophysica Acta*, 1602, pp. 73–87.
95. Pacchiana, R. *et al.* (2014) 'Combining immunofluorescence with in situ proximity ligation assay: a novel imaging approach to monitor protein-protein interactions in relation to subcellular localization', *Histochemistry and Cell Biology*, 142(5), pp. 593–600. doi: 10.1007/s00418-014-1244-8.
96. Parsons, D. W. *et al.* (2005) 'Mutations in a signalling pathway', *Nature*, 436(7052), pp. 792–792. doi: 10.1038/436792a.
97. Patai, Á. *et al.* (2013) 'Serrated pathway: Alternative route to colorectal cancer', 19(5), pp. 607–615. doi: 10.3748/wjg.v19.i5.607.
98. Penfield, J. D. *et al.* (2013) 'The role of cellular senescence in the gastrointestinal mucosa', *Gut and Liver*, 7(3), pp. 270–277. doi: 10.5009/gnl.2013.7.3.270.
99. Phipps, A. I. *et al.* (2013) 'KRAS-mutation status in relation to colorectal cancer survival: the joint impact of correlated tumour markers.', *British journal of cancer*. Nature Publishing Group, 108(8), pp. 1757–64. doi: 10.1038/bjc.2013.118.
100. Pino, M. S. and Chung, D. C. (2010) 'The Chromosomal Instability Pathway in Colon Cancer', *Gastroenterology*, 138(6), pp. 2059–2072. doi: 10.1053/j.gastro.2009.12.065.
101. Piyush, T. *et al.* (2017) 'Interaction of galectin-3 with MUC1 on cell surface promotes EGFR dimerization and activation in human epithelial cancer cells', *Cell Death and Differentiation*. Nature Publishing Group, 24(11), pp. 1931–1947. doi: 10.1038/cdd.2017.119.
102. Popov, N. and Gil, J. (2010) 'Epigenetic regulation of the INK4B-ARF-INK4a locus: In sickness and in health', *Epigenetics*, 5(8), pp. 685–690. doi: 10.4161/epi.5.8.12996.
103. Prior, I. A., Lewis, P. D. and Mattos, C. (2012) 'A Comprehensive Survey of Ras Mutations in Cancer', *Cancer Research*, 72(10), pp. 2457–2468. doi: 10.1158/0008-5472.CAN-11-2612.
104. Qi, G. *et al.* (2015) 'Inhibitory Effect of Various Breads on DMH-Induced Aberrant Crypt Foci and Colorectal Tumours in Rats', *BioMed Research International*. Hindawi Publishing Corporation, 2015, pp. 1–8. doi: 10.1155/2015/829096.
105. Rabien, A. *et al.* (2012) 'Tumor suppressor p16^{INK4a} controls oncogenic K-Ras function in human pancreatic cancer cells', *Cancer Science*, 103(2), pp. 169–175. doi: 10.1111/j.1349-7006.2011.02140.x.
106. Reinacher-Schick, A. *et al.* (2012) 'Effect of KRAS codon13 mutations in patients with advanced colorectal cancer (advanced CRC) under oxaliplatin containing chemotherapy. Results from a translational study of the AIO colorectal study group.', *BMC cancer*, 12, p. 349. doi: 10.1186/1471-2407-12-349.
107. Richi, E. B. *et al.* (2015) 'Health Risks Associated with Meat Consumption: A Review of Epidemiological Studies.', *International journal for vitamin and nutrition research*, 85(1–2), pp. 70–78. doi: 10.1024/0300-9831/a000224.
108. Rojas, A. M. *et al.* (2012) 'The Ras protein superfamily: Evolutionary tree and role of conserved amino acids', *Journal of Cell Biology*, 196(2), pp. 189–201. doi: 10.1083/jcb.201103008.
109. Romagosa, C. *et al.* (2011) 'p16^{Ink4a} overexpression in cancer: a tumor suppressor gene associated with senescence and high-grade tumors', *Oncogene*, 30(18), pp. 2087–2097. doi: 10.1038/onc.2010.614.
110. Roper, J. and Hung, K. E. (2013) 'Molecular Mechanisms of Colorectal Carcinogenesis', in Haigis, Ph.D., K. M. (ed.) *Molecular Pathogenesis of Colorectal Cancer*. K.M. Haigi. New York, NY: Springer New York, pp. 25–66. doi: 10.1007/978-1-4614-8412-7.

111. Rosa, M. *et al.* (2015) 'Overexpression of Vascular Endothelial Growth Factor A in Invasive Micropapillary Colorectal Carcinoma', *Cancer control*, 22(2).
112. Rosseland, C. M., Wierod, L. and Flinder, L. I. (2007) 'Distinct Functions of H-Ras and K-Ras in Proliferation and Survival of Primary Hepatocytes Due to Selective Activation of ERK and PI3K', *Journal of Cellular Physiology*, 215, pp. 818–826. doi: 10.1002/jcp.21367.
113. Rustgi, A. K. (2013) 'BRAF: A Driver of the Serrated Pathway in Colon Cancer', *Cancer Cell*. Elsevier, 24(1), pp. 1–2. doi: 10.1016/j.ccr.2013.06.008.
114. Sakellariou, S. *et al.* (2016) 'Clinical significance of AGE-RAGE axis in colorectal cancer: associations with glyoxalase-I, adiponectin receptor expression and prognosis', *BMC Cancer*. BMC Cancer, 16(1), p. 174. doi: 10.1186/s12885-016-2213-5.
115. Sameer, A. S. *et al.* (2012) 'The blues of P(16)INK(4a): Aberrant promoter methylation and association with colorectal cancer in the Kashmir valley', *Molecular Medicine Reports*, 5(4), pp. 1053–1057. doi: 10.3892/mmr.2012.740.
116. Sanchez-Ruderisch, H. *et al.* (2010) 'Tumor suppressor p16INK4a: Downregulation of galectin-3, an endogenous competitor of the pro-oncogenic effector galectin-1, in a pancreatic carcinoma model', *FEBS Journal*, 277(17), pp. 3552–3563. doi: 10.1111/j.1742-4658.2010.07764.x.
117. Sancho, E., Batlle, E. and Clevers, H. (2004) 'Signaling Pathways in Intestinal Development and Cancer', *Annual Review of Cell and Developmental Biology*, 20(1), pp. 695–723. doi: 10.1146/annurev.cellbio.20.010403.092805.
118. Sarkar, S., Sabhachandani, P. and Konry, T. (2017) 'Isothermal Amplification Strategies for Detection in Microfluidic Devices', *Trends in Biotechnology*, 35(3), pp. 186–189. doi: 10.1016/j.tibtech.2016.09.006.
119. Schubbert, S., Shannon, K. and Bollag, G. (2007) 'Hyperactive Ras in developmental disorders and cancer', *Nature Reviews Cancer*, 7(4), pp. 295–308. doi: 10.1038/nrc2109.
120. Semczuk, A. *et al.* (2004) 'Expression of the cell-cycle regulatory proteins (pRb, cyclin D1, p16ink4a and cdk4) in human endometrial cancer: correlation with clinicopathological features', *Arch Gynecol Obstet*, 269, pp. 104–110. doi: 10.1007/s00404-002-0449-6.
121. Serizawa, N. *et al.* (2015) 'Galectin 3 regulates HCC cell invasion by RhoA and MLCK activation', *Laboratory Investigation*, 95(10), pp. 1145–1156. doi: 10.1038/labinvest.2015.77.
122. Serrano, M. (1997) 'The Tumor Suppressor Protein p16(ink4a)', *Experimental cell research*, 237, pp. 7–13.
123. Setaffy, L. and Langner, C. (2015) 'Microsatellite instability in colorectal cancer: clinicopathological significance', *Pol. J. Pathol.*, 66(3), pp. 203–18. doi: 10.5114/pjp.2015.54953.
124. Shalom-Feuerstein, R. *et al.* (2005) 'Galectin-3 Regulates a Molecular Switch from mN-Ras to K-Ras Usage in Human Breast Carcinoma Cells', *American Association for Cancer Research*, 65(16). doi: 10.1158/0008-5472.CAN-05-0775.
125. Shalom-Feuerstein, R. *et al.* (2008) 'K-Ras Nanoclustering Is Subverted by Overexpression of the Scaffold Protein Galectin-3', *Cancer Research*, 68(16), pp. 6608–6616. doi: 10.1158/0008-5472.CAN-08-1117.
126. Shi, S., Wang, X. and Xia, Q. (2016) 'P16 overexpression in BRAF-mutated gastrointestinal stromal tumors', *Expert Review of Molecular Diagnostics*. doi: 10.1080/14737159.2017.1272413.
127. Shi, Y. *et al.* (2007) 'Inhibition of Wnt-2 and galectin-3 synergistically destabilizes β -catenin and induces apoptosis in human colorectal cancer cells', *International Journal of Cancer*, 121(6), pp. 1175–1181. doi: 10.1002/ijc.22848.
128. Simmonds, P. C. *et al.* (2006) 'Surgical resection of hepatic metastases from colorectal cancer: A systematic review of published studies', *British Journal of Cancer*, 94(7), pp. 982–999. doi: 10.1038/sj.bjc.6603033.
129. Simons, K. and Toomre, D. (2000) 'Lipid rafts and signal transduction', *Nature Reviews Molecular Cell Biology*, 1(1), pp. 31–39. doi: 10.1038/35036052.
130. Smetana, K. *et al.* (2013) 'Context-dependent multifunctionality of galectin-1: a challenge for defining the lectin as therapeutic target', *Expert Opinion on Therapeutic Targets*, 17(4), pp. 379–392. doi: 10.1517/14728222.2013.750651.
131. Smith, G. *et al.* (2010) 'Activating K-Ras mutations outwith "hotspot" codons in sporadic colorectal tumours – implications for personalised cancer medicine', *British Journal of Cancer*, 102, pp. 693–703. doi: 10.1038/sj.bjc.6605534.
132. Song, S. *et al.* (2012) 'Overexpressed galectin-3 in pancreatic cancer induces cell proliferation and invasion by binding ras and activating ras signaling', *PLoS ONE*, 7(8). doi: 10.1371/journal.pone.0042699.
133. Suthahar, N. *et al.* (2018) 'Galectin-3 activation and inhibition in heart failure and cardiovascular disease: An update', *Theranostics*, 8(3), pp. 593–609. doi: 10.7150/thno.22196.
134. Sylvester, B. E. and Vakiani, E. (2015) 'Tumor evolution and intratumor heterogeneity in colorectal carcinoma: insights from comparative genomic profiling of primary tumors and matched metastases.', *Journal of gastrointestinal oncology*, 6(6), pp. 668–75. doi: 10.3978/j.issn.2078-6891.2015.083.
135. Szyllberg, A. *et al.* (2015) 'Serrated Polyps and Their Alternative Pathway to the Colorectal Cancer : A Systematic Review', 2015.
136. Tague, S. E., Muralidharan, V. and D'Souza-Schorey, C. (2004) 'ADP-ribosylation factor 6 regulates tumor cell invasion through the activation of the MEK/ERK signaling pathway.', *Proceedings of the National Academy of Sciences of the United States of America*, 101(26), pp. 9671–6. doi: 10.1073/pnas.0403531101.
137. Tamas, K. *et al.* (2015) 'Rectal and colon cancer: Not just a different anatomic site', *Cancer Treatment Reviews*. Elsevier Ltd, 41(8), pp. 671–679. doi: 10.1016/j.ctrv.2015.06.007.
138. Tan, C. and Du, X. (2012) 'KRAS mutation testing in metastatic colorectal cancer', *World Journal of Gastroenterology*, 18(37), pp. 5171–5180. doi: 10.3748/wjg.v18.i37.5171.
139. Terese Winslow (2005) *Medical and Scientific Illustration*. Available at: <http://www.teresewinslow.com/portshow.asp?nxt=13&sid=B9D1A76E-29D5-43A3-A5C7-E1BF46DF5D37&portfolioid=%7B4B56C61F-9C24-47C6-9F4D-9444E1D75BA2%7D>.
140. Thermo Fisher Scientific (2010) *Thermo Scientific Pierce Protein Interaction Technical Handbook*. 2nd edn. United States.
141. Tomita, N. *et al.* (1992) 'Isolation and Characterization of a Highly Malignant Variant of the SW480 Human Colon Cancer Cell Line', *CANCER RESEARCH*, pp. 6840–6847.
142. Tsai, F. D. *et al.* (2015) 'K-Ras4A splice variant is widely expressed in cancer and uses a hybrid membrane-targeting motif', *PNAS*, 112(3), pp. 779–784. doi: 10.1073/pnas.1412811112.
143. Vara, J. Á. F. *et al.* (2004) 'PI3K/Akt signalling pathway and cancer', *Cancer Treatment Reviews*, 30(2), pp. 193–204. doi: 10.1016/j.ctrv.2003.07.007.
144. Velho, S. *et al.* (2005) 'The prevalence of PIK3CA mutations in gastric and colon cancer', *European Journal of Cancer*, 41(11), pp. 1649–1654. doi: 10.1016/j.ejca.2005.04.022.
145. Vetter, I. R. (2014) 'The Structure of the G Domain of the Ras', in *Ras Superfamily Small G Proteins: Biology and Mechanisms I*, pp. 1–27. doi: 10.1007/978-3-7091-1806-1.
146. Vinci, A. D., Perdelli, L. and Banelli, B. (2005) 'p16(INK4a) promoter methylation and protein expression in breast fibroadenoma and carcinoma', *Int. J. Cancer*, 114, pp. 414–421. doi: 10.1002/ijc.20771.
147. Vladiou, M. C., Labrie, M. and St-Pierre, Y. (2014) 'Intracellular galectins in cancer cells: Potential new targets for therapy (review)', *International Journal of Oncology*, 44(4), pp. 1001–1014. doi: 10.3892/ijo.2014.2267.
148. Walther, A. *et al.* (2009) 'Genetic prognostic and predictive markers in colorectal cancer.', *Nat. Rev. Cancer*, 9(7), pp. 489–99. doi:

- 10.1038/nrc2645.
149. Wassermann, S. *et al.* (2009) 'p16INK4a is a beta-catenin Target Gene and Indicates Low survival in Human Colorectal Tumors', *Gastroenterology*. AGA Institute American Gastroenterological Association, 136(1), p. 196–205.e2. doi: 10.1053/j.gastro.2008.09.019.
150. Watson, A. R. (2007) 'Hyperplastic Polyps, Serrated Adenomas, and the Serrated Polyp Neoplasia Pathway', (Table 1).
151. William Y. Kim, W. Y. and Sharpless, N. E. (2016) 'The Regulation of INK4/ARF in Cancer and Aging', *Cell*, 127. doi: 10.1016/j.cell.2006.10.003.
152. Wong, M. *et al.* (2015) 'Targeted screening for colorectal cancer in high-risk individuals', *Best Practice & Research Clinical Gastroenterology*. Elsevier Ltd, 29(6), pp. 941–951. doi: 10.1016/j.bpg.2015.09.006.
153. Worthley, D.-L. and Leggett, B.-A. (2010) 'Colorectal cancer: molecular features and clinical opportunities.', *The Clinical biochem. Reviews / Australian Association of Clinical Biochemists*, 31(2), pp. 31–38. Available at: <http://eutils.ncbi.nlm.nih.gov/entrez/eutils/elink.fcgi?dbfrom=pubmed&id=20498827&retmode=ref&cmd=prlinks%5Cnpapers2://publication/uuid/8C22FA3D-04DC-4725-BE51-5944DE4C08E1>.
154. Wu, K.-L. *et al.* (2012) 'Overexpression of galectin-3 enhances migration of colon cancer cells related to activation of the K-Ras – Raf – Erk1 / 2 pathway', *J Gastroenterol*, (48), pp. 350–359. doi: 10.1007/s00535-012-0663-3.
155. Xing, S. *et al.* (2016) 'Techniques for the analysis of protein-protein interactions in vivo', *Plant Physiology*, 171(June), p. pp.00470.2016. doi: 10.1104/pp.16.00470.
156. Xue, M., Lai, S. C. and Wang, L. J. (2015) 'Non-invasive DNA methylation biomarkers in colorectal cancer: a systematic review', *Journal of Digestive Diseases*, 16(12), pp. 699–712. doi: 10.1111/cdd.12299.
157. Yamane, L. *et al.* (2014) 'Serrated pathway in colorectal carcinogenesis', *World Journal of Gastroenterology*, 20(10), pp. 2634–2640. doi: 10.3748/wjg.v20.i10.2634.
158. Yanai, S., Nakamura, S. and Matsumoto, T. (2015) 'What would be the best diagnostic strategy of colonoscopy for colorectal neoplasia? (East) The role of magnifying colonoscopy for the diagnosis of colorectal neoplasms: From Japanese colonoscopists' perspective', (August). doi: 10.1002/den.12568.
159. Yeh, J. J. *et al.* (2010) 'KRAS/BRAF mutation status and ERK1/2 activation as biomarkers for MEK1/2 inhibitor therapy in colorectal cancer', *Molecular Cancer*, 8(4), pp. 834–843. doi: 10.1158/1535-7163.MCT-08-0972.KRAS/BRAF.
160. Yoruker, E. E., Mert, U. and Bugra, D. (2012) 'Promoter and histone methylation and p16ink4a gene expression in colon cancer', *EXPERIMENTAL AND THERAPEUTIC MEDICINE*, (4), pp. 865–870. doi: 10.3892/etm.2012.683.
161. You, C. *et al.* (2016) 'Deregulation of the miR-16-KRAS axis promotes colorectal cancer', *Scientific Reports*, 6(May), pp. 1–12. doi: 10.1038/srep37459.
162. Yu, L.-G. (2010) 'Circulating galectin-3 in the bloodstream: An emerging promoter of cancer metastasis.', *World journal of gastrointestinal oncology*, 2(4), pp. 177–180. doi: 10.4251/wjgo.v2.i4.177.
163. Yu, L. G. (2014) 'Peanut agglutinin appearance in the blood circulation after peanut ingestion mimics the action of endogenous galectin-3 to promote metastasis by interaction with cancer-associated MUC1', *Carcinogenesis*, 35(12), pp. 2815–2821. doi: 10.1093/carcin/bgu216.
164. Zaritsky, A. *et al.* (2015) 'Live time-lapse dataset of in vitro wound healing experiments', *GigaScience*, 4(1), pp. 4–8. doi: 10.1186/s13742-015-0049-6.
165. Zhang, D. *et al.* (2013) 'Galectin-3 gene silencing inhibits migration and invasion of human tongue cancer cells in vitro via downregulating β -catenin', *Acta Pharmacologica Sinica*. Nature Publishing Group, 34(1), pp. 176–184. doi: 10.1038/aps.2012.150.
166. Zhang, W. E. I. *et al.* (2016) 'A proximity-dependent assay for specific RNA – protein interactions in intact cells', *RNA (New York, N.Y.)*, 22, pp. 1785–1792. doi: 10.1261/rna.058248.116.7.
167. Zhang, X. *et al.* (2013) 'A CDK4 / 6 inhibitor enhances cytotoxicity of paclitaxel in lung adenocarcinoma cells harboring mutant KRAS as well as wild-type KRAS', (July), pp. 597–605.
168. Zhang, Z., Rosen, D.-G. and Yao, J. L. (2006) 'Expression of p14(ARF), p15(ink4b), p16 (ink4a) and DCR2 increases during prostate cancer progression', *Modern pathology*, 19, pp. 1339–1343.
169. Zinchuk, V., Zinchuk, O. and Okada, T. (2007) 'Quantitative Colocalization Analysis of Multicolor Confocal Immunofluorescence Microscopy Images: Pushing Pixels to Explore Biological Phenomena', *Acta Histochemica Et Cytochemica*, 40(4), pp. 101–111. doi: 10.1267/ahc.07002.

Cells **2018**, *7*(2), 14; doi:[10.3390/cells7020014](https://doi.org/10.3390/cells7020014)

Review

The Yeast *Saccharomyces cerevisiae* as a Model for Understanding RAS Proteins and Their Role in Human Tumorigenesis

Giulia Cazzanelli ¹, Flávia Pereira ^{1,2,3}, Sara Alves ^{1,2,4}, Rita Francisco ¹, Luísa Azevedo ^{1,2,4,5}, Patrícia Dias Carvalho ^{1,2,4}, Ana Almeida ¹, Manuela Côrte-Real ¹, Maria José Oliveira ^{2,3}, Cândida Lucas ¹, Maria João Sousa ^{1,*†} and Ana Preto ^{1,*†}

¹CBMA—Centre of Molecular and Environmental Biology, Department of Biology, University of Minho, Campus de Gualtar, 4710-057 Braga, Portugal

²Instituto de Investigação e Inovação em Saúde, Universidade do Porto, Rua Alfredo Allen 208, 4200-135 Porto, Portugal

³New Therapies Group, INEB-Institute for Biomedical Engineering, 4200-135 Porto, Portugal

⁴IPATIMUP-Institute of Molecular Pathology and Immunology, University of Porto, Rua Júlio Amaral de Carvalho 45, 4200-135 Porto, Portugal

⁵Department of Biology, Faculty of Sciences, University of Porto, Rua do Campo Alegre S/N, 4169-007 Porto, Portugal

*Correspondence: apreto@bio.uminho.pt (A.P.); mjsousa@bio.uminho.pt (M.J.S.); Tel.: +351-253-601524 (A.P.); +351-253-601545 (M.J.S.); Fax: +351-253-678980 (A.P. & M.J.S.)

†These senior authors contributed equally to this work.

Received: 25 December 2017 / Accepted: 12 February 2018 / Published: 19 February 2018

Abstract:

The exploitation of the yeast *Saccharomyces cerevisiae* as a biological model for the investigation of complex molecular processes conserved in multicellular organisms, such as humans, has allowed fundamental biological discoveries. When comparing yeast and human proteins, it is clear that both amino acid sequences and protein functions are often very well conserved. One example of the high degree of conservation between human and yeast proteins is highlighted by the members of the RAS family. Indeed, the study of the signaling pathways regulated by RAS in yeast cells led to the discovery of properties that were often found interchangeable with RAS proto-oncogenes in human pathways, and vice versa. In this work, we performed an updated critical literature review on human and yeast RAS pathways, specifically highlighting the similarities and differences between them. Moreover, we emphasized the contribution of studying yeast RAS pathways for the understanding of human RAS and how this model organism can contribute to unveil the roles of RAS oncoproteins in the regulation of mechanisms important in the tumorigenic process, like autophagy.

Keywords: RAS proteins; *S. cerevisiae*; model; homologues; colorectal cancer; autophagy; KRAS

1. Introduction

The exploitation of eukaryotic organisms as biological models has been fundamental for biological discoveries up to the present day. Among those models, a special position is reserved for the yeast *Saccharomyces cerevisiae*, which continues to be extremely useful for the investigation of basic cellular processes conserved in complex multicellular organisms such as humans, profiting from the availability of a larger set of resourceful techniques [1,2,3]. Almost thirty years ago, the power of yeast as a model organism was already clear, due to “the facility with which the relation between gene structure and protein function can be established” [4].

Importantly, in 1996 *S. cerevisiae* was the first eukaryote to have its complete genome sequenced and published [5] and continuous updates have been made since [6]. A few years later, a set of yeast strains with deletions of most of its annotated open reading frames (ORF) was made available [7,8] and currently, relatively simple methods for introducing gene mutations are well established, allowing the discovery of the biochemical function of the analyzed gene and the outcomes of the gene loss [1]. Supported by these resources, the research on *S. cerevisiae* had important repercussion for unveiling the role of many different proteins in the biology of human cells [1,3]. This was possible because of the high degree of conservation of many of the yeast and human proteins, at the level of both amino acid sequence and function.

One such example of a high degree of conservation is the case of the members of the RAS family of proteins [9,10,11]. RAS genes are the founding members and prototypes of the RAS superfamily of small guanosine triphosphatases (GTPases). The “classical” mammalian RAS proto-oncogenes (HRAS, KRAS and NRAS) are the most extensively studied among all the RAS superfamily members because of their direct involvement in tumorigenesis. The members of RAS are involved in cell proliferation, gene expression, differentiation, migration/invasion, autophagy and apoptosis [12,13,14,15,16,17]. The interest in RAS began in the 1960s with the discovery of Harvey and Kirsten rat sarcoma retroviruses, which were identified as viral genes transduced from the rodent genome and responsible for causing tumors in mice. These genes were respectively termed v-HRAS and v-KRAS [18,19]. Nevertheless, it was only in 1982, with the identification of activated mutant forms of these genes in human cancer cell lines, that intensive biochemical, biological and structural studies of RAS began [20]. In addition to the previously described RAS isoforms, a third isoform was identified in 1983 and named neuroblastoma (N-) RAS [21]. In the same period, the two RAS yeast homologues, RAS1 and RAS2, were identified based on DNA sequence similarity with KRAS and HRAS [9]. The yeast Ras proteins were isolated [22] and their nucleotide sequences were determined [10,11]. The importance of the study of yeast RAS proteins in elucidating mammalian RAS regulation and roles was immediately clear [23,24,25,26,27]. Since then, the studies of the RAS pathway in humans has led to the discovery of properties that were often found

to be interchangeable with the yeast RAS pathway, and vice versa, due to the high degree of similarity among their protein members and upstream regulators. However, it is important to stress that human and yeast proteins are not identical, and likewise, the pathways they control also differ.

In this work, we performed an updated critical literature review on human and yeast RAS pathways, specifically highlighting the similarities and differences between them. Moreover, we emphasized the contribution of studying yeast RAS pathway for the understanding of human RAS oncoproteins and how this model organism can contribute to the unveiling of their role in the regulation of mechanisms important in the tumorigenic process, like autophagy.

2. *S. cerevisiae* as a Model Organism for Studying Human Proteins and Molecular Mechanisms Underlying Associated Diseases

Current understanding of basic aspects of different cell processes, such as cell cycle, DNA replication, vesicular trafficking, aging and cell death has received a major contribution from studies on *S. cerevisiae* [1], supporting the use of this organism as a powerful experimental system. Different factors contribute to the success of yeast as a model organism. First of all, *S. cerevisiae* is a eukaryote, so it shares the cellular structure and organization of higher eukaryotic cells, such as mammalian cells. Secondly, when comparing yeast and other organisms, it is clear that both amino acid sequences and protein functions are conserved. Thirdly, as mentioned above, a broad range of specific molecular tools and resources are available in yeast. Indeed, besides the sequenced genome [5] and a set of yeast ORF deletion strains [7,8], other collections with genome-wide coverage are available, such as a collection of GFP-fused chimera proteins that helps localize endogenous yeast proteins [28,29]. Moreover, the Saccharomyces Genome Database (<http://www.yeastgenome.org/>), which gives detailed and updated information about every yeast gene, is available. All these resources have made it possible to uncover the role of almost 85% of the 5800 protein-coding genes of *S. cerevisiae*, with important repercussions for the biology of other organisms, including humans.

Approximately 17% of yeast genes are members of orthologous gene families associated with human diseases [30] and, conversely, 30% of known genes involved in human diseases have yeast orthologues and can substitute for yeast gene function [31]. The fact that many of the protein functions discovered in yeast can then be translated to higher eukaryotes evidences the relevance of using this model in the study of proteins involved in human disorders. At first glance, it might seem that yeast proteins have little to do with processes involved in human diseases. However, some of these processes can be better analyzed in the simpler environment of yeast cells, like in the case of the aggregations of misfolded proteins implicated in neurodegenerative disorders, such as Parkinson's, Huntington's and Alzheimer's diseases [2,3,32,33]. Besides studying yeast protein functions and then translating them to higher eukaryotes, a different approach can be considered to directly understand the role of human proteins: the creation of humanized yeast by heterologously

expressing human proteins [34] (Figure 1). This strategy is particularly helpful in the discovery of human protein functions associated with a disease in a “neutral” environment, devoid of the different layers of complexity that were acquired during evolution. It is also useful for determining the outcome of protein mutations [1]. The expression of human proteins in yeast can also be instrumental in the discovery of chemical or protein inhibitors of their activity in high-throughput screenings. These assays are based on the fact that human proteins expressed heterologously may cause growth defects in yeast, which can be suppressed by chemical compounds or by the expression of a second human protein [3]. Yeasts have also been used to express human genes that do not have an endogenous functional counterpart. This approach has been successfully exploited in the study of neurological disorders such as Huntington’s, Alzheimer’s and Parkinson’s diseases [32,33,35,36,37,38].

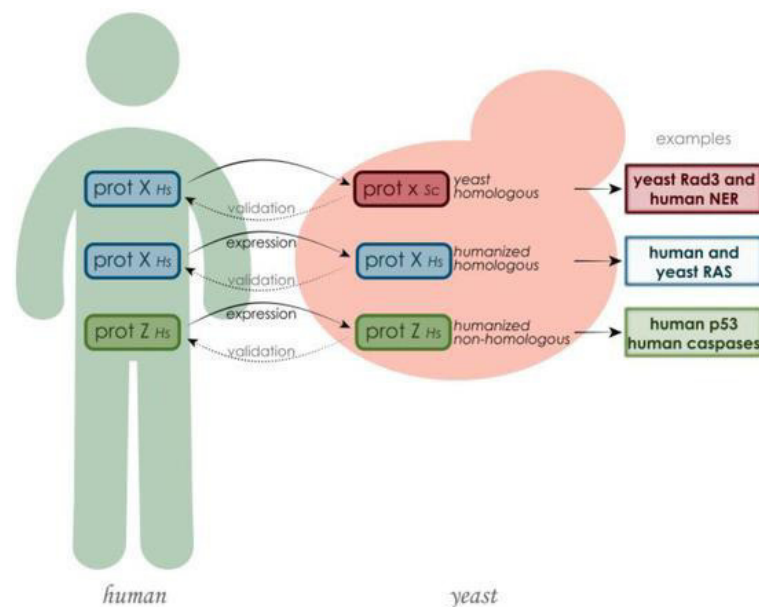


Figure 1. The study of human proteins putatively involved in disease using *S. cerevisiae* as model can be summarized in three main methodologies. If the human protein has a yeast counterpart, the yeast protein can be studied in its environment and its function can be compared with the one in human cells, or the human gene can be cloned and expressed in yeast, in order to be studied in a neutral environment. Also human proteins that do not have a yeast orthologue can be cloned in yeast, especially with the purpose of finding their inhibitors or activators. In every case, the discoveries made in yeast need further validation in human cells.

Importantly, yeast has been applied in the study of proteins relevant for tumorigenesis [39,40] and in the discovery and testing of anticancer agents [41,42,43,44]. For example, yeast deletion mutant collections have been used to identify genes involved in UV sensitivity, and the correspondent human orthologues putatively associated with cancer development [45], and to screen for drug effects, for instance to test sensitivity and/or resistance to the common anticancer drug bleomycin [46]. Several cellular processes important in cancer onset and progression, such apoptosis and cell growth, have also been analyzed in yeast. The heterologous expression of caspases in yeast greatly helped to uncover their mechanism of activation [47]. Importantly, high expression level of

caspsases in yeast caused severe growth defects, and this phenotype facilitated the identification of caspase natural inhibitors, such as IAPs and p35 [47,48], as well as chemical inhibitors and activators [49]. Bcl-2 family members have also been studied in yeast. A Bcl-2 family pro-apoptotic member, Bax, is capable to induce cell death in yeast. Screening for its inhibitors led to the discovery of Bax inhibitor 1, Bar1, HMGB1, bifunctional apoptosis regulator and Calnexin orthologue Cnx1 [50,51,52,53,54], and other inhibitors belonging to the Bcl-2 family, such as Bcl-2 and Bcl-X_L [55]. Studies on p53, one of the most important proteins in cancer development, have also been addressed in yeast. p53 is mutated in approximately 50% of human cancers and, when not mutated, often other proteins involved in p53-mediated pathways are non-functional [56]. There are no orthologues of p53 in yeast, but this protein can maintain most of its activity as transcription factor in *S. cerevisiae* [57,58,59]. Aside from the conserved function, p53 can cause a mild decrease of yeast growth [60,61]. All these factors have been extensively exploited to better analyze the function and regulation of p53. For example, p53 regulation by redox level and thioredoxin reductase were first discovered in yeast and then confirmed in mammals [62,63]. Another study revealed the conservation in yeast of functional transcription-dependent and -independent p53 apoptotic mechanisms [64]. Also the importance of p53 mutations for pathogenesis has been analyzed in yeast, facilitated by the amenability of yeast high-throughput assays. Indeed, all the mutations of p53 representing amino acid substitutions were expressed in yeast and tested for various aspects, including the ability to activate proteins involved in cell cycle and apoptosis [65,66,67].

S. cerevisiae as a Model Organism for Studying Human RAS Proteins

Human RAS proteins have a role in tumorigenesis and are highly conserved in yeast [9,10,11]. Indeed, though they do not activate the same downstream pathways, the upstream regulating events and the resulting effects are often very similar. Therefore, the usage of *S. cerevisiae* as model for dissecting the role of these oncoproteins and the underlying molecular mechanisms was not only possible, but was also extremely useful.

Historically, the study of yeast RAS pathway has brought great insights in the understanding of mammalian RAS pathway. First of all, yeast was very useful for understanding the post-translational process necessary for RAS proteins to translocate to the plasma membrane [68]. In particular, the usage of a *S. cerevisiae* mutant, *dpr1Δ*, made clear that acylation could not be the first translational modification in the processing of RAS proteins [69]. Moreover, the first RAS effector, adenylate cyclase, and the first guanine-nucleotide exchange factor (GEF), Cdc25, were identified in yeast [70,71,72]. These discoveries, especially the one of Cdc25, helped to uncover similar proteins in other organisms, including humans, based on homology [73,74,75]. In addition to GEF proteins, yeast has been useful to deepen the understanding of the other class of RAS regulators, GTPase activating proteins (GAPs), IRA in yeast. Indeed, the functions of GAP-

coding *NF1* gene, whose mutations are responsible for neurofibromatosis type 1, were clarified thanks to the similarity with *IRA* genes of *S. cerevisiae* [76]. Importantly, expression of *NF1* in yeast can suppress the phenotypes caused by deletion of *IRA* genes, such as heat shock sensitivity [77], proving that mammalian and yeast GAPs are interchangeable and highlighting the similarity between yeast and mammalian RAS proteins activation.

3. Human and Yeast RAS Proteins: Similarities and Differences

The human RAS family includes three genes: *HRAS*, *NRAS*, and *KRAS*. These three loci encode four different protein isoforms: HRAS, NRAS, KRAS4A, and KRAS4B. The two KRAS isoforms differ due to the alternative splicing of exon 4 in the KRAS locus. KRAS4A is expressed at low levels, whereas KRAS4B (hereafter referred to as KRAS) is ubiquitously expressed and accounts for 90–99% of all KRAS mRNA [12,78,79,80]. All isoforms are similar (~85%) in their primary amino acid sequence in the G-domain, which is responsible for GTP/GDP binding, whereas the major differences are concentrated in the hypervariable region (HVR) at the C terminus, which is particularly important for post translational modifications (PTMs) and consequent intracellular targeting [81]. Despite their high conservation at the amino acid sequence level, their functions differ significantly and they do not display redundant functionality. The specific roles of RAS proteins may be explained by various factors, such as cellular context, differential interaction with effectors, compartmentalized signaling and PTMs [82]. While HRAS, KRAS4A and NRAS have been shown to be dispensable for normal development in mice, KRAS4B knockout was proven to be embryonically lethal [12].

S. cerevisiae expresses two proteins homologous to human RAS, Ras1 and Ras2. *RAS1* and *RAS2* genes are located in chromosome XV and XIV, respectively [25,83], and encode two highly similar proteins of 36 and 40 kDa [22,84]. Ras1 and Ras2 have the same function, but different expression regulation [85,86]. Initially, they were thought to have different roles in the cell, because Ras1 could not complement growth defects caused by the deletion of *RAS2*, such as reduced growth on non-fermentable carbon sources and low level of intracellular cAMP [25,87,88], and *RAS1* mutants did not present any clear phenotype. However, these effects are now explained by the different regulation of the mRNA production and of protein translation of *RAS1*. Indeed, the level of *RAS1* mRNA and protein synthesis are reduced as cells approach mid-logarithmic phase and when cells are grown on non-fermentable carbon sources [85], while *RAS2* mRNA levels are high during growth phases [86] and on both fermentable and non-fermentable carbon sources [85]. The final confirmation that the only difference between *RAS1* and *RAS2* lies in differential expression was obtained by expressing *RAS1* under the constitutive *ADHI* promoter. In this case, *RAS1* was able to fully suppress the phenotype of $\Delta ras2$ and the hyperactive mutant of *RAS1* showed the same effects as the constitutively expressed *RAS2* [89].

As observed in comparisons within human RAS isoforms and within yeast RAS isoforms, the similarity between human and yeast RAS also resides in the functional G-domain of 180 amino acids, whereas the region of divergence is located at the C-terminal, corresponding to the HVR [9,10,11]. In addition, the yeast RAS molecular weights are higher than those of human RAS, with the size of the proteins being approximately 40 kDa, in contrast with mammalian RAS, which accounts for 21 kDa [22,90] (Figure 2).

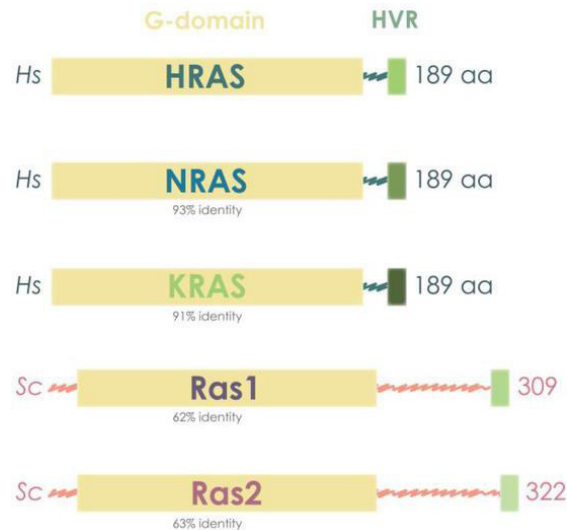


Figure 2. Yeast and human RAS proteins present a highly conserved G domain, which is responsible for GTP/GDP binding. Human RAS proteins are also highly similar among them, HRAS showing 91% of amino acid identity in the G-domain to NRAS and 93% to KRAS. Yeast Ras proteins are bigger, having more than 100 extra amino acids, but still present around 60% amino acid identity in the G-domain to human RAS proteins.

3.1. Human and Yeast RAS Sequence and Structure

We performed a comparative analysis of yeast and human RAS amino acid sequences and confirmed the high similarity in sequence and structure between human and yeast RAS proteins (Figure 3). Specifically, the N-terminal region is strongly conserved, especially in the first half of the sequence. This reflects the important functional constraints involved in the recognition of guanine nucleotide and phosphate, for which the N-terminal is responsible (Figure 3a). In this segment, 58% of residues are identical between any of the yeast RAS proteins and any of the mammalian RAS sequences. As expected, G12 and G13 residues, which are frequently found mutated in cancer, are among those invariant positions (Figure 3a). The human KRAS structure (PDB ID 3GFT) was used to infer the structure of the yeast RAS (Figure 3b) through homology modeling, as previously documented [91,92]. This comparative analysis evidences the similarity between human KRAS and both yeast RAS proteins (Figure 3c) and suggests that the differences in amino acid sequence would still result in a similar fold in humans and yeast proteins (Figure 3c). The main difference between the three mammalian RAS isoforms (KRAS, HRAS and NRAS) and yeast homologues lies at the C-terminal domain, in the HVR, which is critical to membrane localization and function (Figure 3a). Interestingly, yeast RAS proteins contain an extra C-terminal

portion not present in RAS protein from other organisms ([Figure 3a](#)). The extended C-terminal accounts for 120 aa in the case of Ras1 and 131 aa for Ras2, making yeast RAS HVR around 140 aa [[89](#)]. It has not been established yet if this part can form a secondary structure, however its function has been identified. The extended C-terminal was reported to serve as a negative regulatory domain for RAS, promoting its interaction with GDP and therefore the permanence in the inactive status [[93](#)]. Accordingly, it was shown that yeast cells expressing truncated RAS proteins lacking the C-terminal domain (or mammalian RAS proteins, without the extra 120 aa) do not require a functional GEF to be viable, while they do when expressing normal RAS proteins [[89](#)].



(a)

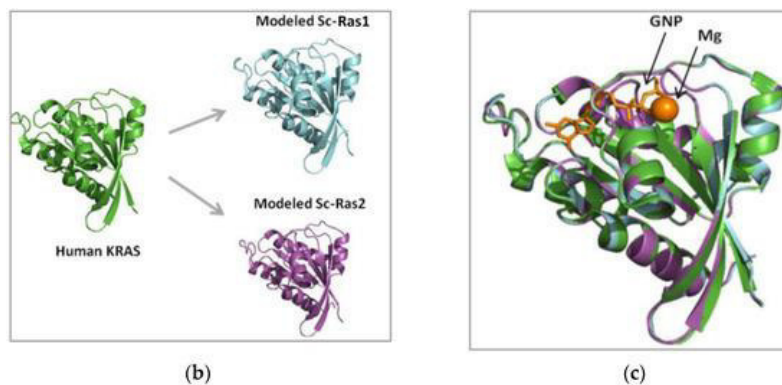


Figure 3. Comparison of RAS proteins between human (Hs) and yeast (Sc) species. (a) Alignment of human KRAS, NRAS and HRAS with yeast Ras1 and Ras2. Identical residues at homologous positions are shown in blue. The Gly12 and Gly13 sites are highlighted in red. The CAAX box is highlighted in green. The lysine repeats of KRAS4A are highlighted in pink. Human sequences were obtained from Ensembl (KRAS4B: ENSP00000308495, KRAS4A: ENSP00000256078, NRAS: ENSP00000358548 and HRAS: ENSP00000309845) and yeast sequences from the *Saccharomyces* Genome Database (RAS1: YOR101W and RAS2: YNL098C). Sequences were aligned in Geneious 5.5.8 [[94](#)], using Muscle [[95](#)]. (b) Models of *S. cerevisiae* Ras1 (blue) and Ras2 (purple) using human KRAS structure (3GFT) as a template (green). (c) The three structures are shown superimposed, revealing the fold similarity. GDP and Mg sites are shown in orange.

3.2. RAS Mechanism of Action and Regulators

Since all RAS proteins share a conserved G-domain, which is the functional domain that binds to GTP/GDP, they all present a common mechanism of action. All RAS proteins work substantially as binary molecules switching between an inactive state, in which they are bound to GDP, and an active state, in which they are bound to GTP. Our understanding of the molecular mechanism underlying the activation of RAS proteins has been greatly facilitated by the similarity between human and yeast RAS proteins. Specifically, the relevance of a glutamine in position 61 for the intrinsic hydrolysis activity of human RAS [96,97] was better understood and confirmed by the comparison with yeast. Indeed, the substitution of the glutamine with a leucine in both human and yeast, position 61 and 68, respectively, reduced the GTPase activity of human and yeast RAS proteins [98]. The activation of RAS proteins leads to the subsequent activation of a signaling cascade, which differs depending on the organism and the specific RAS protein [99,100]. Even though the proteins that interact with RAS for the activation of downstream signaling are different in different organisms and for different RAS isoforms in the same organism, most of them share a conserved domain to interact with RAS proteins, the RAS-binding domain (RBD) or RAS association (RA) domain [100]. Many RAS effectors have been identified by screening cDNA libraries for the presence of RA domain [101,102,103]. The conserved working mechanism of RAS proteins relies on their conserved sequence, in particular on the presence of a set (1 to 5) of G box GDP/GTP-binding motif elements beginning at the N-terminal domain, which together form a G-domain of approximately 20 kDa [104]. Particularly relevant among the G box motifs are switch I and switch II, which regulate the conformational changes between GTP- and GDP-bound RAS proteins [105,106]. The conformations of active and inactive state show pronounced changes corresponding to the regions of switch I and II, and these small variations lead to different affinities of active or inactive RAS proteins toward RAS regulators and effectors [107,108,109].

RAS protein switching between GTP and GDP binding is regulated by two classes of proteins: GAPs and GEFs. GAPs enhance the intrinsically low GTPase activity of RAS proteins, up to 300-fold acceleration [110], in order to reinstate the GDP-bound form of RAS proteins [111], whereas GEFs promote the formation of GTP-bound form, by triggering the dissociation of GDP from RAS proteins, allowing more abundant GTP to bind in its place [112] (Figure 4). As mentioned above, the similarity between human and yeast RAS was a great contribution to the discovery of GEF and their relevance for the proper switch between active and inactive RAS. Indeed, the first GEF, Cdc25, was identified in *S. cerevisiae* [70,71,72]. Based on the homology with Cdc25 and the *Drosophila* GEF, mammalian GEFs were also discovered and identified as RAS switch regulators [73,74,75,113]. The similarities between RAS regulators, in addition to the ones between RAS proteins themselves, contributed to clarifying some aspects of the RAS mechanism. For example, comparing the sequences of various GAPs, including Ira1 and Ira2 from *S. cerevisiae* and

human p120GAP, was very important in understanding which regions of the protein were fundamental for the interaction with RAS [96]. Importantly, to reinforce the similarity between human and yeast RAS regulators, yeast Cdc25 can act as GEF for human RAS [114] and mammalian GAPs can enhance the GTPase activity of yeast RAS proteins [77,115], making GEFs and GAPs interchangeable between human and yeast.

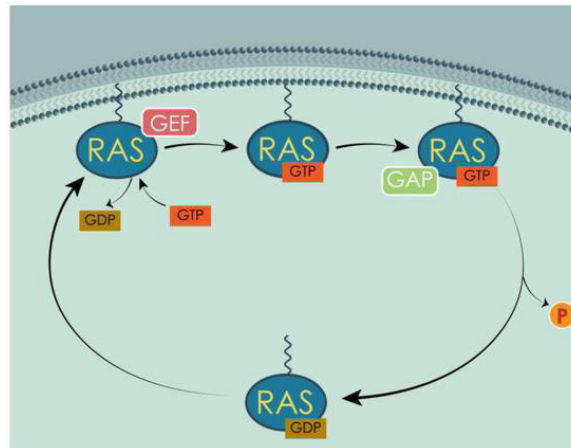


Figure 4. Inactive RAS proteins bound to GDP are localized in the cytoplasm. GEFs catalyze the liberation of GDP from the binding site, allowing GTP, more abundant in the cell, to bind instead. GTP-bound RAS are translocated to the membrane and activated. GAPs enhance the endogenous GTPase activity, hydrolyzing GTP to GDP. RAS is inactive again and goes back to the cytoplasm, where the cycle can begin again, upon proper stimulus.

3.3. Post-Translational Modifications of Human and Yeast RAS

The activity of both human and yeast RAS proteins is not regulated only by their GTP/GDP binding state, but also by PTMs, which determine RAS sub-cellular localization. Indeed, the localization of RAS proteins at the plasma membrane or on endomembranes establishes the class of effectors and regulators available, determining in turn the downstream signaling [99,100]. As happened in the case of the protein regulators of RAS, GAPs and GEFs, yeast had a pivotal role in the study of the PTMs of RAS. In particular, the study in yeast led to the understanding that RAS processing in the CAAX box was necessary for its translocation to the membrane and, therefore, for its proper activity [69,90,116]. Yeast also contributed to the determination of the sequence of PTMs necessary for RAS processing [117,118]. The discoveries made in yeast were soon translated for human RAS, when it was observed that a human RAS protein expressed in yeast underwent the same PTMs in order to function [68].

RAS proteins are synthesized as cytoplasmic proteins [119] and then undergo different PTMs that fully activate and target them to the inner leaflet of the plasma membrane [100]. The C-terminal domain is necessary for this sub-cellular localization, because it contains the CAAX (C = cysteine, A = aliphatic amino acid, X = terminal amino acid) motif indispensable for membrane targeting [99,100,120]. The cysteine in the CAAX motif is the target of farnesyltransferase, which catalyzes the addition of a farnesyl isoprenoid [99,100,121,122,123]. It has been proved experimentally that

the addition of a geranylgeranyl isoprenoid (geranylgeranylation) to the CAAX motif can substitute the farnesylation [124]. However, this PTM has only been observed when farnesyltransferase was blocked by specific inhibitors [124,125,126]. This modification is the first step of RAS processing, followed by other modifications, such as palmitoylation, driven by a second signal contained in the HVR [100]. These two steps are the minimum signal required for transit to and tenure at a membrane, either plasmatic or of internal organelles. This specific differentiation, plasma or endo-membranes, depends exactly on the second step of RAS proteins processing, which is often different for distinct RAS isoforms.

3.4. *Differential Localization of Human and Yeast RAS*

The localization of RAS proteins in either biological system has always been a matter of debate, with interesting results from both mammals and yeasts. In both organisms, RAS proteins can exhibit intracellular localizations, but are almost always associated with membranes. Notably, the specific site in which they reside dictates their function and effects, through the interaction with specific partners [99,100].

Localization of RAS proteins in mammals varies throughout their lifetime. Once in the active form, i.e. farnesylated, RAS proteins organize themselves in pools situated in the Golgi, the endocytic compartments and the endoplasmic reticulum (ER) [127,128,129]. From that step forward, the processing of the different RAS isoforms differs. HRAS is palmitoylated on C181 and C184, NRAS is palmitoylated only on C181 and KRAS4B is not palmitoylated at all [122,130,131]. KRAS4B contains a polybasic region constituted by a stretch of lysines that enables an electrostatic interaction with the negatively charged plasma membrane phospholipids [122,124,130,132,133] and excludes it from a Golgi-dependent trafficking pathway [127]. Once the CAAX processing is complete, RAS isoforms follow different routes. Palmitoylated isoforms visit the Golgi, where they are acylated and thereby trapped in its membranes, from where they traffic, via vesicular transport, to the plasma membrane [134]. KRAS4A is believed to follow this pathway, as this splice variant does not have the polybasic domain of KRAS4B and it is palmitoylated at C180 [131]. In contrast, KRAS4B cannot be trapped in the Golgi and is directly routed from the endoplasmic reticulum to the plasma membrane by a still poorly understood delivery system that could involve cytosolic chaperones [134] (Figure 5).

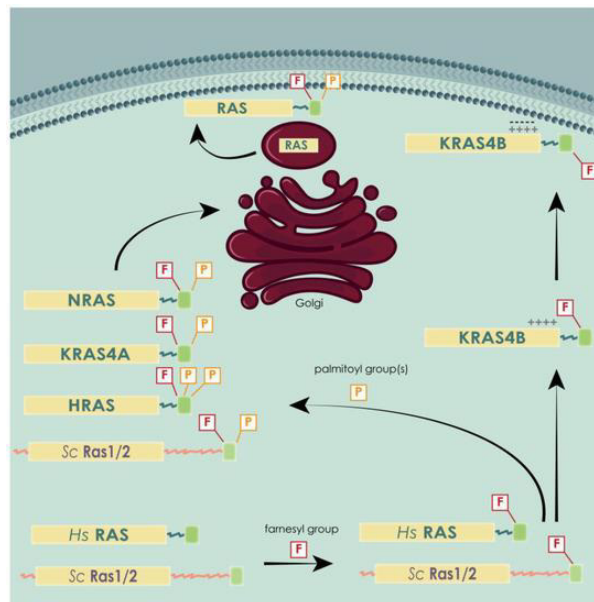


Figure 5. All RAS isoforms undergo a first farnesylation, followed by single palmitoylation in the case of KRAS4A and NRAS, double palmitoylation in the case of HRAS, and no palmitoylation in the case of KRAS4B. This splicing variant is retained in the inner leaflet of the plasma membrane by electrostatic interaction between the positively charged lysines and the negatively charged phospholipids. The three palmitoylated isoforms first pass through the Golgi and are then transported to the membrane via vesicular trafficking. Yeast RAS proteins behave very similar to the palmitoylated human isoforms, also being palmitoylated.

In addition to different PTMs, RAS isoforms also display different final localizations on the membrane. For example, Prior et al. [135] demonstrated, through electron and confocal microscopy, that HRAS in its inactive state is predominantly localized at cholesterol-rich domains inside or outside caveolin-rich domains called caveolae, whereas upon activation it delocalizes to disordered regions of the plasma membrane. As for KRAS, it was described to be located mostly outside caveolae and lipid rafts and preferably in electron-dense regions [135]. Once localized at a membrane, either plasmatic or of an internal organelle, RAS isoforms are not dispersed randomly, but are grouped in organized subdomains, as firstly suggested by Roy et al. [136]. Clustering of RAS proteins at the plasma membrane seems to be related with galectins, namely galectin 1 and 3 [137] and cholesterol content [129,136,138,139]. For many years, plasma membrane localization was considered the main platform from which RAS proteins activated their effectors [140]. However, increasing evidences show that RAS proteins are still capable of activating their signaling pathways when located on endomembranes [127,128,140,141]. The presence in the endosomal system of adaptor proteins that are required to activate RAS [142,143] is a strong indicator that RAS proteins could localize in internal cell compartments and signal from there [142,144]. As further evidence, it was shown that ubiquitination of HRAS and NRAS alters their sub-cellular localization to endosomes [145]. KRAS translocates from the plasma membrane to the early and late endosomes through a clathrin-dependent pathway and independently of CaM and protein kinase C phosphorylation [146]. From late endosomes (LEs), KRAS is eventually targeted to lysosomes, as

indicated by confocal microscope images showing that GFP-KRAS co-localized, to some extent, with both LAMP1 and LAMP2 lysosomal markers. Fluorescent probes revealed that KRAS was active on LEs, and recruited RAF to initiate a MAP kinase signaling cascade [146]. A study from Chiu et al. [140] showed that HRAS and NRAS engaged their RBD in Golgi and ER after stimulation with common mitogens, such as epidermal growth factor (EGF) and insulin, and from there they were able to activate different signaling pathways with different efficiency. KRAS was found to relocate from the plasma membrane to ER and Golgi after being phosphorylated by protein kinase C on serine 181 [147] and to move along the endocytic compartment maintaining the ability to activate MAPK (mitogen-activated protein kinase) upon EGF stimulation [146]. Association with mitochondria has also been reported [148] (Figure 6).

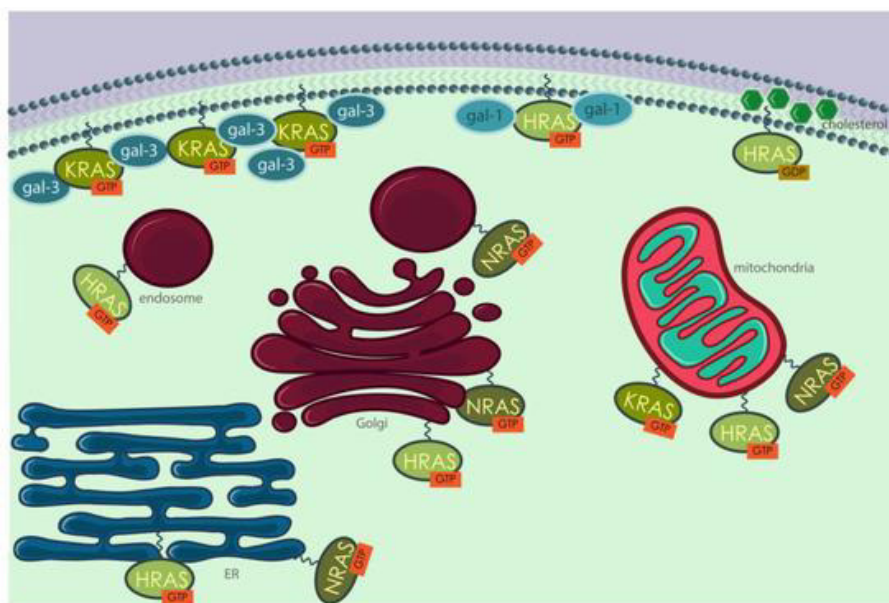


Figure 6. Human RAS proteins are localized in different cellular compartments, almost always associated with membranes. KRAS and HRAS are found in the inner leaflet of the plasma membrane, associated with galectin-3 [151,152] and galectin-1 [153], respectively. Inactive HRAS is very often located in cholesterol-rich structures called caveolae. RAS proteins can also signal from the membranes of internal organelles, such as ER, Golgi, mitochondria and the endosomal system.

In conclusion, RAS post-translational modifications address different RAS isoforms to different localizations, specifically different intracellular organelles, and determine the relative proportion of each isoform in each location. Typically, the relative contribution on endomembranes is NRAS > HRAS and KRAS4A > KRAS4B [149,150], with KRAS4B being more often associated with plasma membranes, whereas NRAS is more frequently found on endomembranes [149].

Yeast RAS proteins also localize in different cell compartments in order to activate different effectors and thereby to control different processes [154]. Indeed, fluorescent tagging of yeast RAS proteins and their partners, including the GAP Ira proteins and the GEF Cdc25, showed that most of these molecules are actually localized on endomembranes [154]. In particular, Ras2 activates

adenylyl cyclase on the plasma membrane and is engaged to the ER by Ras inhibitor 1 (Eri1) [155]. It has also been reported to localize at mitochondrial membranes, together with Ira proteins [154]. More recent studies go further, showing that the localization of active RAS is dependent on PKA activity [156,157].

In summary, the compartmentalized RAS activities have now been validated in many cell types across species. Therefore, the exclusively plasma membrane localization of RAS proteins is evidently an oversimplification [158].

3.5. Human and Yeast RAS Downstream Signaling Pathway

As aforementioned, many studies have highlighted the great similarities between human and yeast RAS proteins at the level of sequence, structure, mechanism of action, PTMs and differential localization. On the other hand, the most evident differences between the intracellular activities of the RAS proteins in the two organisms relate to RAS effectors and their downstream signaling cascades.

Human RAS proteins work as transducers of pro-survival signals from the extracellular space to the intracellular compartment, through different tyrosine kinases receptors (TKRs), among which the most studied is the epidermal growth factor receptor (EGFR). The dimerization of the receptors upon ligand binding triggers a conformational change that activates the catalytic tyrosine kinase domain, enabling the autophosphorylation of the intracellular carboxyl-terminal domain and therefore its activation [159,160,161]. The phosphorylated intracellular domain of TKR recruits GEFs, which activate RAS, enabling it to signal downstream [162]. Activated RAS proteins can bind and activate at least 20 different effectors, among which the best known and characterized are RAF (rapidly-accelerated fibrosarcoma) kinases, phosphatidylinositol 3-kinase (PI3K) and RAL guanine nucleotide dissociation stimulator (RALGDS). Other effectors of RAS proteins are RIN1, T lymphoma invasion and metastasis-inducing 1 (Tiam 1), Af6, Nore1, PLC ϵ and PKC ζ [131,163,164,165] (Figure 7).

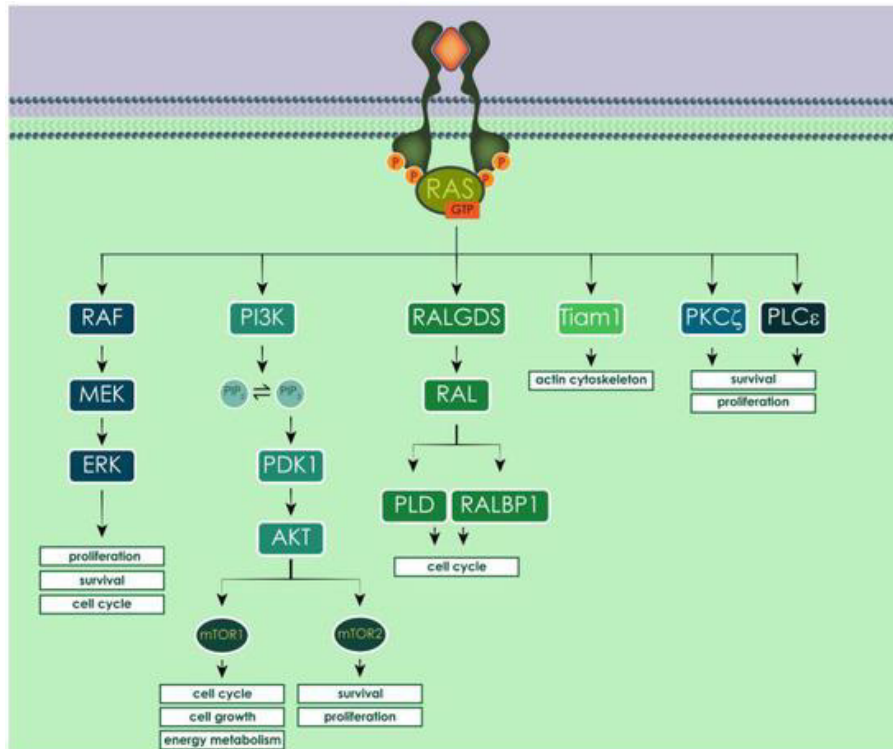


Figure 7. Activated human RAS proteins can activate multiple effectors, having different impact on cell fate. Among the most studied, activated RAF triggers pro-growth signaling through the MAP kinases cascade; PI3K leads to AKT activation and RALGDS stimulated cell cycle progression.

Activated RAF kinases phosphorylate and activate MEK (MAPK/ERK kinase), leading to the activation of ERK (extracellular signal-regulated kinase, also called MAPK). ERK regulates several transcriptional factors that influence cell cycle progression, proliferation and survival (e.g., autophagy) [21]. In the other pathway, activated PI3K catalyzes the production of PIP₃ (phosphatidylinositol-3,4-triphosphate) by phosphorylating PIP₂ (phosphatidylinositol-4,5-diphosphate), a process reversed by the phosphatase PTEN (phosphatase and tensin homolog deleted in chromosome ten). PIP₃ activates phosphatidylinositol dependent kinase 1 (PDK1), which recruits AKT to the plasma membrane and activates it [166]. The main downstream effector of activated AKT is mTOR (mammalian target of rapamycin), which is an atypical serine/threonine kinase that can form two distinct complexes, depending on which proteins interact with it. The mTOR complex 1 (mTORC1) mainly promotes the transcription of genes involved in cell growth, cell cycle progression and energy metabolism. The mTOR complex 2 (mTORC2) mainly phosphorylates AKT, originating an auto-sustaining positive feedback loop, which results in cell survival and proliferation. Moreover, AKT activation enhances telomerase activity, inhibits apoptosis blocking the release of cytochrome *c* from the mitochondria and inactivating pro-apoptotic factors such as Bad and pro-caspase 9, and regulates modulators of angiogenesis through the activation of nitric oxide synthase [167,168,169,170]. RAS, when interacting with RALGDS, stimulates RAL (RAS-like) GTPases, inducing the activation of phospholipase D1 (PLD) and CDC42/RAC-GAP-RAL binding protein 1 (RALBP1). These, among other pro-survival functions,

promote the progression of the cell cycle, inhibiting transcription factors implicated in cell cycle arrest, such as the FORKHEAD transcription factors [131,163]. Another important RAS effector is Tiam 1, which is a Rho family GTPase that regulates the actin cytoskeleton and activates p21 activated protein kinases (PAKs) and c-Jun N-terminal kinase (JNK) [134].

Similarly to human RAS, yeast RAS proteins transduce signals in response to the nutritional conditions of the environment from outside to inside the cell, especially glucose availability [93,171,172] (Figure 8). Contrarily to human RAS and TKRs, the transducer of the growth signal from the outside to the inside of the yeast cell is still not known.

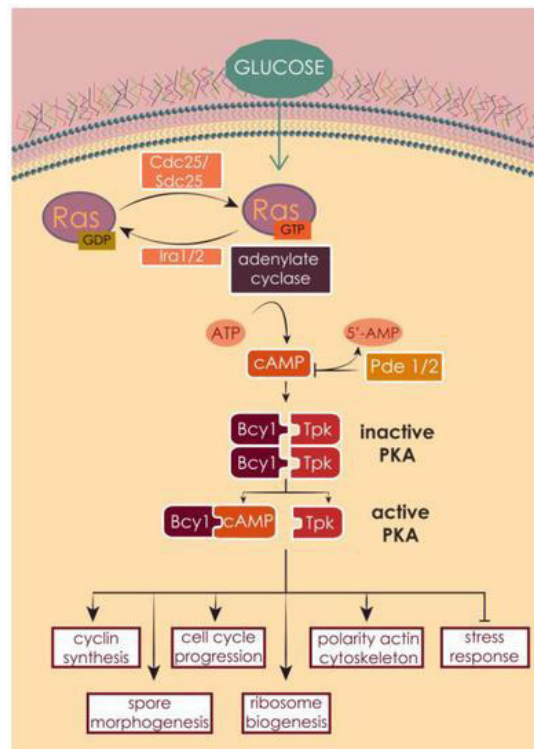


Figure 8. Ras1 and Ras2 are activated upon nutrient availability signaling, glucose in particular. The GEF proteins Cdc25 or Sdc25 catalyze the liberation of GDP and the binding of GTP. Active RAS proteins activate in turn adenylate cyclase, which produces cAMP. This second messenger binds to the inhibitory unit of PKA, releasing the catalytic unit, which phosphorylates multiple downstream targets, leading to the activation of a variety of cellular processes or to the inhibition of transcription factors that control stress response. The pathway can be inactivated by the hydrolysis of cAMP by the phosphodiesterases Pde1 and Pde2, and by the GTPase activity of the GAPs Ira1 and Ira2.

Yeast RAS proteins exert this function mainly in controlling the 3',5'-cyclic adenosine monophosphate (cAMP) metabolism. cAMP acts as second messenger in the regulation of several fundamental cellular processes, such as protein phosphorylation, accumulation of storage carbohydrates, mitochondrial functions [173,174,175,176,177,178,179,180,181], sporulation [182], sensitivity to heat shock [183] and cell cycle progression [25,184,185,186]. RAS proteins, once activated, interact with adenylate cyclase at the plasma membrane [187], which synthesizes cAMP from guanine nucleotides [27,70,93,172,188,189,190,191,192]. The main target of cAMP is protein kinase A (PKA), which is composed by a catalytic subunit, encoded by

the genes *TPK1*, *TPK2* and *TPK3* [193,194], and by a regulatory subunit encoded by *BCY1*. PKA exists in the cell as an inactive heterotetrameric holoenzyme composed by two catalytic and two regulatory subunits [193,194]. cAMP binds to the regulatory unit Bcy1, which relieves its inhibitory effect on the catalytic subunit, allowing the phosphorylation of several downstream targets [171,172,188]. cAMP synthesis is one of several PKA targets, suggesting a strong negative feedback regulation [195,196] and adenylate cyclase itself has been proposed as a PKA target [188]. PKA has a wide variety of substrates, whose activation leads to a dramatic change in the transcriptional program, which helps the cells to adapt to new nutrient conditions, in particular favoring cell growth and proliferation. PKA regulates the metabolism of storage carbohydrates, ribosomal biogenesis, stress response [197,198], polarity of actin cytoskeleton [199], spore morphogenesis [200], cyclins synthesis and subsequent cell cycle progression [25,70,201,202], cell size and growth [171].

3.6. RAS Effects on Growth, Apoptosis and Autophagy

3.6.1. RAS Effects on Cell Cycle in Human and Yeast

In both human and yeast, RAS is activated in response of the presence of growth and pro-survival signals, specifically growth factors in the case of human RAS [159,161] and glucose in the case of yeast RAS [93,171,172]. Though RAS stimulates growth, meant as an increase in cell number, these effects are not always achieved in the same way in human and yeast due to the different level of organism complexity. RAS stimulates cell cycle progression associated with increase in cell size and protein synthesis [171,197,203,204,205] (Figure 9). However, in the case of human, cell population growth is also promoted by inhibiting apoptosis and stimulating accessory processes such as angiogenesis [163,164,206].

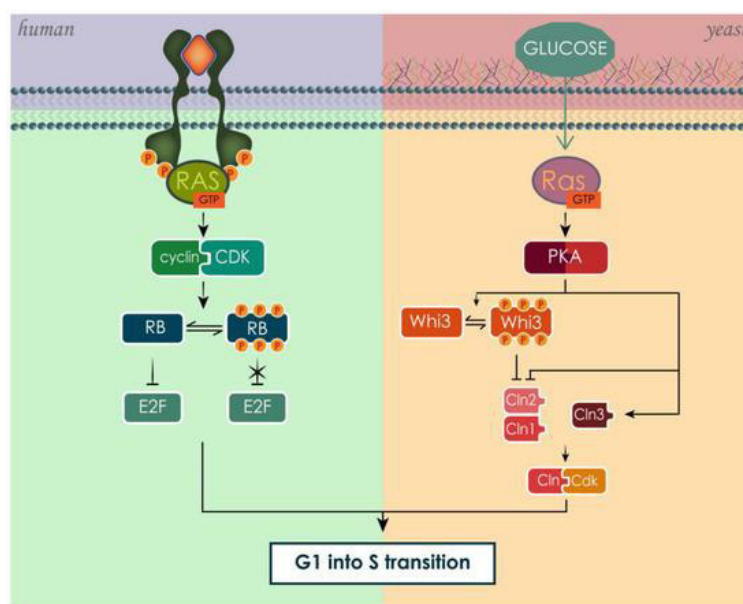


Figure 9. The activation of RAS proteins leads to G1 to S phase progression through the cell cycle in both human and yeast. In both cases, RAS stimulates the formation of functional complexes between cyclins and CDK.

The RAS pathway in mammals controls the cell cycle through a variety of different proteins, resulting ultimately in the inactivation of the retinoblastoma (RB) family of pocket proteins [203,207]. RB proteins are found in a hypo-phosphorylated state in resting cells, which confers them the ability to sequester members of the E2F transcription-factor family. These transcription factors, once free from RB inhibition, modulate the transcription of genes involved in the progression of cell cycle from G1 to S phase, especially involved in the regulation of DNA synthesis [205]. The phosphorylation of RB by cyclin-CDK (cyclin-dependent kinase) complexes frees the E2F transcription factors from inhibition. Cyclins and CDKs regulate the progression of the cell cycle by associating in active complexes [204,205]. The connection between RAS-driven pathways and the cell cycle was confirmed by experiments that utilized RAS neutralizing antibodies [208,209,210]. Cells subjected to this type of treatment stopped growth in G1 and presented hypo-phosphorylated RB. On the other hand, expression of oncogenic mutated RAS enabled cells to enter the cell cycle independently from growth factors, progressing through the cell cycle uncontrollably [211,212]. This occurs because the activating mutation of KRAS leads to its constitutive activation, by turning it more resistant to GAPs activity, and consequently, constitutively activating its downstream signaling pathway [79,213].

The RAS/cAMP/PKA pathway in yeast regulates not only the cell cycle, but also ribosome production, increase in cell size and mass and growth rate [171,197]. These processes are strictly interdependent. In fact, if on one hand the specific growth rate is determined by the rate of mass accumulation, which in turn depends on nutrient availability, on the other hand cell cycle progression and cell size both depend on specific growth rate and mass accumulation [214,215,216,217,218]. RAS/cAMP/PKA pathway can influence the cell cycle, modulating the expression of cyclins (Clns) [219], whose complexation with cyclin-dependent kinases (Cdks) is necessary to enter in S phase. In particular, RAS suppresses the expression of Cln1 and Cln2, but not of Cln3 [219,220]. Cln3 in this way counteracts the inhibition of the other Clns, mediating their growth-dependent expression [219]. In addition, PKA has been found to directly phosphorylate Whi3, a negative regulator of G1 cyclins, inhibiting its functions and thus promoting the passage into S phase [221].

3.6.2. RAS Effects on Cell Death in Human and Yeast

In addition to regulate cell proliferation, promoting cell cycle progression, RAS pathways control cell survival by modulating apoptosis [222,223,224]. Contrarily to what happens for cell cycle and proliferation, in the case of apoptosis the outcomes of RAS activation are opposite in human and yeast. Indeed, the human RAS pathway is one of the main anti-apoptotic pathways and when up-regulated it can immortalize the cells. On the opposite side, yeast RAS upregulation can lead to programmed cell death through the overexpression of genes that negatively control stress response.

RAS-mediated survival signals promote apoptosis evasion, especially through PI3K pathway. In particular, AKT can phosphorylate Bad, a pro-apoptotic member of the Bcl-2 family, and this phosphorylation causes Bad to bind to 14-3-3 in an inactive complex, instead of sequestering the anti-apoptotic proteins Bcl-2 and Bcl-X_L [225]. In addition to AKT, PI3K can activate another important survival factor, NF- κ B, through the activation of Rac [226,227,228]. NF- κ B is a potent transcription factor that induces the transcription of several anti-apoptotic genes, such as inhibitors of apoptosis proteins (IAPs) [229]. Rac, and consequently NF- κ B, can also be activated by RAS directly through Tiam 1, in a PI3K independent manner [230]. A third RAS-mediated pathway to activate NF- κ B is the phosphorylation of I- κ B kinase (IKK) by AKT [231]. The RAF/MEK/ERK signaling cascade also contributes to the regulation of apoptosis, sometimes converging its signals to the same targets as the PI3K branch, like in the cases of the pro-apoptotic protein Bad [232,233,234,235] and the transcription factor CREB, which induces the expression of pro-survival proteins [233,236]. In addition, RAS has been shown to help escaping apoptosis by downregulating Par-4, a pro-apoptotic transcription repressor, through MEK activity [237], and by inducing p53 degradation, thereby annulling p53-mediated apoptosis induction [238]. Moreover, RAS signal activity through the RAF/MEK/ERK cascade modulates the expression level of several proteins belonging to the Bcl-2 family [239,240] (Figure 10).

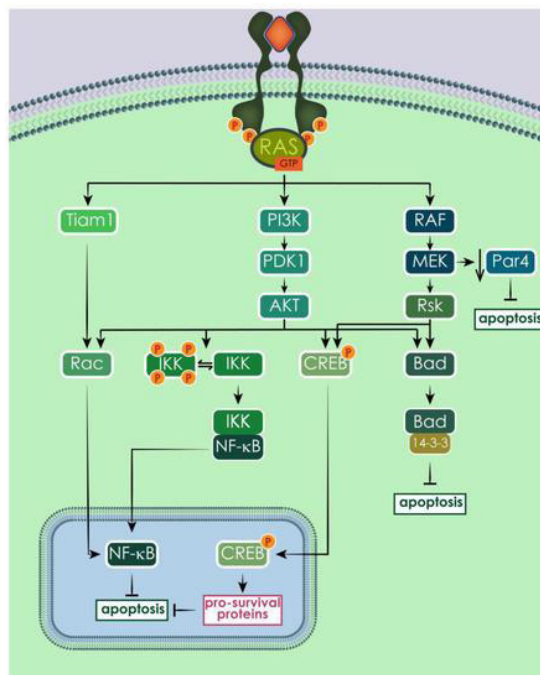


Figure 10. Human RAS proteins protect the cells from apoptosis mainly through the activation of PI3K and the consequent activation of AKT. Among AKT multiple targets there are Rac, IKK, CREB and Bad. Rac can be activated also by Tiam 1, activating in turn NF- κ B, an important pro-survival factor. AKT phosphorylates also Bad, promoting the inhibition of the pro-apoptotic factor 14-3-3 and the consequent inhibition of apoptosis, and CREB, promoting the transcription of pro-survival genes. CREB is phosphorylated also by Rsk, activated by RAF/MEK/ERK signaling cascade. In addition, MEK promotes the downregulation of the pro-apoptotic protein Par4, contributing to apoptosis inhibition.

The RAS/cAMP/PKA pathway is a major intracellular player in regulated cell death (RCD) process also in yeast [241,242,243]. It has been observed that increased activation of RAS signaling in yeast cells induces the appearance of typical apoptotic markers, such as phosphatidylserine externalization, increased reactive oxygen species (ROS) accumulation and DNA degradation, among others [244,245]. Three stimuli that lead to RAS/cAMP/PKA hyper-activation and subsequent cell death are osmotin, changes in actin dynamic and ammonium [245,246,247,248]. Osmotin, a protein produced by plants in defense to pathogenic fungi, when in contact with *S. cerevisiae* binds to Pho36, a G-protein-like homologous of the mammalian adiponectin receptor, causing the inappropriate inactivation of RAS signaling, ultimately leading to RCD of the yeast [246]. A different stimulus for RAS-mediated apoptosis in yeast is mediated by actin cytoskeleton. Mutations or addition of drugs can change actin dynamics, causing the formation of F-actin aggregates, which in turn trigger the constitutive activation of Ras2 and apoptosis [245]. In aging yeast cultures, ammonium was found to induce cell death leading to the shortening of the chronological lifespan, an effect that was mediated through the activation of the RAS/cAMP/PKA pathway [247,248]. The role of mitochondria is fundamental in yeast RCD, this organelle being the main responsible of ROS accumulation when dysfunctional [241]. ROS accumulation is a central event in yeast RCD [249,250,251,252,253] and in both osmotin- and actin-induced RCD, it seems to be the main responsible for cell death, since the addition of antioxidants could suppress the apoptotic phenotype [246,254]. RAS/cAMP/PKA pathway regulates also cell death in acidic environment [255]. Intracellular acidification caused by acetic acid, a known inducer of apoptosis in yeast, leads to RAS/cAMP/PKA activation, which causes consequent cell death [188,250,256]. Supporting the pivotal role of RAS in yeast apoptosis, deletion of *RAS* genes suppresses the apoptotic phenotype of the cells and leads to necrosis instead, while, in an acidic environment, hyper-activation of RAS pathway by constitutively active allele *RAS2^{val19}* or by deletion of *PDE2* increases apoptotic cell death [255].

3.6.3. RAS Effects on Autophagy in Humans and Yeast

Similarly to what happens for cell cycle and apoptosis, both human and yeast RAS are involved in other cellular processes relevant for cell survival and cancer progression. Indeed, both organisms use RAS proteins, among others, to regulate autophagy. In humans, RAS proteins can promote or inhibit autophagy, depending on the cell context and on the RAS isoform, whereas in yeast RAS activation leads to autophagy repression. The autophagic mechanisms are highly conserved in budding yeast and higher eukaryotes. Autophagy is a catabolic process that targets cellular components, such as damaged cell structures/organelles, long-lived proteins and pathogens for lysosomal degradation [257,258]. Autophagy involves the engulfment of intracellular constituents into double membrane vesicles, termed autophagosomes, which then fuse with lysosomes in

mammals or with the vacuole in yeast, where the autophagic contents are degraded [259]. The formation of the autophagosome is controlled by autophagy-related (Atg) proteins, first identified in yeast. More than 30 yeast *ATG* genes have been discovered, and orthologues of many of these genes have been identified and characterized in higher eukaryotes, including humans, suggesting that autophagy is a highly conserved pathway through evolution [260]. At basal levels, autophagy is constitutively active, recycling the cell contents to maintain cellular homeostasis and integrity. Additionally, autophagy can be activated in response to starvation and other conditions of metabolic stress, to provide an alternative source of energy that limits cell death [261]. Autophagy is also implicated in cellular development and differentiation [262], in innate and adaptive immunity [263], as well as in cancer, where its role is highly ambiguous: it may serve as a mechanism of adaptation to stress and consequent avoidance of cell death, or as a route to cell death, by the destruction of the cell itself [264,265,266,267,268,269].

In humans, the regulation of the autophagy process converges at the level of mTOR [270], which is one of the downstream effectors of RAS proteins (Figure 7). The best known pathway that regulates mTORC1 is PI3K/AKT and, when activated, it promotes protein synthesis, cell division and metabolism, while autophagy is suppressed. On the other side, RAF/MEK/ERK signaling cascade activated by amino acid starvation can trigger autophagy in human colorectal carcinoma (CRC) [271]. The dual role of RAS activation on autophagy can be observed also for mutated oncogenic RAS proteins and their effects on survival and proliferation. For example, HRAS^{G12V} can either inhibit autophagy by activating PI3K pathway in NIH3T3 [272], or stimulate autophagy through its effects on RAF/MEK/ERK cascade, NOXA or Beclin 1 expression in human ovarian surface epithelial (HOSE) cells, or through RALB (RAS-like protein B) signaling, or the up-regulation of Bnip3 in mouse embryonic fibroblasts (MEF) cells [273,274,275]. In mouse kidney iBMK and human MCF10A mammary epithelial cells, it was reported that overexpression of oncogenic HRAS^{G12V} or KRAS^{G12V} up-regulates autophagy and promotes cell proliferation [276,277,278]. On the other side, there are also reports showing that RAS-driven autophagy is part of a pro-death mechanism. Specifically, infection of ovarian HOSE cells with HRAS^{G12V} induced autophagy and promoted cell death [273].

In yeast, the involvement of RAS proteins in autophagy happens mostly through the activity of PKA. Once activated, it phosphorylates Rim15 and Msn2/4, preventing the translocation of these proteins to the nucleus to initiate transcription of the autophagy genes, thereby inhibiting autophagy [279,280]. PKA also inhibits autophagy by direct inhibition of Atg13, which is part of the Atg1 complex (ULK1/2 in mammals), essential for autophagy initiation [281]. TOR pathways are also involved in autophagy regulation in yeast and are highly interconnected with the RAS/cAMP/PKA pathway. TOR and RAS often control overlapping effectors, including

the ones involved in autophagy, leading to similar response in the cell, such as inhibition of stress response, aging and cell cycle progression. Importantly, both pathways are activated by the presence of nutrients, glucose in the case of RAS and nitrogen in the case of TOR [171,282,283]. *S. cerevisiae* has two Tor kinases, Tor1 and Tor2, orthologues of human TOR, but only Tor1 gives a significant contribution in the regulation of autophagy [284]. When Tor1 is activated by the presence of nitrogen it represses autophagy by direct inhibition of the Atg1 complex and sequestration of the transcription factors Rim15 and Msn2/4 in the cytoplasm [279,280,281]. Upon starvation induction or treatment with rapamycin, TOR is inhibited and autophagy is induced [285]. In addition to directly inhibit autophagy, TOR also exerts its functions through its main downstream effector Sch9, which is directly phosphorylated and activated by the TORC1 complex [286]. The inactivation of Sch9p and PKA is sufficient to trigger autophagy, suggesting that these kinases are cooperatively involved in negative regulation of this process [287].

4. Involvement of RAS Proteins in Cancer: Yeast as a Model Organism

The role of human RAS proteins in carcinogenesis is well established. Approximately 30% of all human cancers harbors an activating point mutation in RAS, with pancreas (60–90%), colon (30–50%) and lung (20–30%) cancers displaying the highest frequency [79,163,288]. KRAS mutations are common in pancreatic, colorectal, endometrial, biliary tract, lung and cervical cancers. NRAS mutations are more prevalent in myeloid leukemia and HRAS mutations predominate in bladder cancer [79,288,289]. RAS point mutations are found at the highest frequency at codons 12, 13 and 61.

The uncontrolled cell growth typical of tumors with mutated RAS is due to the hyper-activation of RAS proteins. Indeed, mutated RAS are more resistant to GAPs activity. Without being efficiently affected by GAPs, their endogenous GTP hydrolysis is too low and, in this way, RAS proteins are locked in a permanent active state, which increases RAS activity and its downstream signaling [79]. Hyper-activation of RAS signaling can be caused as well by mutations in genes encoding proteins that interact with RAS [290,291]. Another factor that causes hyper-activation of RAS signaling is the overexpression of EGFR [292]. Mutations or amplification of downstream RAS effectors have also been implicated in human cancer development [293,294,295].

Besides the aforementioned contribution of *S. cerevisiae* to clarifying several aspects of mammalian RAS upstream regulation, further evidence has sustained the rationale behind the use of this model organism to study RAS functioning. Mammalian RAS proteins can indeed act as a direct complement for yeast-deficient RAS and vice versa. In the middle of the 1980s, several studies showed that activated human HRAS could suppress the lethality of simultaneous deletion of RAS1 and RAS2 in yeast, because it shows the same ability to activate yeast adenylate cyclase as

yeast Ras1 or Ras2 [23,24,26,68,296]. The functional complementation of *RAS2* deletion in yeast by human *HRAS* was later proved also for different $\Delta ras2$ -induced phenotypes, such as temperature-sensitive growth and temperature-dependent depolarization of the actin cytoskeleton [199]. Conversely, it was shown that a yeast-mammalian hybrid gene expressed in mouse cells had the ability to induce morphological changes extremely similar to those induced by mammalian oncogenic *HRAS* [23]. In addition, a mutant variant of yeast RAS protein that resembles oncogenic *HRAS* was also identified, Ras^{val19}, which was capable to differentially activate adenylate cyclase [26,296]. *KRAS*, in opposition to *HRAS*, is not able to complement the double deletion of *RAS1* and *RAS2*, resulting in a non-viable yeast [23,24]. Results from our group [297] showed that the expression of human *KRAS* in yeast expressing its own *RAS1* and *RAS2* genes (wt) caused a decrease in the strain resistance to high non-permissive temperature, osmotic stress and oxidative stress (Figure 11). Moreover, both wt and $\Delta ras1$ or $\Delta ras2$ yeast strains expressing human *KRAS* were less able to grow on non-fermentable carbon sources like ethanol and glycerol (Figure 11). Exogenous human RAS protein, in addition to the yeast endogenous Ras1 and Ras2, increased sensitivity to stress in wild type, but this phenotype was less pronounced or absent in *RAS* deletion strains. So *KRAS* seems to be able to activate yeast RAS downstream cascades, even if it cannot complement the growth defect caused by the loss of both *RAS* genes [297]. This strongly suggests that human *KRAS*, once inside the yeast cell, has roles that are probably very close to the ones of the endogenous RAS proteins.

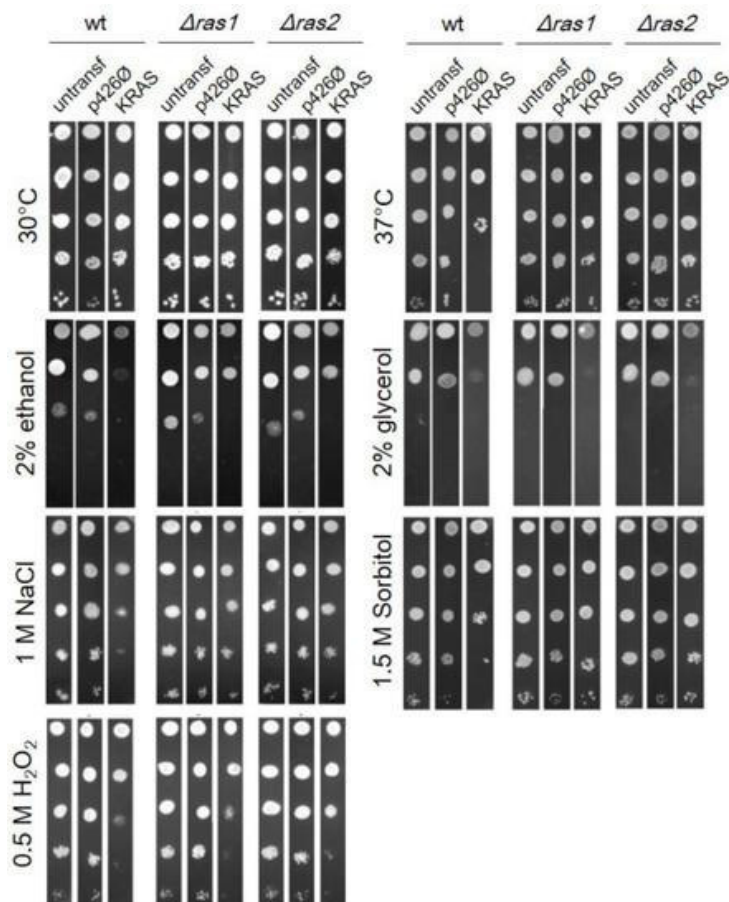


Figure 11. Serial drop test of BY4741 strain expressing human KRAS. *S. cerevisiae* BY4741 wt, $\Delta ras1$ and $\Delta ras2$ were subjected to different stress conditions (stress stimulus described on the side of each box). The direction of the serial dilutions, from 10^{-1} to 10^{-5} , proceeds from top to bottom. The image is representative of one of three independent experiments.

4.1. *S. cerevisiae* as a Model for Studying KRAS-Induced Autophagy in Colorectal Cancer

Recently, our group addressed the role of KRAS proteins in autophagy modulation using yeast as a model [17]. As mentioned above, autophagy is a highly conserved metabolic process that cells use to recycle their components and maintain cellular homeostasis [298]. Importantly, autophagy is also conserved in yeast [260]. In cancer, autophagy is involved on a double front; on one side, autophagy can weaken the cells by degrading their components, but on the other side, the recycling of peptides makes the cells less sensitive to nutrient depletion and therefore to death. This pro-survival role has been evidenced by studies showing that autophagy is implicated in the resistance of tumors to chemotherapy [299]. The RAS pathway is one of the major regulators of autophagy [272,273,275,276,277,278]. Work using a yeast strain lacking *RAS2* and transformed with either *KRAS*^{wt} or its most common mutated alleles (*KRAS*^{G13D}, *KRAS*^{G12D}, *KRAS*^{G12V}) in colorectal carcinoma made it possible to uncover that the activating KRAS mutations, unlike wild-type KRAS, increase the level of the yeast autophagy reporter Atg8 [17]. Further studies with CRC cell lines confirmed that *KRAS* mutated alleles increased autophagy, and showed that this increase was associated with increased survival under starvation conditions. KRAS-induced autophagy was

mediated through upregulation of the RAS/RAF/MEK/ERK pathway and downregulation of the PI3K/AKT pathway, known to activate the autophagy inhibitor mTOR. The humanized yeast in this case helped to determine the role of mutated and wild type KRAS in the autophagic process. This study reinforces that human RAS proteins are functional in yeast and that, as in mammalian cells, they can activate the autophagic machinery, further supporting yeast as an excellent model to study human RAS and its involvement in tumorigenesis through the modulation of autophagy.

4.2. *S. cerevisiae* as a Model for Studying KRAS/gal-3 Interaction in Colorectal Cancer

In addition to showing that human RAS can interact with endogenous yeast proteins, as discussed above for autophagy, we recently disclosed that, reciprocally, yeast RAS activity can be influenced by heterologously expressed human proteins, namely galectin-3 [297]. KRAS has been found to interact specifically with gal-3 in the cytoplasm [137,151,300]. It has been hypothesized that gal-3 may render KRAS less sensitive to GAPs and therefore maintain KRAS in a constitutive active state, increasing the pro-growth signaling transmitted by KRAS. Indeed, it has been noticed that the interaction between gal-3 and KRAS enhances PI3K activity and Raf-1 activation [151]. Gal-3 enhances KRAS activity acting as a scaffold protein, maintaining it in a proper orientation, relevant for its activity regulation [301], and in organized nanoclusters on the cell membrane, facilitating its function [137,152,302]. In addition, it seems that the expression of gal-3 increases not only the activation, but also the expression of KRAS [303]. Since KRAS promotes cell proliferation and inhibition of apoptosis and gal-3 appears to enhance KRAS activity through different mechanisms, it is conceivable that this interaction enhances cancer progression. It has been shown that gal-3 interaction with KRAS potentiates thyroid cancer progression, increasing KRAS signaling and thus proliferation [303]. In addition, gal-3 has been found overexpressed in pancreatic cancer, where it interacts with KRAS-GTP, influencing its active status and its membrane localization. Alterations in gal-3 level and consequent variation in RAS downstream signaling cascades strongly modulate the cancer phenotype. Downregulation of gal-3 decreases growth, invasiveness, anchorage independent growth and tumor growth in an in vivo orthotopic model, whereas gal-3 upregulation stimulates growth proliferation [304]. A colon cancer cell line was found to express gal-3 at high levels, and this expression correlates with the migration ability of cancer cells [305]. Further highlighting the relationship between gal-3 and the RAS pathway in colon cancer, a correlation between high levels of gal-3, RAF and ERK was found tissue samples [305]. Finally, gal-3 seems to be the adaptor for the interaction between KRAS and $\alpha_v\beta_3$ integrin, which causes tumor aggressiveness [306,307]. This further proves the fundamental role of gal-3 in mediating KRAS function and its ability to ablate KRAS-mediated pro-survival signals, when downregulated. To summarize, it has been discovered that an increased expression or availability of cytoplasmic gal-3 could confer to the cells that same tumorigenic properties—namely uncontrolled growth and downregulated apoptosis—as the mutation of an oncogene, in this case *KRAS*. This fact emphasizes the need to better understand the interaction

between these two proteins. For all these reasons, we expressed human gal-3 in yeast and measured some basic phenotypes, such as specific growth rate. Our aim was to build a humanized yeast that could be used as a model to study the interaction between KRAS and gal-3. We observed that the presence of endogenous yeast RAS proteins greatly affected the outcomes of gal-3 expression in yeast. In particular, an increase in the growth rate was observed only in the wild type yeast and not in the two *RAS* deletion mutants when gal-3 was expressed [297]. In human cells, gal-3 interacts with KRAS, stabilizing its active GTP-bound form [151,300,303,304] and its positioning on the inner side of the plasma membrane, the proper location for RAS signaling [137,151,302]. This observation suggests that yeast RAS proteins might interact as well with gal-3. This RAS/gal-3 interaction could therefore have similar effects in yeast and in human cells, namely the stabilization and activation of RAS proteins by gal-3, enhancing RAS signaling, and in this way increasing the growth rate (Figure 12) [297]. In support of this hypothesis is the fact that several other mammalian RAS partners could successfully interact with yeast RAS proteins, like the above-mentioned mammalian GTP activating protein NF1 [77,308] and proteins involved in the autophagic process [17].

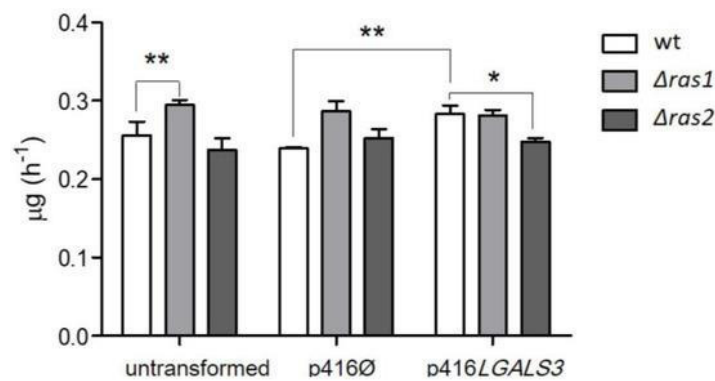


Figure 12. *S. cerevisiae* wt, *Δras1* and *Δras2* transformed with p416LGALS3 were grown on glucose for 28 h from O.D.₆₀₀ 0.05 up to stationary phase. The untransformed yeasts and the yeasts transformed with the empty plasmid (p416 Ø) were used as controls. Specific growth rates were estimated from log phase. Graphs show the average specific growth rate ± SD of three independent experiments. Statistical significant differences are shown: * (p -value ≤ 0.05) and ** (p -value ≤ 0.01).

5. Final Remarks

This review highlights the main similarities and differences between human and yeast RAS proteins and pathways. It becomes clear that RAS proteins from the two organisms share similar features, like the sequence, structure, mechanism of activation and the cellular outcomes they cause. This can still occur, though the intracellular partners and the pathways that RAS proteins activate in human and yeast differ. These differences are yet not enough to prevent RAS regulators and effectors to be functionally interchangeable in the two organisms. The main contributions of *S. cerevisiae* in clarifying different aspects of mammalian RAS regulation, such as the PTMs necessary for membrane anchorage [71,72], GAPs [79,80] and GEFs [75,76] promoting GTP/GDP binding, as

well as the role of RAS in regulation of cell cycle, growth, cell death and autophagy, are also stressed. Yeast has been specifically used to analyze the role of human KRAS in autophagy, a cancer-related process, and was established as a model to study KRAS-induced autophagy.

Here, we wanted to evidence that yeast is a useful model in the study of human RAS proteins because of the functional conservation of RAS proteins roles. Though increasing advanced resources are becoming more available to study higher eukaryotic organisms, the “simple” yeast eukaryotic model together with novel and expedite tools, still seems promising to genetically analyze the molecular mechanisms at the core of human RAS signal transduction pathways and their involvement in tumorigenesis.

Acknowledgments

This work was supported by the strategic program UID/BIA/04050/2013 (POCI-01-0145-FEDER-007569) funded by national funds through the FCT I.P. and by the ERDF through the COMPETE2020—Programa Operacional Competitividade e Internacionalização (POCI). It was also supported by the Portuguese Foundation for Science and Technology (FCT) under the scope of the strategic funding of the UID/BIO/04469/2013 unit and COMPETE 2020 (POCI-01-0145-FEDER-006684) and FCT fellowships: Sara Alves (FCT SFRH/BD/64695/2009). This work was also supported by the Marie Curie Initial Training Network: GLYCOPHARM, PITN-GA-2012-317297 (GC PhD Grant).

Conflicts of Interest

The authors declare no conflict of interest.

Appendix A

In the text, genes and proteins have been written accordingly to the standard nomenclature of the specific organism. In the case of *S. cerevisiae*, wild-type genes were presented as all italicized capital letters and specific yeast proteins as non-italicized, with only the first letter in upper case. Human genes and proteins were written all in capital letters, with the difference that gene names were italicized, whereas protein names were not [309,310]. When RAS proteins were addressed in general, without specifying the exact protein, either in human or yeast, they were written in upper case, non-italicized.

References

1. Botstein, D.; Fink, G.R. Yeast: An experimental organism for 21st Century biology. *Genetics* **2011**, *189*, 695–704. [[Google Scholar](#)] [[CrossRef](#)] [[PubMed](#)]
2. Fields, S.; Johnston, M. Cell biology. Whither model organism research? *Science* **2005**, *307*, 1885–1886. [[Google Scholar](#)] [[CrossRef](#)] [[PubMed](#)]
3. Mager, W.H.; Winderickx, J. Yeast as a model for medical and medicinal research. *Trends Pharmacol. Sci.* **2005**, *26*, 265–273. [[Google Scholar](#)] [[CrossRef](#)] [[PubMed](#)]
4. Botstein, D.; Fink, G.R. Yeast: An experimental organism for modern biology. *Science* **1988**, *240*, 1439–1443. [[Google Scholar](#)] [[CrossRef](#)] [[PubMed](#)]
5. Goffeau, A.; Barrell, B.G.; Bussey, H.; Davis, R.W.; Dujon, B.; Feldmann, H.; Galibert, F.; Hoheisel, J.D.; Jacq, C.; Johnston, M. Life with 6000 genes. *Science* **1996**, *274*, 546–567. [[Google Scholar](#)] [[CrossRef](#)] [[PubMed](#)]
6. Engel, S.R.; Dietrich, F.S.; Fisk, D.G.; Binkley, G.; Balakrishnan, R.; Costanzo, M.C.; Dwight, S.S.; Hitz, B.C.; Karra, K.; Nash, R.S.; et al. The reference genome sequence of *Saccharomyces cerevisiae*: Then and now. *G3* **2014**, *4*, 389–398. [[Google Scholar](#)] [[CrossRef](#)] [[PubMed](#)]
7. Giaever, G.; Chu, A.M.; Ni, L.; Connelly, C.; Riles, L.; Veronneau, S.; Dow, S.; Lucan-Danila, A.; Anderson, K.; Andre, B.; et al. Functional profiling of the *Saccharomyces cerevisiae* genome. *Nature* **2002**, *418*, 387–391. [[Google Scholar](#)] [[CrossRef](#)] [[PubMed](#)]

8. Winzeler, E.A.; Shoemaker, D.D.; Astromoff, A.; Liang, H.; Anderson, K.; Andre, B.; Bangham, R.; Benito, R.; Boeke, J.D.; Bussey, H.; et al. Functional characterization of the *S. cerevisiae* genome by gene deletion and parallel analysis. *Science* **1999**, *285*, 901–906. [[Google Scholar](#)] [[CrossRef](#)] [[PubMed](#)]
9. DeFeo-Jones, D.; Scolnick, E.M.; Koller, R.; Dhar, R. Ras-related gene sequences identified and isolated from *Saccharomyces cerevisiae*. *Nature* **1983**, *306*, 707–709. [[Google Scholar](#)] [[CrossRef](#)] [[PubMed](#)]
10. Dhar, R.; Nieto, A.; Koller, R.; DeFeo-Jones, D.; Scolnick, E.M. Nucleotide sequence of two rasH related genes isolated from the yeast *Saccharomyces cerevisiae*. *Nucleic Acids Res.* **1984**, *12*, 3611–3618. [[Google Scholar](#)] [[CrossRef](#)] [[PubMed](#)]
11. Powers, S.; Kataoka, T.; Fasano, O.; Goldfarb, M.; Strathern, J.; Broach, J.; Wigler, M. Genes in *S. cerevisiae* encoding proteins with domains homologous to the mammalian ras proteins. *Cell* **1984**, *36*, 607–612. [[Google Scholar](#)] [[CrossRef](#)]
12. Ihle, N. Differential Activity of the KRAS Oncogene by Method of Activation: Implications for Signaling and Therapeutic Intervention. Ph.D. Thesis, Faculty of The University of Texas, Houston, TX, USA, 2012. [[Google Scholar](#)]
13. Wittinghofer, A. *Ras Superfamily Small G Proteins: Biology and Mechanisms I*; Springer: Wien, Austria, 2014. [[Google Scholar](#)]
14. Arrington, A.K.; Heinrich, E.L.; Lee, W.; Duldulao, M.; Patel, S.; Sanchez, J.; Garcia-Aguilar, J.; Kim, J. Prognostic and Predictive Roles of KRAS Mutation in Colorectal Cancer. *Int. J. Mol. Sci.* **2012**, *13*, 12153–12168. [[Google Scholar](#)] [[CrossRef](#)] [[PubMed](#)]
15. Liu, X.; Jakubowski, M.; Hunt, J.L. KRAS Gene Mutation in Colorectal Cancer Is Correlated with Increased Proliferation and Spontaneous Apoptosis. *Am. Soc. Clin. Pathol.* **2011**, *135*, 245–252. [[Google Scholar](#)] [[CrossRef](#)] [[PubMed](#)]
16. Smith, G.; Bounds, R.; Wolf, H.; Steele, R.J.; Carey, F.A.; Wolf, C.R. Activating K-Ras mutations outwith ‘hotspot’ codons in sporadic colorectal tumours—Implications for personalised cancer medicine. *Br. J. Cancer* **2010**, *102*, 693–703. [[Google Scholar](#)] [[CrossRef](#)] [[PubMed](#)]
17. Alves, S.; Castro, L.; Fernandes, M.S.; Francisco, R.; Castro, P.; Priault, M.; Chaves, S.R.; Moyer, M.P.; Oliveira, C.; Seruca, R.; et al. Colorectal cancer-related mutant KRAS alleles function as positive regulators of autophagy. *Oncotarget* **2015**, *6*, 30787–30802. [[Google Scholar](#)] [[CrossRef](#)] [[PubMed](#)]
18. Harvey, J.J. An Unidentified Virus Which Causes the Rapid Production of Tumours in Mice. *Nature* **1964**, *204*, 1104–1105. [[Google Scholar](#)] [[CrossRef](#)] [[PubMed](#)]
19. Kirsten, W.H.; Mayer, L.A.; Welander, C.W. Infective and noninfective viral murine leukemias. *Natl. Cancer Inst. Monogr.* **1966**, *22*, 369–377. [[Google Scholar](#)] [[PubMed](#)]
20. Hall, A.; Marshall, C.J.; Spurr, N.K.; Weiss, R.A. Identification of transforming gene in two human sarcoma cell lines as a new member of the ras gene family located on chromosome 1. *Nature* **1983**, *303*, 396–400. [[Google Scholar](#)] [[CrossRef](#)] [[PubMed](#)]
21. Malumbres, M.; Barbacid, M. RAS oncogenes: The first 30 years. *Nat. Rev. Cancer* **2003**, *3*, 459–465. [[Google Scholar](#)] [[CrossRef](#)] [[PubMed](#)]
22. Papageorge, A.G.; DeFeo-Jones, D.; Robinson, P.; Temeles, G.; Scolnick, E.M. *Saccharomyces cerevisiae* synthesizes proteins related to the p21 gene product of ras genes found in mammals. *Mol. Cell. Biol.* **1984**, *4*, 23–29. [[Google Scholar](#)] [[CrossRef](#)] [[PubMed](#)]
23. DeFeo-Jones, D.; Tatchell, K.; Robinson, L.C.; Sigal, I.S.; Vass, W.C.; Lowy, D.R.; Scolnick, E.M. Mammalian and yeast ras gene products: Biological function in their heterologous systems. *Science* **1985**, *228*, 179–184. [[Google Scholar](#)] [[CrossRef](#)] [[PubMed](#)]
24. Kataoka, T.; Powers, S.; Cameron, S.; Fasano, O.; Goldfarb, M.; Broach, J.; Wigler, M. Functional homology of mammalian and yeast RAS genes. *Cell* **1985**, *40*, 19–26. [[Google Scholar](#)] [[CrossRef](#)]
25. Kataoka, T.; Powers, S.; McGill, C.; Fasano, O.; Strathern, J.; Broach, J.; Wigler, M. Genetic analysis of yeast *RAS1* and *RAS2* genes. *Cell* **1984**, *37*, 437–445. [[Google Scholar](#)] [[CrossRef](#)]
26. Toda, T.; Broek, D.; Field, J.; Michaeli, T.; Cameron, S.; Nikawa, J.; Sass, P.; Birchmeier, C.; Powers, S.; Wigler, M. Exploring the function of RAS oncogenes by studying the yeast *Saccharomyces cerevisiae*. *Princess Takamatsu Symp.* **1986**, *17*, 253–260. [[Google Scholar](#)] [[PubMed](#)]
27. Wigler, M.; Field, J.; Powers, S.; Broek, D.; Toda, T.; Cameron, S.; Nikawa, J.; Michaeli, T.; Colicelli, J.; Ferguson, K. Studies of RAS function in the yeast *Saccharomyces cerevisiae*. *Cold Spring Harb. Symp. Quant. Biol.* **1988**, *53*, 649–655. [[Google Scholar](#)] [[CrossRef](#)] [[PubMed](#)]
28. Ghaemmaghami, S.; Huh, W.K.; Bower, K.; Howson, R.W.; Belle, A.; Dephoure, N.; O’Shea, E.K.; Weissman, J.S. Global analysis of protein expression in yeast. *Nature* **2003**, *425*, 737–741. [[Google Scholar](#)] [[CrossRef](#)] [[PubMed](#)]
29. Huh, W.K.; Falvo, J.V.; Gerke, L.C.; Carroll, A.S.; Howson, R.W.; Weissman, J.S.; O’Shea, E.K. Global analysis of protein localization in budding yeast. *Nature* **2003**, *425*, 686–691. [[Google Scholar](#)] [[CrossRef](#)] [[PubMed](#)]
30. Heinicke, S.; Livstone, M.S.; Lu, C.; Oughtred, R.; Kang, F.; Angiuoli, S.V.; White, O.; Botstein, D.; Dolinski, K. The Princeton Protein Orthology Database (P-POD): A comparative genomics analysis tool for biologists. *PLoS ONE* **2007**, *2*, e766. [[Google Scholar](#)] [[CrossRef](#)] [[PubMed](#)]
31. Foury, F. Human genetic diseases: A cross-talk between man and yeast. *Gene* **1997**, *195*, 1–10. [[Google Scholar](#)] [[CrossRef](#)]
32. Zabrocki, P.; Pellens, K.; Vanhelmont, T.; Vandebroek, T.; Griffioen, G.; Wera, S.; Van Leuven, F.; Winderickx, J. Characterization of a-synuclein aggregation and synergistic toxicity with protein tau in yeast. *FEBS J.* **2005**, *272*, 1386–1400. [[Google Scholar](#)] [[CrossRef](#)] [[PubMed](#)]
33. Tenreiro, S.; Franssens, V.; Winderickx, J.; Outeiro, T.F. Yeast models of Parkinson’s disease-associated molecular pathologies. *Curr. Opin. Genet. Dev.* **2017**, *44*, 74–83. [[Google Scholar](#)] [[CrossRef](#)] [[PubMed](#)]
34. Laurent, J.M.; Young, J.H.; Kachroo, A.H.; Marcotte, E.M. Efforts to make and apply humanized yeast. *Brief. Funct. Genom.* **2016**, *15*, 155–163. [[Google Scholar](#)] [[CrossRef](#)] [[PubMed](#)]
35. Outeiro, T.F.; Lindquist, S. Yeast cells provide insight into a-synuclein biology and pathobiology. *Science* **2003**, *302*, 1772–1775. [[Google Scholar](#)] [[CrossRef](#)] [[PubMed](#)]
36. Outeiro, T.F.; Muchowski, P.J. Molecular genetics approaches in yeast to study amyloid diseases. *J. Mol. Neurosci.* **2004**, *23*, 49–60. [[Google Scholar](#)] [[CrossRef](#)]
37. Willingham, S.; Outeiro, T.F.; DeVit, M.J.; Lindquist, S.L.; Muchowski, P.J. Yeast genes that enhance the toxicity of a mutant huntingtin fragment or a-synuclein. *Science* **2003**, *302*, 1769–1772. [[Google Scholar](#)] [[CrossRef](#)] [[PubMed](#)]
38. Fruhmann, G.; Seynnaeve, D.; Zheng, J.; Ven, K.; Molenberghs, S.; Wilms, T.; Liu, B.; Winderickx, J.; Franssens, V. Yeast buddies helping to unravel the complexity of neurodegenerative disorders. *Mech. Ageing Dev.* **2017**, *161*, 288–305. [[Google Scholar](#)] [[CrossRef](#)] [[PubMed](#)]
39. Pereira, C.; Coutinho, I.; Soares, J.; Bessa, C.; Leao, M.; Saraiva, L. New insights into cancer-related proteins provided by the yeast model. *FEBS J.* **2012**, *279*, 697–712. [[Google Scholar](#)] [[CrossRef](#)] [[PubMed](#)]
40. Nitiss, J.L.; Heitman, J. *Yeast as a Tool in Cancer Research*; Springer: Dordrecht, The Netherlands, 2007; p. 433. [[Google Scholar](#)]
41. Matuo, R.; Sousa, F.G.; Soares, D.G.; Bonatto, D.; Saffi, J.; Escargueil, A.E.; Larsen, A.K.; Henriques, J.A. *Saccharomyces cerevisiae* as a model system to study the response to anticancer agents. *Cancer Chemother. Pharmacol.* **2012**, *70*, 491–502. [[Google Scholar](#)] [[CrossRef](#)] [[PubMed](#)]
42. Simon, J.A.; Bedalov, A. Yeast as a model system for anticancer drug discovery. *Nat. Rev. Cancer* **2004**, *4*, 481–492. [[Google Scholar](#)] [[CrossRef](#)] [[PubMed](#)]
43. Menacho-Marquez, M.; Murguia, J.R. Yeast on drugs: *Saccharomyces cerevisiae* as a tool for anticancer drug research. *Clin. Transl. Oncol.* **2007**, *9*, 221–228. [[Google Scholar](#)] [[CrossRef](#)] [[PubMed](#)]

44. Guaragnella, N.; Palermo, V.; Galli, A.; Moro, L.; Mazzoni, C.; Giannattasio, S. The expanding role of yeast in cancer research and diagnosis: Insights into the function of the oncosuppressors p53 and BRCA1/2. *FEMS Yeast Res.* **2014**, *14*, 2–16. [[Google Scholar](#)] [[CrossRef](#)] [[PubMed](#)]
45. Birrell, G.W.; Giaever, G.; Chu, A.M.; Davis, R.W.; Brown, J.M. A genome-wide screen in *Saccharomyces cerevisiae* for genes affecting UV radiation sensitivity. *Proc. Natl. Acad. Sci. USA* **2001**, *98*, 12608–12613. [[Google Scholar](#)] [[CrossRef](#)] [[PubMed](#)]
46. Aouida, M.; Page, N.; Leduc, A.; Peter, M.; Ramotar, D. A genome-wide screen in *Saccharomyces cerevisiae* reveals altered transport as a mechanism of resistance to the anticancer drug bleomycin. *Cancer Res.* **2004**, *64*, 1102–1109. [[Google Scholar](#)] [[CrossRef](#)] [[PubMed](#)]
47. Kang, J.J.; Schaber, M.D.; Srinivasula, S.M.; Alnemri, E.S.; Litwack, G.; Hall, D.J.; Bjornsti, M.A. Cascades of mammalian caspase activation in the yeast *Saccharomyces cerevisiae*. *J. Biol. Chem.* **1999**, *274*, 3189–3198. [[Google Scholar](#)] [[CrossRef](#)] [[PubMed](#)]
48. Wright, M.E.; Han, D.K.; Hockenbery, D.M. Caspase-3 and inhibitor of apoptosis protein(s) interactions in *Saccharomyces cerevisiae* and mammalian cells. *FEBS Lett.* **2000**, *481*, 13–18. [[Google Scholar](#)] [[CrossRef](#)]
49. Hayashi, H.; Cuddy, M.; Shu, V.C.; Yip, K.W.; Madiraju, C.; Diaz, P.; Matsuyama, T.; Kaibara, M.; Taniyama, K.; Vasile, S.; et al. Versatile assays for high throughput screening for activators or inhibitors of intracellular proteases and their cellular regulators. *PLoS ONE* **2009**, *4*, e7655. [[Google Scholar](#)] [[CrossRef](#)] [[PubMed](#)]
50. Xu, Q.; Reed, J.C. Bax inhibitor-1, a mammalian apoptosis suppressor identified by functional screening in yeast. *Mol. Cell* **1998**, *1*, 337–346. [[Google Scholar](#)] [[CrossRef](#)]
51. Zhang, H.; Cowan-Jacob, S.W.; Simonen, M.; Greenhalf, W.; Heim, J.; Meyhack, B. Structural basis of BFL-1 for its interaction with BAX and its anti-apoptotic action in mammalian and yeast cells. *J. Biol. Chem.* **2000**, *275*, 11092–11099. [[Google Scholar](#)] [[CrossRef](#)] [[PubMed](#)]
52. Brezniceanu, M.L.; Volp, K.; Bossier, S.; Solbach, C.; Lichter, P.; Joos, S.; Zornig, M. HMGB1 inhibits cell death in yeast and mammalian cells and is abundantly expressed in human breast carcinoma. *FASEB J.* **2003**, *17*, 1295–1297. [[Google Scholar](#)] [[CrossRef](#)] [[PubMed](#)]
53. Torgler, C.N.; de Tiani, M.; Raven, T.; Aubry, J.P.; Brown, R.; Meldrum, E. Expression of bak in *S. pombe* results in a lethality mediated through interaction with the calnexin homologue Cnx1. *Cell Death Differ.* **1997**, *4*, 263–271. [[Google Scholar](#)] [[CrossRef](#)] [[PubMed](#)]
54. Zhang, H.; Xu, Q.; Krajewski, S.; Krajewska, M.; Xie, Z.; Fuess, S.; Kitada, S.; Pawlowski, K.; Godzik, A.; Reed, J.C. BAR: An apoptosis regulator at the intersection of caspases and Bcl-2 family proteins. *Proc. Natl. Acad. Sci. USA* **2000**, *97*, 2597–2602. [[Google Scholar](#)] [[CrossRef](#)] [[PubMed](#)]
55. Sato, T.; Hanada, M.; Bodrug, S.; Irie, S.; Iwama, N.; Boise, L.H.; Thompson, C.B.; Golemis, E.; Fong, L.; Wang, H.G.; et al. Interactions among members of the Bcl-2 protein family analyzed with a yeast two-hybrid system. *Proc. Natl. Acad. Sci. USA* **1994**, *91*, 9238–9242. [[Google Scholar](#)] [[CrossRef](#)] [[PubMed](#)]
56. Cheok, C.F.; Verma, C.S.; Baselga, J.; Lane, D.P. Translating p53 into the clinic. *Nat. Rev. Clin. Oncol.* **2011**, *8*, 25–37. [[Google Scholar](#)] [[CrossRef](#)] [[PubMed](#)]
57. Yousef, A.F.; Xu, G.W.; Mendez, M.; Brandl, C.J.; Mymryk, J.S. Coactivator requirements for p53-dependent transcription in the yeast *Saccharomyces cerevisiae*. *Int. J. Cancer* **2008**, *122*, 942–946. [[Google Scholar](#)] [[CrossRef](#)] [[PubMed](#)]
58. Fields, S.; Jang, S.K. Presence of a potent transcription activating sequence in the p53 protein. *Science* **1990**, *249*, 1046–1049. [[Google Scholar](#)] [[CrossRef](#)] [[PubMed](#)]
59. Scharer, E.; Iggo, R. Mammalian p53 can function as a transcription factor in yeast. *Nucleic Acids Res.* **1992**, *20*, 1539–1545. [[Google Scholar](#)] [[CrossRef](#)] [[PubMed](#)]
60. Nigro, J.M.; Sikorski, R.; Reed, S.I.; Vogelstein, B. Human p53 and CDC2Hs genes combine to inhibit the proliferation of *Saccharomyces cerevisiae*. *Mol. Cell. Biol.* **1992**, *12*, 1357–1365. [[Google Scholar](#)] [[CrossRef](#)] [[PubMed](#)]
61. Mokdad-Gargouri, R.; Belhadj, K.; Gargouri, A. Translational control of human p53 expression in yeast mediated by 5'-UTR-ORF structural interaction. *Nucleic Acids Res.* **2001**, *29*, 1222–1227. [[Google Scholar](#)] [[CrossRef](#)] [[PubMed](#)]
62. Pearson, G.D.; Merrill, G.F. Deletion of the *Saccharomyces cerevisiae* TRR1 gene encoding thioredoxin reductase inhibits p53-dependent reporter gene expression. *J. Biol. Chem.* **1998**, *273*, 5431–5434. [[Google Scholar](#)] [[CrossRef](#)] [[PubMed](#)]
63. Hu, J.; Ma, X.; Lindner, D.J.; Karra, S.; Hofmann, E.R.; Reddy, S.P.; Kalvakolanu, D.V. Modulation of p53 dependent gene expression and cell death through thioredoxin-thioredoxin reductase by the Interferon-Retinoid combination. *Oncogene* **2001**, *20*, 4235–4248. [[Google Scholar](#)] [[CrossRef](#)] [[PubMed](#)]
64. Coutinho, I.; Pereira, C.; Pereira, G.; Goncalves, J.; Corte-Real, M.; Saraiva, L. Distinct regulation of p53-mediated apoptosis by protein kinase Ca, d, e and z: Evidence in yeast for transcription-dependent and -independent p53 apoptotic mechanisms. *Exp. Cell Res.* **2011**, *317*, 1147–1158. [[Google Scholar](#)] [[CrossRef](#)] [[PubMed](#)]
65. Robert, V.; Michel, P.; Flaman, J.M.; Chiron, A.; Martin, C.; Charbonnier, F.; Paillot, B.; Frebourg, T. High frequency in esophageal cancers of p53 alterations inactivating the regulation of genes involved in cell cycle and apoptosis. *Carcinogenesis* **2000**, *21*, 563–565. [[Google Scholar](#)] [[CrossRef](#)] [[PubMed](#)]
66. Di Como, C.J.; Prives, C. Human tumor-derived p53 proteins exhibit binding site selectivity and temperature sensitivity for transactivation in a yeast-based assay. *Oncogene* **1998**, *16*, 2527–2539. [[Google Scholar](#)] [[CrossRef](#)] [[PubMed](#)]
67. Kato, S.; Han, S.Y.; Liu, W.; Otsuka, K.; Shibata, H.; Kanamaru, R.; Ishioka, C. Understanding the function-structure and function-mutation relationships of p53 tumor suppressor protein by high-resolution missense mutation analysis. *Proc. Natl. Acad. Sci. USA* **2003**, *100*, 8424–8429. [[Google Scholar](#)] [[CrossRef](#)] [[PubMed](#)]
68. Clark, S.G.; McGrath, J.P.; Levinson, A.D. Expression of normal and activated human Ha-ras cDNAs in *Saccharomyces cerevisiae*. *Mol. Cell. Biol.* **1985**, *5*, 2746–2752. [[Google Scholar](#)] [[CrossRef](#)] [[PubMed](#)]
69. Fujiyama, A.; Matsumoto, K.; Tamanoi, F. A novel yeast mutant defective in the processing of ras proteins: Assessment of the effect of the mutation on processing steps. *EMBO J.* **1987**, *6*, 223–228. [[Google Scholar](#)] [[PubMed](#)]
70. Toda, T.; Uno, I.; Ishikawa, T.; Powers, S.; Kataoka, T.; Broek, D.; Cameron, S.; Broach, J.; Matsumoto, K.; Wigler, M. In yeast, RAS proteins are controlling elements of adenylate cyclase. *Cell* **1985**, *40*, 27–36. [[Google Scholar](#)] [[CrossRef](#)]
71. Robinson, L.C.; Gibbs, J.B.; Marshall, M.S.; Sigal, I.S.; Tatchell, K. CDC25: A component of the RAS-adenylate cyclase pathway in *Saccharomyces cerevisiae*. *Science* **1987**, *235*, 1218–1221. [[Google Scholar](#)] [[CrossRef](#)] [[PubMed](#)]
72. Broek, D.; Toda, T.; Michaeli, T.; Levin, L.; Birchmeier, C.; Zoller, M.; Powers, S.; Wigler, M. The *S. cerevisiae* CDC25 gene product regulates the RAS/adenylate cyclase pathway. *Cell* **1987**, *48*, 789–799. [[Google Scholar](#)] [[CrossRef](#)]
73. Wei, W.; Mosteller, R.D.; Sanyal, P.; Gonzales, E.; McKinney, D.; Dasgupta, C.; Li, P.; Liu, B.X.; Broek, D. Identification of a mammalian gene structurally and functionally related to the CDC25 gene of *Saccharomyces cerevisiae*. *Proc. Natl. Acad. Sci. USA* **1992**, *89*, 7100–7104. [[Google Scholar](#)] [[CrossRef](#)] [[PubMed](#)]
74. Bowtell, D.; Fu, P.; Simon, M.; Senior, P. Identification of murine homologues of the *Drosophila* son of sevenless gene: Potential activators of ras. *Proc. Natl. Acad. Sci. USA* **1992**, *89*, 6511–6515. [[Google Scholar](#)] [[CrossRef](#)] [[PubMed](#)]
75. Shou, C.; Farnsworth, C.L.; Neel, B.G.; Feig, L.A. Molecular cloning of cDNAs encoding a guanine-nucleotide-releasing factor for Ras p21. *Nature* **1992**, *358*, 351–354. [[Google Scholar](#)] [[CrossRef](#)] [[PubMed](#)]
76. Xu, G.F.; Lin, B.; Tanaka, K.; Dunn, D.; Wood, D.; Gesteland, R.; White, R.; Weiss, R.; Tamanoi, F. The catalytic domain of the neurofibromatosis type 1 gene product stimulates ras GTPase and complements *ira* mutants of *S. cerevisiae*. *Cell* **1990**, *63*, 835–841. [[Google Scholar](#)] [[CrossRef](#)]

77. Gibbs, J.B.; Schaber, M.D.; Allard, W.J.; Sigal, I.S.; Scolnick, E.M. Purification of ras GTPase activating protein from bovine brain. *Proc. Natl. Acad. Sci. USA* **1988**, *85*, 5026–5030. [[Google Scholar](#)] [[CrossRef](#)] [[PubMed](#)]
78. Wang, Y.; You, M.; Wang, Y. Alternative splicing of the K-ras gene in mouse tissues and cell lines. *Exp. Lung Res.* **2001**, *27*, 255–267. [[Google Scholar](#)] [[CrossRef](#)] [[PubMed](#)]
79. Schubbert, S.; Shannon, K.; Bollag, G. Hyperactive Ras in developmental disorders and cancer. *Nat. Rev. Cancer* **2007**, *7*, 295–308. [[Google Scholar](#)] [[CrossRef](#)] [[PubMed](#)]
80. Zeitouni, D.; Pylayeva-Gupta, Y.; Der, C.J.; Bryant, K.L. KRAS Mutant Pancreatic Cancer: No Lone Path to an Effective Treatment. *Cancers* **2016**, *8*, 45. [[Google Scholar](#)] [[CrossRef](#)] [[PubMed](#)]
81. Matallanas, D.; Arozarena, I.; Berciano, M.T.; Aaronson, D.S.; Pellicer, A.; Lafarga, M.; Crespo, P. Differences on the inhibitory specificities of H-Ras, K-Ras, and N-Ras (N17) dominant negative mutants are related to their membrane microlocalization. *J. Biol. Chem.* **2003**, *278*, 4572–4581. [[Google Scholar](#)] [[CrossRef](#)] [[PubMed](#)]
82. Arozarena, I.; Calvo, F.; Crespo, P. Ras, an actor on many stages: Posttranslational modifications, localization, and site-specified events. *Genes Cancer* **2011**, *2*, 182–194. [[Google Scholar](#)] [[CrossRef](#)] [[PubMed](#)]
83. Tatchell, K.; Chaleff, D.T.; DeFeo-Jones, D.; Scolnick, E.M. Requirement of either of a pair of ras-related genes of *Saccharomyces cerevisiae* for spore viability. *Nature* **1984**, *309*, 523–527. [[Google Scholar](#)] [[CrossRef](#)] [[PubMed](#)]
84. Feuerstein, J.; Goody, R.S.; Wittinghofer, A. Preparation and characterization of nucleotide-free and metal ion-free p21 “apoprotein”. *J. Biol. Chem.* **1987**, *262*, 8455–8458. [[Google Scholar](#)] [[PubMed](#)]
85. Breviario, D.; Hinnebusch, A.; Cannon, J.; Tatchell, K.; Dhar, R. Carbon source regulation of *RAS1* expression in *Saccharomyces cerevisiae* and the phenotypes of ras2-cells. *Proc. Natl. Acad. Sci. USA* **1986**, *83*, 4152–4156. [[Google Scholar](#)] [[CrossRef](#)] [[PubMed](#)]
86. Breviario, D.; Hinnebusch, A.G.; Dhar, R. Multiple regulatory mechanisms control the expression of the *RAS1* and *RAS2* genes of *Saccharomyces cerevisiae*. *EMBO J.* **1988**, *7*, 1805–1813. [[Google Scholar](#)] [[PubMed](#)]
87. Fraenkel, D.G. On ras gene function in yeast. *Proc. Natl. Acad. Sci. USA* **1985**, *82*, 4740–4744. [[Google Scholar](#)] [[CrossRef](#)] [[PubMed](#)]
88. Tatchell, K.; Robinson, L.C.; Breitenbach, M. *RAS2* of *Saccharomyces cerevisiae* is required for gluconeogenic growth and proper response to nutrient limitation. *Proc. Natl. Acad. Sci. USA* **1985**, *82*, 3785–3789. [[Google Scholar](#)] [[CrossRef](#)] [[PubMed](#)]
89. Marshall, M.S.; Gibbs, J.B.; Scolnick, E.M.; Sigal, I.S. Regulatory function of the *Saccharomyces cerevisiae* RAS C-terminus. *Mol. Cell. Biol.* **1987**, *7*, 2309–2315. [[Google Scholar](#)] [[CrossRef](#)] [[PubMed](#)]
90. Fujiyama, A.; Tamanoi, F. Processing and fatty acid acylation of *RAS1* and *RAS2* proteins in *Saccharomyces cerevisiae*. *Proc. Natl. Acad. Sci. USA* **1986**, *83*, 1266–1270. [[Google Scholar](#)] [[CrossRef](#)] [[PubMed](#)]
91. Azevedo, L.; Carneiro, J.; van Asch, B.; Moleirinho, A.; Pereira, F.; Amorim, A. Epistatic interactions modulate the evolution of mammalian mitochondrial respiratory complex components. *BMC Genom.* **2009**, *10*, 266. [[Google Scholar](#)] [[CrossRef](#)] [[PubMed](#)]
92. Carneiro, J.; Duarte-Pereira, S.; Azevedo, L.; Castro, L.F.; Aguiar, P.; Moreira, I.S.; Amorim, A.; Silva, R.M. The evolutionary portrait of metazoan NAD salvage. *PLoS ONE* **2013**, *8*, e64674. [[Google Scholar](#)] [[CrossRef](#)] [[PubMed](#)]
93. Gibbs, J.B.; Marshall, M.S. The ras oncogene—an important regulatory element in lower eucaryotic organisms. *Microbiol. Rev.* **1989**, *53*, 171–185. [[Google Scholar](#)] [[PubMed](#)]
94. Kearse, M.; Moir, R.; Wilson, A.; Stones-Havas, S.; Cheung, M.; Sturrock, S.; Buxton, S.; Cooper, A.; Markowitz, S.; Duran, C.; et al. Geneious Basic: An integrated and extendable desktop software platform for the organization and analysis of sequence data. *Bioinformatics* **2012**, *28*, 1647–1649. [[Google Scholar](#)] [[CrossRef](#)] [[PubMed](#)]
95. Edgar, R.C. MUSCLE: A multiple sequence alignment method with reduced time and space complexity. *BMC Bioinform.* **2004**, *5*, 113. [[Google Scholar](#)] [[CrossRef](#)] [[PubMed](#)]
96. Scheffzek, K.; Ahmadian, M.R.; Kabsch, W.; Wiesmuller, L.; Lautwein, A.; Schmitz, F.; Wittinghofer, A. The Ras-RasGAP complex: Structural basis for GTPase activation and its loss in oncogenic Ras mutants. *Science* **1997**, *277*, 333–338. [[Google Scholar](#)] [[CrossRef](#)] [[PubMed](#)]
97. Majumdar, S.; Acharya, A.; Prakash, B. Structural plasticity mediates distinct GAP-dependent GTP hydrolysis mechanisms in Rab33 and Rab5. *FEBS J.* **2017**, *284*, 4358–4375. [[Google Scholar](#)] [[CrossRef](#)] [[PubMed](#)]
98. Temeles, G.L.; Gibbs, J.B.; D’Alonzo, J.S.; Sigal, I.S.; Scolnick, E.M. Yeast and mammalian ras proteins have conserved biochemical properties. *Nature* **1985**, *313*, 700–703. [[Google Scholar](#)] [[CrossRef](#)] [[PubMed](#)]
99. Wennerberg, K.; Rossman, K.L.; Der, C.J. The Ras superfamily at a glance. *J. Cell Sci.* **2005**, *118*, 843–846. [[Google Scholar](#)] [[CrossRef](#)] [[PubMed](#)]
100. Cox, A.D.; Der, C.J. Ras history: The saga continues. *Small GTPases* **2010**, *1*, 2–27. [[Google Scholar](#)] [[CrossRef](#)] [[PubMed](#)]
101. Spaargaren, M.; Bischoff, J.R. Identification of the guanine nucleotide dissociation stimulator for Ral as a putative effector molecule of R-ras, H-ras, K-ras, and Rap. *Proc. Natl. Acad. Sci. USA* **1994**, *91*, 12609–12613. [[Google Scholar](#)] [[CrossRef](#)] [[PubMed](#)]
102. Kikuchi, A.; Demo, S.D.; Ye, Z.H.; Chen, Y.W.; Williams, L.T. ralGDS family members interact with the effector loop of ras p21. *Mol. Cell. Biol.* **1994**, *14*, 7483–7491. [[Google Scholar](#)] [[CrossRef](#)] [[PubMed](#)]
103. Hofer, F.; Fields, S.; Schneider, C.; Martin, G.S. Activated Ras interacts with the Ral guanine nucleotide dissociation stimulator. *Proc. Natl. Acad. Sci. USA* **1994**, *91*, 11089–11093. [[Google Scholar](#)] [[CrossRef](#)] [[PubMed](#)]
104. Bourne, H.R.; Sanders, D.A.; McCormick, F. The GTPase superfamily: Conserved structure and molecular mechanism. *Nature* **1991**, *349*, 117–127. [[Google Scholar](#)] [[CrossRef](#)] [[PubMed](#)]
105. Milburn, M.V.; Tong, L.; de Vos, A.M.; Brunger, A.; Yamaizumi, Z.; Nishimura, S.; Kim, S.H. Molecular switch for signal transduction: Structural differences between active and inactive forms of protooncogenic ras proteins. *Science* **1990**, *247*, 939–945. [[Google Scholar](#)] [[CrossRef](#)] [[PubMed](#)]
106. Schlichting, I.; Almo, S.C.; Rapp, G.; Wilson, K.; Petratos, K.; Lentfer, A.; Wittinghofer, A.; Kabsch, W.; Pai, E.F.; Petsko, G.A.; et al. Time-resolved X-ray crystallographic study of the conformational change in Ha-Ras p21 protein on GTP hydrolysis. *Nature* **1990**, *345*, 309–315. [[Google Scholar](#)] [[CrossRef](#)] [[PubMed](#)]
107. Scheffzek, K.; Lautwein, A.; Kabsch, W.; Ahmadian, M.R.; Wittinghofer, A. Crystal structure of the GTPase-activating domain of human p120GAP and implications for the interaction with Ras. *Nature* **1996**, *384*, 591–596. [[Google Scholar](#)] [[CrossRef](#)] [[PubMed](#)]
108. Bishop, A.L.; Hall, A. Rho GTPases and their effector proteins. *Biochem. J.* **2000**, *348*, 241–255. [[Google Scholar](#)] [[CrossRef](#)] [[PubMed](#)]
109. Repasky, G.A.; Chenette, E.J.; Der, C.J. Renewing the conspiracy theory debate: Does Raf function alone to mediate Ras oncogenesis? *Trends Cell Biol.* **2004**, *14*, 639–647. [[Google Scholar](#)] [[CrossRef](#)] [[PubMed](#)]
110. Trahey, M.; McCormick, F. A cytoplasmic protein stimulates normal N-ras p21 GTPase, but does not affect oncogenic mutants. *Science* **1987**, *238*, 542–545. [[Google Scholar](#)] [[CrossRef](#)] [[PubMed](#)]
111. Bernards, A.; Settleman, J. GAP control: Regulating the regulators of small GTPases. *Trends Cell Biol.* **2004**, *14*, 377–385. [[Google Scholar](#)] [[CrossRef](#)] [[PubMed](#)]
112. Schmidt, A.; Hall, A. Guanine nucleotide exchange factors for Rho GTPases: Turning on the switch. *Genes Dev.* **2002**, *16*, 1587–1609. [[Google Scholar](#)] [[CrossRef](#)] [[PubMed](#)]

113. Martegani, E.; Vanoni, M.; Zippel, R.; Coccetti, P.; Brambilla, R.; Ferrari, C.; Sturani, E.; Alberghina, L. Cloning by functional complementation of a mouse cDNA encoding a homologue of CDC25, a *Saccharomyces cerevisiae* RAS activator. *EMBO J.* **1992**, *11*, 2151–2157. [[Google Scholar](#)] [[PubMed](#)]
114. Segal, M.; Marbach, I.; Engelberg, D.; Simchen, G.; Levitzki, A. Interaction between the *Saccharomyces cerevisiae* CDC25 gene product and mammalian ras. *J. Biol. Chem.* **1992**, *267*, 22747–22751. [[Google Scholar](#)] [[PubMed](#)]
115. Ballester, R.; Marchuk, D.; Boguski, M.; Saulino, A.; Letcher, R.; Wigler, M.; Collins, F. The NF1 locus encodes a protein functionally related to mammalian GAP and yeast IRA proteins. *Cell* **1990**, *63*, 851–859. [[Google Scholar](#)] [[CrossRef](#)]
116. Goodman, L.E.; Judd, S.R.; Farnsworth, C.C.; Powers, S.; Gelb, M.H.; Glomset, J.A.; Tamanoi, F. Mutants of *Saccharomyces cerevisiae* defective in the farnesylation of Ras proteins. *Proc. Natl. Acad. Sci. USA* **1990**, *87*, 9665–9669. [[Google Scholar](#)] [[CrossRef](#)] [[PubMed](#)]
117. Fujiyama, A.; Tamanoi, F. RAS2 protein of *Saccharomyces cerevisiae* undergoes removal of methionine at N terminus and removal of three amino acids at C terminus. *J. Biol. Chem.* **1990**, *265*, 3362–3368. [[Google Scholar](#)] [[PubMed](#)]
118. Fujiyama, A.; Tsunasawa, S.; Tamanoi, F.; Sakiyama, F. S-farnesylation and methyl esterification of C-terminal domain of yeast RAS2 protein prior to fatty acid acylation. *J. Biol. Chem.* **1991**, *266*, 17926–17931. [[Google Scholar](#)] [[PubMed](#)]
119. Shih, T.Y.; Weeks, M.O.; Young, H.A.; Scholnick, E.M. Identification of a sarcoma virus-coded phosphoprotein in nonproducer cells transformed by Kirsten or Harvey murine sarcoma virus. *Virology* **1979**, *96*, 64–79. [[Google Scholar](#)] [[CrossRef](#)]
120. Cox, A.D.; Der, C.J. Ras family signaling: Therapeutic targeting. *Cancer Biol. Ther.* **2002**, *1*, 599–606. [[Google Scholar](#)] [[CrossRef](#)] [[PubMed](#)]
121. Schafer, W.R.; Kim, R.; Sterne, R.; Thorner, J.; Kim, S.H.; Rine, J. Genetic and pharmacological suppression of oncogenic mutations in ras genes of yeast and humans. *Science* **1989**, *245*, 379–385. [[Google Scholar](#)] [[CrossRef](#)] [[PubMed](#)]
122. Hancock, J.F.; Magee, A.I.; Childs, J.E.; Marshall, C.J. All ras proteins are polyisoprenylated but only some are palmitoylated. *Cell* **1989**, *57*, 1167–1177. [[Google Scholar](#)] [[CrossRef](#)]
123. Casey, P.J.; Solski, P.A.; Der, C.J.; Buss, J.E. p21ras is modified by a farnesyl isoprenoid. *Proc. Natl. Acad. Sci. USA* **1989**, *86*, 8323–8327. [[Google Scholar](#)] [[CrossRef](#)] [[PubMed](#)]
124. Hancock, J.F.; Cadwallader, K.; Paterson, H.; Marshall, C.J. A CAAX or a CAAL motif and a second signal are sufficient for plasma membrane targeting of ras proteins. *EMBO J.* **1991**, *10*, 4033–4039. [[Google Scholar](#)] [[CrossRef](#)]
125. Rowell, C.A.; Kowalczyk, J.J.; Lewis, M.D.; Garcia, A.M. Direct demonstration of geranylgeranylation and farnesylation of Ki-Ras in vivo. *J. Biol. Chem.* **1997**, *272*, 14093–14097. [[Google Scholar](#)] [[CrossRef](#)] [[PubMed](#)]
126. Whyte, D.B.; Kirschmeier, P.; Hockenberry, T.N.; Nunez-Oliva, I.; James, L.; Catino, J.J.; Bishop, W.R.; Pai, J.K. K- and N-Ras are geranylgeranylated in cells treated with farnesyl protein transferase inhibitors. *J. Biol. Chem.* **1997**, *272*, 14459–14464. [[Google Scholar](#)] [[CrossRef](#)] [[PubMed](#)]
127. Apolloni, A.; Prior, I.A.; Lindsay, M.; Parton, R.G.; Hancock, J.F. H-ras but not K-ras traffics to the plasma membrane through the exocytic pathway. *Mol. Cell. Biol.* **2000**, *20*, 2475–2487. [[Google Scholar](#)] [[CrossRef](#)] [[PubMed](#)]
128. Choy, E.; Chiu, V.K.; Silletti, J.; Feoktistov, M.; Morimoto, T.; Michaelson, D.; Ivanov, I.E.; Philips, M.R. Endomembrane trafficking of ras: The CAAX motif targets proteins to the ER and Golgi. *Cell* **1999**, *98*, 69–80. [[Google Scholar](#)] [[CrossRef](#)]
129. Roy, M.O.; Leventis, R.; Silviu, J.R. Mutational and biochemical analysis of plasma membrane targeting mediated by the farnesylated, polybasic carboxy terminus of K-ras4B. *Biochemistry* **2000**, *39*, 8298–8307. [[Google Scholar](#)] [[CrossRef](#)] [[PubMed](#)]
130. Hancock, J.F.; Paterson, H.; Marshall, C.J. A polybasic domain or palmitoylation is required in addition to the CAAX motif to localize p21ras to the plasma membrane. *Cell* **1990**, *63*, 133–139. [[Google Scholar](#)] [[CrossRef](#)]
131. Rajalingam, K.; Schreck, R.; Rapp, U.R.; Albert, S. Ras oncogenes and their downstream targets. *Biochim. Biophys. Acta* **2007**, *1773*, 1177–1195. [[Google Scholar](#)] [[CrossRef](#)] [[PubMed](#)]
132. Hancock, J.F.; Cadwallader, K.; Marshall, C.J. Methylation and proteolysis are essential for efficient membrane binding of prenylated p21K-ras(B). *EMBO J.* **1991**, *10*, 641–646. [[Google Scholar](#)] [[PubMed](#)]
133. Agudo-Ibanez, L.; Crespo, P.; Casar, B. Analysis of Ras/ERK Compartmentalization by Subcellular Fractionation. *Methods Mol. Biol.* **2017**, *1487*, 151–162. [[Google Scholar](#)] [[PubMed](#)]
134. Ahearn, I.M.; Tsai, F.D.; Court, H.; Zhou, M.; Jennings, B.C.; Ahmed, M.; Fehrenbacher, N.; Linder, M.E.; Philips, M.R. FKBP12 binds to acylated H-ras and promotes depalmitoylation. *Mol. Cell* **2011**, *41*, 173–185. [[Google Scholar](#)] [[CrossRef](#)] [[PubMed](#)]
135. Prior, I.A.; Harding, A.; Yan, J.; Sluimer, J.; Parton, R.G.; Hancock, J.F. GTP-dependent segregation of H-ras from lipid rafts is required for biological activity. *Nat. Cell Biol.* **2001**, *3*, 368–375. [[Google Scholar](#)] [[CrossRef](#)] [[PubMed](#)]
136. Roy, S.; Luetterforst, R.; Harding, A.; Apolloni, A.; Etheridge, M.; Stang, E.; Rolls, B.; Hancock, J.F.; Parton, R.G. Dominant-negative caveolin inhibits H-Ras function by disrupting cholesterol-rich plasma membrane domains. *Nat. Cell Biol.* **1999**, *1*, 98–105. [[Google Scholar](#)] [[PubMed](#)]
137. Ashery, U.; Yizhar, O.; Rotblat, B.; Elad-Sfadia, G.; Barkan, B.; Haklai, R.; Kloog, Y. Spatiotemporal organization of Ras signaling: Rasosomes and the galectin switch. *Cell. Mol. Neurobiol.* **2006**, *26*, 471–495. [[Google Scholar](#)] [[CrossRef](#)] [[PubMed](#)]
138. Carozzi, A.J.; Roy, S.; Morrow, I.C.; Pol, A.; Wyse, B.; Clyde-Smith, J.; Prior, I.A.; Nixon, S.J.; Hancock, J.F.; Parton, R.G. Inhibition of lipid raft-dependent signaling by a dystrophy-associated mutant of caveolin-3. *J. Biol. Chem.* **2002**, *277*, 17944–17949. [[Google Scholar](#)] [[CrossRef](#)] [[PubMed](#)]
139. Prior, I.A.; Muncke, C.; Parton, R.G.; Hancock, J.F. Direct visualization of Ras proteins in spatially distinct cell surface microdomains. *J. Cell Biol.* **2003**, *160*, 165–170. [[Google Scholar](#)] [[CrossRef](#)] [[PubMed](#)]
140. Chiu, V.K.; Bivona, T.; Hach, A.; Sajous, J.B.; Silletti, J.; Wiener, H.; Johnson, R.L., 2nd; Cox, A.D.; Philips, M.R. Ras signalling on the endoplasmic reticulum and the Golgi. *Nat. Cell Biol.* **2002**, *4*, 343–350. [[Google Scholar](#)] [[CrossRef](#)] [[PubMed](#)]
141. Hancock, J.F. Ras proteins: Different signals from different locations. *Nat. Rev. Mol. Cell Biol.* **2003**, *4*, 373–384. [[Google Scholar](#)] [[CrossRef](#)] [[PubMed](#)]
142. Jiang, X.; Sorkin, A. Coordinated traffic of Grb2 and Ras during epidermal growth factor receptor endocytosis visualized in living cells. *Mol. Biol. Cell* **2002**, *13*, 1522–1535. [[Google Scholar](#)] [[CrossRef](#)] [[PubMed](#)]
143. Sorkin, A.; McClure, M.; Huang, F.; Carter, R. Interaction of EGF receptor and grb2 in living cells visualized by fluorescence resonance energy transfer (FRET) microscopy. *Curr. Biol.* **2000**, *10*, 1395–1398. [[Google Scholar](#)] [[CrossRef](#)]
144. Mochizuki, N.; Yamashita, S.; Kurokawa, K.; Ohba, Y.; Nagai, T.; Miyawaki, A.; Matsuda, M. Spatio-temporal images of growth-factor-induced activation of Ras and Rap1. *Nature* **2001**, *411*, 1065–1068. [[Google Scholar](#)] [[CrossRef](#)] [[PubMed](#)]
145. Sasaki, A.T.; Carracedo, A.; Locasale, J.W.; Anastasiou, D.; Takeuchi, K.; Kahoud, E.R.; Haviv, S.; Asara, J.M.; Pandolfi, P.P.; Cantley, L.C. Ubiquitination of K-Ras enhances activation and facilitates binding to select downstream effectors. *Sci. Signal.* **2011**, *4*, ra13. [[Google Scholar](#)] [[CrossRef](#)] [[PubMed](#)]
146. Lu, A.; Tebar, F.; Alvarez-Moya, B.; Lopez-Alcala, C.; Calvo, M.; Enrich, C.; Agell, N.; Nakamura, T.; Matsuda, M.; Bachs, O. A clathrin-dependent pathway leads to KRas signaling on late endosomes en route to lysosomes. *J. Cell Biol.* **2009**, *184*, 863–879. [[Google Scholar](#)] [[CrossRef](#)] [[PubMed](#)]

147. Bivona, T.G.; Quatela, S.E.; Bodemann, B.O.; Ahearn, I.M.; Soskis, M.J.; Mor, A.; Miura, J.; Wiener, H.H.; Wright, L.; Saba, S.G.; et al. PKC regulates a farnesyl-electrostatic switch on K-Ras that promotes its association with Bcl-XL on mitochondria and induces apoptosis. *Mol. Cell* **2006**, *21*, 481–493. [[Google Scholar](#)] [[CrossRef](#)] [[PubMed](#)]
148. Rebollo, A.; Perez-Sala, D.; Martinez, A.C. Bcl-2 differentially targets K-, N-, and H-Ras to mitochondria in IL-2 supplemented or deprived cells: Implications in prevention of apoptosis. *Oncogene* **1999**, *18*, 4930–4939. [[Google Scholar](#)] [[CrossRef](#)] [[PubMed](#)]
149. Prior, I.A.; Hancock, J.F. Ras trafficking, localization and compartmentalized signalling. *Semin. Cell Dev. Biol.* **2012**, *23*, 145–153. [[Google Scholar](#)] [[CrossRef](#)] [[PubMed](#)]
150. Wittinghofer, A.; Franken, S.M.; Scheidig, A.J.; Rensland, H.; Lautwein, A.; Pai, E.F.; Goody, R.S. Three-dimensional structure and properties of wild-type and mutant H-ras-encoded p21. *Ciba Found. Symp.* **1993**, *176*, 6–21, discussion 21–27. [[Google Scholar](#)] [[PubMed](#)]
151. Elad-Sfadia, G.; Haklai, R.; Balan, E.; Kloog, Y. Galectin-3 augments K-Ras activation and triggers a Ras signal that attenuates ERK but not phosphoinositide 3-kinase activity. *J. Biol. Chem.* **2004**, *279*, 34922–34930. [[Google Scholar](#)] [[CrossRef](#)] [[PubMed](#)]
152. Shalom-Feuerstein, R.; Plowman, S.J.; Rotblat, B.; Ariotti, N.; Tian, T.; Hancock, J.F.; Kloog, Y. K-ras nanoclustering is subverted by overexpression of the scaffold protein galectin-3. *Cancer Res.* **2008**, *68*, 6608–6616. [[Google Scholar](#)] [[CrossRef](#)] [[PubMed](#)]
153. Paz, A.; Haklai, R.; Elad-Sfadia, G.; Ballan, E.; Kloog, Y. Galectin-1 binds oncogenic H-Ras to mediate Ras membrane anchorage and cell transformation. *Oncogene* **2001**, *20*, 7486–7493. [[Google Scholar](#)] [[CrossRef](#)] [[PubMed](#)]
154. Belotti, F.; Tisi, R.; Paiardi, C.; Rigamonti, M.; Groppi, S.; Martegani, E. Localization of Ras signaling complex in budding yeast. *Biochim. Biophys. Acta* **2012**, *1823*, 1208–1216. [[Google Scholar](#)] [[CrossRef](#)] [[PubMed](#)]
155. Sobering, A.K.; Romeo, M.J.; Vay, H.A.; Levin, D.E. A novel Ras inhibitor, Eri1, engages yeast Ras at the endoplasmic reticulum. *Mol. Cell. Biol.* **2003**, *23*, 4983–4990. [[Google Scholar](#)] [[CrossRef](#)] [[PubMed](#)]
156. Broggi, S.; Martegani, E.; Colombo, S. Nuclear Ras2-GTP Controls Invasive Growth in *Saccharomyces cerevisiae*. *PLoS ONE* **2013**, *8*, e79274. [[Google Scholar](#)] [[CrossRef](#)] [[PubMed](#)]
157. Tisi, R.; Belotti, F.; Martegani, E. Yeast as a model for Ras signalling. *Methods Mol. Biol.* **2014**, *1120*, 359–390. [[Google Scholar](#)] [[PubMed](#)]
158. Cheng, C.-M.; Chang, E.C. Cell Cycle. In *Busy Traveling Ras*; Bioscience, L., Ed.; Landes Bioscience: Houston, TX, USA, 2011; Volume 10, pp. 1180–1181. [[Google Scholar](#)]
159. Saif, M.W. Colorectal cancer in review: The role of the EGFR pathway. *Expert Opin. Investig. Drugs* **2010**, *19*, 357–369. [[Google Scholar](#)] [[CrossRef](#)] [[PubMed](#)]
160. Martinelli, E.; De Palma, R.; Orditura, M.; De Vita, F.; Ciardiello, F. Anti-epidermal growth factor receptor monoclonal antibodies in cancer therapy. *Clin. Exp. Immunol.* **2009**, *158*, 1–9. [[Google Scholar](#)] [[CrossRef](#)] [[PubMed](#)]
161. Normanno, N.; Tejpar, S.; Morgillo, F.; De Luca, A.; Van Cutsem, E.; Ciardiello, F. Implications for KRAS status and EGFR-targeted therapies in metastatic CRC. *Nat. Rev. Clin. Oncol.* **2009**, *6*, 519–527. [[Google Scholar](#)] [[CrossRef](#)] [[PubMed](#)]
162. Schulze, W.X.; Deng, L.; Mann, M. Phosphotyrosine interactome of the ErbB-receptor kinase family. *Mol. Syst. Biol.* **2005**, *1*. [[Google Scholar](#)] [[CrossRef](#)] [[PubMed](#)]
163. Downward, J. Targeting RAS signalling pathways in cancer therapy. *Nat. Rev. Cancer* **2003**, *3*, 11–22. [[Google Scholar](#)] [[CrossRef](#)] [[PubMed](#)]
164. Shields, J.M.; Pruitt, K.; McFall, A.; Shaub, A.; Der, C.J. Understanding Ras: 'it ain't over 'til it's over'. *Trends Cell Biol.* **2000**, *10*, 147–154. [[Google Scholar](#)] [[CrossRef](#)]
165. Herrmann, C. Ras-effector interactions: After one decade. *Curr. Opin. Struct. Biol.* **2003**, *13*, 122–129. [[Google Scholar](#)] [[CrossRef](#)]
166. Efferth, T. Signal transduction pathways of the epidermal growth factor receptor in colorectal cancer and their inhibition by small molecules. *Curr. Med. Chem.* **2012**, *19*, 5735–5744. [[Google Scholar](#)] [[CrossRef](#)] [[PubMed](#)]
167. Scheid, M.P.; Woodgett, J.R. Phosphatidylinositol 3' kinase signaling in mammary tumorigenesis. *J. Mammary Gland Biol. Neoplasia* **2001**, *6*, 83–99. [[Google Scholar](#)] [[CrossRef](#)] [[PubMed](#)]
168. Scheid, M.P.; Woodgett, J.R. PKB/AKT: Functional insights from genetic models. *Nat. Rev. Mol. Cell Biol.* **2001**, *2*, 760–768. [[Google Scholar](#)] [[CrossRef](#)] [[PubMed](#)]
169. Yan, J.; Roy, S.; Apolloni, A.; Lane, A.; Hancock, J.F. Ras isoforms vary in their ability to activate Raf-1 and phosphoinositide 3-kinase. *J. Biol. Chem.* **1998**, *273*, 24052–24056. [[Google Scholar](#)] [[CrossRef](#)] [[PubMed](#)]
170. Wang, X.W.; Zhang, Y.J. Targeting mTOR network in colorectal cancer therapy. *World J. Gastroenterol.* **2014**, *20*, 4178–4188. [[Google Scholar](#)] [[CrossRef](#)] [[PubMed](#)]
171. Busti, S.; Coccetti, P.; Alberghina, L.; Vanoni, M. Glucose signaling-mediated coordination of cell growth and cell cycle in *Saccharomyces cerevisiae*. *Sensors* **2010**, *10*, 6195–6240. [[Google Scholar](#)] [[CrossRef](#)] [[PubMed](#)]
172. Tamanoi, F. Ras signaling in yeast. *Genes Cancer* **2011**, *2*, 210–215. [[Google Scholar](#)] [[CrossRef](#)] [[PubMed](#)]
173. Francois, J.; Hers, H.G. The control of glycogen metabolism in yeast. 2. A kinetic study of the two forms of glycogen synthase and of glycogen phosphorylase and an investigation of their interconversion in a cell-free extract. *Eur. J. Biochem.* **1988**, *174*, 561–567. [[Google Scholar](#)] [[CrossRef](#)] [[PubMed](#)]
174. Francois, J.; Van Schaftingen, E.; Hers, H.G. The mechanism by which glucose increases fructose 2,6-bisphosphate concentration in *Saccharomyces cerevisiae*. A cyclic-AMP-dependent activation of phosphofruktokinase 2. *Eur. J. Biochem.* **1984**, *145*, 187–193. [[Google Scholar](#)] [[CrossRef](#)] [[PubMed](#)]
175. Lopez-Boado, Y.S.; Herrero, P.; Gascon, S.; Moreno, F. Catabolite inactivation of isocitrate lyase from *Saccharomyces cerevisiae*. *Arch. Microbiol.* **1987**, *147*, 231–234. [[Google Scholar](#)] [[CrossRef](#)] [[PubMed](#)]
176. Müller, G.; Bandlow, W. cAMP-dependent protein kinase activity in yeast mitochondria. *Z. Naturforsch. C* **1987**, *42*, 1291–1302. [[Google Scholar](#)] [[PubMed](#)]
177. Ortiz, C.H.; Maia, J.C.; Tenan, M.N.; Braz-Padua, G.R.; Mattoon, J.R.; Panek, A.D. Regulation of yeast trehalase by a monocyclic, cyclic AMP-dependent phosphorylation-dephosphorylation cascade system. *J. Bacteriol.* **1983**, *153*, 644–651. [[Google Scholar](#)] [[PubMed](#)]
178. Pohl, G.; Holzer, H. Phosphorylation and inactivation of yeast fructose-1,6-bisphosphatase by cyclic AMP-dependent protein kinase from yeast. *J. Biol. Chem.* **1985**, *260*, 13818–13823. [[Google Scholar](#)] [[PubMed](#)]
179. Rittenhouse, J.; Moberly, L.; Marcus, F. Phosphorylation in vivo of yeast (*Saccharomyces cerevisiae*) fructose-1,6-bisphosphatase at the cyclic AMP-dependent site. *J. Biol. Chem.* **1987**, *262*, 10114–10119. [[Google Scholar](#)] [[PubMed](#)]
180. Rödel, G.; Müller, G.; Bandlow, W. Cyclic AMP receptor protein from yeast mitochondria: Submitochondrial localization and preliminary characterization. *J. Bacteriol.* **1985**, *161*, 7–12. [[Google Scholar](#)] [[PubMed](#)]
181. Uno, I.; Matsumoto, K.; Adachi, K.; Ishikawa, T. Genetic and biochemical evidence that trehalase is a substrate of cAMP-dependent protein kinase in yeast. *J. Biol. Chem.* **1983**, *258*, 10867–10872. [[Google Scholar](#)] [[PubMed](#)]
182. Cameron, S.; Levin, L.; Zoller, M.; Wigler, M. cAMP-independent control of sporulation, glycogen metabolism, and heat shock resistance in *S. cerevisiae*. *Cell* **1988**, *53*, 555–566. [[Google Scholar](#)] [[CrossRef](#)]
183. Uno, I.; Matsumoto, K.; Hirata, A.; Ishikawa, T. Outer plaque assembly and spore encapsulation are defective during sporulation of adenylate cyclase-deficient mutants of *Saccharomyces cerevisiae*. *J. Cell Biol.* **1985**, *100*, 1854–1862. [[Google Scholar](#)] [[CrossRef](#)] [[PubMed](#)]
184. Matsumoto, K.; Uno, I.; Oshima, Y.; Ishikawa, T. Isolation and characterization of yeast mutants deficient in adenylate cyclase and cAMP-dependent protein kinase. *Proc. Natl. Acad. Sci. USA* **1982**, *79*, 2355–2359. [[Google Scholar](#)] [[CrossRef](#)] [[PubMed](#)]

185. Matsumoto, K.; Uno, I.; Ishikawa, T. Control of cell division in *Saccharomyces cerevisiae* mutants defective in adenylate cyclase and cAMP-dependent protein kinase. *Exp. Cell Res.* **1983**, *146*, 151–161. [[Google Scholar](#)] [[CrossRef](#)]
186. Matsumoto, K.; Uno, I.; Ishikawa, T. Initiation of meiosis in yeast mutants defective in adenylate cyclase and cyclic AMP-dependent protein kinase. *Cell* **1983**, *32*, 417–423. [[Google Scholar](#)] [[CrossRef](#)]
187. Kido, M.; Shima, F.; Satoh, T.; Asato, T.; Kariya, K.; Kataoka, T. Critical function of the Ras-associating domain as a primary Ras-binding site for regulation of *Saccharomyces cerevisiae* adenylate cyclase. *J. Biol. Chem.* **2002**, *277*, 3117–3123. [[Google Scholar](#)] [[CrossRef](#)] [[PubMed](#)]
188. Thevelein, J.M.; de Winde, J.H. Novel sensing mechanisms and targets for the cAMP-protein kinase A pathway in the yeast *Saccharomyces cerevisiae*. *Mol. Microbiol.* **1999**, *33*, 904–918. [[Google Scholar](#)] [[CrossRef](#)] [[PubMed](#)]
189. Broach, J.R.; Deschenes, R.J. The function of ras genes in *Saccharomyces cerevisiae*. *Adv. Cancer Res.* **1990**, *54*, 79–139. [[Google Scholar](#)] [[PubMed](#)]
190. Thevelein, J.M. The RAS-adenylate cyclase pathway and cell cycle control in *Saccharomyces cerevisiae*. *Antonie van Leeuwenhoek* **1992**, *62*, 109–130. [[Google Scholar](#)] [[CrossRef](#)] [[PubMed](#)]
191. Thevelein, J.M. Signal transduction in yeast. *Yeast* **1994**, *10*, 1753–1790. [[Google Scholar](#)] [[CrossRef](#)] [[PubMed](#)]
192. Tatchell, T. RAS genes in the budding yeast *Saccharomyces cerevisiae*. In *Signal Transduction: Prokaryotic and Simple Eukaryotic Systems*; Kurjan, J., Taylor, B.L., Eds.; Academic Press: San Diego, CA, USA, 1993; pp. 147–188. [[Google Scholar](#)]
193. Toda, T.; Cameron, S.; Sass, P.; Zoller, M.; Scott, J.D.; McMullen, B.; Hurwitz, M.; Krebs, E.G.; Wigler, M. Cloning and characterization of BCY1, a locus encoding a regulatory subunit of the cyclic AMP-dependent protein kinase in *Saccharomyces cerevisiae*. *Mol. Cell. Biol.* **1987**, *7*, 1371–1377. [[Google Scholar](#)] [[CrossRef](#)] [[PubMed](#)]
194. Toda, T.; Cameron, S.; Sass, P.; Zoller, M.; Wigler, M. Three different genes in *S. cerevisiae* encode the catalytic subunits of the cAMP-dependent protein kinase. *Cell* **1987**, *50*, 277–287. [[Google Scholar](#)] [[CrossRef](#)]
195. Nikawa, J.; Cameron, S.; Toda, T.; Ferguson, K.M.; Wigler, M. Rigorous feedback control of cAMP levels in *Saccharomyces cerevisiae*. *Genes Dev.* **1987**, *1*, 931–937. [[Google Scholar](#)] [[CrossRef](#)] [[PubMed](#)]
196. Mbonyi, K.; van Aelst, L.; Arguelles, J.C.; Jans, A.W.; Thevelein, J.M. Glucose-induced hyperaccumulation of cyclic AMP and defective glucose repression in yeast strains with reduced activity of cyclic AMP-dependent protein kinase. *Mol. Cell. Biol.* **1990**, *10*, 4518–4523. [[Google Scholar](#)] [[CrossRef](#)] [[PubMed](#)]
197. Zaman, S.; Lippman, S.I.; Zhao, X.; Broach, J.R. How *Saccharomyces* responds to nutrients. *Annu. Rev. Genet.* **2008**, *42*, 27–81. [[Google Scholar](#)] [[CrossRef](#)] [[PubMed](#)]
198. Gancedo, J.M. The early steps of glucose signalling in yeast. *FEMS Microbiol. Rev.* **2008**, *32*, 673–704. [[Google Scholar](#)] [[CrossRef](#)] [[PubMed](#)]
199. Ho, J.; Bretscher, A. Ras regulates the polarity of the yeast actin cytoskeleton through the stress response pathway. *Mol. Biol. Cell* **2001**, *12*, 1541–1555. [[Google Scholar](#)] [[CrossRef](#)] [[PubMed](#)]
200. McDonald, C.M.; Wagner, M.; Dunham, M.J.; Shin, M.E.; Ahmed, N.T.; Winter, E. The Ras/cAMP pathway and the CDK-like kinase Ime2 regulate the MAPK Smk1 and spore morphogenesis in *Saccharomyces cerevisiae*. *Genetics* **2009**, *181*, 511–523. [[Google Scholar](#)] [[CrossRef](#)] [[PubMed](#)]
201. Hubler, L.; Bradshaw-Rouse, J.; Heideman, W. Connections between the Ras-cyclic AMP pathway and G1 cyclin expression in the budding yeast *Saccharomyces cerevisiae*. *Mol. Cell. Biol.* **1993**, *13*, 6274–6282. [[Google Scholar](#)] [[CrossRef](#)] [[PubMed](#)]
202. Sun, J.; Kale, S.P.; Childress, A.M.; Pinswasdi, C.; Jazwinski, S.M. Divergent roles of RAS1 and RAS2 in yeast longevity. *J. Biol. Chem.* **1994**, *269*, 18638–18645. [[Google Scholar](#)] [[PubMed](#)]
203. Peeper, D.S.; Upton, T.M.; Ladha, M.H.; Neuman, E.; Zalvide, J.; Bernards, R.; DeCaprio, J.A.; Ewen, M.E. Ras signalling linked to the cell-cycle machinery by the retinoblastoma protein. *Nature* **1997**, *386*, 177–181. [[Google Scholar](#)] [[CrossRef](#)] [[PubMed](#)]
204. Pruitt, K.; Der, C.J. Ras and Rho regulation of the cell cycle and oncogenesis. *Cancer Lett.* **2001**, *171*, 1–10. [[Google Scholar](#)] [[CrossRef](#)]
205. Coleman, M.L.; Marshall, C.J.; Olson, M.F. RAS and RHO GTPases in G1-phase cell-cycle regulation. *Nat. Rev. Mol. Cell Biol.* **2004**, *5*, 355–366. [[Google Scholar](#)] [[CrossRef](#)] [[PubMed](#)]
206. Downward, J. Cell cycle: Routine role for Ras. *Curr. Biol.* **1997**, *7*, R258–R260. [[Google Scholar](#)] [[CrossRef](#)]
207. Mittnacht, S.; Paterson, H.; Olson, M.F.; Marshall, C.J. Ras signalling is required for inactivation of the tumour suppressor pRb cell-cycle control protein. *Curr. Biol.* **1997**, *7*, 219–221. [[Google Scholar](#)] [[CrossRef](#)]
208. Yang, J.J.; Kang, J.S.; Krauss, R.S. Transformation-restoring factor: A low molecular weight secreted factor required for anchorage-independent growth of oncogene-resistant mutant cell lines. *Oncogene* **1995**, *10*, 1291–1299. [[Google Scholar](#)] [[PubMed](#)]
209. Kang, J.S.; Krauss, R.S. Ras induces anchorage-independent growth by subverting multiple adhesion-regulated cell cycle events. *Mol. Cell. Biol.* **1996**, *16*, 3370–3380. [[Google Scholar](#)] [[CrossRef](#)] [[PubMed](#)]
210. Pruitt, K.; Pestell, R.G.; Der, C.J. Ras inactivation of the retinoblastoma pathway by distinct mechanisms in NIH 3T3 fibroblast and RIE-1 epithelial cells. *J. Biol. Chem.* **2000**, *275*, 40916–40924. [[Google Scholar](#)] [[CrossRef](#)] [[PubMed](#)]
211. Mulcahy, L.S.; Smith, M.R.; Stacey, D.W. Requirement for ras proto-oncogene function during serum-stimulated growth of NIH 3T3 cells. *Nature* **1985**, *313*, 241–243. [[Google Scholar](#)] [[CrossRef](#)] [[PubMed](#)]
212. Feramisco, J.R.; Gross, M.; Kamata, T.; Rosenberg, M.; Sweet, R.W. Microinjection of the oncogene form of the human H-ras (T-24) protein results in rapid proliferation of quiescent cells. *Cell* **1984**, *38*, 109–117. [[Google Scholar](#)] [[CrossRef](#)]
213. Hanahan, D.; Weinberg, R.A. Hallmarks of cancer: The next generation. *Cell* **2011**, *144*, 646–674. [[Google Scholar](#)] [[CrossRef](#)] [[PubMed](#)]
214. Hartwell, L.H.; Unger, M.W. Unequal division in *Saccharomyces cerevisiae* and its implications for the control of cell division. *J. Cell Biol.* **1977**, *75*, 422–435. [[Google Scholar](#)] [[CrossRef](#)] [[PubMed](#)]
215. Vanoni, M.; Vai, M.; Popolo, L.; Alberghina, L. Structural heterogeneity in populations of the budding yeast *Saccharomyces cerevisiae*. *J. Bacteriol.* **1983**, *156*, 1282–1291. [[Google Scholar](#)] [[PubMed](#)]
216. Johnston, G.C.; Ehrhardt, C.W.; Lorincz, A.; Carter, B.L. Regulation of cell size in the yeast *Saccharomyces cerevisiae*. *J. Bacteriol.* **1979**, *137*, 1–5. [[Google Scholar](#)] [[PubMed](#)]
217. Lord, P.G.; Wheals, A.E. Rate of cell cycle initiation of yeast cells when cell size is not a rate-determining factor. *J. Cell Sci.* **1983**, *59*, 183–201. [[Google Scholar](#)] [[PubMed](#)]
218. Mitchison, J.M. *The Biology of the Cell Cycle*; Cambridge University Press: Cambridge, UK, 1971. [[Google Scholar](#)]
219. Baroni, M.D.; Monti, P.; Alberghina, L. Repression of growth-regulated G1 cyclin expression by cyclic AMP in budding yeast. *Nature* **1994**, *371*, 339–342. [[Google Scholar](#)] [[CrossRef](#)] [[PubMed](#)]
220. Tokiwa, G.; Tyers, M.; Volpe, T.; Futcher, B. Inhibition of G1 cyclin activity by the Ras/cAMP pathway in yeast. *Nature* **1994**, *371*, 342–345. [[Google Scholar](#)] [[CrossRef](#)] [[PubMed](#)]
221. Mizunuma, M.; Tsubakiyama, R.; Ogawa, T.; Shitamukai, A.; Kobayashi, Y.; Inai, T.; Kume, K.; Hirata, D. Ras/cAMP-dependent protein kinase (PKA) regulates multiple aspects of cellular events by phosphorylating the Whi3 cell cycle regulator in budding yeast. *J. Biol. Chem.* **2013**, *288*, 10558–10566. [[Google Scholar](#)] [[CrossRef](#)] [[PubMed](#)]
222. Downward, J. Ras signalling and apoptosis. *Curr. Opin. Genet. Dev.* **1998**, *8*, 49–54. [[Google Scholar](#)] [[CrossRef](#)]

223. Chang, F.; Steelman, L.S.; Shelton, J.G.; Lee, J.T.; Navolanic, P.M.; Blalock, W.L.; Franklin, R.; McCubrey, J.A. Regulation of cell cycle progression and apoptosis by the Ras/Raf/MEK/ERK pathway. *Int. J. Oncol.* **2003**, *22*, 469–480. [[Google Scholar](#)] [[PubMed](#)]
224. Cox, A.D.; Der, C.J. The dark side of Ras: Regulation of apoptosis. *Oncogene* **2003**, *22*, 8999–9006. [[Google Scholar](#)] [[CrossRef](#)] [[PubMed](#)]
225. Datta, S.R.; Brunet, A.; Greenberg, M.E. Cellular survival: A play in three Akts. *Genes Dev.* **1999**, *13*, 2905–2927. [[Google Scholar](#)] [[CrossRef](#)] [[PubMed](#)]
226. Sulciner, D.J.; Irani, K.; Yu, Z.X.; Ferrans, V.J.; Goldschmidt-Clermont, P.; Finkel, T. rac1 regulates a cytokine-stimulated, redox-dependent pathway necessary for NF- κ B activation. *Mol. Cell Biol.* **1996**, *16*, 7115–7121. [[Google Scholar](#)] [[CrossRef](#)] [[PubMed](#)]
227. Irani, K.; Xia, Y.; Zweier, J.L.; Sollott, S.J.; Der, C.J.; Fearon, E.R.; Sundaresan, M.; Finkel, T.; Goldschmidt-Clermont, P.J. Mitogenic signaling mediated by oxidants in Ras-transformed fibroblasts. *Science* **1997**, *275*, 1649–1652. [[Google Scholar](#)] [[CrossRef](#)] [[PubMed](#)]
228. Joneson, T.; Bar-Sagi, D. Suppression of Ras-induced apoptosis by the Rac GTPase. *Mol. Cell Biol.* **1999**, *19*, 5892–5901. [[Google Scholar](#)] [[CrossRef](#)] [[PubMed](#)]
229. Mayo, M.W.; Baldwin, A.S. The transcription factor NF- κ B: Control of oncogenesis and cancer therapy resistance. *Biochim. Biophys. Acta* **2000**, *1470*, M55–M62. [[Google Scholar](#)] [[PubMed](#)]
230. Lambert, J.M.; Lambert, Q.T.; Reuther, G.W.; Malliri, A.; Siderovski, D.P.; Sondel, J.; Collard, J.G.; Der, C.J. Tiam1 mediates Ras activation of Rac by a PI(3)K-independent mechanism. *Nat. Cell Biol.* **2002**, *4*, 621–625. [[Google Scholar](#)] [[CrossRef](#)] [[PubMed](#)]
231. Romashkova, J.A.; Makarov, S.S. NF- κ B is a target of AKT in anti-apoptotic PDGF signalling. *Nature* **1999**, *401*, 86–90. [[Google Scholar](#)] [[CrossRef](#)] [[PubMed](#)]
232. Blume-Jensen, P.; Janknecht, R.; Hunter, T. The kit receptor promotes cell survival via activation of PI 3-kinase and subsequent Akt-mediated phosphorylation of Bad on Ser136. *Curr. Biol.* **1998**, *8*, 779–782. [[Google Scholar](#)] [[CrossRef](#)]
233. Bonni, A.; Brunet, A.; West, A.E.; Datta, S.R.; Takasu, M.A.; Greenberg, M.E. Cell survival promoted by the Ras-MAPK signaling pathway by transcription-dependent and -independent mechanisms. *Science* **1999**, *286*, 1358–1362. [[Google Scholar](#)] [[CrossRef](#)] [[PubMed](#)]
234. Fang, X.; Yu, S.; Eder, A.; Mao, M.; Bast, R.C., Jr.; Boyd, D.; Mills, G.B. Regulation of BAD phosphorylation at serine 112 by the Ras-mitogen-activated protein kinase pathway. *Oncogene* **1999**, *18*, 6635–6640. [[Google Scholar](#)] [[CrossRef](#)] [[PubMed](#)]
235. Tan, Y.; Ruan, H.; Demeter, M.R.; Comb, M.J. p90(RSK) blocks bad-mediated cell death via a protein kinase C-dependent pathway. *J. Biol. Chem.* **1999**, *274*, 34859–34867. [[Google Scholar](#)] [[CrossRef](#)] [[PubMed](#)]
236. Du, K.; Montminy, M. CREB is a regulatory target for the protein kinase Akt/PKB. *J. Biol. Chem.* **1998**, *273*, 32377–32379. [[Google Scholar](#)] [[CrossRef](#)] [[PubMed](#)]
237. Nalca, A.; Qiu, S.G.; El-Guendy, N.; Krishnan, S.; Rangnekar, V.M. Oncogenic Ras sensitizes cells to apoptosis by Par-4. *J. Biol. Chem.* **1999**, *274*, 29976–29983. [[Google Scholar](#)] [[CrossRef](#)] [[PubMed](#)]
238. Ries, S.; Biederer, C.; Woods, D.; Shifman, O.; Shirasawa, S.; Sasazuki, T.; McMahon, M.; Oren, M.; McCormick, F. Opposing effects of Ras on p53: Transcriptional activation of mdm2 and induction of p19ARF. *Cell* **2000**, *103*, 321–330. [[Google Scholar](#)] [[CrossRef](#)]
239. Tsuchida, T.; Kijima, H.; Hori, S.; Oshika, Y.; Tokunaga, T.; Kawai, K.; Yamazaki, H.; Ueyama, Y.; Scanlon, K.J.; Tamaoki, N.; et al. Adenovirus-mediated anti-K-ras ribozyme induces apoptosis and growth suppression of human pancreatic carcinoma. *Cancer Gene Ther.* **2000**, *7*, 373–383. [[Google Scholar](#)] [[CrossRef](#)] [[PubMed](#)]
240. Navarro, P.; Valverde, A.M.; Benito, M.; Lorenzo, M. Activated Ha-ras induces apoptosis by association with phosphorylated Bcl-2 in a mitogen-activated protein kinase-independent manner. *J. Biol. Chem.* **1999**, *274*, 18857–18863. [[Google Scholar](#)] [[CrossRef](#)] [[PubMed](#)]
241. Gourlay, C.W.; Du, W.; Ayscough, K.R. Apoptosis in yeast—mechanisms and benefits to a unicellular organism. *Mol. Microbiol.* **2006**, *62*, 1515–1521. [[Google Scholar](#)] [[CrossRef](#)] [[PubMed](#)]
242. Frohlich, K.U.; Fussi, H.; Ruckstuhl, C. Yeast apoptosis—From genes to pathways. *Semin. Cancer Biol.* **2007**, *17*, 112–121. [[Google Scholar](#)] [[CrossRef](#)] [[PubMed](#)]
243. Carmona-Gutierrez, D.; Eisenberg, T.; Buttner, S.; Meisinger, C.; Kroemer, G.; Madeo, F. Apoptosis in yeast: Triggers, pathways, subroutines. *Cell Death Differ.* **2010**, *17*, 763–773. [[Google Scholar](#)] [[CrossRef](#)] [[PubMed](#)]
244. Phillips, A.J.; Crowe, J.D.; Ramsdale, M. Ras pathway signaling accelerates programmed cell death in the pathogenic fungus *Candida albicans*. *Proc. Natl. Acad. Sci. USA* **2006**, *103*, 726–731. [[Google Scholar](#)] [[CrossRef](#)] [[PubMed](#)]
245. Gourlay, C.W.; Ayscough, K.R. Actin-induced hyperactivation of the Ras signaling pathway leads to apoptosis in *Saccharomyces cerevisiae*. *Mol. Cell Biol.* **2006**, *26*, 6487–6501. [[Google Scholar](#)] [[CrossRef](#)] [[PubMed](#)]
246. Narasimhan, M.L.; Damsz, B.; Coca, M.A.; Ibeas, J.I.; Yun, D.J.; Pardo, J.M.; Hasegawa, P.M.; Bressan, R.A. A plant defense response effector induces microbial apoptosis. *Mol. Cell* **2001**, *8*, 921–930. [[Google Scholar](#)] [[CrossRef](#)]
247. Santos, J.; Sousa, M.J.; Leao, C. Ammonium is toxic for aging yeast cells, inducing death and shortening of the chronological lifespan. *PLoS ONE* **2012**, *7*, e37090. [[Google Scholar](#)] [[CrossRef](#)] [[PubMed](#)]
248. Santos, J.; Leao, C.; Sousa, M.J. Ammonium-dependent shortening of CLS in yeast cells starved for essential amino acids is determined by the specific amino acid deprived, through different signaling pathways. *Oxid. Med. Cell. Longev.* **2013**, *2013*, 161986. [[Google Scholar](#)] [[CrossRef](#)] [[PubMed](#)]
249. Madeo, F.; Frohlich, E.; Ligr, M.; Grey, M.; Sigrist, S.J.; Wolf, D.H.; Frohlich, K.U. Oxygen stress: A regulator of apoptosis in yeast. *J. Cell Biol.* **1999**, *145*, 757–767. [[Google Scholar](#)] [[CrossRef](#)] [[PubMed](#)]
250. Ludovico, P.; Sousa, M.J.; Silva, M.T.; Leao, C.; Corte-Real, M. *Saccharomyces cerevisiae* commits to a programmed cell death process in response to acetic acid. *Microbiology* **2001**, *147*, 2409–2415. [[Google Scholar](#)] [[CrossRef](#)] [[PubMed](#)]
251. Silva, R.D.; Sotoca, R.; Johansson, B.; Ludovico, P.; Sansonetti, F.; Silva, M.T.; Peinado, J.M.; Corte-Real, M. Hyperosmotic stress induces metacaspase- and mitochondria-dependent apoptosis in *Saccharomyces cerevisiae*. *Mol. Microbiol.* **2005**, *58*, 824–834. [[Google Scholar](#)] [[CrossRef](#)] [[PubMed](#)]
252. Mitsui, K.; Nakagawa, D.; Nakamura, M.; Okamoto, T.; Tsurugi, K. Valproic acid induces apoptosis dependent of Yca1p at concentrations that mildly affect the proliferation of yeast. *FEBS Lett.* **2005**, *579*, 723–727. [[Google Scholar](#)] [[CrossRef](#)] [[PubMed](#)]
253. Weinberger, M.; Ramachandran, L.; Feng, L.; Sharma, K.; Sun, X.; Marchetti, M.; Huberman, J.A.; Burhans, W.C. Apoptosis in budding yeast caused by defects in initiation of DNA replication. *J. Cell Sci.* **2005**, *118*, 3543–3553. [[Google Scholar](#)] [[CrossRef](#)] [[PubMed](#)]
254. Gourlay, C.W.; Ayscough, K.R. Identification of an upstream regulatory pathway controlling actin-mediated apoptosis in yeast. *J. Cell Sci.* **2005**, *118*, 2119–2132. [[Google Scholar](#)] [[CrossRef](#)] [[PubMed](#)]
255. Lastauskiene, E.; Zinkeviciene, A.; Citavicius, D. Ras/PKA signal transduction pathway participates in the regulation of *Saccharomyces cerevisiae* cell apoptosis in an acidic environment. *Biotechnol. Appl. Biochem.* **2014**, *61*, 3–10. [[Google Scholar](#)] [[CrossRef](#)] [[PubMed](#)]
256. Mollapour, M.; Phelan, J.P.; Millson, S.H.; Piper, P.W.; Cooke, F.T. Weak acid and alkali stress regulate phosphatidylinositol bisphosphate synthesis in *Saccharomyces cerevisiae*. *Biochem. J.* **2006**, *395*, 73–80. [[Google Scholar](#)] [[CrossRef](#)] [[PubMed](#)]
257. Klionsky, D.J. Autophagy. *Curr. Biol.* **2005**, *15*, R282–R283. [[Google Scholar](#)] [[CrossRef](#)] [[PubMed](#)]
258. Massey, A.; Kiffin, R.; Cuervo, A.M. Pathophysiology of chaperone-mediated autophagy. *Int. J. Biochem. Cell Biol.* **2004**, *36*, 2420–2434. [[Google Scholar](#)] [[CrossRef](#)] [[PubMed](#)]
259. Yang, Z.; Klionsky, D.J. An overview of the molecular mechanism of autophagy. *Curr. Top. Microbiol. Immunol.* **2009**, *335*, 1–32. [[Google Scholar](#)] [[PubMed](#)]

260. He, C.; Klionsky, D.J. Regulation mechanisms and signaling pathways of autophagy. *Annu. Rev. Genet.* **2009**, *43*, 67–93. [[Google Scholar](#)] [[CrossRef](#)] [[PubMed](#)]
261. Ravikumar, B.; Sarkar, S.; Davies, J.E.; Futter, M.; Garcia-Arencibia, M.; Green-Thompson, Z.W.; Jimenez-Sanchez, M.; Korolchuk, V.I.; Lichtenberg, M.; Luo, S.; et al. Regulation of mammalian autophagy in physiology and pathophysiology. *Physiol. Rev.* **2010**, *90*, 1383–1435. [[Google Scholar](#)] [[CrossRef](#)] [[PubMed](#)]
262. Levine, B.; Klionsky, D.J. Development by self-digestion: Molecular mechanisms and biological functions of autophagy. *Dev. Cell* **2004**, *6*, 463–477. [[Google Scholar](#)] [[CrossRef](#)]
263. Levine, B.; Deretic, V. Unveiling the roles of autophagy in innate and adaptive immunity. *Nat. Rev. Immunol.* **2007**, *7*, 767–777. [[Google Scholar](#)] [[CrossRef](#)] [[PubMed](#)]
264. Boya, P.; Gonzalez-Polo, R.A.; Casares, N.; Perfettini, J.L.; Dessen, P.; Larochette, N.; Metivier, D.; Meley, D.; Souquere, S.; Yoshimori, T.; et al. Inhibition of macroautophagy triggers apoptosis. *Mol. Cell. Biol.* **2005**, *25*, 1025–1040. [[Google Scholar](#)] [[CrossRef](#)] [[PubMed](#)]
265. Galluzzi, L.; Vicencio, J.M.; Kepp, O.; Tasdemir, E.; Maiuri, M.C.; Kroemer, G. To die or not to die: That is the autophagic question. *Curr. Mol. Med.* **2008**, *8*, 78–91. [[Google Scholar](#)] [[PubMed](#)]
266. Kroemer, G.; Jaattela, M. Lysosomes and autophagy in cell death control. *Nat. Rev. Cancer* **2005**, *5*, 886–897. [[Google Scholar](#)] [[CrossRef](#)] [[PubMed](#)]
267. Maiuri, M.C.; Zalckvar, E.; Kimchi, A.; Kroemer, G. Self-eating and self-killing: Crosstalk between autophagy and apoptosis. *Nat. Rev. Mol. Cell Biol.* **2007**, *8*, 741–752. [[Google Scholar](#)] [[CrossRef](#)] [[PubMed](#)]
268. Tsujimoto, Y.; Shimizu, S. Another way to die: Autophagic programmed cell death. *Cell Death Differ.* **2005**, *12* (Suppl. 2), 1528–1534. [[Google Scholar](#)] [[CrossRef](#)] [[PubMed](#)]
269. Mathew, R.; Karantza-Wadsworth, V.; White, E. Role of autophagy in cancer. *Nat. Rev. Cancer* **2007**, *7*, 961–967. [[Google Scholar](#)] [[CrossRef](#)] [[PubMed](#)]
270. Meijer, A.J.; Codogno, P. Autophagy: Regulation by energy sensing. *Curr. Biol.* **2011**, *21*, R227–R229. [[Google Scholar](#)] [[CrossRef](#)] [[PubMed](#)]
271. Pattingre, S.; Bauvy, C.; Codogno, P. Amino acids interfere with the ERK1/2-dependent control of macroautophagy by controlling the activation of Raf-1 in human colon cancer HT-29 cells. *J. Biol. Chem.* **2003**, *278*, 16667–16674. [[Google Scholar](#)] [[CrossRef](#)] [[PubMed](#)]
272. Furuta, S.; Hidaka, E.; Ogata, A.; Yokota, S.; Kamata, T. Ras is involved in the negative control of autophagy through the class I PI3-kinase. *Oncogene* **2004**, *23*, 3898–3904. [[Google Scholar](#)] [[CrossRef](#)] [[PubMed](#)]
273. Elgendy, M.; Sheridan, C.; Brumatti, G.; Martin, S.J. Oncogenic Ras-induced expression of Noxa and Beclin-1 promotes autophagic cell death and limits clonogenic survival. *Mol. Cell* **2011**, *42*, 23–35. [[Google Scholar](#)] [[CrossRef](#)] [[PubMed](#)]
274. Wu, S.Y.; Lan, S.H.; Cheng, D.E.; Chen, W.K.; Shen, C.H.; Lee, Y.R.; Zuchini, R.; Liu, H.S. Ras-related tumorigenesis is suppressed by BNP3-mediated autophagy through inhibition of cell proliferation. *Neoplasia* **2011**, *13*, 1171–1182. [[Google Scholar](#)] [[CrossRef](#)] [[PubMed](#)]
275. Kim, J.H.; Kim, H.Y.; Lee, Y.K.; Yoon, Y.S.; Xu, W.G.; Yoon, J.K.; Choi, S.E.; Ko, Y.G.; Kim, M.J.; Lee, S.J.; et al. Involvement of mitophagy in oncogenic K-Ras-induced transformation: Overcoming a cellular energy deficit from glucose deficiency. *Autophagy* **2011**, *7*, 1187–1198. [[Google Scholar](#)] [[CrossRef](#)] [[PubMed](#)]
276. Guo, J.Y.; Chen, H.Y.; Mathew, R.; Fan, J.; Strohecker, A.M.; Karsli-Uzunbas, G.; Kamphorst, J.J.; Chen, G.; Lemons, J.M.; Karantza, V.; et al. Activated Ras requires autophagy to maintain oxidative metabolism and tumorigenesis. *Genes Dev.* **2011**, *25*, 460–470. [[Google Scholar](#)] [[CrossRef](#)] [[PubMed](#)]
277. Kim, M.J.; Woo, S.J.; Yoon, C.H.; Lee, J.S.; An, S.; Choi, Y.H.; Hwang, S.G.; Yoon, G.; Lee, S.J. Involvement of autophagy in oncogenic K-Ras-induced malignant cell transformation. *J. Biol. Chem.* **2011**, *286*, 12924–12932. [[Google Scholar](#)] [[CrossRef](#)] [[PubMed](#)]
278. Lock, R.; Roy, S.; Kenific, C.M.; Su, J.S.; Salas, E.; Ronen, S.M.; Debnath, J. Autophagy facilitates glycolysis during Ras-mediated oncogenic transformation. *Mol. Biol. Cell* **2011**, *22*, 165–178. [[Google Scholar](#)] [[CrossRef](#)] [[PubMed](#)]
279. Cebollero, E.; Reggiori, F. Regulation of autophagy in yeast *Saccharomyces cerevisiae*. *Biochim. Biophys. Acta* **2009**, *1793*, 1413–1421. [[Google Scholar](#)] [[CrossRef](#)] [[PubMed](#)]
280. Chen, Y.; Klionsky, D.J. The regulation of autophagy—Unanswered questions. *J. Cell Sci.* **2011**, *124*, 161–170. [[Google Scholar](#)] [[CrossRef](#)] [[PubMed](#)]
281. Stephan, J.S.; Yeh, Y.Y.; Ramachandran, V.; Deminoff, S.J.; Herman, P.K. The Tor and PKA signaling pathways independently target the Atg1/Atg13 protein kinase complex to control autophagy. *Proc. Natl. Acad. Sci. USA* **2009**, *106*, 17049–17054. [[Google Scholar](#)] [[CrossRef](#)] [[PubMed](#)]
282. Conrad, M.; Schothorst, J.; Kankipati, H.N.; Van Zeebroeck, G.; Rubio-Teixeira, M.; Thevelein, J.M. Nutrient sensing and signaling in the yeast *Saccharomyces cerevisiae*. *FEMS Microbiol. Rev.* **2014**, *38*, 254–299. [[Google Scholar](#)] [[CrossRef](#)] [[PubMed](#)]
283. Longo, V.D.; Fabrizio, P. Chronological aging in *Saccharomyces cerevisiae*. *Subcell. Biochem.* **2012**, *57*, 101–121. [[Google Scholar](#)] [[PubMed](#)]
284. Jacinto, E.; Lorbberg, A. TOR regulation of AGC kinases in yeast and mammals. *Biochem. J.* **2008**, *410*, 19–37. [[Google Scholar](#)] [[CrossRef](#)] [[PubMed](#)]
285. Noda, T.; Ohsumi, Y. Tor, a phosphatidylinositol kinase homologue, controls autophagy in yeast. *J. Biol. Chem.* **1998**, *273*, 3963–3966. [[Google Scholar](#)] [[CrossRef](#)] [[PubMed](#)]
286. Urban, J.; Soulard, A.; Huber, A.; Lippman, S.; Mukhopadhyay, D.; Deloche, O.; Wanke, V.; Anrather, D.; Ammerer, G.; Riezman, H.; et al. Sch9 is a major target of TORC1 in *Saccharomyces cerevisiae*. *Mol. Cell* **2007**, *26*, 663–674. [[Google Scholar](#)] [[CrossRef](#)] [[PubMed](#)]
287. Yorimitsu, T.; Zaman, S.; Broach, J.R.; Klionsky, D.J. Protein kinase A and Sch9 cooperatively regulate induction of autophagy in *Saccharomyces cerevisiae*. *Mol. Biol. Cell* **2007**, *18*, 4180–4189. [[Google Scholar](#)] [[CrossRef](#)] [[PubMed](#)]
288. Forbes, S.A.; Bindal, N.; Bamford, S.; Cole, C.; Kok, C.Y.; Beare, D.; Jia, M.; Shepherd, R.; Leung, K.; Menzies, A.; et al. COSMIC: Mining complete cancer genomes in the Catalogue of Somatic Mutations in Cancer. *Nucleic Acids Res.* **2011**, *39*, D945–D950. [[Google Scholar](#)] [[CrossRef](#)] [[PubMed](#)]
289. Karnoub, A.E.; Weinberg, R.A. Ras oncogenes: Split personalities. *Nat. Rev. Mol. Cell Biol.* **2008**, *9*, 517–531. [[Google Scholar](#)] [[CrossRef](#)] [[PubMed](#)]
290. Pendergast, A.M.; Quilliam, L.A.; Cripe, L.D.; Bassing, C.H.; Dai, Z.; Li, N.; Batzer, A.; Rabun, K.M.; Der, C.J.; Schlessinger, J.; et al. BCR-ABL-induced oncogenesis is mediated by direct interaction with the SH2 domain of the GRB-2 adaptor protein. *Cell* **1993**, *75*, 175–185. [[Google Scholar](#)] [[CrossRef](#)]
291. Donovan, S.; Shannon, K.M.; Bollag, G. GTPase activating proteins: Critical regulators of intracellular signaling. *Biochim. Biophys. Acta* **2002**, *1602*, 23–45. [[Google Scholar](#)] [[CrossRef](#)]
292. Yarden, Y. The EGFR family and its ligands in human cancer. Signalling mechanisms and therapeutic opportunities. *Eur. J. Cancer* **2001**, *37* (Suppl. 4), S3–S8. [[Google Scholar](#)] [[CrossRef](#)]
293. Barault, L.; Veyrie, N.; Jooste, V.; Lecorre, D.; Chapusot, C.; Ferraz, J.M.; Lievre, A.; Cortet, M.; Bouvier, A.M.; Rat, P.; et al. Mutations in the RAS-MAPK, PI(3)K (phosphatidylinositol-3-OH kinase) signaling network correlate with poor survival in a population-based series of colon cancers. *Int. J. Cancer* **2008**, *122*, 2255–2259. [[Google Scholar](#)] [[CrossRef](#)] [[PubMed](#)]

294. Oliveira, C.; Velho, S.; Moutinho, C.; Ferreira, A.; Preto, A.; Domingo, E.; Capelinha, A.F.; Duval, A.; Hamelin, R.; Machado, J.C.; et al. KRAS and BRAF oncogenic mutations in MSS colorectal carcinoma progression. *Oncogene* **2007**, *26*, 158–163. [[Google Scholar](#)] [[CrossRef](#)] [[PubMed](#)]
295. Samuels, Y.; Velculescu, V.E. Oncogenic mutations of PIK3CA in human cancers. *Cell Cycle* **2004**, *3*, 1221–1224. [[Google Scholar](#)] [[CrossRef](#)] [[PubMed](#)]
296. Broek, D.; Samiy, N.; Fasano, O.; Fujiyama, A.; Tamanoi, F.; Northup, J.; Wigler, M. Differential activation of yeast adenylate cyclase by wild-type and mutant RAS proteins. *Cell* **1985**, *41*, 763–769. [[Google Scholar](#)] [[CrossRef](#)]
297. Cazzanelli, G. Study the Roles of Human Galectin-3 Using the Yeast *Saccharomyces cerevisiae* and Colorectal Cancer Cells as Eukaryotic Models. Ph.D. Thesis, the University of Minho, Braga, Portugal, 2017. [[Google Scholar](#)]
298. Yang, Z.; Klionsky, D.J. Mammalian autophagy: Core molecular machinery and signaling regulation. *Curr. Opin. Cell Biol.* **2010**, *22*, 124–131. [[Google Scholar](#)] [[CrossRef](#)] [[PubMed](#)]
299. Chen, N.; Karantza, V. Autophagy as a therapeutic target in cancer. *Cancer Biol. Ther.* **2011**, *11*, 157–168. [[Google Scholar](#)] [[CrossRef](#)] [[PubMed](#)]
300. Shalom-Feuerstein, R.; Cooks, T.; Raz, A.; Kloog, Y. Galectin-3 regulates a molecular switch from N-Ras to K-Ras usage in human breast carcinoma cells. *Cancer Res.* **2005**, *65*, 7292–7300. [[Google Scholar](#)] [[CrossRef](#)] [[PubMed](#)]
301. Abankwa, D.; Gorfe, A.A.; Inder, K.; Hancock, J.F. Ras membrane orientation and nanodomain localization generate isoform diversity. *Proc. Natl. Acad. Sci. USA* **2010**, *107*, 1130–1135. [[Google Scholar](#)] [[CrossRef](#)] [[PubMed](#)]
302. Bhagatji, P.; Leventis, R.; Rich, R.; Lin, C.J.; Silviu, J.R. Multiple cellular proteins modulate the dynamics of K-ras association with the plasma membrane. *Biophys. J.* **2010**, *99*, 3327–3335. [[Google Scholar](#)] [[CrossRef](#)] [[PubMed](#)]
303. Levy, R.; Grafi-Cohen, M.; Kraiem, Z.; Kloog, Y. Galectin-3 promotes chronic activation of K-Ras and differentiation block in malignant thyroid carcinomas. *Mol. Cancer Ther.* **2010**, *9*, 2208–2219. [[Google Scholar](#)] [[CrossRef](#)] [[PubMed](#)]
304. Song, S.; Ji, B.; Ramachandran, V.; Wang, H.; Hafley, M.; Logsdon, C.; Bresalier, R.S. Overexpressed galectin-3 in pancreatic cancer induces cell proliferation and invasion by binding Ras and activating Ras signaling. *PLoS ONE* **2012**, *7*, e42699. [[Google Scholar](#)] [[CrossRef](#)] [[PubMed](#)]
305. Wu, K.L.; Huang, E.Y.; Jhu, E.W.; Huang, Y.H.; Su, W.H.; Chuang, P.C.; Yang, K.D. Overexpression of galectin-3 enhances migration of colon cancer cells related to activation of the K-Ras-Raf-Erk1/2 pathway. *J. Gastroenterol.* **2013**, *48*, 350–359. [[Google Scholar](#)] [[CrossRef](#)] [[PubMed](#)]
306. Markowska, A.I.; Liu, F.T.; Panjwani, N. Galectin-3 is an important mediator of VEGF- and bFGF-mediated angiogenic response. *J. Exp. Med.* **2010**, *207*, 1981–1993. [[Google Scholar](#)] [[CrossRef](#)] [[PubMed](#)]
307. Seguin, L.; Kato, S.; Franovic, A.; Camargo, M.F.; Lesperance, J.; Elliott, K.C.; Yebra, M.; Mielgo, A.; Lowy, A.M.; Husain, H.; et al. An integrin b(3)-KRAS-RalB complex drives tumour stemness and resistance to EGFR inhibition. *Nat. Cell Biol.* **2014**, *16*, 457–468. [[Google Scholar](#)] [[CrossRef](#)] [[PubMed](#)]
308. Han, J.W.; McCormick, F.; Macara, I.G. Regulation of Ras-GAP and the neurofibromatosis-1 gene product by eicosanoids. *Science* **1991**, *252*, 576–579. [[Google Scholar](#)] [[CrossRef](#)] [[PubMed](#)]
309. Chen, M.; Rymond, B. Appendix A1: Yeast Nomenclature Systematic Open Reading Frame (ORF) and Other Genetic Designations. In *Alternative pre-mRNA Splicing*; Wiley-VCH Verlag GmbH & Co. KGaA: Weinheim, Germany, 2012; pp. 603–607. [[Google Scholar](#)]
310. Sherman, F. Getting started with yeast. *Methods Enzymol.* **2002**, *350*, 3–41. [[Google Scholar](#)] [[PubMed](#)]